AFFINE MODELS: CHANGE POINT DETECTION AND APPLICATIONS

Konstantinos Bisiotis

A thesis submitted in partial fulfilment
of the requirements for the degree of
Doctor of Philosophy in Statistics

Athens University of Economics and Business
Department of Statistics
School of Information Sciences

Athens, Greece
August, 2021

AFFINE MODELS: CHANGE POINT DETECTION AND APPLICATIONS

Κωνσταντίνος Μπισιώτης

ΔΙΑΤΡΙΒΗ

Που υποβλήθηκε στο Τμήμα Στατιστικής
του Οικονομικού Πανεπιστημίου Αθηνών
ως μέρος των απαιτήσεων για την απόκτηση
Διδακτορικού Διπλώματος στη Στατιστική

Οικονομικό Πανεπιστήμιο Αθηνών
Τμήμα Στατιστικής
Σχολή Επιστημών και Τεχνολογίας της
Πληροφορίας

Αθήνα, Ελλάδα
Αύγουστος, 2021

Dedication

Abstract

The purpose of the present thesis is the application of statistical process control (SPC) techniques, specifically control charts in Gaussian affine term structure models (ATSM). In recent years SPC methods have been widely popular not only in industrial applications but also in several non-industrial scientific areas such as in finance. Gaussian ATSMs under no-arbitrage conditions have been a very important research tool in the area of term structure of interest rates. Financial time series are usually subject to changes at unknown time points and the detection of these change points are of great importance.

In our work we propose several control chart procedures that develop the ATSMs from the change point perspective. First, we extent the class of term structure models estimated using the minimum chi square estimation (MCSE) method by constructing fixed-income government bond portfolios. The proposed bond portfolio strategies from the ATSM in most of the cases perform better than traditional bond portfolio strategies. Next, the control charts are applied for monitoring the optimal portfolio weights. Second, we construct control chart procedures for monitoring the parameters of an ATSM and examine their ability of detecting changes for various types of shifts in the yield curve. Also, we propose a technique for reestimating the target process of the control chart procedure in case of a detection of a change. The results show that there is no single chart that performs well in all types of shifts but a combination of control chart is needed. Third, we propose and construct control charts for monitoring shifts in the autoregressive and moving average matrix of a VARMA ATSM. The estimation procedure of the model is a two-step process where in the first step among standard estimation procedures we apply a minimum distance estimation method based on the impulse responses and define its advantages in the forecasting of the yield curve. In the second step, we estimate the market prices of risk given the estimates of the first step by minimizing the sum of squared fitting errors of bond yields.

ΠΕΡΙΛΗΨΗ

Ο σκοπός της παρούσας διατριβής είναι η εφαρμογή τεχνικών του Στατιστικού Ελέγχου Ποιότητας, συγκεκριμένα των διαγραμμάτων ελέγχου σε Gaussian affine term structure models (ATSM). Τα τελευταία χρόνια μεθοδολογίες του Στατιστικού Ελέγχου Ποιότητας δεν είναι μόνο δημοφιλής σε βιομηχανικές εφαρμογές αλλά και σε αρκετές μη- βιομηχανικές εφαρμογές όπως για παράδειγμα στα χρηματοοικονομικά. Τα Gaussian ATSMs χωρίς arbitrage είναι ένα πολύ σημαντικό εργαλείο στην κατηγορία των μοντέλων για τη σχέση επιτοκίων και αποδόσεων των κρατικών ομολόγων. Οι Χρηματοοικονομικές σειρές συχνά υπόκεινται σε αλλαγές σε άγνωστα χρονικά σημεία και ο εντοπισμός αυτών των σημείων είναι μεγάλης σημασίας.

Στην παρούσα εργασία μας προτείνουμε διάφορα διαγράμματα ελέγχου με τα οποία επεκτείνουμε τα ATSMs κάτω από την οπτική των σημείων αλλαγής. Κύριοι στόχοι της διατριβής είναι οι εξής: Πρώτον, να επεκτείνουμε την κατηγορία των ATSM τα οποία εκτιμώνται με τη μέθοδο ελαχίστων χ^2 (MCSE), κατασκευάζοντας χαρτοφυλάκια σταθερού εισοδήματος κρατικών ομολόγων. Οι προτεινόμενες στρατηγικές για χαρτοφυλάκια ομολόγων από το ATSM στις περισσότερες περιπτώσεις παρουσιάζουν καλύτερα αποτελέσματα από παραδοσιακές τεχνικές κατασκευής χαρτοφυλακίων ομολόγων. Στη συνέχεια τα διαγράμματα ελέγχου εφαρμόζονται για την παρακολούθηση των βέλτιστων βαρών του χαρτοφυλακίου. Δεύτερον, να κατασκευάσουμε διαγράμματα ελέγχου για την παρακολούθηση των παραμέτρων ενός ATSM και να εξετάσουμε την ικανότητά τους να εντοπίζουν τις αλλαγές για διαφόρους τύπους μετατοπίσεων στην καμπύλη των αποδόσεων των κρατικών ομολόγων. Επιπλέον, προτείνουμε μια τεχνική για την επανεκτίμηση της διαδικασίας στόχου για τα διαγράμματα ελέγχου σε περίπτωση που το διάγραμμα εντοπίσει ένα σημείο αλλαγής. Τα αποτελέσματα δείχνουν ότι δεν υπάρχει ένα διάγραμμα ελέγχου που να αποδίδει καλά σε όλους τους τύπους των μετατοπίσεων αλλά ένας συνδυασμός από διαγράμματα ελέγχου είναι απαραίτητος. Τρίτον, να προτείνουμε και κατασκευάσουμε διαγράμματα ελέγχου για την παρακολούθηση αλλαγών σε ένα διανυσματικό αυτοπαλινδρομούμενο μοντέλο κινούμενου μέσου (VARMA) ATSM. Η εκτίμηση του μοντέλου είναι μια διαδικασία με δυο βήματα όπου στο πρώτο βήμα εφαρμόζουμε εκτός από συνηθισμένες μεθόδους στη βιβλιογραφία και

μια μέθοδο εκτίμησης ελάχιστής απόστασης βασισμένη στις αιφνίδιες αντιδράσεις (impulse responses) και αναφέρουμε τα πλεονεκτήματα της στην πρόγνωση της καμπύλης αποδόσεων των ομολόγων. Το δεύτερο βήμα περιλαμβάνει την εκτίμηση των market price of risk ελαχιστοποιώντας το άθροισμα των τετραγώνων των σφαλμάτων των αποδόσεων των ομολόγων.

Acknowledgements

Contents

List of Figures

List of Tables

Chapter 1

Introduction

1.1 Gaussian affine term structure models

Gaussian affine term structure models (ATSMs) have been a very popular research tool in the area of term structure of interest rates mainly due to the fact that provide closed-form solutions for bond pricing under no arbitrage conditions. The class of ATSMs developed by Vasicek (1977), Duffie and Kan (1996), Dai and Singleton (2000) have been used among others for measuring risk premia (see e.g Duffee (2002), Cochrane and M. Piazzesi (2009)), characterize the monetary policy rule (Wu and Rudebusch (2004),) exploring the effect of macroeconomic developments on the term structure (Ang and Piazzesi (2003), Bauer (2009)) and to infer market expectations of inflation from the spread between nominal and inflation-indexed Treasury yields (Christensen et al. (2010)). Ang and Piazzesi (2003) first mentioned the importance of including macroeconomic factors in the model in order to explain the yield curve dynamics and improve its forecasting ability.

The fundamental works of Vasicek (1977) and Cox et al. (2005) referred to one-factor state variable models. However, this single-factor specification is not sufficient to describe the dynamics of the yield curve. This drawback led to the introduction of multifactor ATSMs. The inclusion of macroeconomic factors in the model improves the fit of the model estimates and can explain a substantial amount of variation in the future bond yields. Another drawback of one-factor affine models is the implication that interest rates with different maturities are perfectly correlated. One-factor affine models, such as the Vasicek model, do not have a large range of shapes and will provide a poor fit to some initial yield curves. Multifactor ATSMs, which are the

focus of our work, generalized these models and improve the goodness of fit and the forecasting performance by including macro factors as state variables.

The yield curve has been found to be a good predictor of future real activity and inflation (Harvey (1988), Mishkin (1990) and Estrella and Hardouvelis (1991)). Since the work of Harvey (1988) the slope of the yield curve, defined as the difference between long-term and short-term interest rates, has been documented as an indicator for future economic activity. The behavior of the yield curve variates across the business cycles. For example, during recessions, long-term bond yields tend to be high in contrast with yields on short-term bonds which tend to be low. As a result in recessions we have upward sloping yield curve activity (Ang et al. (2006)). Estrella and Hardouvelis (1991) and Estrella and Mishkin (1996) focused on the US yield curve as a predictor of real economic activity and recessions. Estrella and Trubin (2006) provided evidence that the yield curve slope can be used in forecasting recessions in real-time. We remind that an inverted yield curve is being thought of as a precursor of a recession. Macroeconomic and financial time series are subject to various structural breaks and ignoring them may lead to estimation problems and this has a significant impact in the out-of-sample forecasts. As a result the detection of change points is of great importance for the description of the dynamic term structure models (see e.g Hamilton (1988), Bansal and Zhou (2002), Dai et al. (2007)). Regime shifts in yield curve could be due to several reasons such as business cycles (Bansal and Zhou (2002)), changes in monetary policy (Ang et al. (2011)), inflation (Ang et al. (2008)) and the risk premium (Dai et al. (2007)).

1.2 Sequential process monitoring

In recent years statistical process monitoring (SPM) techniques, specially control charts, have been applied to non-industrial fields such as the surveillance of optimal portfolio weights. A control chart should provide to the investor a signal that there is a possibly change in the process of portfolio weights (Golosnoy and Schmid (2007)). The control chart procedure is consisted of the control statistic and a rejection area (Montgomery (2013)). If the value of the control statistic lies in the rejection area then the control chart gives a signal that the monitoring process is out-of-control. A control chart statistic is computed from the quality characteristics that we observe and is plotted against an upper control limit (UCL) and a lower control limit (LCL). If the value of the control chart statistic exceeds the specified control limits then a signal is given that the process has been changed. A basic component of a control chart procedure is the average run length (ARL), which is the average number of

subgroups before a signal from the control chart is given in order to indicate that the process is out-of-control. Suppose that Z_t is the control chart statistic and c a control limit that determines the rejection area of the process. The run length which is the number of samples before a signal is given, is

$$N = \inf\{t \in \mathbb{N} : Z_t > c\} \tag{1.2.1}$$

and the ARL is equal to $E(N)$. In the in-control state the ARL (ARL_0) should be large and in the out-of-control-state (ARL_1) it has to be small. Alternatively someone can use the median run length (MRL), the median number of sample points before the first out-of-control signal is detected. Since the development of control charts by Shewhart in 1924 (Montgomery (2013)), various charts and procedures are being proposed and used in order to monitor processes. Roberts (1959) introduced the exponentially weighted moving average (EWMA) control chart. Multivariate process control techniques were introduced by Hotelling (1947). For more details about multivariate Exponentially Weighted Moving Average (MEWMA) see e.g. Lowry et al. (1992).

1.3 Thesis overview and our contribution

The research we present in this dissertation deal with monitoring and detecting structural changes in multivariate Gaussian ATSMs using SPM techniques, specifically control charts. In Chapter 2 we present an overview of the applications of control chart procedures in finance. In Chapter 3 we monitor the parameters of an ATSM via control charts and we propose a technique for the reestimation of the monitoring procedure when a change point is detected. Next, in Chapter 4 first we extent the class of ATSMs estimated with the the MCSE approach introduced by Hamilton and Wu (2012) in the construction of fixed-income portfolios consisted of government bonds. Second, we construct appropriate control charts for monitoring the optimal portfolio weights. Finally, in Chapter 5 we refer to Vector autoregressive moving average (VARMA) affine models for the term structure and monitoring the autoregressive and moving average parameter of the state factor evolution process. Also, we propose an estimation approach based on impulse responses previously applied on Dynamic stochastic general equilibrium (DSGE) models in order to improve forecasts for medium and long end yields. Conclusions and suggestions for future research can be found in Chapter 6.

Chapter 2

Control charts in financial applications: An overview

2.1 Introduction

Statistical process control (SPC) has been used for many decades to monitor one or several quality characteristics of a process simultaneously (Montgomery (2013)). Control charts are one of the major tools of SPC. The main goal of a control chart is to monitor the underlying process, based on information observed from individual items or subgroups of items. The use of a control chart helps not only to monitor a process but also to improve its performance. The monitoring of several quality characteristics of a process simultaneously is called multivariate statistical process control (MSPC) or in case of one quality characteristic we have univariate SPC (Woodall and Montgomery (2014), Montgomery (2013)). Bersimis et al. (2007) presented the basic procedures that use control charts for the implementation of MSPC.

A control chart statistic is computed from the quality characteristics that we observe and plotted against an upper control limit (UCL) and a lower control limit (LCL). If the control chart statistic exceeds the specified control limits then a signal is given that the process has been changed. Statistical processes are usually implemented in the following two phases: 1) Phase I, where control charts are used for retrospectively testing whether the process was in control when the first samples were being drawn. This phase includes the determination of the process being statistically in control. Also, the historical data of Phase I is used for estimating the parameters of the monitoring process. 2) Phase II, where control charts are used for monitoring the

new observations of the process for any change from the in-control state (see e.g. Bersimis et al. (2007), Woodall (2000)). In financial applications in contrast to industrial applications the distinction between Phase I and Phase II control charts is difficult (Golosnoy et al. (2007)).

A basic component of a control chart procedure is the ARL, which is the average number of subgroups before a signal from the control chart is given in order to indicate that the process is out-of-control. The ARL is often used to compare the performance between control charts. Suppose that Z_t is the control chart statistic and h a control limit that determines the rejection area of the process. The run length which is the number of observations before a signal is given, is denoted by:

$$N = \inf\{t \in \mathbb{N} : Z_t > h\}, \tag{2.1.1}$$

and the ARL is equal to $E(N)$. In the in-control state the ARL (ARL_0) should be large but in the out-of-control-state it has to be small. Alternatively someone can use the MRL, the median number of sample points before the first out-of-control signal is detected. Since the development of control charts by Shewhart (1931), various charts and procedures are being proposed and used in order to monitor processes. We remind that in the Shewhart procedure only the last observation is taken into consideration. Multivariate process control techniques were introduced by Hotelling (1947). Roberts (1959) introduced the EWMA control chart. The EWMA control chart is a good alternative to the Shewhart control chart when we are interested in detecting small shifts, because these control charts are very effective against small process shifts (Montgomery (2013)). The control statistic in the univariate case is based on exponentially weighted moving average defined as:

$$Z_t = (1 - \lambda)Z_{t-1} + \lambda X_t, \tag{2.1.2}$$

where $t = 1, 2, \ldots$, $0 < \lambda \leq 1$ is a smoothing constant parameter and Z_0 is the target value with $Z_0 = E_0(X_t)$. The notation E_0 denotes the mean calculated when the process is in-control. The control chart gives a signal at time $t \geq 1$ if $Z_t \geq h$. The constant $h > 0$ is chosen such as ARL_0 to be equal to a certain value. Large values of the smoothing parameter λ give more weight to recent observations and small values give more weight to past observations. If $\lambda = 1$ then the EWMA chart reduces to the Shewhart chart.

Lowry et al. (1992) generalized the univariate EWMA control chart procedure to the multivariate case. MEWMA control charts are constructed by applying a multivariate EWMA recursion directly to the components of the monitoring characteristic X_t.

The advantage of this approach is that each characteristic element obtains its own smoothing factor and as a result allows more flexibility compared to the univariate EWMA (Golosnoy and Schmid (2007)). The MEWMA statistic is given by:

$$\mathbf{Z}_t = (\mathbf{I} - \mathbf{R})\mathbf{Z}_{t-1} + \mathbf{R}\mathbf{X}_t, \tag{2.1.3}$$

where $\mathbf{Z_0} = E_0(\mathbf{X_t})$, $\mathbf{I}$ is the $(k-1) \times (k-1)$ identity matrix and $\mathbf{R} = diag(r_1, \ldots, r_{k-1})$ is a diagonal matrix with elements $0 < r_i \leq 1$ for $i \in \{1, ..., k-1\}$. A signal is given if:

$$\mathbf{Z}_t^{'} \cdot Cov_0(\mathbf{Z}_t)^{-1} \cdot \mathbf{Z}_t > h, \tag{2.1.4}$$

where the control limit $h > 0$ is chosen so as to achieve a specified ARL_0 and Cov_0 is the covariance matrix when the process is in-control. The EWMA is used extensively in time series modeling and forecasting and since it can be viewed as a weighted average of all past and current observations, it is very insensitive to the normality assumption.

The CUSUM chart was proposed by Page (1954) for monitoring small shifts. The CUSUM control chart is used to monitor a process based on samples taken from the process at given time periods. The measurements of the samples at given times constitute a subgroup. The CUSUM chart shows the accumulated information of current and previous samples. CUSUM control charts are a good alternative when small shifts are important (Montgomery (2013)). CUSUM control charts can be constructed for individual observations or for groups of observations. Suppose μ_0 is the target of the process when the process is in-control for the quality characteristic X. The statistics C^+ and C^- are the one sided upper and lower cusum limit respectively. Defined by the iterative scheme:

$$C_t^+ = \max[0, C_{t-1}^+ + X_t - \mu_0 - k]$$

$$C_i^- = \max[0, C_{t-1}^+ + \mu_0 - k - X_t],$$

where k is the reference value or else the control chart constant parameter. A signal from the CUSUM scheme is given for upward shift if $C_t^+ > h$ and for downward shifts if $C_t^- < h$. The multivariate cumulative sum control chart (MCUSUM) is an extension of the univariate CUSUM control chart analysis. It is a procedure that uses the cumulative sum of deviations of each random vector previously observed compared to the nominal value to monitor the vector of means of a multivariate

process (Cunha et al. (2013)). This chart was proposed by Crosier (1988). The scalar quantities of the univariate case are now replaced by vectors:

$$C_t = \sqrt{(\mathbf{S}_t + \mathbf{X}_t - \mu_0)' \mathbf{\Sigma}^{-1} (\mathbf{S}_t + \mathbf{X}_t - \mu_0)}, \tag{2.1.5}$$

where $\mathbf{\Sigma}$ is the variance matrix of the data and $\mathbf{S}_i$ are the cumulative sums defined as:

$$\mathbf{S}_i = \begin{cases} 0, & \text{if} \quad C_t \leq \kappa \\ (\mathbf{S}_{t-1} + \mathbf{X}_t - \mu_0)(1 - \frac{k}{C_t}), & \text{if} \quad C_t > \kappa, \end{cases}$$

where the reference value $\kappa > 0$ is related to the magnitude of change and $S_0 = 0$. An out of control signal is given if $\mathbf{Z}_t > h$, with h being the control limit, $\mathbf{Z}_t = (\mathbf{S}_t' \mathbf{\Sigma}^{-1} \mathbf{S}_t)$. An alternative way to construct a vector accumulating multivariate CUSUM is given by Pignatiello and Runger (1990) . The CUSUM and EWMA are control charts with memory which means that a parameter controls the impact of the past values. For more details about MEWMA and MCUSUM control charts see for example Lowry et al. (1992) and Ncube and Woodall (1985) respectively.

SPC tools are used in various industrial and non-industrial areas such as medicine, environment, chemical analysis, healthcare and public-health surveillance (Tsui et al. (2008), Frisén (2011)), network monitoring and change-point problems. For a review in non-industrial application of MSPC see Bersimis et al. (2018). In recent years SPC methods have also gained popularity in many financial applications such as stock trading and portfolio monitoring (Frisén (2008), Golosnoy et al. (2010)). Jumah et al. (2012), among other quality control techniques referred to SPC methods in the improvement of trading, banking and service sectors. Bock et al. (2007) provided a comparison of surveillance methods and decision rules for finance. Various other applications of control charts include for example that of Schmid and Tzotchev (2004) that applied multivariate EWMA control charts in order to detect a change in the parameters of the Cox–Ingersoll–Ross (CIR) model for the evolution of interest rates. Yousefi et al. (2019) implemented control chart techniques on non-normal and autocorrelated data for monitoring the performance of a project. Berlemann et al. (2012) applied EWMA and CUSUM charts for the detection of U.S. house price bubbles and especially the estimation of their likely starting points. Freese (2015) is focused on the detection of U.S. regional bubbles having data from different markets. Rębisz (2015) applied control charts for country risk monitoring for various countries using the credit ratings. Golosnoy and Roestel (2019) used CUSUM control charts for real time monitoring of shifts in inflation expectations and specially to forward break-even inflation (FBI) series.

In financial applications the underlying data are in most cases no longer independent and as a result control charts for dependent data have to be considered. Knoth and Schmid (2004) presented a review for control charts in time series generally. Therein, the case of dependent data is taken into consideration and the new control chart schemes that are presented are based on the time series structure, specially for autoregressive (AR) and autoregressive moving average processes (ARMA). Control charts for dependent data are usually residual-based or modified control charts. Residual-based charts are constructed from a transformation of the original data so that the resulting data are independent and standard control charts can now be applied (see e.g. Alwan and Roberts (1988), Harris and Ross (1991), Pan and Jarrett (2007)). Modified control charts use standard control chart procedures but the control limits are adjusted in order to account for the autocorrelation (see e.g. Vasilopoulos and Stamboulis (1978), Schmid (1995)). Another category of control charts, in order to overcome the problem of dependent data, is based on the difference between two subsequent values of the measured characteristic and it is known as difference control charts (see Golosnoy and Schmid (2007)).

Okhrin and Schmid (2007) presented a review of the methods used for monitoring univariate and multivariate linear time series. They discussed various modified and residual control charts with focus on the monitoring of the variance of financial series. Okhrin and Schmid (2007) reviewed EWMA and CUSUM control charts for the surveillance of univariate and multivariate generalized autoregressive conditional heteroskedasticity (GARCH) processes. The authors considered a local measure of the variance based on the squared observations, the forecasts of the conditional variance and on the residuals. In a comparison study when the performance measure is the ARL both the EWMA and the CUSUM type charts based on the conditional volatility performed better. In contrast, in terms of maximum average delay the residual charts are preferred. Garthoff et al. (2014) introduced control charts for simultaneous monitoring of the mean and the variance of multivariate nonlinear time series. Owlia et al. (2017) applied residual Shewhart control charts to monitor time dependent GARCH financial processes in the presence of outliers in the data. The existence of outliers in the sample data can cause problems in the design of the control charts. A thorough discussion of control charts for dependent data in finance is given in the book of Frisén (2008).

The aim of this work is to present the basic economic and financial application fields of statistical process monitoring from the perspective of control charts with focus on portfolio monitoring and stock markets. The application of control chart schemes in finance can be seen as a three-step procedure. In the first step the main purpose

is the definition or the construction of the monitoring process. The second step refers to the choice of the appropriate control chart and depends on the data of the monitoring process. Finally, the third step is related with the interpretation of the signals obtained from the control charts. The challenge in this step is the economic interpretation of these signals specially in monitoring of optimal portfolio weights as we will see later. The transfer of sequential monitoring methods such as control charts from industrial applications to finance it is not always obvious and many difficulties arise. For example in some applications of SPC in industry when the first false alarm signal appears, it is possible that the whole process is stopped. In applications such as portfolio monitoring as we will see later the process can not be stopped or the reasons of the change to be eliminated (Golosnoy et al. (2011)). Another issue is the structure of the monitoring process which in most financial cases is more complicated than in the industrial applications.

The research papers reviewed in our work are presented thematically according to their application area in finance. Specifically, in Section 2 we review some specific applications of control charts in stock markets and stock trading. Section 3 is devoted to applications of SPC in portfolio monitoring with focus in multivariate control charts. In conclusion, we point out some issues for further research.

2.2 Control Charts and Stock Markets

Control charts have been applied in recent years in the decision process for stock trading and investigate the behaviour of stock markets. In this section, we review several research papers with focus firstly on applications of control charts in the filter trading rule and later on applications of Shewhart and other procedures generally in stock markets.

2.2.1 Filter trading rule and control charts

The use of SPC methods for the study of changes in stock market price levels was first proposed by Roberts (1959). Next, Hubbard (1967) constructed control charts so as to to determine the stock price trend and compare it with the gross national product (GNP) and personal income trends. Also, Hubbard (1967) sets up decision rules for buying or holding stocks. The data used are logarithmic monthly values of Moody's Composite 200 Stock Average from 1950 to 1967.

Alexander (1961) and Alexander (1964) introduced filter trading rules followed by the work of Fama and Blume (1966). The filter trading rule is a mechanical trading

rule, defined as a sequence of signals for buying and selling stocks. Briefly, the buy signal is given if for example the daily closing price of an observed stock moves up at least a certain percent x from a subsequent low. The investor sells the stock when a signal is given,i.e., when the closing prices drops at least a certain percent y from a subsequent high. The values x and y are the filter sizes for the trading rule and represent the minimum acceptable percentage change of the stock value for the investor.

Lam and Yam (1997) motivated by the filter trading rule used CUSUM techniques to create a trading strategy in the stock market equivalent to the filter trading rule. Starting from a sell signal at time $t = 0$ the filter trading rule is to generate a buy signal at day n if $\frac{r_t}{\min p_i} \geq x$, $i = 1, \ldots, n$, where x is the filter size of the trading rule and p_t the closing stock price. The CUSUM procedure for the filter trading rule has as reference value $k = 0$, the control limit is $h = \log(1 + x)$ and has the following form:

$$S_n = \sum_{i=1}^{n} y_i = q_n - q_0, \tag{2.2.1}$$

with the difference of the current stock log price from a historical low $S_n^{'}$ defined recursively as:

$$\begin{cases} S_0^{'} = 0 \\ S_n^{'} = \max(S_{n-1}^{'} + y_n,\ 0), \end{cases}$$

where $q_t = \log(p_t)$ is the logarithm of the closing stock prices p_t and $y_t = q_t - q_{t-1},\ t = 1, 2, \ldots$ is the continuously compounded daily return from a stock investment. A signal is given if $S_n^{'} > h$. The filter size of the trading rule is $x = e^h - 1$. Lam and Yam (1997) generalized the classical filter trading rule by setting the reference value $k \neq 0$. First they consider the general CUSUM procedure with $k > 0$ and $h = 0$ which means that such a general filter trading rule will give a buy signal to the investor when the one-day return exceeds k. This happens when:

$$\frac{p_t - p_{t-1}}{p_{t-1}} > e^{-k} - 1, \tag{2.2.2}$$

and the opposite when this general filter trading rule generates a sell signal to the investor. This procedure can be an investment strategy if we believe that a rising trend in the stock market starts with a large single day rise and a downward trend that usually starts with a large drop in a single day. However, Lam and Yam (1997) mentioned that a main drawback of this general filter trading rule (with $h = 0,\ k > 0$) is the absence of a stop-loss mechanism.

Yi et al. (2006) applied CUSUM techniques in predicting regime shifts in stock market indices but in contrast with Lam and Yam (1997) , they take into account transaction fees. The same CUSUM technique is used in 30 different stock markets and its performance is compared. Suppose that x_i is the daily index of a certain stock market and r the logarithmic return with $r_i = \log(\frac{x_i}{x_{i-1}})$. Define $y_i = r_i - k$, where k is the reference value in the CUSUM procedure, then an upward or downward shift is detected by the following rule:

$$C_i \geq h, \text{ upward shift} \quad \text{and} \quad C_i^{'} \leq -h, \text{ downward shift},$$

where h is the threshold value of the CUSUM procedure and $C_i = \max(C_{i-1} + y_i, 0)$, $C_i^{'} = \max(C_{i-1}^{'} + y_i, 0)$, $i = 1, \cdots, n$. The starting values are $C_0 = 0$ and $C_0^{'} = 0$. The result of different values for the parameters k, h is different trading cycles and CUSUM performances. We mention that the performance of each trading cycle is measured using the total profit (TP) or the daily profit (DP). The total profit (TP) and daily profit (DP) of the CUSUM procedure that contains n trading cycles, the time between a buy and a sell signal, for the case of not taking into account transaction fees are given by:

$$TP = \frac{SP_1}{BP_1} \cdot \frac{SP_2}{BP_2} \cdots \cdot \frac{SP_n}{BP_n}, \; DP = \frac{TP - 1}{D_1 + D_2 + \cdots + D_n},$$

with SP the selling price and BP the buying price. After taking the transaction fees into consideration, the total profit and the daily profit of the CUSUM procedure are:

$$TP^{'} = \frac{SP_1}{BP_1} \cdot \frac{SP_2}{BP_2} \cdot \cdots \cdot \frac{SP_n}{BP_n} \cdot (1 - \alpha)^{2n}, \; DP^{'} = \frac{TP^{'} - 1}{D_1 + D_2 + \cdots + D_n},$$

where $0 < \alpha < 1$, $TP^{'} < TP$, $DP^{'} < DP$, α is the proportion of the total trading amount charged as the trading fee for each stock buying or selling and D_i, $i = 1, 2, \ldots, n$, are the days in which the stock is held in the ith trading cycle. The result of taking transaction fees into consideration is the deterioration of the performance of the CUSUM procedures. Yi et al. (2006) concluded that if transaction fees are included they find no acceptable values of k and h. In this situation the performance of the CUSUM procedure is not so good as when the transaction fees are very small or excluded.

Žmuk (2016) in the spirit of the work of Alexander (1961) and Alexander (1964) applied residual-based control charts to improve the decision-making process in short- and long-run stock trading. The empirical application included open and average prices of CROBEX10 index stocks on the Zagreb Stock Exchange and three types of

control charts: individual units (I-chart), EWMA and CUSUM. The possible presence of autocorrelation in open and average stock prices is dealt with the Autoregressive Integrated Moving Average (ARIMA) models. Like Lam and Yam (1997) no transaction fees are taken into consideration but also the simulation of the stock trading scenarios excluded the existence of outliers. In the long-term trading analysis based on opening prices the stocks showed a higher variability level than in the short term. The use of the residual-based CUSUM control charts resulted in the highest investor trading score in most of the cases. The results of using average prices are almost similar to that of opening prices. Generally, higher profits for the investor are achieved with the use of opening prices than average prices in the short-run analysis. Additionally, the total portfolio profit in the short-run was achieved by using the residual-based CUSUM control chart in all possible stock trading cases. In the long-run, the residual-based CUSUM control chart achieved the highest portfolio profit except for the case with the average trading stock prices and the use of 2-sigma control limits. In the short run stock trading based on average prices and using different control limit levels outperformed overall portfolio profits and individually profits based on that from opening prices. In the long run, stock trading based on opening prices outperformed the trading based on average prices.

Xin et al. (2013) used CUSUM control charts under the spectrum of filter trading rule in a two-regime Markov switching model (MSM) for the returns of the underlying security. The parameters of the control scheme are the decision interval h and the reference value k, which are the filter size and the filter trading rule respectively. The two-regime model has the regime I and regime II in which the security returns follow different distributions. Under the two-regime model, the market transits between bear and bull state. Generally, the transition probability matrix of a hidden Markov chain for two regimes has the following form:

$$M = \begin{pmatrix} p_{11} & p_{12} \\ p_{21} & p_{22} \end{pmatrix}.$$

This transition probability matrix has the constraints that the four probabilities should be all nonzero and it is invertible. The reference value is set equal to zero which means that the filter trading rule monitors whether the stock return series belongs to a bull or bear market. The four states of the proposed system are: long position under a bull market, long position under a bear market, short position under a bull market and short position under a bear market. An extension of this scheme included the values of the filter trading rule S_t^+, S_t^- which are the up-sided and down-sided CUSUM statistics respectively with stating values equal to zero. At the empirical application, the performance of the filter trading rule under the filter size

that gives the largest expected unit time profit, is profitable. Also in many cases the annualized log-returns of filter trading rule outperforms the log-returns of the buy-and-hold strategy.

Cooper and Van Vliet (2012) dealt with high frequency trading (HFT) data and developed statistical techniques and tests alternative to traditional SPC that examine each trading event using the generalized lambda distribution (GLD). The need for their proposed control schemes is due to the fact that in high frequency trading systems large amount of trades per minute or per second are executed, something that makes difficult their real-time control. Also, traditional SPC methods usually assume normality in contrast with HFT systems that produce skewed outputs with long tails which supports the selection of the generalized lambda distribution. The suggested statistical tests applied on the distribution of sample means and ranges like in traditional SPC and the distribution of the actual trading profits using the GLD. The distribution of the actual trading profits is called whole distribution of the SPC. The monitored procedure with the whole distribution SPC and the generalized lambda distribution refers to the actual data and each observation is tested rather than each sample mean or range, like in traditional SPC. Every observation now is compared to the presumed underlying distribution. As a result the whole distribution SPC method does not rely on the central limit theorem in order to generate the required statistics. The comparison analysis between traditional SPC and the whole distribution SPC is done through a simulation study. The results, according to Cooper and Van Vliet (2012) , showed that the whole distribution SPC reacts quicker than traditional SPC to changes even if new single events differ from the reference distribution. However, there is a trade-off between the number of observations used in the tests and their sensitivity. A small number of observations can give more quickly the change detection in contrast with a large number which can lead to false signals.

Kumiega et al. (2014) following the work of Cooper and Van Vliet (2012) used the generalized lambda distribution and SPC methods in high frequency trading so as to assess the performance of the investments. A basic issue in high-frequency trading is if a trading system will generate sufficient profits so as to cover its costs. The traditional financial tools appear to have problems to correctly quantify the ability of an HFT system for algorithmic trading firms (ATFs) to cover that costs. The traditional risk measures compared with SPC methods are the Sharpe, Information and Sortino ratios. Drawbacks for their use in assessing the performance of the system is for example that they ignore costs such as research and development (R&D) and operating expenses or fail to capture a series of operations of a ATF such as

capital reallocation to other trading systems. The authors examined the performance of in-control HFT systems so as to meet ATF specifications for profitability. After the definition of investor's trading strategy and the lower limit of capability of the system, a backtesting was performed and the capability of the system to meet returns on investment (ROI) requirements it was verified. We remind that the capability of a process measures the ability to satisfy some specifications. The simulation example and the use of X-bar chart for sample mean returns and an R chart of simulated HFT returns identify that the process is in-control. The capability study is necessary so as ATFs know if an HFT system will cover its own R&D costs. The capability of the trading system is measured with the quantity C_{pl} defined as:

$$C_{pl} = \frac{\mu_n - LSL}{3\sigma_n},$$

where μ_n is the mean of all the samples, σ_n is the standard deviation of the sample means and LSL is the lower specification limit of the costs that a capable firm must satisfy. Lower values of C_{pl} of a system may require the firm to reduce costs or reduce variation through trading process improvement.

Cooper et al. (2015) extended the work of Kumiega et al. (2014) and developed a new robust performance measurement methodology for algorithmic trading without any assumption for normality. Except for taking into account that returns may not necessarily follow the normal distribution they introduced the concept of multi-scale capability of the system. The notion of multi-scale capability refers to the fact that different time scales may be applied to the operation of the algorithm, the capital allocation decision to the trading strategy and the funding decisions of investors and there is a need for a framework for unifying measurement of capability. The authors defined a set of conditions for the definition of which trading strategy is consider to be good for the investor and a methodology for ranking trading strategies according to a term structure of capability. The applied trading strategy at each time must generate a stable distribution of returns and HFT operate when the distribution of returns are in-control. An important part of the methodology is the definition of the expected loss when a left tail event happens when the process is in-control and the trading strategy needs to be changed. The purpose of the firm is not only to achieve profits in the long run but to perform in an acceptable level in the short run so as to cover its costs. The authors provided a framework for the relationship between the performance of the system in the short run and the distribution in the long run. The process in order to be capable uses a generalization of the C_{pl} value that must

satisfy the following condition:

$$GC_{pl}(n) = \frac{\mu_n - c}{\mu_n - Q(a)_n} > 1, \tag{2.2.3}$$

where c is the allocated fixed and variable costs so as to research, build and operate the trading system, the distance from the mean to the proxy for the left tail endpoint $3\sigma_n$ is replaced by the non-normal $\mu_n - Q(a)_n$ for some level a. The mean μ_n follows the generalized lambda distribution and $Q(.)$ is the percentile function of the generalized lambda distribution. The acceptable value of n in order $GC_{pl}(n) > 1$ is the time for which the trading strategy is profitable and may vary across firms. Also the level of the percentile α is the risk tolerance of the trading firm. Low values mean that c is believed to be exceeded and high values mean that the desired profitability is not believed to be achieved. Generally, the values of n that equation (2.2.3) is valid are related with the financing decision that the firm face. Possible serial correlation in the time series of returns is dealt with using differences in an EWMA recursion of returns and the new control limits can be computed using the moving range (MR) method.

Dumičić and Žmuk (2015) mentioned in their work difficulties for using statistical control charts for making decisions about trading on the stock market on short term period. They applied univariate control schemes in opening and average prices of stocks from the CROBEX10 market index from the Zagreb Stock Exchange. No additional payments (such as dividends) for the investors are taken into consideration. The control schemes are the individual (I), the EWMA and CUSUM control charts. For the case of taking open stock prices they find for the various control schemes too many observations out of the control limits. An observation out-of-control will give a signal to the investor to perform a trading action. The authors indicate that many of these signal are probably false alarms. The same problem, many out-of-control limits observations, appears and in the case of using average stock prices making the use of control charts in portfolio analysis, according to the authors dubious. Possible explanations for this problem, according to Dumičić and Žmuk (2015), may be the fact that stock prices show non-normal distribution and exhibit autocorrealtion. More appropriate control chart procedures could be a solution to this problem. In recent year many procedures have been developed for non-normal and autocorrelated data.

An interest application of control charts is on the algorithm-controlled finance (ACF) trading machines. ACF trading machines consist not only of the interacting trade selection algorithms for taking positions in the financial markets but also with the

technology required to automate some or all of the processes required for trade selection and execution (Hassan et al. (2010)). Hassan et al. (2010) mentioned the problems of traditional risk measurement techniques and the need for SPC methods such as control charts in order to describe, monitoring and improve the performance of ACF systems. Between industrial systems and ACF systems there are some basic differences. In ACF systems risk managers can inspect the entire set of data, input and output, and more importantly in finance systems the process is assumed to be normal in contrast to industrial that normality is achieved through sampling methodology. Also in finance the process it can not be stopped in case of out-of-control situations but it can continue only to close existing open trading positions. The authors among others apply X-bar and R charts so as to monitor the performance in a trading machine. They use an X-bar on the returns and define appropriate criteria for the out-of-control situation. The stochastic variables of a trading machine are the mean and the variation of the inputs and outputs. It is obvious that any change to the algorithm of the trading machine applied in order to bring the machine into the in-control condition should lead to rebacktesting of the system and define the new benchmark values. Hassan et al. (2010) compared the results from classical risk control measures with these of SPC such as the control charts we previously mentioned. For the statistical arbitrage pairs trading investment example traditional risk measures such as average annual return, volatility and Sharpe ratio for the in-sample period indicate that this trading machine could be acceptable for an investor. However, quality techniques applied on the outputs (specifically the returns), such as an X-bar chart, do not support this result and give signals where the trading algorithm is out-of-control. Additionally, out-of-sample results show that the ACF system performed poorly in term of returns and more volatile in contrast with the in-sample backtesting of the system. The signals of the SPC tools helped the immediate correction and improvement of the trading system. Also, the authors dealt with serial correlation, a common problem in financial data and mention as a possible drawback of the SPC methods the sensitivity due to noisy financial data which led to false alarms. They removed the serial correlation from the return distribution applying EWMA techniques and re-performed the SPC methods. The purpose of designing an ACF trading system is the absence of autocorrelation and the repeatability in the results. The examined system generated a white noise and after testing on the error terms the monitoring results were found the same with the serially correlated data.

Bilson et al. (2010) examined the use of SPC methods in trading systems. They apply X-bar and R charts on the returns of two applications of trading systems, the first in a Long-Short pairs trading strategy using statistical arbitrage and the second in a foreign currency trading strategy. Their results are compared with those

of traditional quantitative risk management methods trying to find differences in the decisions an investor makes based on these approaches. Another task is if the proposed SPC methods predict better the poor performance of the system and reduce the potential losses of the investor. The results are in accordance with that of Hassan et al. (2010) and SPC methods generate signals contrary to the signals generated by the traditional risk measures. Both applications referred to risk due to unknown probability distributions of the outputs. The first application referred to the risk of creating a finance trading model that over-fits the data and the results measured with traditional methods show that came from a known probability distribution. The second application is the risk of running a trading model after the model faces uncertainty and stops working according to to a market structure shift. SPC methods identified the change in the outputs of the trading model in contrast with the results using backtesting and traditional risk measures that the trading system produced acceptable returns.

2.2.2 Shewhart procedures and volatility in stock market returns

Govindaraju and Godfrey (2011) explored the volatility of a stock market using Shewhart procedures. Following Shewhart (1931) they broke down volatility into common (C) causes and special (S) causes volatility. In financial applications it may be difficult the distinction between special and common causes. Common causes are responsible for the controlled variation while special causes for the uncontrolled variation. Short term variability mainly is due to common causes and usually can be estimated. In addition, long-term variability includes all the variation due to special causes. Govindaraju and Godfrey (2011) used rational subgrouping so as to check if a variation is common or special cause. The distribution function F of a variable of interest X can be written as a mixture of the distribution functions of X under common and special causes:

$$F(X) = (1-\alpha)F_C(X|\text{common causes}) + \alpha F_S(X|\text{special causes}), \tag{2.2.4}$$

where $F_C(.)$ and $F_S(.)$ are the distribution functions of X under common and special causes respectively. In case that the process is in-control then the mixing proportion α is zero. The sample standard deviation of the entire data $\{x_t\}$, $t = 1, \ldots, n$ contains both common and special causes standard deviations and is given by:

$$\hat{\sigma}_T = \sqrt{\frac{1}{n-1}\sum_{i=1}^{n}(x_i - \bar{x})^2}, \tag{2.2.5}$$

and suppose the sample standard deviation of the jth subgroup is given by:

$$\hat{\sigma}_j = \sqrt{(x_{2j} - \bar{x}_j)^2 + (x_{2j-1} - \bar{x}_j)^2}, \tag{2.2.6}$$

where $\bar{x}_j = \frac{1}{2}(x_{2j} + x_{2j-1})$ is the mean of the jth subgroup, $j = 1, \ldots, m$ and $m = \frac{n}{2}$, of the observations and adjusting for the bias using a correction factor c_4 we have:

$$\hat{\sigma}_C = \frac{1}{c_4 m} \sum_{j=1}^{m} \hat{\sigma}_j. \tag{2.2.7}$$

When the time-dependent effect of special causes is removed the estimated standard deviation is an estimate of the persistent volatility. The results of the empirical application show that much of the volatility in stock returns is due to common causes and can be considered as the permanent risk. Also the concept of common cause variability can be applied to the portfolio selection. The trade-off between risk and return in a portfolio will depend on the choice of total risk or special cause variation used. Long term investors are interested for special cause variation and analogously define their investment choices.

Premarathna et al. (2016) extended the work of Govindaraju and Godfrey (2011) and examined the risk/return and skewness/kurtosis trade-offs in a stock market using Shewhart methodology. The data are separated into rational subgroups and expected in each subgroup to be as homogeneous as possible. The subgroups are partitioned for common and special causes variation.

The decision rule for determining variation subject to special causes, is based on the trimmed mean of subgroup standard deviation:

$$\bar{S}_\alpha = \frac{1}{m - 2\alpha} \left\lceil \sum_{i=m\alpha+1}^{m-k\alpha} \bar{s}_i \right\rceil, \tag{2.2.8}$$

where α denotes the percentage of subgroup data that has to be trimmed, $\lceil . \rceil$ denotes the ceiling function and $\bar{s}_i$ is the ith subgroup corrected average standard deviation. When a rational subgroup has a within-subgroup standard deviation that exceeds a certain limit, then in that time period a special cause of variation affects the volatility in the process and this subgroup should be removed from the calculation of $\bar{S}_\alpha$. The control limit using the new $\bar{S}_\alpha$ is recalculated. This procedure is repeated until they get an upper control limit that is based solely on subgroups whose variation is based only on common cause variation. Premarathna et al. (2016) in order to ensure the termination of the decision process set that if the number of subgroups is below the

Poisson upper control limit then the subgroup removal process is stopped. From the empirical application they found negative mean/standard deviation trade-off in periods of special cause variation and positive trade-off in common cause periods. As a result the proposed method cleared up trade-offs that were not observed in the total periods of data. The negative trade-offs in the special cause periods are connected with increase in market volatility. The skewness/kurtosis trade-off is negative in both total and special cause periods and has not been observed before. Also the overall trade-off is mainly driven by events during the special cause periods.

2.2.3 Other financial applications

Severin and Schmid (1998) introduced and compared univariate modified and residual-based control schemes for monitoring GARGH processes applied to daily stock market returns. The modified control schemes are the modified Shewhart, EWMA and CUSUM chart. The results from the simulation and empirical study favor the use of modified EWMA chart. Severin and Schmid (1996) proposed control charts for GARCH processes in order to detect changes in the volatility of financial asset returns. They focused on modified Shewhart, EWMA, CUSUM and residual control charts. An important prerequisite for the application of these control schemes is the existence of second moments. For the modified Shewhart and EWMA chart various properties for the distribution of the run length are proved. These methods are compared in a simulation study with the target process to be an ARCH(1) process and an empirical study is made on stock market data.

Schipper and Schmid (2001) mentioned that in the presence of variance changes, the opinion that EWMA and CUSUM control charts are suitable to detect small shifts rather than large is not always true. Schipper and Schmid (2001) presented EWMA and CUSUM charts for detecting changes in the variance of a GARCH process and applied them to monitor stock market returns. Suppose that Y_t is the GARCH target process with mean μ_0 and variance γ_0 and X_t is the observed process of the data. The observed process in connection with the target process is modeled as follows:

$$X_t = \begin{cases} Y_t, & \text{for} \quad 1 \leq t < \tau \\ \mu_0 + \Delta(Y_t - \mu_0), & \text{for} \quad t \geq \tau, \end{cases}$$

with $\Delta \geq 1$ and $\tau \in \mathbb{N}$. The distribution of Y_t is assumed to be known. The exponential weighted moving average and the cumulative sum, for the construction of the EWMA and CUSUM chart respectively, are applied to the residuals of the process, the squared observations, the logarithm of the squared observations and the

conditional variance. Next we present the EWMA recursions for the four cases we mentioned previously:

$$\text{Residual Chart} : Z_t = (1-\lambda)Z_{t-1} + \lambda\frac{X_t^2}{\hat{\sigma}_t^2},$$

$$\text{Squared observations} : Z_t = (1-\lambda)Z_{t-1} + \lambda(X_t-\mu_0)^2,$$

$$\text{Logarithm of the Squared Observations} : Z_t = (1-\lambda)Z_{t-1} + \lambda \ln\frac{(X_t-\mu_0)^2}{\gamma_0},$$

$$\text{Conditional Variance} : Z_t = (1-\lambda)Z_{t-1} + \lambda\hat{\sigma}_{t+1}^2,$$

for $t \geq 1,\ \lambda \in (0,1],\ \sigma_t^2$ is the conditional variance and $Var(X_t) = \gamma_0$ for $t < \tau$. In a comparison simulation study of these control schemes with the cases of the target processes to be a GARCH(1,1), the EWMA control chart based on the conditional variance outperforms the other schemes and provides in almost all cases the minimal ARL_1. A suggested value for the smoothing parameter is $\lambda = 0.1$.

Śliwa and Schmid (2005) were the first that applied control chart procedures for monitoring multivariate nonlinear time series and cross-covariances in particular. The underlying target process is assumed to be a GARCH(1,1) process. Two different types of MEWMA and univariate EWMA control charts are proposed for the surveillance of the multivariate GARCH processes. The first type is based on the exponential smoothing of each component for various examples of local measures for the covariances of the observed and the residual process. In the second type the Mahalanobis distance between the local covariance measure and its in-control mean is calculated and then the univariate EWMA recursion is estimated. The proposed control schemes are applied to stock markets data.

Golosnoy et al. (2012) applied Shewahart and CUSUM control charts for monitoring the daily integrated volatility. The dynamics of daily integrated log-volatility are modeled through a linear state-space representation. This state-space representation links the observable volatility measure to the unobservable log-daily volatility. The daily integrated volatility σ_t^2 is not directly observable and the authors use three alternative estimators: the realized volatility RV_t measure, the bipower variations BV_t measure and the staggered bipower variations SBV_t. The proposed state-space representation for the log-volatility $\omega_t = \log(\sigma_t^2)$ is:

$$\omega_{t+1} - \mathrm{a} = \phi(\omega_t - \mathrm{a}) + \epsilon_{t+1}, \quad \epsilon_{t+1} \sim N(0,q) \tag{2.2.9}$$

$$s_t = \omega_t + \gamma_t, \quad \gamma_t \sim N(0,\upsilon_t), \tag{2.2.10}$$

where the measure s_t is $\log(RV_t)$, $\log(BV_t)$ or $\log(SBV_t)$, a is the unconditional expectation of the log integrated volatility, q is the innovations variance and $|\phi| < 1$. Additionally, the innovations ϵ_t, γ_t are assumed to be uncorrelated with each other and not autocorrelated. The volatility modeled with this state-space representation assumes that there is no jumps in the price equation of the underlying asset. Jumps and changes in the parameters may have as a result changes in the distribution of volatility forecasting errors. The authors mentioned the need for differentiation of this two sources of change. The validity of this state-space model and its ability to provide proper volatility forecasts is tested via statistical monitoring techniques.These techniques are applied on the standardized volatility forecasting errors:

$$S_\eta = \frac{\eta}{(p_{t|t-1} + \upsilon_t)^{\frac{1}{2}}},$$

where $\eta_t = s_t - s_{t|t-1}$ the forecasting errors and the conditional variance is $p_{t|t-1} = var(\omega_t - \omega_{t+1})$. The observable forecasting errors η_t follow a normal distribution with mean 0 and variance $p_{t|t-1}+\upsilon_t$. When the control chart on the forecasting errors or the standardized forecasting errors give a signal then the model described in the previous state-space representation does not provide proper volatility forecasts and action needs to be taken. In addition to the Shewhart chart, CUSUM-type control schemes are applied such as the CUSUM, the fluctuation sum and the recursive residual chart (for more see Andreou and Ghysels (2008) and Horváth et al. (2006)). The detecting ability of the proposed control schemes is examined through a simulation and an empirical study. In the simulation study also it is investigated the case of forecasting errors that do not follow normal distribution but t-distribution. The results in the simulation study showed that changes causing the largest average forecasting losses are detected with relative ease from all control charts. When detecting changes in the mean the CUSUM, the fluctuation sum and the recursive residual control schemes showed similar abilities and performed better than the Shewhart chart. The opposite happened when the authors detected increases in the variance q. The use of innovations that follow the t-distribution led to lower ARL_0. The empirical example consisted of daily data of four highly liquid stocks traded on the New York Stock Exchange (NYSE). The Shewhart charts based on all volatility measures provided similar number of signals for both in- and out-of-sample case. An interesting fact is that the majority of signals in the control charts occurred at the same days for all volatility measures. The authors mention that the signals could be categorized as isolated and clustered. The isolated signals can often be interpreted as outliers and clustered signals which are of the main interest indicate possibly problems with the model adequacy. The fact that obtained signals occur at different times from

detected jumps may be an indicator to possible structural changes in the volatility model. This application of control chart techniques needs to be expanded for more complicated volatility models and to be examined in the case of reestimation of the model when a signal is detected and how this affects the number and time of signals.

The use of classic control charts has as a prerequisite that the data are known exactly. Kaya et al. (2017) examined the case in monitoring the volatility in a financial market when the data cannot be fully determined. They overcame this problem by applying the so called fuzzy control charts for monitoring the variability of a process. The authors introduced two new fuzzy control charts the fuzzy individual measurements control chart (FIMCC) and the fuzzy moving range control chart for (FMRCC). For this purpose the fuzzy set theory (FST) (see e.g. Zadeh (1965)) has been used along with control charts. For more about fuzzy control charts see Raz and Wang (1990), Wang and Raz (1990), Gülbay and Kahraman (2006), Erginel (2008) and Morabi et al. (2015). In the empirical example stock prices are forecasted using the exponential smoothing method for the BIST-30 Index. Next, the fuzzy values of stock prices are calculated. The proposed control schemes not only detect small shifts of stock prices but also increase the flexibility of control limits to analyze the variability of stock prices.

Doroudyan et al. (2017) used Shewhart control charts so as to monitor and detect changes in a financial processes modeled with ARMA-GARCH time series structure and apply their method to monitor Tehran Stock Exchange price index (TEPIX). The control statistic is based on the residuals of the model. According to the type of shifts in Tehran Stock Exchange trends, Shewhart control charts was proposed for monitoring TEPIX. Simulation studies reveal the robustness and the change detection power of the proposed monitoring method. Suppose $X_1, X_2, \ldots, X_n$ denote the observations of the financial process with ARMA(p,q)-GARCH (p,q) structure. They estimated the parameters of the model with maximum likelihood estimation (MLE) and subsequently the residuals ε_t and h_t. The control statistic is denoted as:

$$z_t = \frac{\varepsilon_t}{\sqrt{h_t}}. \tag{2.2.11}$$

The process is assumed to be in control state until

$$z_t > UCL \quad \text{or} \quad z_t < LCL.$$

The control limits UCL and LCL are determined such that the ARL_0 is equal to some predetermined values. According to Doroudyan et al. (2017) the financial process goes to out-of-control state when at least one of the model parameters deviates from

the in-control state. They found that the Shewhart method is almost symmetric in the changes in the parameters of the ARMA process which means that positive and negative shifts have almost the same ARL_1. For the GARCH part only the positive shifts are considered.

Garthoff and Schmid (2017) developed control chart procedures for simultaneously monitoring the mean and the covariance matrix of multivariate financial non-linear time series with heavy tails. The examined financial time series are the constant conditional correlation model (CCC), the extended constant conditional correlation model (ECCC), the dynamic conditional correlation model (DCC) and the generalized dynamic conditional correlation model (GDCC). The proposed EWMA or CUSUM type control charts are based on residuals that follow t-distribution.The data are daily logarithmic returns of the stock market indices FTSE and CAC. The p-dimensional target process $\boldsymbol{Y_t}$ is assumed to be a conditional correlation model and has the following form:

$$\boldsymbol{Y}_t = \boldsymbol{\mu} + \boldsymbol{\Sigma}_t^{1/2}\boldsymbol{\epsilon}_t, \tag{2.2.12}$$

where $\boldsymbol{\mu}$ is the constant overall mean, $\boldsymbol{\Sigma}_t = \boldsymbol{D}_t\boldsymbol{R}_t\boldsymbol{D}_t$ is the covariance matrix with the diagonal matrix $\boldsymbol{D}_t = diag(\sigma_{1t}, ..., \sigma_{pt})$ that includes conditional standard deviations and the conditional correlation matrix R_t of Y_t. The proposed EWMA and CUSUM control charts are applied on some characteristic quantities of non linear processes of the data. The two characteristic quantities are:

$$T_t^{(1)} = \begin{pmatrix} \boldsymbol{\eta}_t \\ vech(\boldsymbol{\eta}_t\boldsymbol{\eta}_t^{'}) \end{pmatrix}, \tag{2.2.13}$$

and

$$T_t^{(2)} = \begin{pmatrix} \boldsymbol{\eta}_t \\ \boldsymbol{\eta}_t\boldsymbol{\eta}_t^{'} \end{pmatrix}, \tag{2.2.14}$$

where η_t is a transformation of the residuals and $vech$ the half-vectorization. In the in control state the variables η_t are independent and t-distributed and in the out-of-control state they are neither independent nor identically distributed. From the ARL point of view the simulation study for the first characteristic quantity favours the MCUSUM based on the cumulative sum of the quantity. For the second characteristic quantity, the MEWMA chart based on the recursion of the characteristic quantity, has the best performance for detecting small changes in covariances. For larger changes in covariances the Mahalanobis EWMA outperforms the other control charts. For larger changes in both the mean and covariance the control schemes on the second characteristic quantity perform better. The use of maximum conditional expected

delay (MCED) as a measure of performance has as a result the MEWMA chart based on the EWMA recursion outperforms the other control charts. Omitting covariances and monitoring the variances can improve the performance of the control schemes. The MCUSUM is appropriate for shifts in the mean. The empirical application confirms that neglecting covariances in the monitoring procedure reduces the number of full-sample signals. Li (2016) among other methods for detection of structural breaks in multivariate normally distributed intraday stock data for a relative short time period use control charts. Specifically, a modification of the control statistic of a univariate EWMA chart that contains the singular value decomposition (SVD) of the covariance matrix. The results are compared with other methods for the detection of structural breaks and advantages and disadvantages of the proposed control chart procedure are presented. This is an area that more advanced control charts could be more useful.

2.3 Control Charts and Portfolio Monitoring

The modern portfolio theory introduced by Markowitz (1952) focuses on the trade-off between the expected return and the risk of an investment. The investors through the asset allocation try to maximize their returns every time by taking the best decisions. Portfolio optimization has attracted the interest of academia and practitioners alike, with the theory of stochastic optimal control in its various forms playing a dominant role. For example, in the area of continuous time stochastic models (see e.g. Korn and Korn (2001)) we have various extensions along the lines of jump diffusion, Markov switching models or hybrid systems (see e.g. Azevedo et al. (2014) or Savku and Weber (2018), Savku and Weber (2021)) as well as extensions using inside information or model uncertainty (see e.g. Baltas and Yannacopoulos (2019), Baltas et al. (2018), Papayiannis and Yannacopoulos (2018)). Furthermore, in recent years SPC techniques, which are the main interest of this section, have been applied to the portfolio diversification problem as tool for decision making. Possible structural breaks in the distribution of the asset returns may result in changes in the optimal portfolio weights and action needs to be taken from the investor's point.

2.3.1 Portfolio optimization framework

Consider n risky assets in the financial market and suppose that $\boldsymbol{X}_t$ is the k-dimensional vector of asset returns at a certain time t. Denote $E(\boldsymbol{X}) = \boldsymbol{\mu}$ and $var(\boldsymbol{X}) = \boldsymbol{\Sigma}$ the expected returns and the variance of the returns distribution respectively. Also we assume that the asset returns are identically and independently

distributed following a multivariate normal distribution. The Markowitz portfolio theory assumes that portfolios can be completely characterized by their expected return and variance. The formulation of mean-variance portfolio is:

$$\begin{aligned} \underset{w}{\text{minimize}} \quad & \boldsymbol{w}^{'}\boldsymbol{\Sigma}\boldsymbol{w} - \frac{1}{\delta}\boldsymbol{w}^{'}\boldsymbol{\mu} \\ \text{subject to} \quad & \boldsymbol{w}^{'}\mathbf{1} = 1, \end{aligned} \tag{2.3.1}$$

where $\boldsymbol{w}$ is the vector of portfolio weights, $\mathbf{1}$ is a vector of ones and δ is the risk aversion coefficient.

The global minimum variance portfolio (GMVP) is the portfolio with the lowest possible variance given the assets covariance matrix. For its estimation only the knowledge of the covariance matrix of the asset returns is required and as a result the GMVP weights do not suffer from estimation risk in the mean asset returns.The vector of optimal weights is the solution to the following minimization problem:

$$\begin{aligned} \underset{w}{\text{minimize}} \quad & \boldsymbol{w}^{'}\boldsymbol{\Sigma}\boldsymbol{w} \\ \text{subject to} \quad & \boldsymbol{w}^{'}\mathbf{1} = 1, \end{aligned} \tag{2.3.2}$$

The vector of optimal weights $\mathbf{w}$ is given by:

$$\boldsymbol{w} = \frac{\boldsymbol{\Sigma^{-1}}\mathbf{1}}{\mathbf{1}'\boldsymbol{\Sigma^{-1}}\mathbf{1}}. \tag{2.3.3}$$

The covariance matrix $\boldsymbol{\Sigma}$ is usually estimated from the sample covariance matrix. Suppose that $X_1, \ldots, X_n$ are the n-period asset returns, then:

$$\hat{\boldsymbol{\Sigma}}_{t,n} = \frac{1}{n-1}\sum_{j=t-n+1}^{t}(\boldsymbol{X_j} - \boldsymbol{\mu_{t,n}})(\boldsymbol{X_j} - \boldsymbol{\mu_{t,n}})^{'} \tag{2.3.4}$$

$$\hat{\boldsymbol{\mu}}_{t,n} = \frac{1}{n}\sum_{v=t-n+1}^{t}\boldsymbol{X_v}. \tag{2.3.5}$$

2.3.2 Portfolio monitoring

Yashchin et al. (1997) used a three-step CUSUM procedure for monitoring and detecting changes in the performance of actively managed portfolios compared to a defined benchmark performance. In contrast to the performance measurement approach the portfolio monitoring can identify regime changes or shifts in performance.

Investors estimate their current portfolio performance every time and take action according to the results from the control schemes. The information ratio, the ratio of a portfolio's returns that exceed a particular benchmark to its tracking error, is chosen as a measure of the portfolio performance and monitored from the CUSUM procedure. The generated sequence of excess returns is uncorrelated and follows approximately the normal distribution. The current information ratio of the portfolio is given as:

$$\hat{IR} = \frac{12e_i}{\hat{\sigma}_{i-1}}, \tag{2.3.6}$$

where e_i and $\hat{\sigma}_i$ is the logarithmic excess return and the annualized tracking error of the portfolio in month i respectively. Next, the log-likelihood ratio based on the k most recent observation is estimated. The estimation of the value of k that maximizes the log-likelihood ratio defines the optimum performance measurement interval. The log-likelihood ratio is defined as the natural logarithm of the ratio of the probability that the observed sequence of returns was generated by a bad portfolio manager to the probability that it was generated by a good portfolio manager. The maximization of the log-likelihood ratio is of great importance because it makes the CUSUM procedure robust to the distribution of portfolio returns and fast to detect a change in the portfolio performance. Finally, the log-likelihood ratio is compared to a threshold value and if it exceeds this value means that the performance has changed from good to bad and action is need to be taken. If the investigation shows that this is a false alarm the likelihood ratio is set to 0 and the procedure is restarted. The empirical findings of Yashchin et al. (1997) indicate that it takes on average 41 months to detect a bad performance, which is much faster than a t-test. For a good portfolio manager the average time between false alarms is 84 months. The probability that it will outperform its benchmark over any specified horizon is simply related to its information ratio.

Gandy (2012) monitored the performance of credit portfolios using survival analysis approach in CUSUM procedures. The credit portfolio changes either by the addition of new credits or when current credits leave the portfolio in case of default or full payment. Three scenarios are examined for the arrival of new customers and for the changes in the portfolio. Specifically, the customer's arrival rate follow a Poisson process or the arrival rate is doubled at time t = 1 or the arrival rate is reduced to half at time t = 1. The credit portfolio can have no change during the monitoring period (No-change condition), the default rate at t=1.5 increases by 50% (Crisis condition) and the default rate from t=1.5 and onwards for all new customers is 50%. The proposed survival analysis CUSUM procedure is compared through a

simulation study for the portfolio monitoring of default rate using sliding window with CUSUM control charts based on default rates and CUSUM control charts based on defaults within a given time after customer's arrival. The alternative strategies, with the exception of the CUSUM charts using a fixed follow-up time, are sensitive to changes in the portfolio population. This has as a result the increase of the default rates and the number of false alarms. The survival analysis of the CUSUM procedure detect faster the alarm times because they can use the information about credit defaults without any delay.

Golosnoy (2018) proposed Shewhart and Hotelling control schemes for the surveillance of the portfolio characteristic beta from the one factor capital asset pricing model (CAPM). The Shewhart control chart is appropriate for the case of the univariate quantity beta when we have a single portfolio. Hotelling schemes are relevant when there is a set of portfolios and the monitoring quantity beta is a multivariate vector.

Riegel Sant'Anna et al. (2019) used EWMA procedures in order to monitor the rebalancing process of index tracking (IT) portfolio. When a signal is given then the portfolio composition is changed and the portfolio needs to be updated using a rebalancing strategy. The EWMA control charts are applied on portfolio's daily returns and daily volatility. The measure of daily returns is the tracking error (TE), which is the difference between portfolio daily returns and index daily returns. The surveillance of index tracking portfolios is implemented on cointegration-based and optimization-based portfolios. The empirical study on data from the Brazilian Ibovespa stock index and the US S&P 100 index compares the SPC rebalancing approach with portfolios with the traditional fixed rebalancing windows. The results showed similar findings for both techniques in terms of returns and volatility. In markets with large volatility the SPC approach is more consistent than the fixed rebalancing window approach.

2.3.3 Monitoring optimal portfolio weights

Markowitz's portfolio theory is a single-period myopic portfolio allocation problem where the investor in every time period tries to maximize its quadratic utility function. Okhrin and Schmid (2006) examined several distributional properties for optimal portfolio weights of four mean-variance portfolio strategies: expected quadratic utility optimal portfolio, global minimum variance portfolio, tangency portfolio and sharpe ratio portfolio. The assumption is that asset returns follow a stationary normal distribution. The estimation of optimal weights depends on the mean and

variance of the asset returns but because the true values are unknown instead of these quantities their sample counterparts are used. Okhrin and Schmid (2006) derived the exact and asymptotic distribution along with the first two moments of the optimal portfolio weights for the various cases. The asymptotic distributions are estimated both when asset returns are uncorrelated and correlated. For example, in the case of uncorrelated k risky asset returns for n time periods, the vector of the first k-1 optimal weights ($\boldsymbol{w}^*$) in the GMVP follows a multivariate t-distribution with $n-k+1$ degrees of freedom. The choice of use of k-1 elements instead of k in every vector of optimal weights is because the sums of the elements are equal to one, their covariance matrices are not regular and the rank of all covariance matrices is equal to k-1. The mean and the variance are given by:

$$E(\hat{\boldsymbol{w}}_{t,n}) = \boldsymbol{w} \text{ and } Var(\hat{\boldsymbol{w}}_{t,n}) = \frac{1}{n-k-1}\frac{\boldsymbol{Q}}{\mathbf{1'\Sigma^{-1}1}}, \tag{2.3.7}$$

respectively, where $\boldsymbol{Q} = \boldsymbol{\Sigma^{-1}} - \frac{\boldsymbol{\Sigma^{-1}11'\Sigma'}}{\mathbf{1'\Sigma^{-1}1}}$ (see Bodnar and Schmid (2008), Golosnoy and Schmid (2009)).

Bodnar and Schmid (2008) investigated the distributional properties of the expected return and the variance of various portfolio strategies. The knowledge of the distributional properties and the first two moments is of crucial interest for the construction of control charts for the surveillance of optimal portfolio weights. Caution should be taken when somebody relies on asymptotic results of the asymptotic counterparts of the exact moments because they can differ significantly from the exact moments and the results to be inaccurate. The observed process is considered to be in control if $E(\hat{\boldsymbol{w}}_{t,n}) = \boldsymbol{w}$ holds for all $t \geq 1$, otherwise the observed process is denoted to be out-of-control. The first approach is directly based on the process of the estimated weights $\hat{\boldsymbol{w}}_{t,n}$. The second one considers the process of the first differences $\{\boldsymbol{\Delta}_{t,n}\}$, defined as $\boldsymbol{\Delta}_{t,n} = \hat{\boldsymbol{w}}_{t,n} - \hat{\boldsymbol{w}}_{t-1,n}$ and its disadvantage is that depends on the estimation window length n.

Under the assumption that asset returns $\{\boldsymbol{X_t}\}$ are independent and identically normally distributed, with mean $\boldsymbol{\mu}$ and covariance matrix $\boldsymbol{\Sigma}$, Golosnoy and Schmid (2007) proposed several EWMA control charts for monitoring the weights of the GMVP. The estimation of optimal weights require the knowledge of the covariance matrix of asset returns. Since the true covariance matrix is unknown, the sample covariance is used for the estimation.The estimated sample weights are highly autocorrelated and for this reason the proposed control schemes are the modified EWMA charts as well as control charts based on the differences of one time lag of the sample weights. The use of differences has as a result to reduce the high autocor-

relation within the original portfolio weight series. For each control scheme control charts based on the multivariate EWMA recursion and Mahalanobis distance are constructed. For $t \leq 0$ it is assumed that there are no changes in the underlying process and for $t \geq 1$ the observed process is in control if it is equal to the target process, otherwise it is said to be out-of-control. The out-of-control situation is modeled by changing the main diagonal or the off-diagonal elements of the covariance matrix or both. Golosnoy and Schmid (2007) examined two types of changes in the covariance matrix of asset returns. The first type affects only the mean of the optimal portfolio weights. The second type which is appropriate for financial applications the changes are modeled in a way that represent the change of a bull market to a bear market. The first category of control charts monitors the process of the estimated weights $\hat{\boldsymbol{w}}_{t,n}$ and the second the process of the first differences of the portfolio weights: $\boldsymbol{\Delta}_{t,n} = \hat{\boldsymbol{w}}_{t,n} - \hat{\boldsymbol{w}}_{t-1,n}$. For example, in the case of modified control charts, the distance between the estimated GMVP weights $\hat{\boldsymbol{w}}^*_{t,n}$ and the target weights $\boldsymbol{w}^* = E_0(\hat{\boldsymbol{w}}^*_{t,n})$ are measured by the Mahalanobis distance. E_0 is the mean of optimal portfolio weights estimated when the process is in-control. This leads to:

$$T_{t,n} = (\hat{\boldsymbol{w}}^*_{t,n} - \boldsymbol{w}^*)' \boldsymbol{\Omega}^{*-1} (\hat{\boldsymbol{w}}^*_{t,n} - \boldsymbol{w}^*), t \geq 1. \tag{2.3.8}$$

The EWMA recursion is given by:

$$Z_{t,n} = (1 - \lambda) Z_{t-1,n} + \lambda T_{t,n}, \tag{2.3.9}$$

for $t \geq 1$. The starting value $Z_{0,n}$ is set equal to $E_0(T_t) = k - 1$. In the case of the multivariate EWMA control chart, the vector $\boldsymbol{Z}_{t,n}$ can be presented as:

$$\boldsymbol{Z}_{t,n} = (\boldsymbol{I} - \boldsymbol{R})^t \boldsymbol{Z}_{0,n} + \boldsymbol{R} \sum_{\upsilon=0}^{t-1} (\boldsymbol{I} - \boldsymbol{R})^\upsilon \hat{\boldsymbol{w}}^*_{t-\upsilon,n}, \tag{2.3.10}$$

where $\boldsymbol{R} = diag(r_1, \cdots, r_{k-1})$ is a $(k-1) \times (k-1)$ diagonal matrix with diagonal elements $0 < r_i \leq 1$, $i \in \{1, \cdots, k-1\}$. Consequently it holds that $E_0(\boldsymbol{Z}_{t,n}) = \boldsymbol{w}^*$. The covariance matrix of the multivariate EWMA statistic $\boldsymbol{Z}_{t,n}$ in the in-control state is given by:

$$Cov_0(\boldsymbol{Z_{t,n}}) = \boldsymbol{R}(\sum_{i,j=0}^{t-1} (\boldsymbol{I} - \boldsymbol{R})^i Cov_0(\hat{\boldsymbol{w}}^*_{t-i,n}, \hat{\boldsymbol{w}}^*_{t-j,n})(\boldsymbol{I} - \boldsymbol{R})^J)\boldsymbol{R}. \tag{2.3.11}$$

A signal is given if:

$$(\boldsymbol{Z}_{t,n} - E_0(\boldsymbol{Z}_{t,n}))' Cov_0(\boldsymbol{Z}_t)^{-1} (\boldsymbol{Z}_{t,n} - E_0(\boldsymbol{Z}_{t,n})) > c.$$

The control limit c which defines the rejection area in every control scheme is estimated through a simulation study for a predetermined value of the ARL (usually in financial applications is equal to 120 days or 1/2 year of daily observations, see Golosnoy et al. (2007)). After a signal is given the financial analyst should examine it and decide for further actions in concern with the portfolio allocation. The estimation of the covariance of the control statistic $\boldsymbol{Z}_{t,n}$ when the process is in control requires the estimation of the covariance matrix between the weights. Golosnoy and Schmid (2007) studied and approximated the limit behavior of $Cov_0(\boldsymbol{Z}_{t,n})$ as n tends to infinity. An alternative method is through Monte Carlo Simulation study. The empirical application study of a portfolio favoured the use of difference control charts in practice because they are able to give an alarm almost immediately with high probability for large changes. However, the proposed control schemes showed poor detection ability for some out-of-control situations such as in the case of modified charts when the variances but not the covariances are changed. Due to these poor detection abilities, Golosnoy et al. (2010) proposed some new characteristics for monitoring optimal portfolio weights in a GMVP. They suggested an alternative process $\{\boldsymbol{q}_t\}$ to the optimal weight process and a process $\{\boldsymbol{p}_{t,n}\}$ alternative to the difference process. For a sequence of independent and normally distributed k-dimensional random vectors $\boldsymbol{X_t}$ it holds that in the in-control state as $n \to \infty$, $n\boldsymbol{\Delta}_{t,n} - \boldsymbol{p}_{t,n} \xrightarrow{p} 0$, where:

$$\boldsymbol{p}_{t,n} = -\boldsymbol{Q}((\boldsymbol{X}_t - \boldsymbol{\mu})(\boldsymbol{X}_t - \boldsymbol{\mu})^{'} - (\boldsymbol{X}_{t-n} - \boldsymbol{\mu})(\boldsymbol{X}_{t-n} - \boldsymbol{\mu})^{'})\boldsymbol{w}, \tag{2.3.12}$$

and $\boldsymbol{Q} = \boldsymbol{\Sigma}^{-1} - \frac{\boldsymbol{\Sigma^{-1}11'\Sigma'}}{\boldsymbol{1'\Sigma^{-1}1}}$. An alternative quantity for monitoring the process of optimal weights is:

$$\boldsymbol{q}_t = -\boldsymbol{Q}((\boldsymbol{X}_t - \boldsymbol{\mu})(\boldsymbol{X}_t - \boldsymbol{\mu})^{'} - \boldsymbol{\Sigma})\boldsymbol{w} = -\boldsymbol{Q}(\boldsymbol{X}_t - \boldsymbol{\mu})(\boldsymbol{X}_t - \boldsymbol{\mu})^{'}, \tag{2.3.13}$$

and $E_0(\boldsymbol{q}_t) = 0$, $Cov_0(\boldsymbol{q}_t) = \boldsymbol{Q}$ with $\boldsymbol{p}_{t,n} = 0$ and $\boldsymbol{1}^{'}\boldsymbol{q_t} = 0$.

Suppose that the process $\{\boldsymbol{X}_t\}$ of asset returns for $t \geq 1$ when it is out-of -control, then the out-of-control mean of the characteristic $\boldsymbol{p}_{t,n}$ for $t \geq 1$ is given by:

$$E_1(\boldsymbol{p}_{t,n}) = \begin{cases} -\boldsymbol{Q}\boldsymbol{\Sigma}_1\boldsymbol{w}, & 1 \leq t \leq n \\ \boldsymbol{0}, & t \geq n+1, \end{cases} \tag{2.3.14}$$

and the covariance matrix is defined as:

$$Cov_1(\boldsymbol{p}_{t,n}) = \begin{cases} 2\boldsymbol{Q}(\boldsymbol{\Sigma}_1\boldsymbol{w}\boldsymbol{w}^{'}\boldsymbol{\Sigma}_1 + (\boldsymbol{w}^{'}\boldsymbol{\Sigma}_1\boldsymbol{w})\boldsymbol{\Sigma}_1)\boldsymbol{Q}, & t \geq n+1 \\ -\boldsymbol{Q}(\boldsymbol{\Sigma}_1\boldsymbol{w}\boldsymbol{w}^{'}\boldsymbol{\Sigma}_1 + (\boldsymbol{w}^{'}\boldsymbol{\Sigma}_1\boldsymbol{w})\boldsymbol{\Sigma}_1)\boldsymbol{Q} + \frac{\boldsymbol{Q}}{(\boldsymbol{1'\Sigma^{-1}1})^{-1}}, & 1 \leq t \leq n. \end{cases} \tag{2.3.15}$$

Control charts for the characteristic processes $\boldsymbol{p}_t$ and $\boldsymbol{q}_t$ are constructed for both univariate and multivariate EWMA recursion. The recursion equations are applied to the first k-1 components of the respective characteristic in each case. In a simulation study the performance of the charts is compared in various out-of-control situations with performance measures the ARL and the worst case conditional expected delay (WED). The results favoured the opinion that for the detection of the changes a combination of control charts should be applied. Control charts based on the first differences are those with the worst overall performance. Also control procedures based on the characteristic quantity $\boldsymbol{q}_t$ performed better than those based on $\boldsymbol{p}_t$. If the type of change in the GMVP optimal weights is an increasing variance then the charts based on the characteristic $\boldsymbol{q}_t$ performed better than any other. A disadvantage of these control schemes is that they fail to detect changes due to a decreasing variance. Additionally, changes caused by an increase in correlation, the charts that monitor the quantity $\hat{\boldsymbol{w}}_{t,n}$ outperformed the other control schemes. For changes in both the variances and the correlations the charts for the characteristic $\boldsymbol{q}_t$ had the best performance.

Golosnoy et al. (2011) developed directionally invariant CUSUM control charts for monitoring the GMVP estimated optimal weights $\hat{\boldsymbol{w}}^*_{t,n}$ and the characteristic process $\boldsymbol{q}^*_t$, the multivariate CUSUM-w and CUSUM-q charts respectively. Changes in the GMVP composition are due to changes in the covariance matrix of asset returns. The MCUSUM1 and MCUSUM2 charts of Pignatiello and Runger (1990) and the projection pursuit (PPCUSUM) scheme of Ngai and Zhang (2001) are applied for monitoring these processes. Simulation and empirical study compared the detection ability of the CUSUM schemes with the EWMA schemes for two types of changes. First, only in the variance matrix, which are responsible for large changes in optimal weights, and second in both the variance and the correlation matrix of asset returns, which had as a result small changes in optimal weights. The performance measures of the control charts are the ARL_1 and the worst-case conditional expected delay (WED). The results supported the opinion that the simultaneous use of both w-charts and q-charts is appropriate for the detection of the different types of changes. In the case of changes in the variance, the best performance can be observed for the MCUSUM1-q and the MCUSUM2-w control charts. If the variances of the asset returns are increasing then CUSUM-q charts perform better than the CUSUM-w charts. If the variances are decreasing then the w-charts are more appropriate for the detection of changes in the weights. For changes in both the variances and the correlations the best control scheme is the MEWMA-q control chart. The MCUSUM2-q chart performs better among the CUSUM-q control schemes. The CUSUM-w charts are appropriate for detecting changes which are the result of increasing correlation.

Olha (2007) monitored optimal weights of a GMVP following a different approach by using the distribution of the estimator of the covariance matrix of asset returns in order to construct multivariate and simultaneous control charts. A significant benefit of this approach is that the proposed multivariate and simultaneous control schemes are independent of the covariance matrix of asset returns. The covariance matrix of asset returns is monitored for possible changes that may affect the mean and the covariance of a transformation of the vector of optimal weights. Suppose that $X_1, \ldots, X_n$ the vector of asset returns, Bodnar and Schmid (2004) showed that linear combinations of the components of the GMVP weights, $\boldsymbol{L}\hat{\boldsymbol{w}}$, follow a multivariate t-distribution with mean $\boldsymbol{Lw}$ and covariance $\frac{1}{n-p+1}\frac{\boldsymbol{LRL'}}{\mathbf{1'\Sigma^{-1}1}}$, where $\boldsymbol{L}$ is the $(q \times p)$-dimensional matrix of constants. Olha 2007 proposed the following transformation of the vector of the optimal weights:

$$\hat{\boldsymbol{\nu}} = \sqrt{n-p}\sqrt{\mathbf{1}'\hat{\boldsymbol{\Sigma}}^{-1}\mathbf{1}}(\boldsymbol{L}\hat{\boldsymbol{\Sigma}}^{-1}\boldsymbol{L}' - \frac{\boldsymbol{L}\hat{\boldsymbol{\Sigma}}^{-1}\mathbf{1}\mathbf{1}'\hat{\boldsymbol{\Sigma}}^{-1}L'}{\mathbf{1}'\hat{\boldsymbol{\Sigma}}^{-\mathbf{1}}\mathbf{1}1})^{-\frac{1}{2}}\boldsymbol{L}(\hat{\boldsymbol{w}} - \boldsymbol{w}), \tag{2.3.16}$$

and $\hat{\nu} \sim t_{n-p}(\mathbf{0}, \frac{n-p}{n-p-2}I)$. Structural breaks in the covariance matrix of asset returns have as a result changes in the mean vector and the covariance matrix of the vector $\hat{\boldsymbol{\nu}}$. If a change in the covariance matrix happens then the composition of the optimal weights changes and a new vector $\hat{\boldsymbol{\nu}}$ is estimated with known mean and covariance.

Five types of control charts for multivariate surveillance are constructed: The multivariate Shewhart control chart, the MC1 control chart of Pignatiello and Runger (1990), the multivariate CUSUM control chart, the PPCUSUM control chart of Pignatiello and Runger (1990), and the MEWMA control chart. The proposed control schemes monitor changes in the covariance matrix by testing if the mean of the vector $\eta_{\mathbf{i}}$ differs significantly from the target value μ_η. The quantity η_i is the $q + q(q+1)/2$ dimensional vector of the sequence of the independent covariance matrix estimators of the subsamples that occur if we divide the entire sample of asset returns in m subsets of size n_1. The expected value of the vectors $\eta_{\mathbf{i}}$ in case of no structural breaks in the covariances of the asset returns has at positions $q+1, 2q+1, 3q, 4q-2, 5q-3, \ldots, q+q(q+1)2$ value equal to $\frac{n_1-p}{n_1-p-2}$ and otherwise is zero. Additionally simultaneous monitoring procedures for detecting shifts in the mean and variance for each component of the vector of optimal weights are constructed. The simulation study supports the opinion that the MEWMA and the simultaneous MEWMA control charts outperform the other control schemes because they have the smallest out-of-control average run lengths.

Golosnoy (2007) monitored the change in the optimal weights of a GMVP by monitor-

ing the unconditional covariance matrix of the k assets returns under the assumption of the locally constant volatility approach. The locally constant volatility approach (Hsu et al. (1974)) suggests that the covariance matrix between sudden changes remains constant. The covariance matrix is estimated through a time-varying estimation window. If the control charts give a signal then we choose a shorter estimation window or if there is no signal we increase the length of the window. The result of this approach is the reduction of the out-of-sample variance of the GMVP which is used as a performance measure. The two applied control schemes are proposed by Golosnoy and Schmid (2007) for the vector of k-1 returns. The modified EWMA based on Mahalanobis distance and the EWMA difference control chart based on Mahalanobis distance, designed for detection of mean changes in the weights. The in-control mean $E_0(\hat{\boldsymbol{w}})$ and covariance matrix $Cov_0(\hat{\boldsymbol{w}})$ of optimal weights are estimated with a time varying approach. The time-varying length $m_t \geq n$ is defined from the signal of the control charts. At time $t = 1$ the estimation window m_t is chosen to have a small value m days. In the next time period $t = 2$ if no alarm has occurred, the length of the window increases by one observation $m_{t=2} = m + 1$. If now an alarm occurs at time $t = t + \tau$ then we restart the control charts setting $m_{t+\tau} = m$. For the evaluation of portfolio performance the out-of-sample variance of realized portfolio returns $V(R^p)$ is used. The proposed portfolio monitoring method based on the estimation of the covariance matrix is compared with strategies that contain five alternative covariance matrix estimators: sample estimator, single-index model, shrinkage estimation, exponential smoothing estimator and estimation with GARCH approach. The empirical study on stocks from the the German stock market index DAX shows that the portfolio monitoring strategies with time-varying estimation window achieve smaller out-of- sample GMVP variance than the alternatives in most of cases.

Golosnoy et al. (2020) estimated the optimal GMVP weights following a different approach than previously described with the sample volatility estimators. They estimated the so called realized GMVP weights by using the realized volatility measures computed from intraday data. The benefit of using this approach according to the authors is the better incorporation of the new daily information in the markets to the estimation of the covariance matrix of asset returns. The realized covariance matrix is given by:

$$\mathbf{R_{r,t}} = \sum_{j=1}^{m} \mathbf{r_{t,j}} \mathbf{r_{t,j}}^{'}, \tag{2.3.17}$$

where $r_{t,j}$ are the m uniformly spaced intraday return vectors for day t. The vector

of the realized GMVP weights $\mathbf{w_{r,t}}$ is given by:

$$\mathbf{w_{r,t}} = \frac{\mathbf{R_{r,t}}^{-1}\mathbf{1}}{\mathbf{1'R_{r,t}}^{-1}\mathbf{1}}. \tag{2.3.18}$$

Similar to the work of Okhrin and Schmid (2006) the authors derived both finite sample and asymptotic distributional properties of the realized GMVP weights. Suppose that the realized covariance matrix $\mathbf{R_{r,t}}$ follows the conditional Wishart distribution with degrees of freedom m_t and covariance matrix $\mathbf{\Sigma_t}/m_t$, $\mathbf{\Sigma_t}$ is the true daily covariance matrix of asset returns. The result is that the vector $\mathbf{w_{r,t}}$ follows an $(k-1)$-elliptical t-distribution. In addition to the finite sample properties under certain conditions as $m_t \to \infty$ the vector $\mathbf{w_{r,t}}$ is asymptotically normally distributed. The proposed control chart is the univariate EWMA for $\lambda = 1$ which is the Shewhart control chart and it is applied to the differences between the target portfolio weights $\theta_{\mathbf{r,t}}$ from the GMVP weights of the current day, $\mathbf{\Delta r, t} = \mathbf{w_{r,t}} - \theta_{\mathbf{r,t}}$. The vector of the target weights could be either deterministic or stochastic. As a consequence the Mahalanobis distance of these differences is:

$$T_{r,t} = (\mathbf{\Delta_{r,t}})' Cov(\mathbf{\Delta_{r,t}})^{-1}(\mathbf{\Delta_{r,t}}), \tag{2.3.19}$$

where $Cov(\mathbf{\Delta_{r,t}})$ is the $(k-1) \times (k-1)$ -dimensional positive definite covariance matrix of $\mathbf{\Delta_{r,t}}$. The performance of the control chart is tested through a simulation and empirical example study. Taking into advantage the distributional properties of the optimal weights for this approach of portfolio monitoring further work needs to be done and additional control chart procedures to be applied.

Chapter 3

Control Charts and Affine Term Structure Models

3.1 Introduction

In this chapter we focus on monitoring the parameters of a Gaussian ATSM in order to detect possible changes. Our work is based on the approach of Schmid and Tzotchev (2004) in which monitoring the stability of the vector of the parameters of the ATSM is transformed to monitoring the stability of bond yields. In the Cox-Ingersoll-Ross (CIR) term structure model used by Schmid and Tzotchev (2004) the short rate process has a conditional non-central chi-square distribution in contrast with our affine model that follows a Gaussian process. The change can be either to one parameter, here the factor loadings of the state evolution process, or to the entire set of parameters of the state factor process. Additionally, we simulate parallel and non-parallel shifts in the yield curve and monitoring them in order to detect change points for large and small shifts. For the sequential monitoring of the parameters of our term structure model we use the following control chart procedures: modified EWMA control charts based on the Mahalanobis distance and the MEWMA recursion, MCUSUM, residual control charts based on the Mahalanobis distance and the MEWMA recursion and the multivariate modified EWMA (MMOEWMA) chart. The proposed control chart techniques have been applied empirically to the U.S. term structure and structural break points have been documented.

Kramer and Schmid (1997) extended the MEWMA in monitoring multivariate time series. Rosołowski and Schmid (2003) in addition to modified EWMA control charts

developed control charts based on the residuals instead of the original data for Gaussian processes. Patel and Divecha (2011) and Patel and Divecha (2013) proposed a modified EWMA chart for the univariate and multivariate case respectively for monitoring small and large shifts in a autoregressive AR(1) and a vector autoregressive VAR(1) process. The Multivariate Modified EWMA (MMOEWMA) chart is a modification in MEWMA (see Lowry et al. (1992)) control chart statistic and has the ability to detect small and large shifts in the monitoring process. Their work is applied to chemical and other industrial applications. Here we adapt their work in the multivariate case in financial applications, specifically in interest rate models. Khan et al. (2017) under the assumption that the monitoring quality characteristic follows the normal distribution proposed a control chart which is a generalization of the modified EWMA proposed by Patel and Divecha (2011). The efficiency of their modified EWMA chart is compared with other control charts in terms of the ARL in an industrial example. Their simulation study results showed that the proposed chart has the ability to detect shifts quicker than the traditional EWMA chart of Roberts (1966) and the modified EWMA of Patel and Divecha (2011). Saghir et al. (2020) following the work of Khan et al. (2017) constructed a modified EWMA for monitoring the process variation. The performance of the proposed control chart is evaluated using the average run length (ARL) and the standard deviation of run length (SDRL). The results indicated the quick detection of the out-of-control process when monitoring the process dispersion.

Chib and Kang (2013) examined for possible structural breaks the U.S. yield curve by using an arbitrage-free ATSM applying Bayesian techniques. They assumed when the economy is in one regime can move only forward to another regime or remain to the same regime. This assumption is different from that in Markov regime switching models where the economy can return to a previous condition (regime). All model parameters are subject to changes at unknown time points. For the determination of the number of regimes and the change points in the data set they followed a "backward looking" approach. They compared various term structure models assuming their number of change points, via their marginal likelihood estimates. In our study we follow a different, "forward looking", approach using sequential monitoring techniques for the detection of change points at each time t.

The rest of this chapter is organized as follows. In section 2 we present our data set. In section 3 we briefly present the main framework of our term structure model and the estimation method. Next, section 4 presents the control chart procedures that we apply in our work. Section 5 and section 6 refer to the simulation study and the empirical example along with their results.

3.2 Data

3.2.1 Government Bonds

The U.S. Treasury yields data are monthly continuously compounded spot rates at maturities 3 months and 2,3,4,5 and 10 years from April 1991 to December 2009, provided from the FED St. Louis. The in-control period is defined from April 1991 to December 2000 in total 117 months. The period from January 2001 to December 2009 is the out-of-control period in total 120 months. Figure 3.2.1 plots the time series of the U.S. Treasury yields for the in-control period. With the exception of the 3-month Treasury yield the rest of the yields exhibit similar patterns during the sample period. There are three periods of low bond yields, 1993, at the end of 1995 and in the middle of 1998. The 3-month Treasury bill mimics the other bond yields but in lower level until the end of 1995. For the period until September 1998 behaves smoother than the other yields of our sample and for the rest of the period exhibits the same pattern again in lower levels. Table 3.2.1 presents the autocorrelations for the time series of treasury yields for the first four lags. The results confirm the strong persistence of the bond yields. The summary statistics are displayed in table 3.2.3.

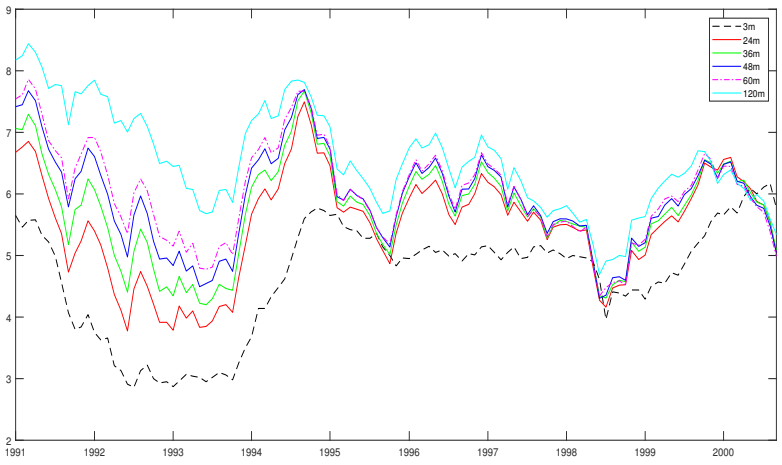

Figure 3.2.1: U.S. Treasury Yields.

3.2.2 Economic variables

In our work we consider two economic variables the Consumer Price Index (CPI) as a proxy for the inflation and the Industrial Production (IP) index growth rate. Data are provided from the FED St. Louis. Figure 3.2.2 plots the CPI for the period 1991:04 to 2000:12. The CPI rates peak at the beginning of our sample, in early 1991, and has a downward trend until the last quarter of 1991 where it stabilizes until April of 1993. The peak at the beginning is mainly due to the inflation pressure generated by oil shocks during the first Gulf War. In the subsequent period, the CPI factor remains at low levels and shows a downward trend from the end of 1996 and reaches the low and at February of 1998 following next an upward trend.

Figure 3.2.3 plots the IP index growth rate. The IP index growth rate factor steadily grows in the period before the first quarter of 1993 starting from negative levels. Until the end of the period the IP index growth remains in positive levels following opposite patterns from the CPI factor. Table 3.2.2 presents the autocorrelations for the two observable factors. The time series of macroeconomic factors exhibit high and medium autocorrelation for the first four lags. The summary statistics are presented in table 3.2.4. All the data used for the model estimation are demeaned.

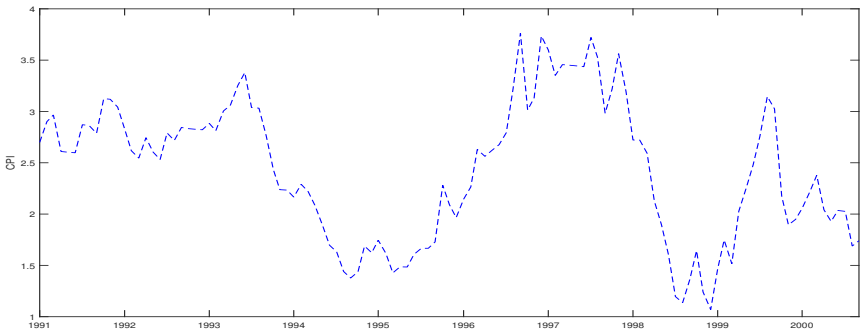

Figure 3.2.2: Consumer Price Index for the period 1991:04 to 2000:12.

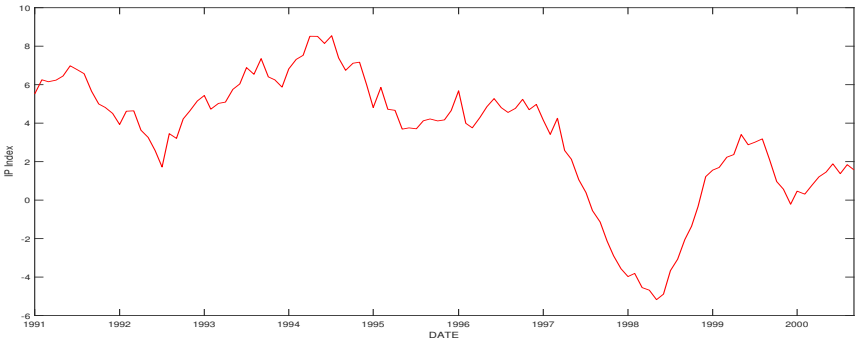

Figure 3.2.3: Industrial Production Index growth for the period 1991:04 to 2000:12.

	Lag 1	Lag 2	Lag 3	Lag 4
3m	0.9693	0.9262	0.8763	0.8163
24m	0.9382	0.8415	0.7357	0.6295
36m	0.9175	0.8003	0.6729	0.5486
48m	0.9077	0.7856	0.6591	0.5299
60m	0.907	0.7844	0.6553	0.5243
120m	0.9294	0.8478	0.7647	0.6759

Table 3.2.1: Autocorrelation of U.S. Treasury yields with maturities 3-,24-,36-,48-,60- and 120-months.

Figure 3.2.4: Yields Term Premia for the period 1991:04 to 2000:12.

	Lag 1	Lag 2	Lag 3	Lag 4
CPI	0.9046	0.7927	0.7088	0.6167
IP	0.9001	0.8111	0.7235	0.6428

Table 3.2.2: Autocorrelation of macroeconomic factors.

Yields	3m	24m	36m	48m	60m	120m
Mean	4.6496	5.4823	5.7203	5.9175	6.0157	6.5375
Skewness	-0.6261	-0.2581	-0.0421	0.1037	0.1879	0.2146
Kurtosis	2.2861	2.4623	2.5806	2.6712	2.6975	2.4887
Std deviation	0.9202	0.8553	0.7918	0.7722	0.7723	0.8213
Maximum	6.17	7.496	7.671	7.695	7.862	8.44
Minimum	2.86	3.774	4.2	4.305	4.344	4.691
Range	3.31	3.722	3.471	3.39	3.518	3.749

Table 3.2.3: Descriptive Statistics for U.S. Treasury yields.

	CPI	IP
Mean	2.6260	1.9482
Skewness	-0.1167	-1.8123
Kurtosis	3.5512	7.8923
Std deviation	1.3761	3.9873
Maximum	6.3796	8.5440
Minimum	-1.9615	3.774
Range	8.3411	23.788

Table 3.2.4: Descriptive Statistics for observable factors.

3.3 Gaussian Affine Term Structure Models

3.3.1 General Framework

We consider a $(N \times 1)$ vector of state variables $\mathbf{X_t}$ that describes the state of the economy. The dynamic evolution process of the state variables has the following Gaussian vector autoregressive form:

$$\mathbf{X_{t+1}} = \boldsymbol{\mu} + \boldsymbol{\phi}\mathbf{X_t} + \boldsymbol{\Sigma}\mathbf{u_{t+1}}, \tag{3.3.1}$$

with $\mathbf{u_{t+1}} \sim N(0, \mathbf{I})$. From equation (3.3.1) it follows that $\mathbf{X_{t+1|t}} \sim N(\boldsymbol{\mu_X}, \boldsymbol{\Sigma\Sigma}')$. The dynamic evolution under the physical probability measure P is

$$\mathbf{X_{t+1}} = \boldsymbol{\mu}^{\boldsymbol{P}} + \boldsymbol{\phi}^{\boldsymbol{P}}\mathbf{X_t} + \boldsymbol{\Sigma}\mathbf{u}^{\mathbf{P}}_{\mathbf{t+1}}, \tag{3.3.2}$$

and under the risk-neutral pricing measure Q is

$$\mathbf{X_{t+1}} = \boldsymbol{\mu}^{\boldsymbol{Q}} + \boldsymbol{\phi}^{\boldsymbol{Q}}\mathbf{X_t} + \boldsymbol{\Sigma}\mathbf{u}^{\mathbf{Q}}_{\mathbf{t+1}}. \tag{3.3.3}$$

The time-varying market prices of risk, $\lambda_\mathbf{t}$, are affine functions of the underlying state variables $\mathbf{X_t}$:

$$\boldsymbol{\lambda_t} = \boldsymbol{\lambda_0} + \boldsymbol{\lambda_1}\mathbf{X_t}. \tag{3.3.4}$$

Suppose r_t is the continuously compounded short term interest rate. The short rate is an affine function of the state variables:

$$r_t = \delta_0 + \boldsymbol{\delta}_\mathbf{1}'\mathbf{X_t}. \tag{3.3.5}$$

The stochastic discount factor (SDF) M_{t+1} is exponentially affine in the evolution process and is defined as

$$\begin{aligned} M_{t+1} &= exp(-\frac{1}{2}\boldsymbol{\lambda}_\boldsymbol{t}'\boldsymbol{\lambda_t} - r_t - \boldsymbol{\lambda_1 u_{t+1}}) \\ &= exp(-\frac{1}{2}\boldsymbol{\lambda}_\boldsymbol{t}'\boldsymbol{\lambda_t} - \delta_0 - \boldsymbol{\delta_1}\mathbf{X_t} - \boldsymbol{\lambda_1}\mathbf{u_{t+1}}). \end{aligned}$$

From the parameters of the P-measure we can obtain the corresponded parameters under the Q-measure and reversely by the following equations:

$$\boldsymbol{\mu}^{\boldsymbol{Q}} = \boldsymbol{\mu}^{\boldsymbol{P}} - \boldsymbol{\Sigma}\lambda_0, \tag{3.3.6}$$

$$\boldsymbol{\phi}^{\boldsymbol{Q}} = \boldsymbol{\phi}^{\boldsymbol{P}} - \boldsymbol{\Sigma\lambda_1}. \tag{3.3.7}$$

The zero-coupon bonds are priced using the stochastic discount factor from the following recursive relation:

$$P_t^n = E_t(M_{t+1}P_{t+1}^{n-1}), \tag{3.3.8}$$

where P_t^n is the price of a zero-coupon bond of maturity n periods at time t. Equation (3.3.8) means that the bond prices are exponential affine functions of the underlying state variables:

$$P_t^n = exp(a_n + \boldsymbol{b_n'}\mathbf{X_t}). \tag{3.3.9}$$

The continuously compounded yield on an n-period zero-coupon bond at time t is

$$y_t^n = -\frac{1}{n} log P_t^n. \tag{3.3.10}$$

From equation (3.3.9) we have that

$$Y_t^n = A_n + \mathbf{B_n'}\mathbf{X_t}, \tag{3.3.11}$$

with $A_n = -\frac{a_n}{n}$ and $\mathbf{B_n} = -\frac{\mathbf{b_n}}{n}$. The parameters α_n and $\mathbf{b_n}$ are estimated from the set of recursive equations

$$a_{n+1} = a_n + \mathbf{b_n'}(\mu - \mathbf{\Sigma}\lambda_0) + \frac{1}{2}\mathbf{b_n'}\mathbf{\Sigma}\mathbf{\Sigma}'\mathbf{b_n} - \delta_0, \tag{3.3.12}$$

$$\mathbf{b_{n+1}} = \mathbf{b_n'}(\boldsymbol{\phi} - \mathbf{\Sigma}\boldsymbol{\lambda_1}) - \boldsymbol{\delta_1'}, \tag{3.3.13}$$

with starting values $A_1 = -\delta_0$, $\mathbf{B_1} = -\boldsymbol{\delta_1}$. Yield risk premia is the difference between the observed yields and the hypothetical yields given by the expectations hypothesis:

$$yr_t^n = \frac{1}{n}\sum_{i=1}^{n-1}(lnP_t^i - lnP_t^{i+1} - E_t(y_{t+i}^1)). \tag{3.3.14}$$

In order to estimate our term structure model we follow the approach of Chen and Scott (1993) and assume that a subset of the yields are estimated without a measurement error. This holds for for l linear combinations of observed yields, where l is the number of latent factors in the model and the remaining $N-l$ linear combinations differ from the predicted value by a small measurement error. Let $\mathbf{Y_t^1}$ denotes the $l \times 1$ vector consisting of those linear combinations of yields that are treated as priced without error and $\mathbf{Y_t^2}$ the remaining $(N-l) \times 1$ linear combinations. Then, the measurement specification of government yields is

$$\begin{bmatrix} Y_t^1 \\ Y_t^2 \end{bmatrix} = \begin{bmatrix} A_t^1 \\ A_t^2 \end{bmatrix} + \begin{bmatrix} B_t^1 \\ B_t^2 \end{bmatrix} + \begin{bmatrix} X_t^l \\ X_t^m \end{bmatrix} \begin{bmatrix} 0 \\ \Sigma_e \end{bmatrix} u_t^e, \tag{3.3.15}$$

where $\mathbf{\Sigma_e}$ is taken to be diagonal and we denote as $\mathbf{u_t} = [\mathbf{0}\ \ \mathbf{\Sigma_e}]'\mathbf{u_t^e}$. A_t^i and B_t^i for $i = 1, 2$ are calculated by stacking 3.3.12 and 3.3.13 respectively for the appropriate maturity n and $\mathbf{\Sigma_e}$ determines the variance of the measurement error with $\mathbf{u_t^e} \sim N(\mathbf{0}, \mathbf{I})$. We impose in our model the following parameter restrictions $\mathbf{\Sigma_{lm}} = \mathbf{0}, \mathbf{\Sigma_{ll}} = \mathbf{I_l}\delta_{\mathbf{1l}} \geq \mathbf{0}, \boldsymbol{\mu}_{\boldsymbol{l}}^{\boldsymbol{Q}} = \mathbf{0}$ and $\mathbf{\Sigma_{mm}}$ is a lower triangular matrix.

The structure of the factor loading $\boldsymbol{\phi}_{\boldsymbol{ll}}^{\boldsymbol{Q}}$ is that proposed by Hamilton and Wu (2012). The reduced form parameters, i.e. the parameters of a restricted vector autoregression for the yields, are collected in vector $\boldsymbol{\pi}$ and can be conveniently estimated by least squares methods. Given $\hat{\boldsymbol{\pi}}$, the structural parameter vector $\boldsymbol{\theta}$ can be estimated by the MCSE method. The MCSE estimator is based on the assumption that the reduced form parameters coincide with a function of the structural parameters, $\hat{\boldsymbol{\pi}} = g(\boldsymbol{\theta})$.

3.3.2 Model Identification

The structural form of the affine model that we previously presented can be changed to a reduced form according to Hamilton and Wu (2012).We briefly present the set of equations for the reduced form (for more details see Hamilton and Wu (2012)):

$$X_t^m = A_m^* + \phi_{mm}^* X_{t-1}^m + \phi_{m1}^* Y_{t-1}^1 + u_{mt}^*, \tag{3.3.16}$$

$$Y_t^1 = A_1^* + \phi_{1m}^* X_{t-1}^m + \phi_{11}^* Y_{t-1}^1 + \psi_{1m}^* X_t^m + u_{1t}^*, \tag{3.3.17}$$

$$Y_t^2 = A_2^* + \phi_{2m}^* X_t^m + \phi_{21}^*, Y_t^1 + u_{2t}^* \tag{3.3.18}$$

where

$$A_1^* = A_1 + B_{1l}c_l - B_{1l}\rho_{ll}B_{1l}^{-1}A_1, \tag{3.3.19}$$

$$A_2^* = A_2 - B_{2l}B_{1l}^{-1}A_1, \tag{3.3.20}$$

$$A_m^* = c_m - \rho_{ml}B_{1l}^{-1}A_1, \tag{3.3.21}$$

$$\phi_{11}^* = B_{1l}\rho_{ll}B_{1l}^{-1}, \tag{3.3.22}$$

$$\phi_{1m}^* = B_{1l}\rho_{ll} - B_{1l}\rho_{ll}B_{1l}^{-1}B_{1m}, \tag{3.3.23}$$

$$\phi_{2m}^* = B_{2m} - B_{2l}B_{1l}^{-1}B_{1m}, \tag{3.3.24}$$

$$\phi_{21}^* = B_{2l}B_{1l}^{-1}, \tag{3.3.25}$$

$$\phi_{m1}^* = \rho_{ml}B_{1l}^{-1}, \tag{3.3.26}$$

$$\phi_{mm}^* = \rho_{mm} - \rho_{ml}B_{1l}^{-1}B_{1m}, \tag{3.3.27}$$

$$\psi_{1m}^* = B_{1m}, \tag{3.3.28}$$

and

$$Var\begin{bmatrix} u^*_{mt} \\ u^*_{1t} \\ u^*_{2t} \end{bmatrix} = \begin{bmatrix} \Omega^*_m & 0 & 0 \\ 0 & \Omega^*_1 & 0 \\ 0 & 0 & \Omega^*_2 \end{bmatrix} = \begin{bmatrix} \Sigma_{mm}\Sigma'_{mm} & 0 & 0 \\ 0 & B_{1l}B'_{1l} & 0 \\ 0 & 0 & \Sigma_e\Sigma'_e \end{bmatrix}. \tag{3.3.29}$$

Full information maximum likelihood estimation is obtained by treating the three blocks,$u^*_{1t}, u^*_{2t}, u^*_{mt}$ separately since they are independent. Also δ_0 cannot be estimated separately from the OLS regression (3.3.5) because the risk-free rate serves a dependent variable not only in the regression (3.3.5) but also but also in the regression (3.3.19). Following the technique of Hamilton and Wu (2012) in order the model to be just identified we take three further restrictions on the matrix of the factor loadings $\boldsymbol{\phi^Q}$.

Table B.0.1 presents the mapping between structural and reduced form parameters with $N_f = N_l + N_m$ where N_l is the number of unobserved pricing factors and N_m the number of observable factors. When the number of parameters in the structural form of the model is equal to the number of reduced-form parameters then the model is just-identified. Also, when the reduced form parameters are more than those in the structural form, the case where the model imposes overidentifying restrictions, one can still estimate structural parameters as functions of the unrestricted reduced-form estimates. The problem arises when more than one value for the parameter vector in the structural form is associated with the same reduced-form parameter vector, then the model is unidentified. As a result, there is no way to use the observed data to distinguish between the alternative possibilities of parameters (Hamilton and Wu (2012)).

3.3.3 Estimation of the Gaussian term structure model

The main idea of the MCSE method is to use the Wald test to test the hypothesis that $\boldsymbol{\pi} = g(\boldsymbol{\theta})$, where $\boldsymbol{\theta}$ is a known vector of parameters. As we mentioned earlier we denote by $\boldsymbol{\pi}$ the vector consisting of all reduce-form parameters. Suppose $\mathcal{L}(\boldsymbol{\pi}; \mathbf{Y_t})$ is the log-likelihood for the entire sample and $\hat{\boldsymbol{\pi}} = arg\,max\mathcal{L}(\boldsymbol{\pi}; \mathbf{Y_t})$ is the vector of full information maximum likelihood (FIML) estimates. Also, we assume that $\hat{\mathbf{R}}$ is a consistent estimate of the information matrix, which satisfies the following equation

$$\mathbf{R} = -\frac{1}{T}E\left[\frac{\vartheta^2\mathcal{L}(\boldsymbol{\pi}; \mathbf{Y})}{\vartheta\boldsymbol{\pi}\vartheta\boldsymbol{\pi}'}\right]. \tag{3.3.30}$$

The MCSE is then given by:

$$\min_{\boldsymbol{\theta}} T(\hat{\boldsymbol{\pi}} - g(\boldsymbol{\theta}))' \mathbf{R} (\hat{\boldsymbol{\pi}} - g(\boldsymbol{\theta})), \tag{3.3.31}$$

where $\mathbf{R}$ is the information matrix of the full information maximum likelihood function $\mathcal{L}(\boldsymbol{\theta}; \mathbf{Y})$. The minimal value that is found by this estimator would have an asymptotic $\chi^2(q)$ distribution under the null hypothesis where q is the dimension of $\boldsymbol{\pi}$. According to Rothenberg (1973) from (3.3.31) we can choose an estimate $\hat{\boldsymbol{\theta}}$ which minimizes the chi-square statistic for the estimation.

In the case of a just identified model the minimum value attainable for (3.3.31) is zero. Then equation (3.3.31) equivalently become

$$\min_{\boldsymbol{\theta}} (\hat{\boldsymbol{\pi}} - g(\boldsymbol{\theta}))' (\hat{\boldsymbol{\pi}} - g(\boldsymbol{\theta})). \tag{3.3.32}$$

When the objective function (3.3.34) is equal to zero the estimators that result from the maximum likelihood estimation and the MCSE method are asymptotically equivalent. The information matrix for all reduced-form parameters takes the form

$$\hat{R} = \begin{bmatrix} \hat{R}_m & 0 & 0 \\ 0 & \hat{R}_1 & 0 \\ 0 & 0 & \hat{R}_2 \end{bmatrix} \tag{3.3.33}$$

where

$$\hat{R}_i = \begin{bmatrix} \hat{\Omega}_i^{*-1} \otimes T^{-1} \sum_{t=1}^{T} x_{it} x_{it}' & 0 \\ 0 & \frac{1}{2} D_{qi}' (\hat{\Omega}_i^{*-1} \otimes \hat{\Omega}_i^{*-1}) D_{qi} \end{bmatrix}, \tag{3.3.34}$$

for D_N the $N^2 \times N(N+1)/2$ duplication matrix satisfying $D_N vech(\Omega) = vec(\Omega)$. The structural measurement errors $\boldsymbol{\Sigma_e}$ only exist in the block $\boldsymbol{\Omega_2^*}$ and these parameters are just-identified by the diagonal elements of $\hat{\boldsymbol{\Omega}}_{\mathbf{2}}^*$. Then the minimum chi square estimates of $\boldsymbol{\Sigma_e}$ are obtained from the square roots of diagonal elements of $\boldsymbol{\Omega_2^*}$. The factor loadings submatrix for the latent factors takes the following form

$$\phi_{ll}^{Q} = \begin{bmatrix} \phi_{33} & 0 & 0 \\ \phi_{43} & \phi_{44} & \phi_{45} \\ \phi_{53} & \phi_{54} & \phi_{55} \end{bmatrix}, \tag{3.3.35}$$

where $\phi_{44} = \phi_{55}$ and $\phi_{45} < \phi_{54}$.In order to optimize the objective function,we need to estimate 66 unknown parameters, 5 in $\boldsymbol{\delta_1}$,1 in δ_0, 25 in $\boldsymbol{\phi}$, 22 in $\boldsymbol{\phi^Q}$, 6 in $\boldsymbol{\Sigma}$, 5 in $\boldsymbol{\mu}$ and 2 in $\boldsymbol{\mu^Q}$. Since we estimate the model parameters we can estimate the coefficients

$\alpha_n, \mathbf{b_n}$ from the recursive equations (3.3.12), (3.3.13). Based on these estimations from equation (3.3.11) and the yields that are measured with no error we can solve numerically for the unknown latent factors. The results of the parameter estimation under the risk-neutral and historical probability measure are presented in table 4.3.1.

3.4 Sequential monitoring of the term structure model

3.4.1 General framework

For the monitoring of the Gaussian ATSM we use the control chart procedures described in this chapter. Before we proceed in the sequential monitoring analysis it is essential first to introduce some basic concepts of our analysis.

Following the approach of Schmid and Tzotchev (2004) instead of monitoring directly the vector of parameters $\boldsymbol{\xi} = (\boldsymbol{\mu}, \boldsymbol{\phi}, \boldsymbol{\mu^Q}, \boldsymbol{\phi^Q}, \boldsymbol{\Sigma})$ we monitor the bond yield process $\mathbf{Y_t^n}$ since a change in the entire vector of parameters or in a part of it could affect the yield curve using the set of equations described in section 4.3. When the process is in-control we assume that there is no change in the vector of the model parameters $\boldsymbol{\xi}$. The theoretical bond yields are estimated through equation (3.3.11) and are affine non-linear functions of the state variables $\mathbf{X_t}$. As a result, under the in-control condition at every time t the expected value of the observed zero coupon bond yields $\mathbf{Y_t^{n*}}$ will be equal to the expected value of the target bond yields $\mathbf{Y_t^n}$ estimated from equation (3.3.11). This means that when the process is in-control we want

$$E_0(\mathbf{Y_t^{n*}}) = E_0(\mathbf{Y_t}^{\mathbf{n}}),$$

or else

$$\begin{aligned} E_0(\mathbf{Y_t^n}) &= A_n + \mathbf{B_n^{'}} \mathbf{X_t} \\ &= -\frac{a_n}{n} - \frac{\mathbf{b_n^{'}}}{n} \mathbf{X_{0,t}}, \end{aligned}$$

for ever maturity n. The notion 0 means that the underlying quantity refers to the in-control condition. The selection of the period where the process is in-control could be quite challenging in finance.

At every time point t a control statistic is appropriately constructed. In order to decide if the process is out-of-control at time t, it is necessary the determination of a control limit h that defines the rejection area. If the value of the control statistic lies within the acceptance area then the monitoring process is considered to be in

the in-control state. The critical value h is determined in such a way that the ARL to be equal to a predetermined value k_1 via a simulation study. When the process is in the in-control state, the average run length (ARL_0) denotes the average number of observations or samples until a signal is obtained. In our analysis we assume that the value of the ARL_0 is equal to 11 months. In order to find the control limit a starting value of the control limit is chosen. Under the assumption that the process is in-control and the target values are identified, the data for the state evolution process and the bond yields are generated for their distributions are presented at section 4.3. These simulated values are applied to each control chart procedure and the stopping times, when the control statistic exceeds the control limit, of the control chart are recorded. This procedure is repeated for 10^4 iterations and the estimated run length in the in-control state is the average of simulated stopping times. If now the estimated ARL_0 is greater or lower from its prespecified value by an error equal to 1% a new value for the control limit is chosen. Using this new control limit a new iteration procedure is performed so as to estimate the stopping times and the ARL_0. This procedure is repeated for 10^4 iterations. The control limits that fulfill the error condition are chosen as the appropriate control limits. The detection ability of a control chart can be evaluated and compared with other control charts via the ARL_1. The ARL_1 indicates the average number of observations or samples that is required until the control chart provides a signal when there is a change in the target process. It is obvious that we desire the value of ARL_1 to be as small as it can be and the opposite for the ARL_0.

3.4.2 Control chart procedures

For the sequential monitoring we use six categories of control chart procedures: Modified EWMA control chart based on the Mahalanobis distance (ModMah), modified chart based on the Multivariate EWMA Statistic (ModMEWMA), EWMA Residual chart based on the Mahalanobis Distance (ResidMah), Residual chart Based on the multivariate EWMA Statistic (ResidMEWMA), Multivariate Cumulative Sum control chart (MCUSUM) and Multivariate Modified EWMA control chart (MMOEWMA).

3.4.2.1 EWMA control charts

The EWMA control charts are very effective for the detection of small shifts in the monitoring process (Montgomery (2013)). Lowry et al. (1992) generalized the univariate EWMA control chart procedure for the multivariate case.

Suppose that $\mathbf{Y_t^{n,*}} = [Y_t^{1,*}, \ldots, Y_t^{N,*}]$ is the vector of observed zero-coupon bond yields at time t with maturity $n = 1, 2, \ldots, N$. The univariate EWMA control chart is based on the (univariate) EWMA recursion applied on the Mahalanobis distance. The Mahalanobis distance is referred to be the distance of observed yields from to its in-control mean $\mu_\mathbf{t} = \mathbf{E_0}(\mathbf{Y_t^{n,*}})$ and is measured by

$$T_{t,n} = (\mathbf{Y_t^{n,*}} - \boldsymbol{\mu_t})' \mathbf{Cov_0}(\mathbf{Y_t^{n,*}})^{-1} (\mathbf{Y_t^{n,*}} - \boldsymbol{\mu_t}), t \geq 1. \tag{3.4.1}$$

The univariate EWMA statistic based on the Mahalanobis distance is given by

$$Z_{t,n} = (1 - \lambda) Z_{t-1,n} + \lambda T_{t,n}, \tag{3.4.2}$$

for $t \geq 1$. The starting value $Z_{0,n}$ is set equal to $E_0(T_{t,n}) = N$. A signal is given if $Z_{t,n} > h$. The control limit $h > 0$ that determines the rejection area, is estimated through simulation for a predetermined value of the in-control average run length (ARL_0). For the calculation of the control statistic we need to estimate the moments for the observed yields when the process is in-control (for details see Appendix A.1). The in-control mean $\boldsymbol{\mu}_t$ is defined as

$$E_0(\mathbf{Y_t^{n,*}}) = A_n + \mathbf{B_n'}(\boldsymbol{\mu^Q} + \boldsymbol{\phi^Q} E_0(\mathbf{X_{t+1}})). \tag{3.4.3}$$

The in-control covariance matrix $\mathbf{Cov_0}(\mathbf{Y_t^{n,*}})$ is

$$\mathbf{Cov_0}(\mathbf{Y_t^{n,*}}) = \mathbf{B_n'}(\boldsymbol{\phi^Q} Var_0(\mathbf{X_t}) \boldsymbol{\phi^{Q'}} + \boldsymbol{\Sigma}) \mathbf{B_n} + \mathbf{U}, \tag{3.4.4}$$

where $\boldsymbol{\Sigma}$ is the covariance matrix in equation (3.3.1) and $\mathbf{U} = E(\mathbf{u_t u_t'})$.

MEWMA control charts are constructed by applying a multivariate EWMA recursion directly to the components of the monitoring characteristic $\mathbf{Y_t^{n,*}}$. The advantage of this approach is that each characteristic element obtains its own smoothing factor and as a result allows for more flexibility compared to the univariate EWMA (Golosnoy and Schmid (2007)). The multivariate EWMA statistic has the following form

$$\mathbf{Z}_{t,n} = (\mathbf{I} - \mathbf{R})^t \mathbf{Z}_{t-1,n} + \mathbf{R} \mathbf{Y_t^{n,*}}, t \geq 1, \tag{3.4.5}$$

or else

$$\mathbf{Z}_{t,n} = (\mathbf{I} - \mathbf{R})^t \mathbf{Z}_{0,n} + \mathbf{R} \sum_{\upsilon=0}^{t-1} (\mathbf{I} - \mathbf{R})^\upsilon \mathbf{Y_t^{n,*}}, \tag{3.4.6}$$

where $\mathbf{I}$ is the $k \times k$ identity matrix and $\mathbf{R} = diag(r_1, r_2, \ldots, r_k)$ is $k \times k$ diagonal matrix with diagonal elements $0 < r_i \leq 1$, $i \in \{1, 2, \ldots, k\}$, k is the total number of bond yields at each time t. The starting value $\mathbf{Z}_{0,n}$ is $E_0(\mathbf{T}_{t,n}) = A_n + \mathbf{B_n} E_0(\mathbf{X_t})$,

with E_0 is denoted the mean value when the monitoring process is in-control. The covariance matrix of the multivariate EWMA statistic $\mathbf{Z}_{t,n}$ in the in-control state is given by

$$Cov_0(\mathbf{Z_{t,n}}) = \mathbf{R}\Big(\sum_{i,j=0}^{t-1}(\mathbf{I}-\mathbf{R})^i Cov_0(\mathbf{Y_t^{n,*}})(\mathbf{I}-\mathbf{R})^J\Big)\mathbf{R}. \tag{3.4.7}$$

Assuming that $Cov_0(\mathbf{X_t}, \mathbf{u_t}) = \mathbf{0},\ E(\mathbf{u_t}) = \mathbf{0},\ E(\mathbf{u_t u_t})' = \mathbf{U},\ E(\mathbf{u_t u_s})' = \mathbf{0}, t \neq s$, then

$$Cov_0(\mathbf{Z_{t,n}}) = \mathbf{R}\big(\mathbf{B_n'}(\boldsymbol{\mu^Q}\boldsymbol{\mu_{0,X}} + \boldsymbol{\phi^Q}\sigma^2_{\mathbf{0,X}})\mathbf{B_n} + \mathbf{U}\big)\frac{\mathbf{I}}{\mathbf{I}-(\mathbf{I}-\mathbf{R})^2}\mathbf{R}. \tag{3.4.8}$$

A signal is given if

$$(\mathbf{Z}_{t,n} - E_0(\mathbf{Z}_{t,n}))' Cov_0(\mathbf{Z}_t)^{-1}(\mathbf{Z}_{t,n} - E_0(\mathbf{Z}_{t,n})) > h$$

where the expected value of the control statistic when the process is in-control is

$$E_0(\mathbf{Z}_t) = (\mathbf{I}-\mathbf{R})^{\mathbf{t}}\mathbf{Z_0} + A + \mathbf{B_n'}(\mathbf{I}-(\mathbf{I}-\mathbf{R})^{\mathbf{t}}\boldsymbol{\mu_{0,X}}. \tag{3.4.9}$$

where $\boldsymbol{\mu_{0,X}} = E_0(\mathbf{X_t})$. The EWMA is used extensively in time series modeling and since it can be viewed as a weighted average of all past and current observations, it is very insensitive to the normality assumption of the monitoring process. Small values of the smoothing parameter give more weight to recent values. For the proof of the previous equations see appendix A.1.1 and appendix A.1.2.

3.4.2.2 Residual based control charts

For the residual control charts the procedures based on the Mahalanobis distance and the multivariate EWMA statistic for the series of the observed zero-coupon bond yields are now replaced by the residuals. We assume that the vector of residuals is defined as the deviations of the observed yields at time t from their conditional expectations when the process is in-control, $E_0(\mathbf{Y_t^{n,*}}/\mathbf{Y_{t-1}^{n,*}})$. We suppose that the vector of the residuals is $\mathbf{d_t} = Y_t^{n,*} - E_0(\mathbf{Y_t^{n,*}}/\mathbf{Y_{t-1}^{n,*}})$. Also we assume that $Cov_0(X_t, \mathbf{u_t}) = \mathbf{0},\ E(\mathbf{u_t}) = 0,\ E(\mathbf{u_t u_t})' = \mathbf{U}$ and $E(\mathbf{u_t u_s})' = 0,$ for all $t \neq s$, then $E_0(\mathbf{d_t}) = \mathbf{0}$ and $E_0(\mathbf{d_t}, \mathbf{d_s}) = \mathbf{0},$ for all $t \neq s$. The control statistic for the Residual EWMA chart based on the Mahalanobis distance is

$$Z_t = (1-\lambda)^t Z_0 + \lambda T_{d,t},\ t \geq 1, \tag{3.4.10}$$

with the Mahalanobis distance

$$T_{d,t} = \mathbf{d_t'}\boldsymbol{\Sigma_d^{-1}}\mathbf{d_t}.$$

Also, the in-control covariance matrix of the vector of the residuals is

$$Cov_0(\mathbf{d_t}) = \mathbf{B_n^{'}}(\boldsymbol{\phi}^{Q} V_0(\mathbf{X_{t-1}})\boldsymbol{\phi}^{Q'} + \mathbf{\Sigma_t})\mathbf{B_n} + \mathbf{U}, \tag{3.4.11}$$

For the residual chart based on MEWMA statistic the control statistic is

$$\boldsymbol{Z}_t = (\boldsymbol{I} - \boldsymbol{R})\boldsymbol{Z}_{t-1} + \boldsymbol{R}\boldsymbol{d}_t,\ t \geq 1, \tag{3.4.12}$$

with $\boldsymbol{Z}_t = \mathbf{0}$. The covariance matrix of the control statistic is given by

$$Cov_0(\mathbf{Z_t}) = \mathbf{R}\big(\mathbf{B_n^{'}}\mathbf{\Sigma_Y}\mathbf{B_n} + \mathbf{U}\big)\frac{\mathbf{I}}{\mathbf{I} - (\mathbf{I} - \mathbf{R})^{\mathbf{2}}}\mathbf{R}. \tag{3.4.13}$$

For the proof of the previous equations see appendix A.1.3.

3.4.2.3 Multivariate CUSUM control charts

The CUSUM control chart is used to monitor a process based on samples taken from the process at given time periods. The CUSUM chart shows the accumulated information of current and previous samples. CUSUM control charts are a good alternative when small shifts are important (Montgomery (2013)) and can be constructed for individual observations or for groups of observations. Now we consider the case of individual observations and monitoring the process mean. The MCUSUM is an extension of the univariate CUSUM control chart. It is a procedure that uses the cumulative sum of deviations of each random vector previously observed, compared to the nominal value to monitor the vector of means of a multivariate process (Cunha et al. (2013)). In our analysis we follow the MCUSUM control chart proposed by Crosier (1988). The MCUSUM procedure can be derived as

$$C_t = \sqrt{(\mathbf{S_t} + \mathbf{Y_t^{n,*}} - \mu_{\mathbf{0}})'\mathbf{\Sigma}^{-1}(\mathbf{S_t} + \mathbf{Y_t^{n,*}} - \mu_{\mathbf{0}})}, \tag{3.4.14}$$

where $\mathbf{\Sigma}$ is the variance-covariance matrix of the data, $\mu_{\mathbf{0}}$ is the in-control mean of the bond yields and $\mathbf{S}_i$ are the cumulative sums defined as

$$\mathbf{S}_i = \begin{cases} 0 & \text{if} \quad C_t \leq \kappa, \\ (\mathbf{S}_{t-1} + \mathbf{Y_t^{n,*}} - \mu_{\mathbf{0}})(1 - \frac{\kappa}{C_t}) & \text{if} \quad C_t > \kappa, \end{cases}$$

where the reference value $\kappa > 0$ is related to the magnitude of change and $\mathbf{S_0} = \mathbf{0}$. An out-of-control signal is given if $\mathbf{Z}_t > h$, with h being the control limit estimated for a pre-defined ARL_0 and $\mathbf{Z}_t = (\mathbf{S}_t'\mathbf{\Sigma}^{-1}\mathbf{S}_t)$.

3.4.2.4 Multivariate Modified EWMA (MMOEWMA) control charts

Patel and Divecha (2013) introduced the MMOEWMA control chart for detecting both large and small shifts in a first order vector autoregressive VAR(1) process. Their approach is an extension of their univariate Modified EWMA chart (Patel and Divecha (2011)). The MMOEWMA control chart statistic is a correction of the MEWMA chart statistic by adding the sum of the last change in the monitoring process. An advantage of the Modified MEWMA chart is that corrects MEWMA statistic from the inertia problem. The MMOEWMA control statistic takes into consideration each current change in the underlying process by giving full weight in addition to the past observations. In our work we adapt and extend their work in a financial application estimating appropriately the expected value and the covariance of the control statistic.

The control statistic for the MMOEWMA control chart based on the multivariate EWMA recursion is

$$\mathbf{Z_t} = (\mathbf{I} - \mathbf{R})\mathbf{Z_{t-1}} + \mathbf{R}\mathbf{Y_{t-1}} + (\mathbf{Y_t} - \mathbf{Y_{t-1}}),\ t \geq 1, \tag{3.4.15}$$

It can be proved by repeated substitution in equation (3.4.15) that

$$\mathbf{Z_t} = (\mathbf{I} - \mathbf{R})^{\mathbf{t}}\mathbf{Z_0} + \mathbf{R}\sum_{j=0}^{t-1}(\mathbf{I} - \mathbf{R})^{\mathbf{j}}\mathbf{Y_{t-j}} + \sum_{j=0}^{t-1}(I - R)^j(\mathbf{Y_{t-j}} - \mathbf{Y_{t-j-1}}). \tag{3.4.16}$$

The expected value of the statistic is

$$E_0(\mathbf{Z_t}) = (\mathbf{I} - \mathbf{R})^{\mathbf{t}}\mathbf{Z_0} + A_n + \mathbf{B_n^{'}}(\mathbf{I} - (\mathbf{I} - \mathbf{R})^{\mathbf{t}}\boldsymbol{\mu_{0,X}},$$

where $\boldsymbol{\mu_X} = E_0(\mathbf{X_t})$. Under the assumption that $Cov_0(X_t, \mathbf{u_t}) = 0$, $E(\mathbf{u_t}) = \mathbf{0}$, $E(\mathbf{u_t}\mathbf{u_t})^{'} = \mathbf{U}$, we estimate the covariance matrix of the control statistic $\mathbf{Z_t}$ is

$$Cov_0(\mathbf{Z_t}) = \mathbf{R}\big(\big(\mathbf{B_n^{'}}\boldsymbol{\Sigma_Y}\mathbf{B_n} + \mathbf{U}\big)\frac{\mathbf{I}}{\mathbf{I} - (\mathbf{I} - \mathbf{R})^{\mathbf{2}}}\big)\mathbf{R} + \mathbf{R}\frac{\mathbf{I}}{\mathbf{I} + \mathbf{R}}\boldsymbol{\Sigma_Y}.$$

The MMOEWMA control chart gives an out-of-control signal when

$$(\mathbf{Z_t} - E_0(\mathbf{Z}_t))^{'}(Cov_0(\mathbf{Z_t}))^{-1}(\mathbf{Z_t} - E_0(\mathbf{Z}_t)) > h,$$

where $h > 0$ is estimated for a determined value of ARL through a simulation study. For the proof of the previous equations see appendix A.1.4.

3.5 Simulation Study

In this section we define the various shifts in the yield curve and eventually the out-of-control situations. Also, we analyse the detection power of the different types of control charts in order to detect changes in the parameters of the term structure model and the yield curve through simulations.

3.5.1 Basic framework

The performance and the detection ability of the proposed control charts is analyzed through a simulation study for different shocks in the parameters of the term structure model. The out-of-control simulation study that determines the ability of a control chart to detect the changes in the monitoring process is divided in three cases using an estimation window of $n = 40$. First, we examine changes in the factor loadings of the state evolution process that as we know from (3.3.11) affect the yield curve equation. Second, we simulate a shift in the set of parameters of our model that has as a result a parallel shift in the yield curve. Finally, we simulate non-parallel shifts in the yield curve and for all cases we consider both positive and negative shocks. The smoothing parameter λ in the univariate EMWA control charts based on the Mahalanobis distance is $\lambda = \{0.1, 0.2, 0.25, 0.35, 0.45, 0.5, 0.75, 0.9\}$. The multivariate EWMA control charts are constructed with all smoothing parameters in the main diagonal equal $r = r_1 = r_2 = \cdots = r_N = \lambda I$. The reference parameter for the MCUSUM control charts takes the values $g = \{0.1, 0.3, 0.5, 0.7, 1, 1.5, 2, 2.5\}$. For each control chart scheme for positive or negative shocks we have 5000 iterations.

For the simulation of the in-control process in each control chart procedure, specifically the mean and the covariance matrix of the state evolution process and the bond yields, we use the following procedure:
Step 1 Generate data from the state evolution process $\mathbf{X} \sim N(\mu, \mathbf{\Sigma\Sigma}')$ with known $\boldsymbol{\mu}$ and $\mathbf{\Sigma}$.
Step 2 Generate residual data for the bond yield process $\boldsymbol{U} \sim N(0, \mathbf{I})$.
Step 3 Estimate the covariance matrix of the filtered states $\mathbf{X_{t|t-1}}$ using equation 3.3.1.
Step 4 Estimate the covariance matrix of zero-coupon bond yields at time t conditional on the information until $t-1$, $\mathbf{Y_{t|t-1}}$, using equation (3.3.11).

3.5.2 Modeling the out-of-control cases

3.5.2.1 Change in the factor loadings of the state evolution process

We assume for the out-of-control situation that there is a change in the matrix of the factor loadings $\boldsymbol{\phi}^{Q}$ of the state evolution process $\mathbf{X_t}$. A change in the factor loadings affects the yields of all maturities and causes a shift in the yield curve. Suppose that the new value after the change is

$$\boldsymbol{\phi}^{\boldsymbol{Q},*} = (\boldsymbol{I} + \boldsymbol{D})\boldsymbol{\phi}^{Q}$$

where $\boldsymbol{D}$ is the size of the shock which can be positive or negative. The change $\boldsymbol{D}$ in the parameter $\boldsymbol{\phi}^{Q}$ is a diagonal matrix which takes the values $d = \{\pm 0.05, \pm 0.1, \pm 0.15, \pm 0.2, \pm 0.25, \pm 0.3, \pm 0.35, \pm 0.4\}$, in total 16 proportional changes. Here we assume that the changes are equal. We examine and analyze the results for positive and negative changes separately for convenience. Also we assume that the change it happens at time $t = 1$. The in-control mean and covariance matrix of the control statistic in each control chart are estimated using the results from section 4.4. For every control scheme we have in total 64 cases.

3.5.2.2 Parallel shifts in the Yield curve

The second out-of-control situation is when we assume changes in the entire parameter set $\boldsymbol{\xi} = \{\boldsymbol{\mu}, \boldsymbol{\phi}, \boldsymbol{\mu}^{\boldsymbol{Q}}, \boldsymbol{\phi}^{\boldsymbol{Q}}, \boldsymbol{\Sigma}\}$ of the target process. The new values after the changes are

$$\boldsymbol{\xi}^{*} = \{\boldsymbol{\mu}^{*}, \boldsymbol{\phi}^{*}, \boldsymbol{\mu}^{\boldsymbol{Q},*}, \boldsymbol{\phi}^{\boldsymbol{Q},*}, \boldsymbol{\Sigma}^{*}\}$$

or

$$\boldsymbol{\xi}^{*} = \{(\boldsymbol{I} + \boldsymbol{D})\boldsymbol{\mu}, (\boldsymbol{I} + \boldsymbol{D})\boldsymbol{\phi}, (\boldsymbol{I} + \boldsymbol{D})\boldsymbol{\mu}^{\boldsymbol{Q}}, (\boldsymbol{I} + \boldsymbol{D})\boldsymbol{\phi}^{\boldsymbol{Q}}, (\boldsymbol{I} + \boldsymbol{D})\boldsymbol{\Sigma}\}$$

where $d = \{\pm 0.05, \pm 0.1, \pm 0.15, \pm 0.2, \pm 0.25, \pm 0.3, \pm 0.35, \pm 0.4\}$ the size of the shocks. The modeling of the changes we described has as a result the observed yield curve to shift in a parallel way. Litterman and Scheinkman (1991) show that the parallel shift explains on average around 89 percent of the variation of the U.S. yield curve. We follow the assumption of Schmid and Tzotchev (2004) that the parallel shift holds even for the shorter maturities. A parallel shift in the yield curve is a shift in in the yields on all maturities of the same size. The shocks in the parameters of the state process $\mathbf{X_t}$ are incorporated in the yield curve equation through (3.3.11). The new observed yields are estimated by adding to the theoretical yields the error term $\mathbf{u}_t \sim N(0, \mathbf{I})$. For every control scheme that we examine parallel shifts we have in total 64 cases.

3.5.2.3 Non-parallel shifts in the Yield Curve

In reality, bond yields does not always have parallel shifts, an argument that Litterman and Scheinkman (1991) mention in their work. A non-parallel shift in the yield curve indicates that the yields do not change by the same number of basis points across the curve for all maturities (Fabozzi (2007)).We have two types of non-parallel yield curve shifts: First a twist in the slope of the yield curve and second a change in the curvature of the yield curve. A twist in the yield curve can be a either a flattening or a steepening of the yield curve. The flattening indicates that the spread between the short-term and the long-term yield has decreased. This can happen when either the short-term yields are increasing more than longer-term yields or long-term rates declining more than the short-term rates. A reason for this behavior may be that the market expects the FED to increase the Fed Funds rate (FFR) or due to lower longer term inflation expectations. A steepening of the yield curve occurs when the yield spread between the long-term and the short-term Treasury has increased. This happens when long-term yields increase more than short-term yields, or long-term yields decline by less than short-term yields. The steepening of the yield curve usually is a result of the market's increase expectation for inflation or if the market demands a higher risk premium.

The second type of non-parallel shifts is a change in the curvature of the yield curve known as butterfly shifts. The changes on yields of the short-term and long-term maturities differ from the changes on the yields in the intermediate maturities. Butterfly shifts are divided into positive and negative shifts. A positive butterfly means that the yield curve has less curvature. Specifically, when bond yields increase, the yields with the short-term and long-term maturities increase more than the yields with intermediate maturities. If now bond yields decrease, the yields with the short- and long-term maturities decrease less than the intermediate maturities. In the opposite, a negative butterfly means the yield curve has more curvature. If now, bond yields in the short- and long-term maturities increase, then yields in the intermediate maturities will increase more. Finally, when yields with short- and long-term maturity decrease, then yields in the intermediate maturities decrease less.

Fabozzi (2007) mentioned that these types of shifts in the yield curve have not been found to be independent and that yields in the short-end tend to be more volatile than yields in the long-end of the yield curve. In our simulation approach even though there is a large number of cases, we present some examples for steepening and change in the curvature of the yield curve, having positive and negative shocks.

Steepening of the Yield Curve

For the steeping of the yield curve we assume in the case of the increase of the yield curve that the increase in the 10-year Treasury bond yield is greater than the increase in the 3-month bond yield. Also, we assume that the increase d_i of the bond yield with maturity $i = 1, \ldots, n$ months has the following restriction: $d_3 < d_{24} < d_{36} < d_{48} < d_{60} < d_{120}$. The second case we consider is when the decrease in the longer-end maturity bond, the 10-year bond, is greater than the decrease in the shorter-end maturity bond yield, the 3-month bond. The restriction in this situation is: $-d_3 < -d_{24} < -d_{36} < -d_{48} < -d_{60} < -d_{120}$. For simplicity we assume that the change happens in the slope of the yield curve equation and each yield with maturity i has from his previous $i-1$ maturity a shift of 3 percent. The opposite happens for negative shocks. As a result the change in each vector of zero-coupon bond yields at time t has the following form for positive shocks

$$\mathbf{I}+\mathbf{D} = \begin{bmatrix} 1+d_3 & 0 & 0 & 0 & 0 & 0 \\ 0 & 1+d_{24} & 0 & 0 & 0 & 0 \\ 0 & 0 & 1+d_{36} & 0 & 0 & 0 \\ 0 & 0 & 0 & 1+d_{48} & 0 & 0 \\ 0 & 0 & 0 & 0 & 1+d_{60} & 0 \\ 0 & 0 & 0 & 0 & 0 & 1+d_{120} \end{bmatrix},$$

and for negative shocks

$$\mathbf{I}-\mathbf{D} = \begin{bmatrix} 1-d_3 & 0 & 0 & 0 & 0 & 0 \\ 0 & 1-d_{24} & 0 & 0 & 0 & 0 \\ 0 & 0 & 1-d_{36} & 0 & 0 & 0 \\ 0 & 0 & 0 & 1-d_{48} & 0 & 0 \\ 0 & 0 & 0 & 0 & 1-d_{60} & 0 \\ 0 & 0 & 0 & 0 & 0 & 1-d_{120} \end{bmatrix}.$$

The new theoretical bond yields $\mathbf{Y^n_{1,t}}$ after the positive shift are

$$\mathbf{Y^n_{1,t}} = A_n + (\mathbf{I}+\mathbf{D})\mathbf{B}^{'}_{\mathbf{n}}\mathbf{X_t},$$

and after the negative shift

$$\mathbf{Y^n_{2,t}} = A_n + (\mathbf{I}-\mathbf{D})\mathbf{B}^{'}_{\mathbf{n}}\mathbf{X_t}.$$

The starting shocks for the 3-month Treasury bond yield are seven:$\{\pm 5\%, \pm 10\%, \pm 15\%, \pm 20\%, \pm 25\%, \pm 30\%$ and $\pm\, 35\%\}$. The rest of the bond yield shocks are estimated as previously described. For this simulation example we have for each control chart procedure 56 out-of-control cases.

Change in Curvature of the Yield Curve

For the case when we have changes in the curvature of the yield curve we examine two situations. First, in negative butterfly shifts when the bond yields decrease, the 3-month and the 10-year bond decrease more than the 2-,3-,4-,5-year bond. For simplicity we assume that changes in the 10-year bond are less than these on 3-month bond, $-d_{120} < -d_3$. The shocks for the 3-month yield are $-d_3 = \{-0.05 - 0.1 - 0.15 - 0.2 - 0.25 - 0.3\}$ and for the 10-year yield are $-d_{120} = \{-0.03 - 0.06 - 0.1 - 0.12 - 0.16 - 0.22\}$. Finally the shocks in the intermediate yields are modeled as follows

$$\mathbf{I - D_1} = \begin{bmatrix} 1-d_{24} & 0 & 0 & 0 \\ 0 & 1-d_{36} & 0 & 0 \\ 0 & 0 & 1-d_{48} & 0 \\ 0 & 0 & 0 & 1-d_{60} \end{bmatrix},$$

where $d_i = (1 - d_1)d_{i-1},\ i = 3, 4, 5$. The vector of the starting shocks is $d_1 = \{0.01, 0.03, 0.06, 0.08, 0.1, 0.16\}$ and each subsequent shock for the intermediate mature that occurs from a yield with maturity i to $i+1$ is 3 percent. The total number of the out-of-control cases are 48 in each control chart scheme.

Second, for the positive butterfly shifts the 3-month and 10-year bond yields decrease less than yields in the intermediate maturities. The shocks for the 3-month yield are $-d_3 = \{-0.03 - 0.06 - 0.09 - 0.12 - 0.15 - 0.2\}$ and for the 10-year yield are $-d_{120} = \{-0.05 - 0.1 - 0.12 - 0.15 - 0.2 - 0.25\}$.

$$\mathbf{I - D_1} = \begin{bmatrix} 1-d_{24} & 0 & 0 & 0 \\ 0 & 1-d_{36} & 0 & 0 \\ 0 & 0 & 1-d_{48} & 0 \\ 0 & 0 & 0 & 1-d_{60} \end{bmatrix},$$

where $d_i = (1 - d_1)d_{i-1},\ i = 3, 4, 5$, the vector of the starting shocks are $d_1 = \{-0.07 - 0.12 - 0.14 - 0.18 - 0.25 - 0.30\}$.

3.5.3 Simulation study results

In this section we present the simulation results for the changes in the yield curve that we described in the previous section. We demonstrate the best $ARLs_1$ for each case and the appropriate smoothing parameters. In addition, we briefly discuss for

the proposed control charts how the detection of the out-of-control situation evolves for the various values of the smoothing parameter or reference values (in the case of MCUSUM procedure).

3.5.3.1 Change in the factor loading of the state factor process

The results from the simulation study when we have positive shocks in the factor loading of the state process are summarized in table 3.5.1. Among the control chart procedures the best performing charts are the chart based on the multivariate MEWMA (ModMEWMA), the residual chart based on the multivariate EWMA statistic (ResMEWMA) and the MMOEWMA chart. Large shifts in the factor loadings $\boldsymbol{\rho^Q}$ are detected faster in the ModMEWMA and MMOEWMA control charts. In contrast the ResMEWMA control chart is not performing very well. However, it detects faster the small shifts specially when shocks are 5%. All these three charts detect with relative ease the intermediate shifts. Appendix B.1.1 presents the analytical results for the simulation study in case of positive shocks. The results support small values for the smoothing parameter, specifically less than 0.35.

Analyzing now the best performing charts, in the ModMEWA chart as we see in table B.1.2 for a given smoothing parameter value as the shock increases the ARL_1 decreases. The same behavior has the MMOEWMA control chart. The opposite happens for the ResMEWMA chart (see table B.1.4) which makes it unsuitable for detecting large shifts.

Table 3.5.2 presents the best $ARLs_1$ when we have negative shocks in the factor loading of the state process. Again the best performing control charts are the ModMEWMA, the ResMEWMA and the MMOEWMA. Small shifts are detected faster from the ModMEWMA chart, medium shocks from the ResMEWMA control chart and all three charts detect large shifts. The best smoothing parameters values for the ModMEWMA chart are $\lambda = \{0.1, 0.45\}$, for the ResMEWMA and medium and large shifts, the appropriate values of λ are less than 0.5. In general, negative shocks in the matrix of factor loadings are detected faster than positive shocks.

In ModMEWMA and MMOEWMA control chart procedures for a certain level of the smoothing parameter λ, the ARL_1 decreases as the size of the negative shock increases. However, in the ResMEMWA control chart this happens only for $\lambda \leq 0.5$ and for values greater than 0.5 the ARL_1 remains relatively constant despite the size of the negative shock (see table B.1.10).

d	ModMah	ModMEWMA	ResMah	ResMEWMA	MCUSUM	MMOEWMA
0.05	9.97 (0.5)	5.12 (0.35)	9.38 (0.45)	1.01 (0.1)	8(2)	6.66 (0.1)
0.1	9.99 (0.5)	3.52 (0.1)	9.7 (0.45)	1.04 (0.1)	8.22 (2)	3.36 (0.1)
0.15	10.17 (0.5)	2.07 (0.1)	9.68 (0.45)	1.08 (0.1)	8.17 (2)	2.02(0.1)
0.2	10.32 (0.5)	1.45 (0.1)	9.94 (0.25)	1.26 (0.1)	8.25 (2)	1.41(0.1)
0.25	10.33 (0.5)	1.17 (0.1)	10.17 (0.75)	1.86 (0.1)	8.48 (2)	1.17(0.1)
0.3	10.65 (0.5)	1.06 (0.1)	10.32 (0.75)	3.18 (0.1)	8.23(2)	1.05 (0.1)
0.35	10.86 (0.3)	1.02 (0.1)	10.54 (0.75)	6.06 (0.1)	8.79 (2)	1.01(0.1)
0.4	10.96 (0.5)	1.00 (0.1)	10.73 (0.25)	10.25 (0.9)	8.78 (2)	1 (*)

Table 3.5.1: Best out-of-control ARLs values for each positive shock in factor loadings, for n=40 and in-control ARL=11. The corresponding smoothing parameter values are given in parentheses.

d	ModMah	ModMEWMA	ResMah	ResMEWMA	MCUSUM	MMOEWMA
-0.05	9.43 (0.5)	5.69 (0.45)	8.55 (0.25)	9.87 (0.5)	7.99(2)	7 (0.35)
-0.1	9.29 (0.5)	4.59 (0.45)	8.53 (0.2)	5.66 (0.1)	8.57 (0.7)	4.06 (0.1)
-0.15	8.92 (0.5)	3.7 (0.45)	7.84 (0.2)	1.38 (0.1)	7.85 (2)	2.35(0.1)
-0.2	8.73 (0.5)	2.8 (0.45)	6.29 0.25)	1.01 (0.1)	7.74 (2)	1.62(0.1)
-0.25	8.77 (0.5)	2.17 (0.1)	5.98 (0.25)	1 (0.1)	7.46 (2)	1.25(0.1)
-0.3	8.6 (0.5)	1.7 (0.1)	6.72 (0.25)	1 (*)	7.57(2)	1.1 (0.1)
-0.35	8.38 (0.3)	1.4 (0.1)	5.56 (0.25)	1 (*)	7.35 (2)	1.03(0.1)
-0.4	8.24 (0.5)	1.26 (0.1)	5.98 (0.25)	1 (*)	7.6 (2)	1 (0.1)

Table 3.5.2: Best out-of-control ARLs values for each negative shock in factor loadings, for n=40 and in-control ARL=11. The corresponding smoothing parameter values are given in parentheses.

3.5.3.2 Parallel shifts in the Yields curve

The results from the simulation study when we impose parallel shifts in the yield curve for positive and negative shifts are summarized in tables 3.5.3 and 3.5.4 respectively. Regarding to positive shifts all control charts detect large shifts with relative ease. For small shifts the best performing chart is the MCUSUM for value of the reference parameter equal to 0.1. Also, with the exception of the ModMehal chart, medium shifts are detected from all chart procedures. All control chart procedures display the same behavior in terms of ARL_1. As the positive shock in the yield curve increases the ARL_1 decreases for each level of the smoothing parameter or the reference value in the case of the MCUSUM chart.

For negative parallel shifts in the yield curve the best performing charts are the ModMEWMA, ResMah, ResMEWMA and the MMOEWMA. The ModMahal performs well only for negative shifts greater than 20%. The MMOEWMA control scheme is appropriate for medium and large negative shifts with proposed smoothing parameter values less than 0.35. Finally, for negative shocks less than 20% in the MMOEWMA control charts we propose $\lambda = \{0.1, 0.2, 0.25\}$. All control charts have a problem in detecting very small negative shifts with the ResMah performing better for $\lambda = 0.1$. Comparing the result for positive and negative parallel shifts for the detection of positive parallel shifts we have an additional control chart scheme that can be useful, the MCUSUM control chart, and small positive shifts are detected faster than the negative ones. Also, for both types of shifts the charts are on average on the same level to detect medium and large shifts. In comparison with changes in the factor loadings of the state process parallel shifts are detected faster.

The results for the ResMah control chart procedure except for one subcase are all under or equal to six months. Also, in all control charts for a given smoothing parameter value as the shock increases the ARL_1 decreases. For the Mahal, ModMEWMA and ResMah positive shifts in the factor loading of the state process are detected faster than those due to parallel shifts in the yield curve. Positive parallel shifts in the yield curve in ResMEWMA, MCUSUM and MMOEWMA are generally detected faster than positive shifts in the state evolution process.

d	ModMah	ModMEWMA	ResMah	ResMEWMA	MCUSUM	MMOEWMA
0.05	16.48 (0.9)	4.38 (0.45)	3.97	8.04 (0.9)	2.81 (0.1)	3.68 (0.35)
0.1	14.09 (0.9)	3.5 (0.45)	2.38	5.75 (0.1)	1.02 (0.1)	4.68 (0.2)
0.15	10.89 (0.9)	2.69 (0.45)	1.44	1.35 (0.1)	1 (*)	2.82 (0.2)
0.2	7.39 (0.5)	1.98 (0.1)	1.07	1.01 (0.1)	1(*)	1.9 (0.2)
0.25	2.84 (0.1)	1.41 (0.1)	1 (*)	1 (*)	1 (*)	1.4(*)
0.3	11.23 (0.1)	1.19 (0.1)	1 (*)	1 (*)	1 (*)	1.17(*)
0.35	1.01 (0.1)	1.07 (0.1)	1 (*)	1 (*)	1(*)	1.06(*)
0.4	1 (0.1)	1.02(0.1)	1 (*)	1 (*)	1 (*)	1(*)

Table 3.5.3: Best out-of-control ARLs values for each positive shock in the case of parallel shift in the yield curve , for n=40 and in-control ARL=11. The corresponding smoothing parameter values are given in parentheses.

In every control chart procedure for negative parallel shifts the larger values of $ARL_1 s$ are concentrated in small shifts. Except for the MCUSUM control chart where its detection ability seems not to be affected from the size of the shock and fails to

detect any change from the in-control condition quickly. Negative parallel shifts are detected slower than the positive ones in almost all the control charts.

d	ModMah	ModMEWMA	ResMah	ResMEWMA	MCUSUM	MMOEWMA
-0.05	16.59 (0.9)	4.44 (0.45)	3.9 (0.1)	8.11 (0.9)	8.07(2)	7.07 (0.35)
-0.1	14.34 (0.9)	3.55 (0.45)	2.53 (0.1)	5.5 (0.1)	8.09 (2)	4.29 (0.1)
-0.15	10.8 (0.9)	2.66 (0.45)	1.46 (0.1)	1.4*0.1)	7.94 (2)	2.51(0.1)
-0.2	7.13(0.2)	1.94 (0.1)	1.07 (0.1)	1.01(0.1)	8.16 (2)	1.7 (0.1)
-0.25	2.68 (0.1)	1.44 (0.1)	1 (0.1)	1(0.1)	8.14 (2)	1.31 (0.1)
-0.3	1.24(0.1)	1.19 (0.1)	1 (0.1)	1 (*)	8.01 (2)	1.12 (0.1)
-0.35	1(0.1)	1.07 (0.1)	1 (*)	1(*)	8.05(2)	1.04 (0.1)
-0.4	1 (0.1)	1.05(0.1)	1 (*)	1 (*)	7.95 (2)	1.02(0.1)

Table 3.5.4: Best out-of-control ARLs values for each negative shock in the case of parallel shift in the yield curve , for n=40 and in-control ARL=11. The corresponding smoothing parameter values are given in parentheses.

3.5.3.3 Non-parallel shifts in the Yield curve

The results for a twist in the yield curve considering positive and negative shifts are introduced in tables 3.5.5 and 3.5.6 respectively. For both cases the best overall performance have the ResMah and the MCUSUM control charts. Also for medium and large positive shocks the ModMah, the ModMEWMA and the ResMEWMA perform very well. The appropriate values for the smoothing parameter are for the ModMah 0.1, for the ModMEWMA chart less than 0.5, and for the rest of the control schemes we have various choices as we can see from the results in Appendix B.3.1.

The ModMah chart for shocks of the size 5% and 10% detects the changes, with very few exceptions, very slowly. The ResMah chart detects the out-of-control situation for every combination of shock and smoothing parameter relatively fast since no ARL_1 exceeds the period of five months. For the negative shifts again the best performance have the ResMah and the MCUSUM control charts with the first to detect faster the small shifts. However, when we have medium and large shifts the ModMEWMA and the ResMEWMA perform very well and the ModMah detects fast only the large negative shifts.

d	ModMah	ModMEWMA	ResMah	ResMEWMA	MCUSUM	MMOEWMA
0.05	11.17 (0.05)	5.23 (0.45)	1.57 (0.1)	11.36 (0.9)	2.15 (0.1)	11.08(0.75)
0.1	2.95 (0.1)	3.82 (0.45)	1.1 (0.1)	4.5 (0.1)	1 (*)	11.3(0.5)
0.15	1 (0.1)	2.71 (0.45)	1 (0.1)	1.06 (0.1)	1 (*)	11.14 (0.35)
0.2	1 (0.1)	1.72 (0.1)	1 (0.1)	1 (0.1)	1 (*)	11.06 (0.75)
0.25	1 (0.1)	1.31 (0.1)	1 (*)	1 (*)	1 (*)	11.13 (0.75)
0.3	1 (*)	1.13 (.1)	1 (*)	1 (*)	1 (*)	11.2 (0.75)
0.35	1 (*)	1.04 (0.1)	1 (*)	1 (*)	1 (*)	11.4 (0.35)

Table 3.5.5: Best out-of-control ARLs values for each positive shock in the case of non-parallel shift in the yield curve , for n=40 and in-control ARL=11. The corresponding smoothing parameter values are given in parentheses.

The ModMEWMA control chart detects faster the medium and large negative shifts than the positive ones. In both types of shifts the MMOEWMA chart fails to detect fast the changes in the yield curve even the large ones. Again, as in the case of positive shocks, the ResMah gives a signal quickly for every combination of shock and λ with values less than five months. The MMOEWMA chart on the opposite, despite the choice of the shock and the the smoothing parameter fails to detect fast the non-parallel shifts with the values of the ARL_1 to remain above the level of ten months. In general, negative shocks are detected in most of the cases faster than the positive ones.

d	ModMah	ModMEWMA	ResMah	ResMEWMA	MCUSUM	MMOEWMA
-0.05	21.87 (0.9)	5.59 (0.45)	1.58 (0.1)	11.22 (0.9)	2.25 (0.1)	11.35 (0.9)
0.1	4.31 (0.2)	4.26 (0.45)	1.11 (0.1)	4.41 (0.1)	1 (*)	11.27 (0.75)
-0.15	14.18 (0.9)	2.38 (0.1)	1 (0.1)	1.05 (0.1)	1 (*)	11.21 (0.75)
-0.2	9.75 (0.5)	1.54 (0.1)	1 (*)	1 (0.1)	1 (*)	11.02 (0.75)
-0.25	4.18 (0.2)	1.23 (0.1)	1 (*)	1 (*)	1 (*)	11.28 (0.75)
-0.3	1.74 (0.2)	1.07 (0.1)	1 (*)	1 (*)	1 (*)	11.12 (0.75)
-0.35	1.07 (0.2)	1.02 (0.1)	1 (*)	1 (*)	1 (*)	10.99 (0.75)

Table 3.5.6: Best out-of-control ARLs values for each negative shock in the case of parallel shift in the yield curve , for n=40 and in-control ARL=11. The corresponding smoothing parameter values are given in parentheses.

Table 3.5.7 summarizes the best $ARLs_1$ when we have negative shocks in positive butterfly shifts in the yield curve. Good performance in small negative shocks has only the ResMah control charts in contrast with the other control schemes that detect slowly the out-of-control situation. Large shifts are detected without delay

from ModMEWMA, ResMEWMA and MCUSUM. The ModMah detects large shifts with relative ease and the MMOEWMA control chart has the worst performance for detection of large shifts. Better performance in medium shift have the ResMEWMA and the MCUSUM control chart. The ModMah fails to detect quick the small and medium shifts. Except for the ModMah and the MMOEWMA chart which generally have their best results for large values of λ (greater than 0.75), the other control chart procedures favor small values.

d	ModMah	ModMEWMA	ResMah	ResMEWMA	MCUSUM	MMOEWMA
-0.05	21.73(0.9)	5.92 (0.45)	1.75(0.1)	12.16 (0.9)	6.75 (0.1)	11.11 (0.35)
-0.1	18.83 (0.9)	5.33 (0.45)	1.38 (0.1)	12.4 (0.75)	1.86 (0.1)	11.1 (0.75)
-0.15	16.59 (0.9)	4.2 (0.45)	1.17 (0.1)	6.83 (0.1)	1 (0.1)	11.27 (0.75)
-0.2	13.32 (0.9)	3.02(0.1)	1.05(0.1)	2.2 (0.1)	1(*)	11.19 (0.75)
-0.25	7.72 (0.2)	2.04 (0.1)	1 (0.1)	1.1 (0.1)	1 (*)	11.42 (0.75)
-0.3	3.11(0.2)	1.43 (0.1)	1 (*)	1 (0.1)	1(*)	11.15 (0.75)

Table 3.5.7: Best out-of-control ARLs values for each negative shock in the case of positive butterfly the yield curve, for n=40 and in-control ARL=11. The corresponding smoothing parameter values are given in parentheses.

The best results in terms of $ARLs_1$ for positive shocks when we have positive butterfly shifts in the yield curve are presented in table 3.5.8. The best performing control charts are the ResMah and the MCUSUM control chart. They detect any shift small or big very fast. The detection power of ResMEWMA is very good for intermediate and big shifts where the ModMEWMA chart is a good alternative for big shifts only. We mention that in the ModMEWMA chart for $\lambda \geq 0.5$ the chart fails to detect intermediate and small shifts.

d	ModMah	ModMEWMA	ResMah	ResMEWMA	MCUSUM	MMOEWMA
0.05	21.66 (0.9)	10.62 (0.1)	1.18 (0.1)	11.07 (.9)	1.23(0.1)	11.41 (0.75)
0.1	19.08 (0.9)	5.6 (0.1)	1 (0.1)	3.74 (0.1)	1 (*)	11.26 (0.75)
0.15	16.27 (0.9)	4.06 (0.1)	1 (0.1)	1.64 (0.1)	1 (*)	11.2 (0.5)
0.2	13.46 (0.9)	2.64 (0.1)	1 (*)	1.02 (0.1)	1 (*)	11.4 (0.35)
0.25	7.52 (0.2)	1.56 (0.1)	1 (*)	1 (*)	1 (*)	11.4 (0.35)
0.3	3.05 (0.2)	1.23 (0.1)	1 (*)	1 (*)	1 (*)	11.01 (0.5)

Table 3.5.8: Best out-of-control ARLs values for each positive shock in the case of non-parallel shift in positive butterfly the yield curve, for n=40 and in-control ARL=11. The corresponding smoothing parameter values are given in parentheses.

Table 3.5.9 presents the best ARL_1s for negative butterfly shifts when the yields decrease or else for negative shocks. The chart with the best overall performance detecting very fast small, medium and large shifts is the ResMah control charts with suggested smoothing parameter equal to 0.1. Also, the MCUSUM chart performs almost equally with the ResMah but expect with the detection of small shifts where the latter performs better. The ModMEWMA and the ResMEWMA chart detect relatively fast the large shifts.

d	ModMah	ModMEWMA	ResMah	ResMEWMA	MCUSUM	MMOEWMA
-0.03	14.61 (0.2)	6 (0.45)	1.65 (0.1)	12.19(0.9)	6.62(0.1)	11.11(0.75)
-0.06	13.25(0.2)	5.27 (0.45)	1.39(0.1)	11.08(0.9)	1.97 (0.1)	11.35 (0.9)
-0.09	10.93 (0.2)	4.29 (0.45)	1.16(0.1)	6.9 (*)	1 (0.1)	11.19 (0.75)
-0.12	8.96(0.2)	3.07 (0.1)	1.06 (0.1)	2.21 (0.1)	1 (*)	11.42 (0.9)
-0.15	6.56(0.2)	2.07 (0.1)	1(0.1)	1.11 (0.1)	1(*)	11.31 (0.75)
-0.2	4.34 (0.2)	1.43 (0.1)	1 (*)	1 (0.1)	1 (*)	11.37(0.75)

Table 3.5.9: Best out-of-control ARLs values for each negative shock in the case of negative butterfly shift in the yield curve, for n=40 and in-control ARL=11. The corresponding smoothing parameter values are given in parentheses.

Finally, table 3.5.10 presents the best results for negative butterfly shifts when we have positive shifts in the yields. The best overall performance in terms of ARL_1s has the MCUSM control chart except for small shifts where the ResMah detect the shifts faster. Additionally, ModMEWMA, ResMEWMA detect quickly large shifts for values of the smoothing parameter $\lambda = 1$. In comparison with table 3.5.9 negative shocks are detected faster than positive ones for almost all control chart procedures. The ModMah, the ResMah and the MCUSUM control chart fail in many occasion to detect the changes in the yield curve. The first two charts fail to detect small shifts and in the third chart this problems extends to intermediate shifts.

In conclusion, we have simulated various parallel and non-parallel shifts in the yield curve and examined the detection power of various control charts for a variety of smoothing parameters. There is no single chart that performs well in all the cases but many detects the changes in a large number of occasions. As a result we propose the use of more than one control charts in order to detect the shifts. Another important aspect is the size of shock and as we see from the results the performance of many charts fluctuate and depends if the shock is small, intermediate or large. The shocks due to a change in the factor loading of the state evolution process of the term structure model are detected faster than parallel shifts in the yield curve.

d	ModMah	ModMEWMA	ResMah	ResMEWMA	MCUSUM	MMOEWMA
0.03	22.73 (0.9)	5.81 (0.45)	4.8 (0.9)	48.18(0.9)	6.93 (0.1)	11.42(0.9)
0.06	20.88 (0.9)	4.94(0.45)	4.52 (0.9)	32.73(0.2)	1.97 (0.1)	11.25(0.9)
0.09	17.93 (0.9)	4.07 (0.45)	4.05 (0.9)	12.89(0.1)	1.01 (0.1)	11.39(0.9)
0.12	14.92 (0.9)	3.18 (0.45)	3.65 (0.9)	5.69(0.1)	1 (0.1)	11.25(0.35)
0.15	11.55 (0.9)	2.18 (0.1)	2.99 (0.9)	2.72(0.1)	1 (*)	11.28(0.9)
0.2	7.77 (0.1)	1.49 (0.1)	2.45 (0.9)	1.16(0.1)	1 (*)	11.19(0.9)

Table 3.5.10: Best out-of-control ARLs values for each positive shock in the case of negative butterfly shift in the yield curve, for n=40 and in-control ARL=11. The corresponding smoothing parameter values are given in parentheses.

The MMOEWMA chart is appropriate for changes in the factor loadings and parallel shifts but fails to detect non-parallel shifts in the yield curve. In contrast, the MCUSUM chart performs better when detects non-parallel shifts than parallel or changes in the factor loadings. The control chart procedure with the worst overall performance is the univariate EWMA based on the Mahalanobis distance. The residual chart based on Mahalanobis distance is more appropriate for the detection of parallel and non-parallel shifts in the yield curve. Finally, the best overall performance have the MEWMA and the residual chart based on the MEWMA statistic.

3.6 Empirical example

The control chart procedures that we previously proposed are applied to a Gaussian ATSM of the U.S. yield curve for the detection of structural breaks. We assume that the in-control period of the term structure is from April 1991 to December 2000. The results from this class of affine model estimated from historical data are obtained from section 3.3 under the no arbitrage assumption. The out-of-sample and monitoring process is from January 2001 to December 2009 which contains the global financial crisis of 2007-08.

We have used the six proposed control chart procedures for various values of the smoothing parameters. Specifically, for the univariate EWMA control chart based on the Mahalanobis distance we have chosen the smoothing parameters 0.1,0.75,0.9. The MEWMA control chart is constructed for $\lambda = \{0.25, 0.5, 0.75\}$. The smoothing parameter values for the Residual EWMA control chart based on the Mahalanobis distance are 0.25,0.35 and 0.5. Also, the Residual MEWMA chart is constructed for $\lambda = \{0.25, 0.45\}$. The MMOEWMA control chart for $\lambda = \{0.45, 0.9\}$ and the reference value of the MCUSUM is chosen to be equal to 2.5.

When the control chart gives a signal then the financial analyst should examine and evaluate it. We remind that as in many financial applications even if a signal is given the process in contrast to industrial applications can not be stopped. The statistical monitoring processes we use do not give more insight to the causes of an out-of-control condition. One of the main problems is what happens in the statistical monitoring procedure when the control chart gives a signal. Golosnoy and Schmid (2007) in their work for monitoring optimal weights in a GMVP referred to an analogous problem. They apply two procedures the first without reestimation of the target process and the second with reestimation. In our work we follow this approach and estimate after a signal a new target process for the yield curve. Golosnoy and Schmid (2007) mentioned a series of problems in order to reestimate the target process such as if the data remain under the assumption of normality and if they are identically and independent distributed. Their new target process is estimated taking into consideration the last 250 observation of their daily data.

In our work we estimate first the control charts under no reestimation of the target process when a signal happens and second we reestimate it under the assumption that the normality of the data we assumed in section 3.3 continues to be valid. However, instead of using the last observations prior to the signal that is given from the control chart we apply the following procedure: First after a signal is detected we let the process run and collect the data for a small period after and apply a two sample T-test for the means with unequal variances. The two samples we test is one with data before the signal when the process is in-control and the second is the small period afterwards the signal. The null hypothesis is that there is no-change in the means. If we reject the null hypothesis then we estimate the new target process. The data set we use for the estimation contains not only data prior to the signal but also for a small period afterwards, here six months. A serious disadvantage of this approach could be if a second change happens in that time period. So, we think this type of approach could be more appropriate for detecting more permanent shocks such as those connected with business cycles. The National Bureau of Economic Research (NBER) estimates the mean duration of contractions to be above 10 months (for more see [1]).

[1] https://www.nber.org/cycles.html

3.6.1 Control charts without reestimation of the target process

For the case without reestimation of the target process the control statistics are presented in Appendix C.0.1, for the smoothing parameters we previously mentioned, from January 2001 to December 2009. The control statistics for the univariate EWMA based on the Mahalanobis distance for $\lambda = \{0.75, 0.9\}$ show similar pattern and which is less smoother than this for $\lambda = \{0.1\}$. Also, we mention that all control statistics for the charts selected, with the exception for those for the MMOEWMA chart, show an increasing trend after 2007. Additionally, control statistics for EWMA and Residual charts based on Malahanobis distance as long as for the MMOEWMA chart begin from a high level and show a downward trend for a certain period.The control statistic for the MCUSUM chart and reference value equal to 2.5 exhibits less fluctuations in comparison with the other charts.

Next we present the control chart under no reestimation for the control limits obtained from a simulation study as described in section 5.5.2 and the dates of their signals. This approach do not use the information obtained from each change point in the control charts (Schmid and Tzotchev (2004)). The EWMA chart based on the Mahalanobis distance and $\lambda = 0.9$, detects six changes (see figure 3.6.1). The dates of the signals are September 2002, December 2002, February 2003, March 2004, December 2007 and November 2008. The other univariate EWMA control charts for $\lambda = 0.1$ and $\lambda = 0.75$ detect two changes. The first chart in December 2002 and March 2008 and the latter in September 2002 and in January 2008. We remind that according to NBER the early 2000s recession started from March 2001 until November 2001. Also the Great recession that started in December 2007 and ended in June 2009 was a consequence of the global financial crisis of 2007-08. The charts that detect the early 2000s recession are that for $\lambda = 0.1, 0.75$. However, all three charts detects with delay the crisis of 2007. The financial crisis represents a period of increased yield volatility. The change at the beginning of 2003 follows the internet bubble bursting and the stock market downturn of 2002.

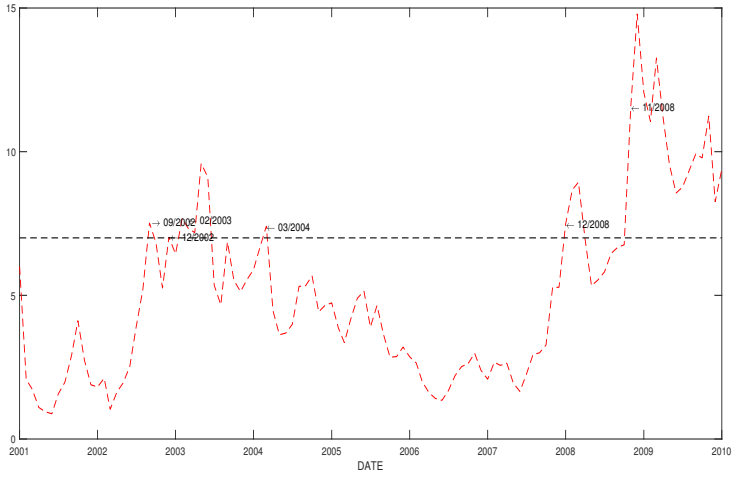

Figure 3.6.1: Control chart for the case of EWMA control chart based on Mahalanobis distance when $\lambda = 0.9$. The sample period is 2001:01 to 2009:12.

The MEWMA control chart for $\lambda = 0.25$ provides two signals, the first in September 2002 and the second in December 2007 (see figure 3.6.2). The MEWMA chart with the choice for smoothing parameter equal to 0.5 gives three signals in September 2002, in June 2005 and in January 2008. The residual chart based on the Mahalanobis distance for $\lambda = 0.25$ detects three structural changes (see figure 3.6.3). The first is at the beginning of the monitoring period in January 2001 and the next two in October 2002 and in February 2008. The residual chart based on the Mahalanobis distance for $\lambda = 0.2$ detects the first change at the same time as the chart for $\lambda = 0.25$ but the other two a month later in each case. The residual chart based on the Mahalanobis distance for $\lambda = 0.35$ in comparison with that for $\lambda = 0.25$ detects an additional change in October 2008. All three charts of this class give a signal near the beginning of the recession of 2001 but detect with delay the crisis of 2007.

The residual chart based on MEWMA statistic and $\lambda = 0.25$ gives a signal in August 2002 and the other in December 2007 (see figure 3.6.4). The chart with $\lambda = 0.45$ detects five changes: March and October 2003, March 2004, September 2008 and December 2008.

The MCUSUM control charts for reference parameter equal to 2.5 detects three structural changes (see figure 3.6.5), in September and December of 2002 and in January 2008. The MMOEWMA chart detects changes in February 2001, in October

2002, in March 2004, in March 2005 and finally in November 2008 (see figure 3.6.6). In all charts the control statistics of the monitoring process after the signals they detect in 2007 or 2008 remain clearly in the out-of-control condition and , except from MMOEWMA chart, exhibit an upward trend. Only in MEWMA control chart when $\lambda = 0.75$ the process returns to the in-control case.

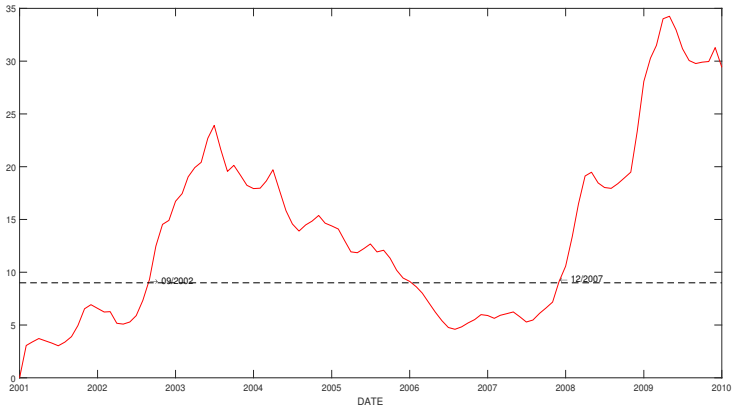

Figure 3.6.2: Control chart for the case of MEWMA control chart when $\lambda = 0.25$. The sample period is 2001:01 to 2009:12.

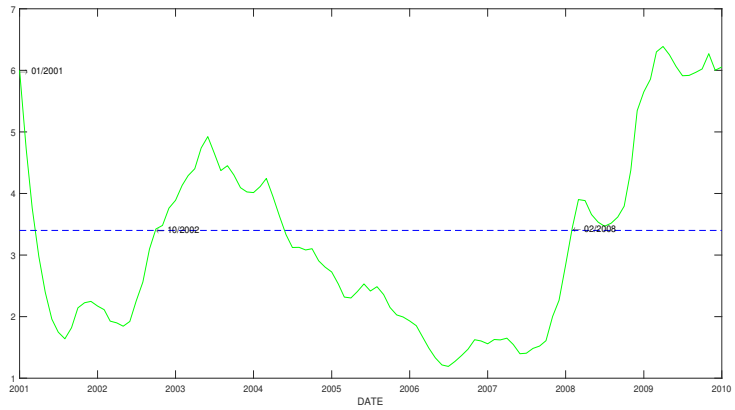

Figure 3.6.3: Control chart for the case of Residual EWMA control chart when $\lambda = 0.25$. The sample period is from 2001:01 to 2009:12.

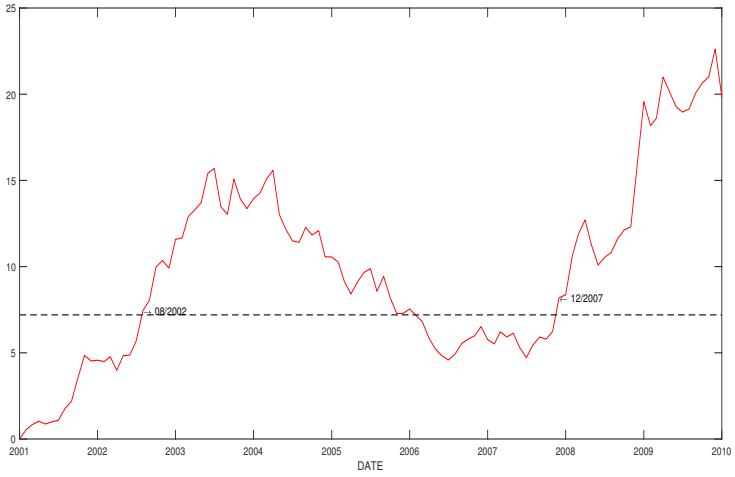

Figure 3.6.4: Control chart for the case of Residual MEWMA control chart when $\lambda = 0.45$. The sample period is from 2001:01 to 2009:12.

We mention that Chib and Kang (2013) for the sample period between 1972:Q1 and 2007:Q4 supported the existence of three change-points. However, their model do not capture the early 2000's recession and the stock crash after the events at September 11, 2001. Most of the control charts we propose in the practical example give a signal either in earlier 2001 or during 2002 in various dates. Only the MEWMA chart for $\lambda = 0.75$ does not give a signal in the beginning of our monitoring period and the ResMEWMA for smoothing parameter equal to 0.75 detect a change at the early 2003.

For the financial crisis of 2007-2008 beginning in August 2007 and the Great Recession of 2007-2009 that lead to, all control charts detect changes during the years 2007 and 2008 in different dates. The ResMEWMA chart for $\lambda = 0.45$ and the MEWMA chart for $\lambda = 0.25$ detect a structural change at December 2007. The rest of the charts detects a change or two during the 2008. We remind that on September 15, 2008 we have Lehman Brothers bankruptcy. The following changes detected: in the MEWMA chart for $\lambda = 0.5$ in June 2006, in ResMah chart for $\lambda = 0.5$ in February 2004, in ResMEWMA for $\lambda = 0.5$ in March 2004 and in MMOEWMA chart for $\lambda = 0.45$ in March 2004 and March 2005 are not attributed to a certain economic activity.

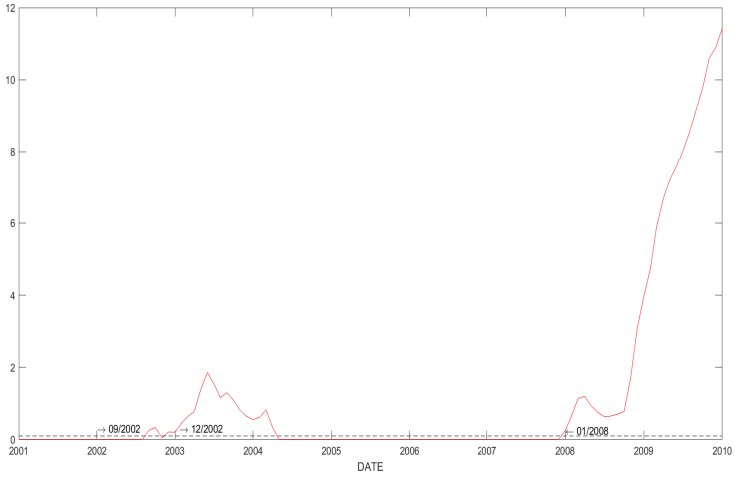

Figure 3.6.5: Control chart for the case of MCUSUM control chart when $g = 2.5$. The sample period is from 2001:01 to 2009:12.

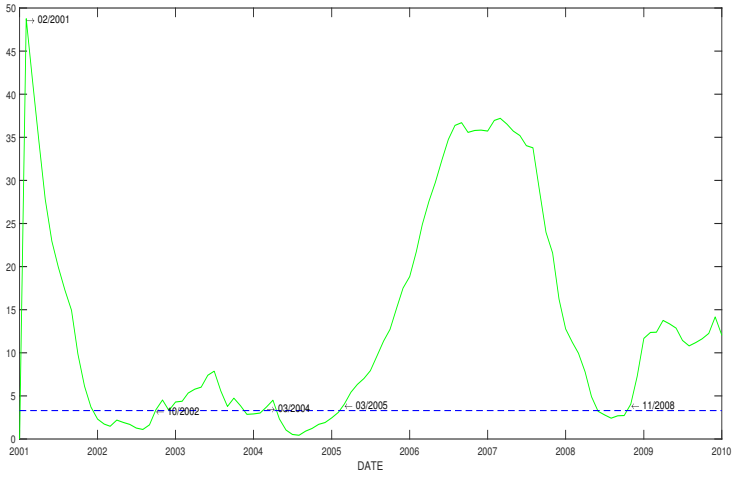

Figure 3.6.6: Control chart for the case of MMOEWMA control chart when $\lambda = 0.45$. The sample period is from 2001:01 to 2009:12.

Bech and Lengwiler (2012) analyzed the dynamics of the U.S. yield curve from 1998 to 2011 and they identified four phases. The first is the so called "normal" phase

from 1998 to mid-2004. Next, is the "moderation' phase that ends in August 2007 connected to the BNP Paribas's announcement that it was freezing three funds invested in subprime securities. which is commonly taken to mark the beginning of the financial crisis. Next is the "liquidity crisis phase" that begins on August 9,2007 and ends on December 16, 2008. This period is characterized by increased volatility in yields of short and medium maturity and liquidity problems. The last phase is the "zero lower bound phase" that begins after the Federal Reserve has reached the zero lower bound until 2011. In this period it is observed large volatility in the long maturities of the yield curve. Chen and Niu (2014) proposed an adaptive dynamic Nelson-Siegel (ADNS) model that improves forecasts of the yield curve and detect structural breaks in level, slope and curvature of the yield curve. They detect among others break in the yield curve at the beginning of 2003 and the financial crisis and recession in 2008.

3.6.2 Control charts with reestimation of the target process

A basic problem after the control chart gives a signal and a change is verified from the financial analyst, is the estimation of the new target process and eventually the new control limits. For the estimation of the new target process after a change is detected we follow the next procedure: First when the control chart gives a signal we perform a two sample t-test for the equality of the means with unequal variances for the observed yields in order to confirm if a change in the mean process happened. Before we perform the test we need to define the size of the data sample we need in order to reestimate the control limits. A main drawback of the data we use in the term structure model is their low frequency since we have monthly data. The difficulty is that for the estimation of the quantities we described in the previous section we need enough data. So as to overcome this problem after a signal is given we observed the process for a limited time period for example until six months and collect the appropriate data. If a signal is given and the monitoring process returns in a very short period (e.g. after one or two months) again under control this is may due to the fact that the change is not persistent. We perform the two sample T-test for the equality of the means with unequal variance having in the one sample this six-month data set. If the results of the test confirm the change we estimate the term structure model for an estimation window equal to 25 months that contains this period of up to six months after the signal. We remind that Golosnoy and Schmid (2007) for the portfolio monitoring estimated the new target process based on the last 250 observations an approach that may do not capture the change in the model parameters when the shock in the monitoring process is large. In our approach we

include in the estimation period and a small time period after the change hoping to improve the estimation results. We maintain the normality assumptions for the interest rate model as introduced in section 3.3. This approach could be helpful in cases of detecting changes due to business cycles where changes are persistent for a relative large time period. However, the task of control limits reestimation after a change is detected for low frequency data remains quite difficult and challenging.

After the reestimation of the target process and the calculation of the new control limits the univariate EWMA control charts based on the Mahalanobis distance detect less changes than in the case without estimating the new control limits. Specifically when $\lambda = 0.9$, the control chart now detects after the reestimation four changes: September,2002, February and October 2005 and October 2008. For $\lambda = 0.1$ we have instead of previously three now two changes January, 2001 and December, 2008. The last of the univariate EWMA charts for $\lambda = 0.75$ detects four changes: February 2003, August 2005 and May 2006 and January 2008. We remind that the early 2000s recession in United Stated according to NBER lasted eight months, March to November 2001. Except for the chart with smoothing parameter equal to 0.1 the other two control charts detect changes after that period. Stock indices after recovering from the September 11,2001 attacks then starting in March 2002 the stock indices reach a low in October of the same year. The chart with $\lambda = 0.9$ gives a signal in September.

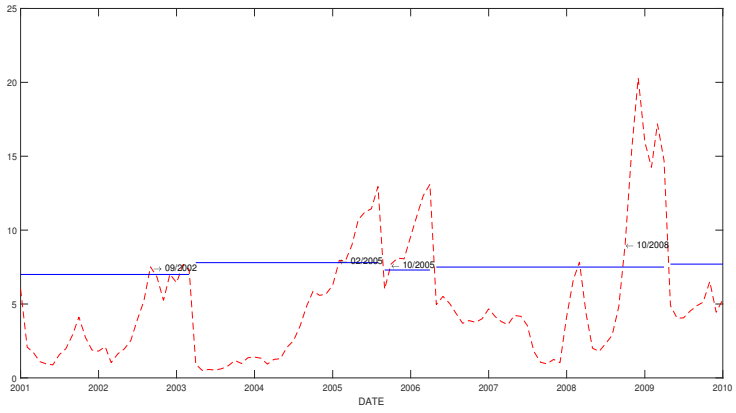

Figure 3.6.7: Control chart for the case of EWMA control chart based on Mahalanobis distance when $\lambda = 0.9$ and reestimation of the target process. The sample period is 2001:01 to 2009:12.

The MEWMA control charts for $\lambda = 0.25, 0.5$ detect more changes than the case without reestimating the target process. At the first occasion with smoothing parameter equal to 0.25 a change happens at September 2002, June 2006 and December 2007. For $\lambda = 0.5$ additional to the first change which is at the same time as previous we have signals for changes at July 2003, April 2006 and March 2008. The change in April 2006 can not be associated with some specific economic event. The remaining MEWMA procedure gives no other signal than that at December 2008 and fails to detect any change during the recession of 2001 or the subsequent stock market crash.

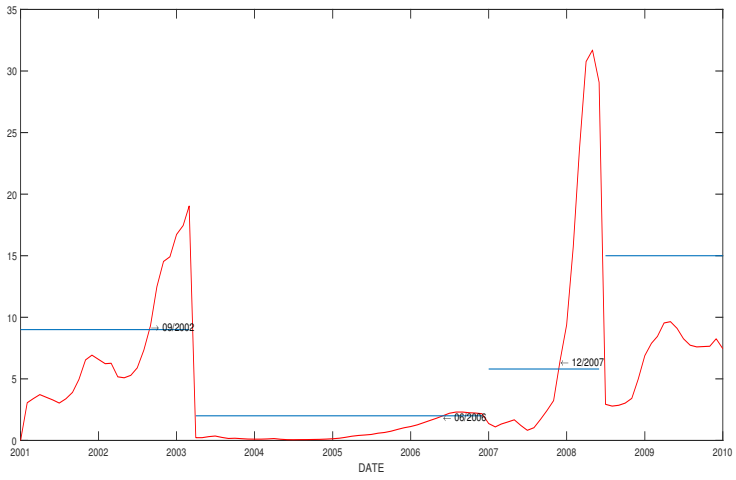

Figure 3.6.8: Control chart for the case of MEWMA control chart when $\lambda = 0.25$ and reestimation of the target process. The sample period is from 2001:01 to 2009:12.

The residual EWMA control charts for $\lambda = 0.2, 0.25$ detect more changes than previously without reestimation and the opposite for $\lambda = 0.35, 0.5$. Figure 3.6.9 presents the four change points for $\lambda = 0.25$: January 2001, October 2002, January 2006 and January 2008 a month after the beginning of the Great Recession of 2007-2009. The rest three residual EWMA charts based on the Mahalanobis distance that we examine all detect a change at the beginning of the monitoring period (January 2001) and a change in the year 2008. The chart with $\lambda = 0.2$ in June and the other two a change in December. The charts for $\lambda = 0.35$ and $\lambda = 0.5$ detect the same changes in numbers and dates.

The residual MEWMA control chart with $\lambda = 0.45$ detects, as the corresponding chart without reestimation discussed in the previous section, a change in August 2002 and two additional in December 2004 and August 2007. Now the MCUSUM

chart detects a change in December 2002 and a change in January 2008. Finally the MMOEWMA chart gives three signals for change: February 2001, April 2006 and February 2007. House prices in the U.S. reached at the peak and start to decline in the middle of 2006 (Baker (2008)) that eventually lead to the subprime mortgage crisis of 2007 and 2010, and contributed significantly to the U.S. financial crisis.

In general, the choice of the appropriate control scheme depends on the size and the type of the shifts in the yield curve and a combination of control charts is suggested. Schmid and Tzotchev (2004) mentioned that the use of control charts in a one-factor CIR model that uses historical data for estimation may be problematic. In contrast, we conclude that control chart procedure could be a useful tool for detecting structural breaks in multifactor interest rate models and specially ATSM taking into advantage the richer structure they have from the one-factor models. Also the MMOEWMA control chart, applied for the first time in a term structure setting, can be appropriate for detecting parallel shifts in the yield curve.

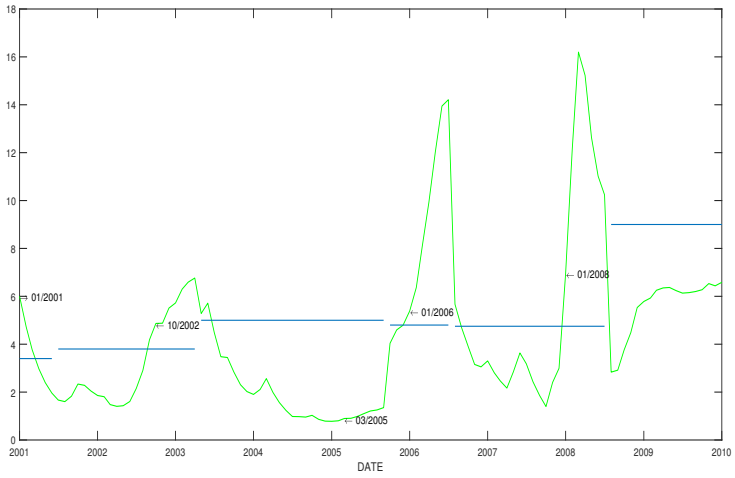

Figure 3.6.9: Control chart for the case of Residual EWMA control chart based on Mahalanobis distance when $\lambda = 0.25$ and reestimation of the target process. The sample period is 2001:01 to 2009:12.

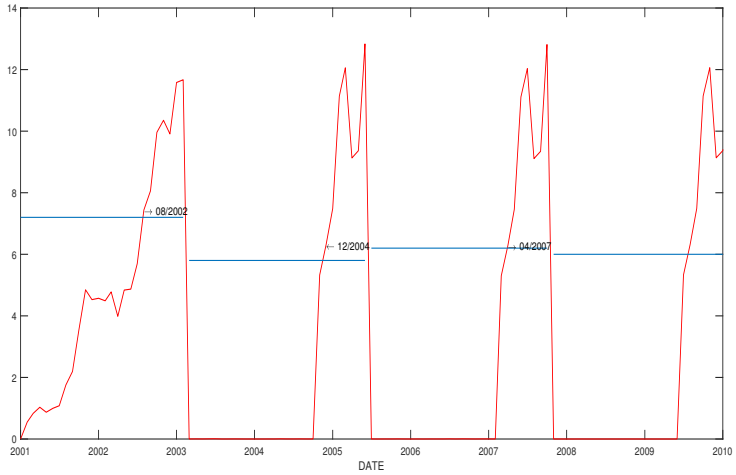

Figure 3.6.10: Control chart for the case of Residual MEWMA control chart when $\lambda = 0.45$ and reestimation of the target process. The sample period is 2001:01 to 2009:12.

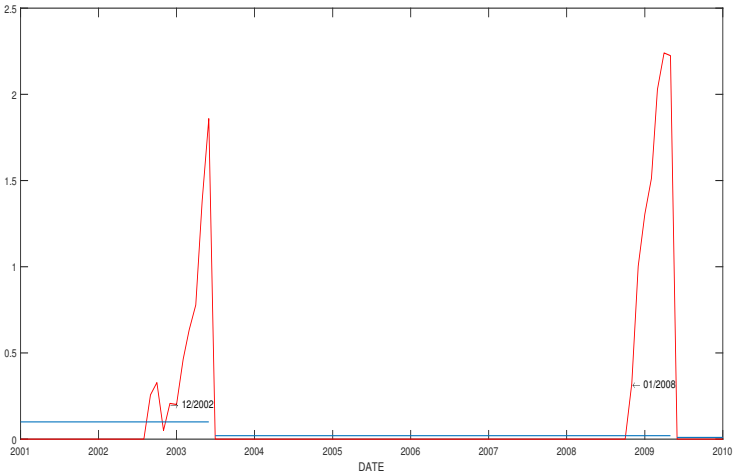

Figure 3.6.11: Control chart for the case of MCUSUM control chart when $g = 2.5$ and reestimation of the target process. The sample period is 2001:01 to 2009:12.

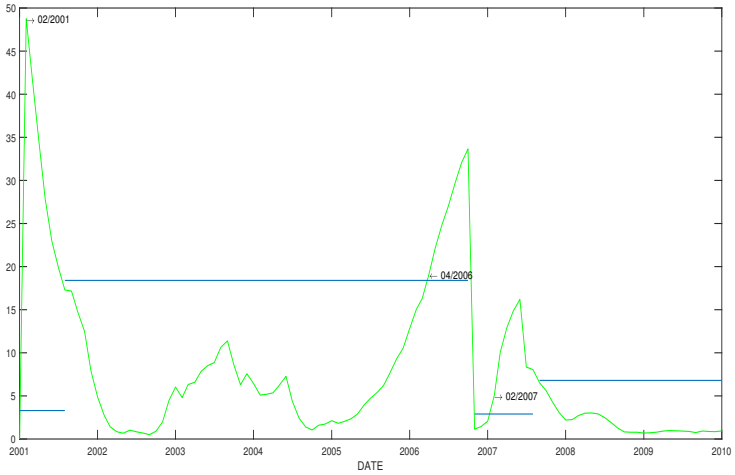

Figure 3.6.12: Control chart for the case of MMOMEWMA control chart when $\lambda = 0.45$ and reestimation of the target process. The sample period is 2001:01 to 2009:12.

Chapter 4

Affine Term Structure Models: Applications in Portfolio Optimization and Change Point Detection

4.1 Introduction

In this chapter first we estimate the term structure model for yield curve with data form the United States following the MCSE method proposed by Hamilton and Wu (2012). Next, we construct a fixed-income portfolio using the results obtained from the term structure model. Dynamic factor models for the yield curve are used to generate yield forecasts for a set of selected maturities and subsequently used to compute expected fixed-income returns. The main problem for fixed-income portfolios is the prediction of the distribution of returns for a number of maturities. Caldeira et al. (2016) selected the optimal vector of portfolio weights conditional on the investor's expected returns and risk preferences. Following the estimation of the yield curve model we generate forecasts of bond returns, which subsequently used for the mean-variance optimization problem. We mention that an important element of this procedure is the ability to obtain good forecast results from the term structure model. The incorporation of macroeconomic factors into term structure models has the advantage of increasing the model's predictive ability. In our analysis we perform forecasts of one-period ahead estimates of fixed-income returns. The distribution of

bond returns follows that of the ATSM, which is the multivariate normal distribution. The estimated mean-variance bond portfolios are compared with traditional bond portfolio strategies and we show that can be a reasonable alternative to them.

Dynamic term structure models play an important role in fixed-income asset pricing and strategic asset allocation. However, the connection between dynamic factor models and portfolio optimization only in recent years has been explored. Fabozzi and Fong (1994) used fixed-income portfolios in order to approximate the duration of a benchmark portfolio or to replicate the performance of this benchmark. The literature is mainly focused on the construction and performance of equity portfolios under the mean-variance approach (see for example DeMiguel et al. (2009) and DeMiguel et al. (2009)).

The main difficulty in portfolio optimization using dynamic factor models is the estimation of the bond expected returns and the covariance matrix of bond returns. If we can estimate expected bond returns and their variance-covariance matrix, the portfolio optimization procedure is similar to that of equity portfolios (Fabozzi and Fong (1994)). According to Meucci (2010) since both bond price and bond return are non-ergodic processes the traditional statistical techniques cannot be used to directly model the expected return and volatility of bond yields. Following the work of Caldeira et al. (2016) we obtain closed-form solutions for the expected bond returns and the covariance matrix of bond returns but for a different class of dynamic factor models, the ATSM of Hamilton and Wu (2012). Puhle (2008) and Korn and Koziol (2006) proposed the use of the Vasicek (1977) model for the yield curve for the mean-variance bond portfolios optimization. The main drawback of their approach is that that the one-factor Vasicek model has limited forecasting power in contrast with the forecasting ability of dynamic factor models (Duffee (2002)).

The structure of this chapter is as follows. In section 2 we describe our data set. In section 3 we estimate the term structure model, the one- period ahead expected returns and the variance of the bond yields for a specified out-of-sample period. In section 4 we present the results for the fixed-income portfolio optimization. Section 5 deals with the application of control charts to optimal weights of a GMVP. Sections 6 and 7 present the results of a simulation study and an empirical example, respectively.

4.2 Data

Our data set consists of fixed-maturity, end-of-month continuously compounded yields on U.S. zero-coupon bonds from January 1981 to December 2009, totally

348 monthly observations. This data set of monthly time series of yields was constructed from Jungbacker et al. (2012) from the Center for Research in Security Prices (CRSP) unsmoothed Fama and Bliss (1987) forward rates and is publicly available in the Journal of Applied Econometrics Data Archive. For our work we have chosen yields with maturities 3,48,60,72,84 and 120 months for the time period from January 1981 to December 2009. Figures 4.2.1, 4.2.2 plot the time series of US Treasury yields. The average yield curve is downward sloping. It is known that usually periods where the yield curve displays a downward trend then bond returns exhibit good performance.

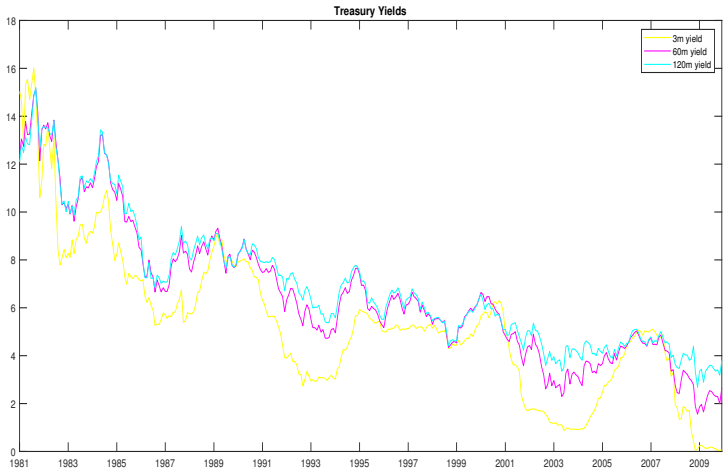

Figure 4.2.1: U.S. Treasury Yields. The graph illustrates annualized monthly zero-coupon bond yields of maturity 3 months, 5 years, and 10 years. The sample period is 1981:01 to 2009:12.

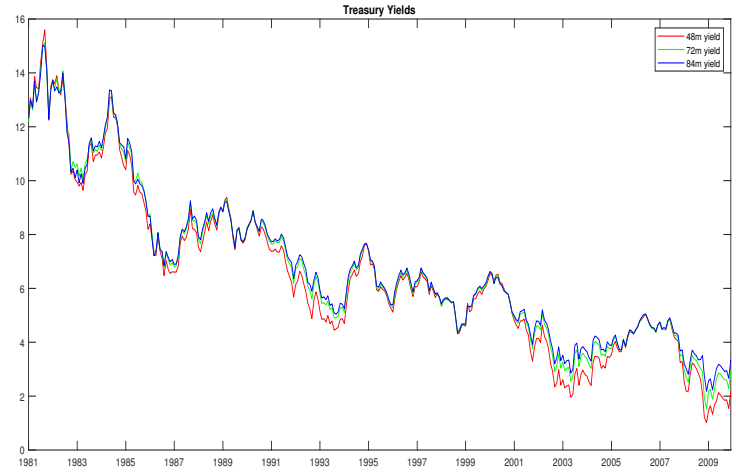

Figure 4.2.2: U.S. Treasury Yields. The graph illustrates annualized monthly zero-coupon bond yields of maturity 4 months, 6 years, and 7 years. The sample period is 1981:01 to 2009:12.

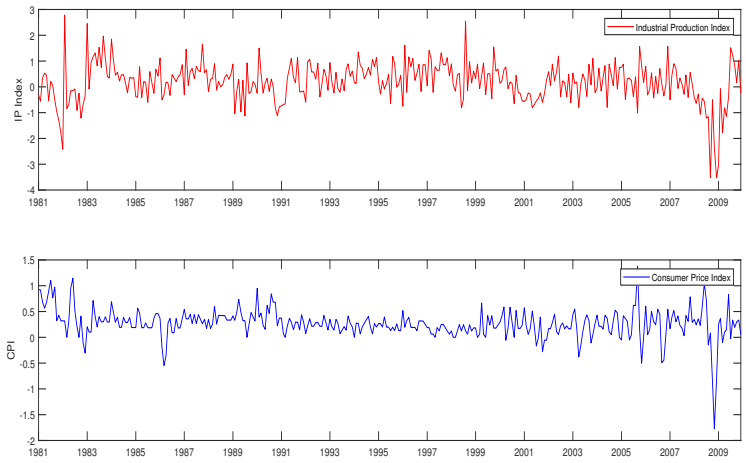

Figure 4.2.3: Macroeconomic factors. The figure illustrates the two macroeconomic factors Industrial Production Index and Consumer Price Index for the sample period 1981:1 to 2009:12

As we mention earlier we follow the recent literature in the term structure models and

we use both macroeconomic and latent factors. The incorporation of macroeconomic factors contributes to the improvement of yield curve forecasting. Good yield curve predictions are important in order to achieve better results in terms of fixed-income portfolio performance. We use two macroeconomic factors, the CPI monthly time series seasonally adjusted and as a proxy for the monthly GDP the monthly Industrial Production (IP) growth. IP is almost 80% of the GDP and so can be used as a proxy. The CPI measures the average changes in the price level of a basket of goods. The IP growth measures the growth rate of the production of goods. The IP growth rates and the CPI time series are obtained from the Federal Reserve St. Luis database. The data series for all the sample period are displayed in figure 4.2.3. The CPI starts from a high level and in average falls during the recession of 1981-82. In the subsequent period follows a upward trend before the fall in the fourth quarter of 1990. Next, the CPI stays mainly in the same level until an upward trend during the period from the end of 1999 until March 2008. For the period from the third quarter 2008 until middle of 2009 we have a period of economic downturn due to the recent global financial crisis. IP Index growth rate is seasonally adjusted. Most of the movements of the IP Index growth rate follows that of the business cycles. However, the time series of CPI has more smooth fluctuations.

Table 4.2.1 presents some descriptive statistics for the yields and table 4.2.2 for the macroeconomic observable factors. The yield levels show mild excess kurtosis at short maturities which decreases with maturity and positive skewness at all maturities. Also in tables 4.2.3 and 4.2.4 we present the autocorrelations of these time series for lags 1,5,12,20 and 24. An important fact is that, the time series of all bond yields are highly autocorrelated showing strong persistence. IP growth rates exhibit medium level autocorrelation and the CPI low autocorrelation. Also, figures C.0.1,C.0.2 and C.0.3 show the autocorrelograms of our data series. In figure C.0.4 we have plot the yields term premia, the difference between the 10-year yield and the 3-month yield. The term premia at the beginning of our sample period starts from a negative position and continuously increases from 1981:09 to 2009:12 and remains to positive levels with the exception of time periods 1989:05 to 1989:07, 1989:10 to 1989:11, 2000:07 to 2000:12 and 2006:07 to 2007:04. During the recession periods the term premia exhibits an upward trend. The estimation procedure is performed for the in-sample period from 1981:01 to 1999:12 while the out-of-sample period is from 2000:01 to 2009:12.

	3m	48m	60m	72m	84m	120m
Mean	5.3335	6.4689	6.5854	6.7159	6.8025	6.9385
Skewness	0.8014	0.7117	0.7477	0.7597	0.8143	0.8817
Kurtosis	4.0964	3.111	3.0446	2.9959	3.0382	3.0774
Std deviation	3.1443	3.0252	2.9415	2.9185	2.8444	2.724
Maximum	16.019	15.599	15.129	15.108	15.024	15.194
Minimum	0.041	1.019	1.556	1.525	2.179	2.679
Range	15.978	14.58	13.573	13.583	12.845	12.515

Table 4.2.1: Descriptive statistics of U.S. Treasury yields. The table reports summary statistics of Treasury yields with maturities 3-,48-,60-,72-,84-,120-months.

	CPI	IP Index
Maximum	1.4	2.7841
Minimum	-1.8	-3.5293
Mean	0.3	0.1875
Median	0.3	0.2343
Mode	0.0	-3.5293
St. Deviation	0.3	0.7770
Variance	0.1	0.6037
Skewness	-1.0	-0.7906
Kurtosis	12.8	6.7616
Range	3.1	6.3134
Sum	92.5	65.2391
Sem	0.0	0.0416

Table 4.2.2: Descriptive Statistics of Macroeconomic factors. The macroeconomic factors are the Consumer Price Index (CPI) and the Industrial Production Index (IP) seasonally adjusted.The sample period is 1981:01 to 2009:12.

Macro Factors	Lag 1	Lag 5	Lag 12	Lag 20	Lag 24
CPI	0.4730	0.0049	-0.0616	0.0107	0.0268
IP Index	0.2852	0.2249	-0.0107	-0.0028	-0.1105

Table 4.2.4: Autocorrelation of macroeconomic factors, Consumer Price Index and Industrial Production Index.The sample period is 1981:01 to 2009:12.

Yields	Lag 1	Lag 5	Lag 12	Lag 20	Lag 24
3 month	0.9724	0.8597	0.6538	0.4385	0.3848
48 month	0.9833	0.9025	0.7497	0.6009	0.5681
60 month	0.9834	0.9056	0.7593	0.6209	0.5915
72 month	0.9841	0.9108	0.771	0.6381	0.609
84 month	0.984	0.9099	0.7676	0.639	0.6159
120 month	0.9844	0.9123	0.7701	0.6504	0.6321

Table 4.2.3: Autocorrelation of U.S. Treasury yields for the sample period 1981:01 to 2009:12.

4.3 A No-Arbitrage Affine Term Structure Model

4.3.1 Model specification

In general, we adopt the modeling approach of Pericoli and Taboga (2008) but under the estimation method proposed by Hamilton and Wu (2012). Here we present the equations of Hamilton and Wu (2012) that are most relevant for our model and retain mostly of their notation for simplicity. The state variables evolution process $\mathbf{X_t}$ follows a vector autoregressive process:

$$\mathbf{X_{t+1}} = \boldsymbol{\mu} + \boldsymbol{\rho}\mathbf{X_t} + \boldsymbol{\Sigma}\mathbf{u_{t+1}}, \tag{4.3.1}$$

with u_{t+1} a Gaussian standard error term. We consider two representations of equation (4.3.1) which represent two different specifications of the risk-neutral pricing measure Q and the pricing measure of a risk-averse investor under the physical probability measure P. As a result equation (4.3.1) takes the following form under these two measures:

$$\mathbf{X_{t+1}} = \boldsymbol{\mu}^{\boldsymbol{Q}} + \boldsymbol{\rho}^{\boldsymbol{Q}}\mathbf{X_t} + \boldsymbol{\Sigma}\mathbf{u}^{\mathbf{Q}}_{\mathbf{t+1}}, \tag{4.3.2}$$

$$\mathbf{X_{t+1}} = \boldsymbol{\mu}^{\boldsymbol{P}} + \boldsymbol{\rho}^{\boldsymbol{P}}\mathbf{X_t} + \boldsymbol{\Sigma}\mathbf{u}^{\mathbf{P}}_{\mathbf{t+1}}. \tag{4.3.3}$$

The time-varying market prices of risk, $\boldsymbol{\lambda_t}$, are affine functions of the underlying state variables $\mathbf{X_t}$:

$$\boldsymbol{\lambda_t} = \boldsymbol{\lambda}_0 + \boldsymbol{\lambda_1}\mathbf{X_t}. \tag{4.3.4}$$

The relation of the parameters of the P-measure to the Q-measure are given by:

$$\boldsymbol{\mu}^{\boldsymbol{Q}} = \boldsymbol{\mu}^{\boldsymbol{P}} - \boldsymbol{\Sigma}\lambda_0, \tag{4.3.5}$$

$$\boldsymbol{\rho}^{\boldsymbol{Q}} = \boldsymbol{\rho}^{\boldsymbol{P}} - \boldsymbol{\Sigma}\boldsymbol{\lambda_1}. \tag{4.3.6}$$

Also, we assume that the short rate is an affine function of the state variables:

$$r_t = \delta_0 + \boldsymbol{\delta_1'} \mathbf{X_t}. \tag{4.3.7}$$

The pricing kernel in the ATSM is

$$M_{t,t+1} = exp(-r_t - \frac{1}{2}\boldsymbol{\lambda_t'}\boldsymbol{\lambda_t} - \boldsymbol{\lambda_t'}, \mathbf{u_{t+1}}) \tag{4.3.8}$$

with $\boldsymbol{\lambda_t} = 0$ in the case of risk neutrality. The pricing kernel allows us to price any asset in the economy such as nominal bond prices. Substituting equation (4.3.3) in (4.3.7) we have that

$$M_{t,t+1} = exp(-\delta_0 - \boldsymbol{\delta_1'}\mathbf{X_t} - \frac{1}{2} - \boldsymbol{\lambda_t'}\boldsymbol{\lambda_t} - \boldsymbol{\lambda_t'}\mathbf{u_{t+1}}). \tag{4.3.9}$$

Bond prices can be estimated recursively as follows

$$P_t^n = E_t(M_{t+1}P_{t+1}^{n-1}), \tag{4.3.10}$$

P_t^n is the price of a zero-coupon bond with maturity n periods at time t. It can be shown that solving equation (4.3.10) is equivalent to solving equation

$$P_t^n = E_t^Q\left[exp(-\sum_{i=0}^{n-1} r_{t+i})\right], \tag{4.3.11}$$

where E_t^Q is the expectation under the risk-neutral probability measure Q. From equation (4.3.10) we derive that bond prices are exponential affine functions of the state variables:

$$P_t^n = exp(\alpha_n + \mathbf{b_n'}\mathbf{X_t}), \tag{4.3.12}$$

where

$$\alpha_{n+1} = \alpha_n + \mathbf{b_n'}(\boldsymbol{\mu} - \boldsymbol{\Sigma}\lambda_0) + \frac{1}{2}\mathbf{b_n'}\boldsymbol{\Sigma}\boldsymbol{\Sigma}'\mathbf{b_n} - \delta_0, \tag{4.3.13}$$

$$\mathbf{b_{n+1}} = \mathbf{b_n'}(\boldsymbol{\rho} - \boldsymbol{\Sigma}\boldsymbol{\lambda_1}) - \boldsymbol{\delta_1'}, \tag{4.3.14}$$

with starting values $a_1 = -\delta_0$ and $\mathbf{b_1} = -\boldsymbol{\delta_1}$. Also, yield risk premia is the difference between the observed yields and the hypothetical yields given by the expectations hypothesis:

$$yrp_t^n = \frac{1}{n}\sum_{i=1}^{n-1}(lnP_t^i - lnP_t^{i+1} - E_t(Y_{t+i}^1)). \tag{4.3.15}$$

Now, the yield of a n-period zero coupon bond is:

$$Y_t^n = -\frac{logP_t^n}{n} = A_n + \mathbf{B_n'X_t}. \tag{4.3.16}$$

where $A_n = \frac{\alpha_n}{n}$ and $\mathbf{B_n} = \frac{\mathbf{b_n}}{n}$. If we knew $\mathbf{X_t}$ and the values of $\boldsymbol{\mu^Q}$ and $\boldsymbol{\rho^Q}$ along with $\delta_0, \boldsymbol{\delta}_1$ and $\boldsymbol{\Sigma}$ we could use (4.3.13), (4.3.14) and (4.3.16) to predict the yield for any maturity n.

To estimate our model, we follow the approach of Chen and Scott (1993) and equation (4.3.16) holds exactly for as many yields as the number l of latent factors. The remaining $N_e = T_o - l$ linear combinations of observed yields differ from the predicted value by a small measurement error, T_o is the total number of yields. The choice of the maturity sets measured with error or not is driven by the interest in obtaining a very good estimate of the 10-year yield. Let $\mathbf{Y_t^1}$ denote the $l \times 1$ vector consisting of those linear combinations of yields that are priced without error and $\mathbf{Y_t^2}$ the remaining $(N_e \times 1)$ linear combinations that are priced with measurement error. The measurement specification is defined as

$$\begin{bmatrix} Y_t^1 \\ Y_t^2 \end{bmatrix} = \begin{bmatrix} A^1 \\ A^2 \end{bmatrix} + \begin{bmatrix} B^1 \\ B^2 \end{bmatrix} X_t + \begin{bmatrix} 0 \\ \Sigma_e \end{bmatrix} u_t^e, \tag{4.3.17}$$

where $\mathbf{\Sigma_e}$ is typically taken to be diagonal. A^i and B^i, $i = 1, 2$, are calculated by stacking (4.3.13) and (4.3.14), respectively, for the appropriate n. $\mathbf{\Sigma_e}$ determines the variance of the measurement error with $u_t^e \sim N(\mathbf{0}, \boldsymbol{I}_{N_e})$.

In our model we assume that yields maturing at 3,60,120 months are priced without error $\mathbf{Y_t^1} = (y_t^3, y_t^{60}, y_t^{120})$ and yields with maturities of 48,72 and 84 months are priced with error, $\mathbf{Y_t^2} = (y_t^{48}, y_t^{72}, y_t^{84})$. Overall, we have six different maturities from which $N_e = 3$ are priced with error. Following Hamilton and Wu (2012) for the model description, equation (5.3.14) has the following form

$$\begin{bmatrix} Y_t^3 \\ Y_t^{60} \\ Y_t^{120} \\ Y_T^{48} \\ Y_t^{72} \\ Y_t^{84} \end{bmatrix} = \begin{bmatrix} a_3 \\ a_{60} \\ a_{120} \\ a_{48} \\ a_{72} \\ a_{84} \end{bmatrix} + \begin{bmatrix} b_3' \\ b_{60}' \\ b_{120}' \\ b_{48}' \\ b_{72}' \\ b_{84}' \end{bmatrix} X_t + \begin{bmatrix} 0 \\ 0 \\ 0 \\ \Sigma_e \end{bmatrix} u_t^e, \tag{4.3.18}$$

The latent factors $\mathbf{X_t^u}$ are estimated from equation (5.3.14) from the yields measured without error and the observed factors $\mathbf{X_t^o}$ since they are known and $\mathbf{X_t} = [\mathbf{X_t^0} \;\; \mathbf{X_t^u}]'$

as follows

$$\mathbf{X_t^u} = \mathbf{B^{2,-1}}(\mathbf{Y_t^1} - A^1 - \mathbf{B^1 X_t^o}). \tag{4.3.19}$$

We also maintain the parameter restrictions imposed by Pericoli and Taboga (2008) and Hamilton and Wu (2012). These are $\mathbf{\Sigma_{lm}} = \mathbf{0}$, $\mathbf{\Sigma_{ll}} = \mathbf{I_{N_l}}$, $\delta_{\mathbf{1l}} \geq \mathbf{0}$ and $\mu_{\mathbf{l}}^{\mathbf{Q}} = \mathbf{0}$, where $\mathbf{\Sigma_{mm}}$ is a lower triangular matrix.

Ang and Piazzesi (2003) assumed that there is no interaction between macro dynamics and the unobserved latent factors. This means that $\rho_{\mathbf{ml}}$ and $\rho_{\mathbf{lm}}$ are set equal to zero. In our study we allow the interaction between the macroeconomic and latent factors. The structure of the loadings of the latent factors, $\rho_{\mathbf{ll}}^{\mathbf{Q}}$, is that proposed by Hamilton and Wu (2012).

The log-forward rate at time t for prices between time $n-1$ and n is given by

$$f_t^n = P_t^{n-1} - P_t^n. \tag{4.3.20}$$

We denote the log-holding period return (HPR) from buying an n-year bond at time t and selling it as an $n-1$ year bond at time $t+1$ as

$$r_{t+1}^n = P_{t+1}^{n-1} - P_t^n, \tag{4.3.21}$$

and the excess log-returns as

$$rx_{t+1}^n = r_{t+1}^n - Y_t^{(3)}, \tag{4.3.22}$$

where $Y^{(3)}$ is the 3-month U.S. Treasury bill rate.

4.3.2 Identification

The structural form of the affine model that we previously presented can be changed to a reduced form according to Hamilton and Wu (2012). We briefly present the set of equations for the reduced form (for more details see Hamilton and Wu (2012)):

$$X_t^m = A_m^* + \phi_{mm}^* X_{t-1}^m + \phi_{m1}^* Y_{t-1}^1 + u_{mt}^*, \tag{4.3.23}$$
$$Y_t^1 = A_1^* + \phi_{1m}^* X_{t-1}^m + \phi_{11}^* Y_{t-1}^1 + \psi_{1m}^* X_t^m + u_{1t}^*, \tag{4.3.24}$$
$$Y_t^2 = A_2^* + \phi_{2m}^* X_t^m + \phi_{21}^* Y_t^1 + u_{2t}^*, \tag{4.3.25}$$

with

$$A_1^* = A_1 + B_{1l}\mu_l - B_{1l}\rho_{ll}B_{1l}^{-1}A_1, \tag{4.3.26}$$

$$A_2^* = A_2 - B_{2l}B_{1l}^{-1}A_1, \tag{4.3.27}$$
$$A_m^* = \mu_m - \rho_{ml}B_{1l}^{-1}A_1, \tag{4.3.28}$$
$$\phi_{11}^* = B_{1l}\rho_{ll}B_{1l}^{-1}, \tag{4.3.29}$$
$$\phi_{1m}^* = B_{1l}\rho_{ll} - B_{1l}\rho_{ll}B_{1l}^{-1}B_{1m}, \tag{4.3.30}$$
$$\phi_{2m}^* = B_{2m} - B_{2l}B_{1l}^{-1}B_{1m}, \tag{4.3.31}$$
$$\phi_{21}^* = B_{2l}B_{1l}^{-1}, \tag{4.3.32}$$
$$\phi_{m1}^* = \rho_{ml}B_{1l}^{-1}, \tag{4.3.33}$$
$$\phi_{mm}^* = \rho_{mm} - \rho_{ml}B_{1l}^{-1}B_{1m}, \tag{4.3.34}$$
$$\psi_{1m}^* = B_{1m}, \tag{4.3.35}$$

and

$$Var\begin{bmatrix} u_{mt}^* \\ u_{1t}^* \\ u_{2t}^* \end{bmatrix} = \begin{bmatrix} \Omega_m^* & 0 & 0 \\ 0 & \Omega_1^* & 0 \\ 0 & 0 & \Omega_2^* \end{bmatrix} = \begin{bmatrix} \Sigma_{mm}\Sigma_{mm}^{'} & 0 & 0 \\ 0 & B_{1l}B_{1l}^{'} & 0 \\ 0 & 0 & \Sigma_e\Sigma_e^{'} \end{bmatrix}, \tag{4.3.36}$$

Full information maximum likelihood (FIML) estimation is obtained by treating the three blocks, $\mathbf{u_{1t}^*}, \mathbf{u_{2t}^*}, \mathbf{u_{mt}^*}$ separately since they are independent. Also, δ_0 can not be estimated separately from the OLS regression (4.3.7) because the risk-free rate is the dependent variable in the regression (4.3.7) and in the regression (4.3.3). Following the approach of Hamilton and Wu (2012) in order the model to be just identified we take three further restrictions on the matrix of the factor loadings $\rho^{\mathbf{Q}}$.

Table B.0.1 presents the mapping between structural and reduced form parameters. When the number of parameters in the structural form of the model is equal to the number of reduced-form parameters then the model is just identified. Also, when the reduced form parameters are more that those in the structural form, this is the case where the model imposes overidentifying restrictions but one can still estimate the structural parameters as functions of the unrestricted reduced-form estimates. The problem arises when more than one value for the parameter vector in the structural form is associated with the same reduced-form parameter vector, then the model is unidentified. As a result, there is no way to use the observed data to distinguish between the alternative parameter values (Hamilton and Wu (2012)).

4.3.3 Estimation of the Affine term structure model

The reduced form parameters are collected in a vector $\boldsymbol{\pi}$ and can be estimated by least squares methods. Then, the vector of the structural parameters $\boldsymbol{\theta}$ can be estimated

by the minimum chi square method. The main assumption of the method is that the reduced form parameters are equal to a function of the structural parameters, $\hat{\boldsymbol{\pi}} = g(\boldsymbol{\theta})$. The MCSE method uses the Wald test in order to test the hypothesis that $\boldsymbol{\pi} = g(\boldsymbol{\theta})$. Suppose now that $\mathcal{L}(\boldsymbol{\pi}; \mathbf{Y})$ is the log- likelihood for the entire sample and $\hat{\boldsymbol{\pi}} = \arg max \mathcal{L}(\boldsymbol{\pi}; \mathbf{Y})$ is the vector of the full information maximum likelihood estimates. Also, we assume that $\hat{\mathbf{R}}$ is a consistent estimate of the information matrix that satisfies the following equation

$$R = -\frac{1}{T} E\left[\frac{\vartheta^2 \mathcal{L}(\pi; Y)}{\vartheta \pi \vartheta \pi'}\right]. \tag{4.3.37}$$

The minimum chi square estimation is then given by:

$$\min_{\boldsymbol{\theta}} T(\hat{\boldsymbol{\pi}} - g(\boldsymbol{\theta}))' \mathbf{R} (\hat{\boldsymbol{\pi}} - g(\boldsymbol{\theta})), \tag{4.3.38}$$

where $\mathbf{R}$ is the information matrix of the full information maximum likelihood function $\mathcal{L}(\boldsymbol{\theta}; \mathbf{Y})$. The minimal value that is found by this estimator would have an asymptotic $\chi^2(q)$ distribution under the null hypothesis where q is the dimension of $\boldsymbol{\pi}$.

In the case of a just identified model the minimum value attainable for (4.3.38) is zero. Then equation (4.3.38) equivalently becomes

$$\min_{\boldsymbol{\theta}} (\hat{\boldsymbol{\pi}} - g(\boldsymbol{\theta}))' (\hat{\boldsymbol{\pi}} - g(\boldsymbol{\theta})). \tag{4.3.39}$$

When the objective function (4.3.38) is equal to zero the estimators that result from the maximum likelihood estimation and the minimum chi square estimation are asymptotically equivalent (Hamilton and Wu (2012). The information matrix $\mathbf{R}$ for all reduced-form parameters takes the following form (Pollock (1989))

$$\hat{\mathbf{R}} = \begin{bmatrix} \hat{R}_m & 0 & 0 \\ 0 & \hat{R}_1 & 0 \\ 0 & 0 & \hat{R}_2 \end{bmatrix}, \tag{4.3.40}$$

where

$$\hat{\mathbf{R}}_\mathbf{i} = \begin{bmatrix} \hat{\Omega}_i^{*-1} \otimes T^{-1} \sum_{t=1}^{T} x_{it} x_{it}' & 0 \\ 0 & \frac{1}{2} D_{qi}' (\hat{\Omega}_i^{*-1} \otimes \hat{\Omega}_i^{*-1}) D_{qi} \end{bmatrix}, \tag{4.3.41}$$

for $\mathbf{D_N}$ the $N^2 \times N(N+1)/2$ duplication matrix satisfying $\mathbf{D_N} \text{vech}(\Omega) = \text{vec}(\Omega)$. The structural measurement errors $\boldsymbol{\Sigma}_\mathbf{e}$ only exist in the block $\boldsymbol{\Omega}_\mathbf{2}^*$ and these parameters are just identified by the diagonal elements of $\hat{\Omega}_2^*$. Then the minimum chi square

estimates of $\mathbf{\Sigma_e}$ are obtained from the square roots of diagonal elements of $\mathbf{\Omega_2^*}$. The factor loadings submatrix takes for the latent factors under the risk-neutral measure Q has the following form

$$\rho_{ll}^{Q} = \begin{bmatrix} \rho_{l_1 l_1} & 0 & 0 \\ \rho_{l_2 l_1} & \rho_{l_2 l_2} & \rho_{l_2 l_3} \\ \rho_{l_3 l_1} & \rho_{l_3 l_2} & \rho_{l_3 l_3} \end{bmatrix}, \tag{4.3.42}$$

where $\rho_{l_2 l_2} = \rho_{l_3 l_3}$ and $\rho_{l_2 l_3} < \rho_{l_3 l_2}$. In order to optimize the objective function, we need to estimate 66 unknown parameters, 5 in $\boldsymbol{\delta_1}$,1 in δ_0, 25 in $\boldsymbol{\rho}$, 22 in $\boldsymbol{\rho^Q}$, 6 in $\mathbf{\Sigma}$, 5 in $\boldsymbol{\mu}$ and 2 in $\boldsymbol{\mu^Q}$. Since we estimate the model parameters we can estimate the coefficients $\alpha_n, \mathbf{b_n}$ from the recursive equations (4.3.13), (4.3.14). The results of the parameter estimation under the risk-neutral and historical probability measure are presented in table 4.3.1.

In addition, for a preliminary view of the response of Treasury yields to macroeconomic factors we run unrestricted OLS regressions. Table B.0.2 reports the estimation results from the regressions of Treasury yields with maturities 3 months, 60 months and 120 months on the two macreconomic factors. The adjusted R^2 is from 11% to 22%. This result suggests that macroeconomic factors should help explain the dynamics of bond yields. Also we observe that the adjusted R^2 and so the explanatory power of the macro factors, increases as bond maturity increases.

4.3.3.1 Forecasts

After the estimation we try to test the forecasting ability of our yield curve model. The yield curve could provide information about the future path of the economy (Cochrane and M. Piazzesi (2009)). The estimation of forecasts for the model is a crucial procedure for the estimation of the moments of bond returns and consequently for the portfolio optimization. We implement an out-of sample forecast for a period of 120 monthly time series of yields, from 2000:01 to 2009:12, for various forecast horizons in order to examine whether our model provides a good forecast of the yield curve dynamics. Also, in order to examine the forecasting ability of our model we calculate the root mean square errors (RMSE) and the mean absolute error (MAE).

$\rho^{\mathbf{Q}}$	1.1564	0.0417	-0.0513	0.0379	-0.0803
	(0.0015)	(0.0005)	(0.0029)	(0.0009)	(0.0002)
	-0.1827	0.9415	-0.0693	0.0282	0.0112
	(0.0018)	(0.0028)	(0.0019)	(0.0038)	(0.0012)
	0.3301	-0.0839	0.5979	0	0
	(0.0018)	(0.0034)	(0.0012)		
	-0.0830	-0.0584	-0.0633	0.9775	0.0476
	(0.0016)	(0.0004)	(0.0010)	(0.0003)	(0.0000)
	0.0766	0.0277	-0.0494	0.1284	0.9775
	(0.0011)	(0.0021)	(0.0019)	(0.0030)	(0.0003)
δ_0	-0.0036				
	(1.2126e-05)				
$\boldsymbol{\delta_1}$	1.3367e-05	2.3692e-6	3.5697e-04	2.1568e-4	1.6369e-4
	(7.4344e-06)	(7.0254e-06)	(4.1176e-06)	(5.2728e-06)	(4.7532e-06)
$\boldsymbol{\mu^Q}$	0.5151	0.7697	0	0	0
	(2.3627e-05)	(2.8129e-06)			
$\boldsymbol{\Sigma}$	0.2388	0	0	0	0
	(2.3552e-06)				
	0.0637	0.7076	0	0	0
	(2.4858e-06)	(2.2066e-6)			
	0	0	1	0	0
	0	0	0	1	0
	0	0	0	0	1
$\boldsymbol{\mu}$	-0.0208	0.6422	0.7131	-0.0605	-0.4171
	(3.9700e-04)	(3.4757e-04)	(3.7405e-04)	(4.3087e-04)	(3.7323e-04)
$\boldsymbol{\rho}$	0.4025	-0.0032	0.0264	0.0099	0.0191
	(2.3839e-04)	(9.7510e-04)	(0.0031)	(0.0048)	(0.0058)
	0.3538	0.1414	-0.1949 0.0548	0.0239	
	(1.0182e-04)	(7.1410e-05)	(0.0028)	(0.0016)	(0.0012)
	0.5871	0.0545	0.7882	0.0482	0.0263
	(1.3142e-04)	(3.4708e-04)	(0.0020)	(0.0037)	(0.0037)
	0.8148	-0.1672	0.0443	0.9668	0.0017
	(1.4495e-04)	(5.6863e-04)	(0.0023)	(0.0051)	(0.0038
	-1.2708	0.1074	0.1000	-0.0227	0.9346
	(8.8173e-05)	(2.4898e-04)	(0.0029)	(0.0030)	(0.0023)

Table 4.3.1: Parameter estimates under both risk neutral measure and historical probability measure along with their with asymptotic standard errors (in parentheses).

Table 4.3.2 presents the results for RMSEs and MAEs for the yields with maturities

3 months and 4,5,6,7 and 10 years. Lower values of root mean square error and mean absolute error denote better forecasts. Root mean square errors are estimated according to the following equation

$$RMSE = \sqrt{\frac{1}{T}\sum_{t=1}^{T}(\hat{Y}_t^n - Y_t^n)^2} \tag{4.3.43}$$

where $\hat{Y}_t^n$ and Y_t^n are the predicted and the actual yields respectively of a bond with maturity n months and T indicates the total length of the forecasting period, here 120 months. Mean absolute errors are estimated as

$$MAE = \frac{\sum_{i=1}^{T}|Y_i^n - \hat{Y}_i^n|}{T}. \tag{4.3.44}$$

From table 4.3.2 we can generally conclude that our term structure model with the two macroeconomic factors and three latent factors gives satisfactory forecasting results for the six maturities that we have. The results presented are for annualized data.

Yields	3-month	48-month	60-month	72-month	84-month	120-month
RMSE	0.0102	-0.7085	0.4968	-0.3315	-0.3312	-0.3470
MAE	0.2850	0.2647	0.4547	0.2778	0.2652	0.3148

Table 4.3.2: Forecast comparisons. The table presents the comparisons of the out-of-sample forecasts. The out-of-sample forecasting period is from 2000:01 to 2009:12, a total of 120 months. The root mean square error (RMSE) and the mean absolute error (MAE) for annualized data are calculated.

Figure C.0.7 presents the actual bond yields versus the estimated bond yields for the out-of-sample period 2000:01 to 2009:12.For the 3-,48-,72-month yield the fitting is almost identical. The fitted 60-month bond yield is very close to the actual and mimics its course. The 84-month bond yield is almost identical to the actual except for the period 2002:03 to 2005:10 when there is a small deviation. Finally, for the 120-month yield the deviation between the fitted and the actual yields is larger than the 84-month yield but generally performs well.

4.3.4 Impulse Responses

Impulse response functions (IRFs) are used in order to represent the dynamic effect over time of an unanticipated shock. Specifically, we are interest to know the response of one variable to an impulse in another variable in a system that involves a number of variables. An impulse response is a function of forecasts at distant horizons. Figure C.0.11 plots impulse responses for the observable factors and figure C.0.12 plots impulse responses for the latent factors from equation (4.3.1). Impulse responses are estimated for one standard deviation shock and for forecasting period of 16 months ahead. Impulse responses are estimated for the sample period 1981:01 to 2009:12. We can see from figure C.0.11 that a shock in IP Index has a negative impact in CPI showing a U-shaped pattern with reaching the low after 12 months. The response of the IP Index to a shock in Consumer Price Index shows a peak after 7 months but after 12 months has a negative impact.

Fig. 4.3.1 shows the factor weights B_n of the yield curve (equation (4.3.16)). The weight on the most persistent factor (Latent 1) is almost horizontal after a period of 15 months. This means that the first latent factor affects bond yields of all maturities in the same way. The coefficient of the second factor (Latent 2) is downward sloping and it mainly moves the short end of the yield curve. The coefficient on the third latent factor (Latent 3) affect yields at the short end of the yield curve and middle and long-end of the yield curve with different signs (Ang and Piazzesi (2003)). Figure 4.3.2 presents the A_n coefficients of the term structure models for a period of 120 months. The coefficients for a starting period of 10 periods (months) exhibit a downward trend but subsequently increase and stabilize for the rest of the time periods.

4.3.5 The distribution and estimation of bond returns

The main problem of fixed-income portfolios is the prediction of the distribution of asset returns for a set of maturities and the selection of the optimal portfolio weights conditional on expected returns and risk preferences. As a consequence this requires the estimation of the expected asset return for each maturity and their covariance matrix. The ATSM that we previously presented can be used for the construction of a fixed-income portfolio. In this section we derive closed-form expressions for the one-period ahead expected log-returns of bonds and their covariance matrix based on the affine dynamic factor model. These estimates are key concepts to the problem

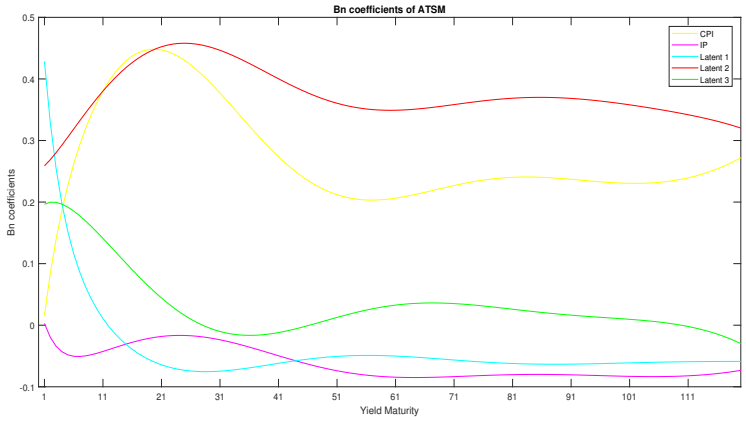

Figure 4.3.1: Factor weights B_n of the yield curve annualized. The figure displays yield weights as a function of maturity $n = 120$ months.

of bond portfolio optimization. Following the discussion in Caldeira et al. (2016) we can obtain expressions for expected bond returns and their covariance matrix based on the distribution of the yield curve model. Specifically, we are interested in the distribution of one-step-ahead forecasts of continuously compounded zero-coupon bond yields.

The Gaussian ATSM presented in equations (4.3.1) and (4.3.16) implies that the distribution of one-step-ahead forecasts of continuously compounded zero-coupon bond yields, is the normal distribution.

The one-step ahead forecasts of bond yields $\mathbf{Y_{t+1|t}} \sim N(\boldsymbol{\mu}_{\boldsymbol{y}_{t+1|t}}, \boldsymbol{\Sigma}_{\boldsymbol{\mu}_{t+1|t}})$ have mean and variance given by

$$\boldsymbol{\mu}_{\boldsymbol{Y}_{t+1|t}} = A_n + \mathbf{B_n^{'}}\hat{\mathbf{X}}_{\mathbf{t+1|t}}, \tag{4.3.45}$$

and

$$\boldsymbol{\Sigma}_{\boldsymbol{\mu}_{t+1|t}} = \mathbf{B_n}\mathbf{S_{t+1|t}}\mathbf{B_n^{'}} + \boldsymbol{\Sigma}, \tag{4.3.46}$$

respectively, where $\hat{\mathbf{X}}_{\mathbf{t+1|t}} = E_t[\mathbf{X_{t+1}}]$ denotes the expected value of the state factors $\mathbf{X_t}$ based on the estimates from the term structure model of equation (4.3.1). $\mathbf{S_{t+1|t}}$ is the covariance matrix not of the true factors $\mathbf{X_t}$ but of the filtered states based on the predicted state factors $\hat{\mathbf{X}}_{\mathbf{t+1|t}}$ (Caldeira et al. (2016)). The covariance of the

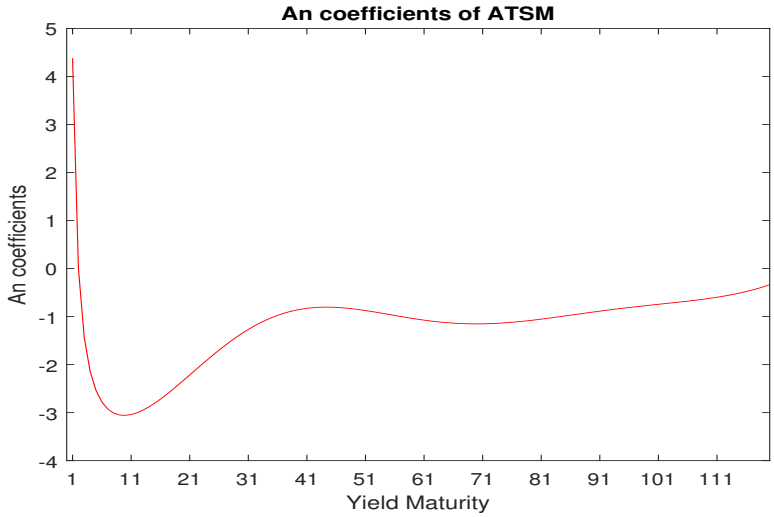

Figure 4.3.2: A_n coefficients of the yield curve annualized. The figure displays coefficients as a function of maturity $n = 120$ months.

predicted states is given by $\hat{\mathbf{S}}_{\mathbf{t+1|t}} = \boldsymbol{\Omega} + \mathbf{B_n}\boldsymbol{\Sigma}\mathbf{B_n'}$. As we mentioned earlier, in order to apply the mean-variance (MV) optimization approach we need the estimation of expected bond returns and their covariance matrix. For this procedure we need to estimate the one-period ahead of log-bond returns. We assume that the investor's one-period return comes from either holding the bond for a fixed maturity or either holding a bond from period t to $t+1$ while its maturity decreases. For the first case of fixed maturities the log-return of holding a bond from period t to $t+1$ is given by

$$\mathbf{rt_{t+1}} = \mathbf{log}\left(\frac{\mathbf{P_{t+1}}}{\mathbf{P_t}}\right) = \mathbf{log}(\mathbf{P_{t+1}}) - \mathbf{log}(\mathbf{P_t}) = -\mathbf{Y_{t+1}} + \mathbf{Y_t}. \tag{4.3.47}$$

One-period-ahead forecasts of log-returns of bonds, $rt_{t+1|t}$, are normally distributed with mean $\boldsymbol{\mu}_{\boldsymbol{rt}_{t+1|t}}$ and covariance matrix $\boldsymbol{\Sigma}_{\mathbf{rt}_{\mathbf{t+1|t}}}$. The mean $\boldsymbol{\mu}_{\boldsymbol{rt}_{t+1|t}}$ is given by:

$$\boldsymbol{\mu}_{\boldsymbol{rt}_{t+1|t}} = -n \cdot \boldsymbol{\mu}_{\boldsymbol{Y}_{t+1|t}} + n \cdot \mathbf{Y^n_{t-1}}. \tag{4.3.48}$$

The elements of the positive definite covariance matrix $\boldsymbol{\Sigma}_{\mathbf{rt}_{\mathbf{t+1|t}}}$ are given by:

$$\boldsymbol{\sigma}_{\boldsymbol{rt}_{t+1|t}} = n^2(\mathbf{B_n'}\mathbf{S_{t+1|t}}\mathbf{B_n} + \sigma_{\mathbf{n_i n_j}}), \tag{4.3.49}$$

where $n = 2, \ldots, N$ is the number of yield maturities, $\sigma_{n_i n_j}$ is the (i, j) element of $\boldsymbol{\Sigma}$.

For the second case, the log-return $\mathbf{r_{i,t}}$ of holding a bond from period t to $t+1$ while its maturity decreases from i to $i-1$ is

$$\mathbf{r_{i,t}} = \mathbf{log}(\frac{\mathbf{P_{t+1}^{i-1}}}{\mathbf{P_t^i}}) = \mathbf{log}(\mathbf{P_{t+1}^{i-1}}) - \mathbf{log}(\mathbf{P_t^i}) = -(\mathbf{i-1})\mathbf{Y_{t+1}^{i-1}} + \mathbf{iY_t^i}. \tag{4.3.50}$$

One-step-ahead forecasts of log-returns of bonds are normally distributed with mean given by

$$\boldsymbol{\mu}_{\boldsymbol{r}_{t+1|t}} = -(i-1)\cdot \boldsymbol{\mu}_{\boldsymbol{Y}_{i-1,t+1|t}} + i\cdot \mathbf{Y_{t-1}^i}. \tag{4.3.51}$$

The out-of-sample expected returns are presented in figure C.0.13. The positive definite covariance matrix $\mathbf{\Sigma_{r_{t+1}|t}}$ has diagonal elements given by:

$$\sigma_{r_{i,t+1|t}} = (i-1)^2(b_{i-1}^{'}\mathbf{S_{t+1|t}}b_{i-1} + \sigma_{i-1}^2), \tag{4.3.52}$$

and non-diagonal elements

$$\sigma_{r_i,r_j} = (i-1)(j-1)(b_{i-1}^{'}\mathbf{S_{t+1|t}}b_{j-1} + \sigma_{i-1,j-1}), \tag{4.3.53}$$

where σ_{i-1}^2 is the $(i-1)$th diagonal element of $\mathbf{\Sigma}$ and $(b_{n_i-1}^{'}\mathbf{S_{t+1|t}}b_{n_j-1}\sigma_{n_i-1n_j-1})$ is the $(i-1, j-1)$ element of the covariance matrix $\mathbf{\Sigma}_{\mu_{t+1|t}}$ of expected bond yields. The choice of the set of maturities depends among others on the investment horizon of the investor. Here, we present the results for the second investment case.

Figure C.0.5 presents the one-step-ahead holding period returns for the out-of-sample period. Figures C.0.6 and C.0.8 present the excess holding period returns without or with risk-free rate, respectively. Excess holding period returns in both cases exhibit the same patern. The risk-free rate is the Federal Funds rate (FFR). Figure C.0.9 shows the five-by-ten year forward rate for the sample period 1982:01 to 2009:12. We see that for the most time of the out-of-sample period remains positve. Figure C.0.10 presents the forward spreads for the entire period from 1982:01 to 2009:12 for holding a bond from period t to t+1 while its maturity decreases from τ_i to τ_{i-1} .We mention that for the entire period the forward spread holding a 3-month bond and a 10-year bond follows a downward trend.

4.4 Fixed-income portfolio optimization

In this section, we adopt the MV and GMV portfolio optimization approach for the construction of optimal bond portfolios based on the Gaussian ATSMs proposed by Hamilton and Wu (2012). The results for the expected bond yield returns and the

covariance obtained in the previous section are used for the bond portfolio optimization. The proposed MV and GMV bond portfolios are compared with traditional yield curve strategies and its performance is evaluated. For every portfolio strategy we examine the cases of allowing or not short selling.

4.4.1 Mean-variance framework

The portfolio theory introduced by Markowitz (1952), provides a basis for portfolio selection and optimization in a single-period set up. The Markowitz's approach assumes an investor that needs two main key ingredients in order to construct an investment portfolio: i) the estimated expected return for each investment and ii) the covariance matrix of returns. Even if the mean-variance approach is a myopic single-period portfolio strategy, investors can have potentially utility gains in comparison with dynamic multi-period investment horizons (see for example W. Brandt (2010) and Caldeira et al. (2016)).

Cheng (1962) adapted the mean-variance model for use in bond portfolio optimization by analyzing the effect of re-investment risk on bond portfolios. He modeled the trade-off between rolling-over short term investments and investing at the spot rate until the end of the investment horizon using probability beliefs on future reinvestment rates (and thus the term structure) as inputs.These beliefs were based on empirical data on historical interest rate movements. Bradley and Crane (1972) provided an improvement on this approach by using a dynamic bond portfolio selection formulation. Korn and Koziol (2006) examined the applicability of term structure models to bond portfolio selection.

The fixed maturity of bonds means that all bonds having maturities less than the investment horizon T_1 will not exist at time T_1. Bond prices are functions of time and interest rates (4.3.11) and so they become non-random at maturity date. Fabozzi and Fong (1994) consider that the major problem of a fixed-income portfolio optimization is that of constructing the variance-covariance matrix of bond returns. As a consequence traditional portfolio optimization models like the Markowitz portfolio method cannot be used directly for the construction of fixed-income portfolios and modifications should be used.

We assume, at the time of the portfolio selection, that investors are only concerned with the expected returns of U.S. Treasury yields for the one-step-ahead forecast horizon and its variance-covariance matrix, with rebalancing every 3 months. Then the mean-variance portfolio problem can be formulated by minimizing the portfolio

variance for a particular one-step-ahead expected bond return, subject or not to a set of additional restrictions on the vector of optimal weights $\mathbf{w}_t$. The mean-variance framework in case that short selling is not allowed (constrained portfolio), has the following form

$$\begin{aligned} \underset{w_t}{\text{minimize}} \quad & \mathbf{w}_t^{'}\boldsymbol{\Sigma}_{\mathbf{rt_{t+1|t}}}\mathbf{w}_t - \delta\mathbf{w}_t^{'}\boldsymbol{\mu}_{\boldsymbol{rt_{t+1|t}}} \\ \text{subject to} \quad & \mathbf{w}_t^{'}\mathbf{1} = \mathbf{1} \\ & \mathbf{w}_t \geq \mathbf{0} \end{aligned} \tag{4.4.1}$$

where $\boldsymbol{\mu}_{rt_{t+1|t}}$ is a $N \times 1$ vector of expected returns of maturities $n_i, i = 1, \ldots, N$, N is the number of yield maturities. $\boldsymbol{\Sigma}_{\mathbf{rt_{t+1|t}}}$ is a $N \times N$ variance-covariance matrix of expected returns estimated from equations (4.3.52) and (4.3.53) and $\mathbf{1}$ is a $N \times 1$ vector of ones, and δ is the risk aversion coefficient. In case where short selling is allowed in the last restriction in equation (4.4.1) $\mathbf{w}_t$ can take and negative values. The optimization problem is subject to a budget constraint, which ensures that all wealth is invested in the investment assets. The mean-variance portfolio problem as we see from equation (4.4.1) solves a quadratic utility function. The result of this optimization gives the vector of the optimal weights for each time period. In case we want to include an additional constraint about the duration of the fixed-income portfolio, then the optimization problem in (4.4.1) takes the following form:

$$\begin{aligned} \underset{w_t}{\text{minimize}} \quad & \mathbf{w}_t^{'}\boldsymbol{\Sigma}_{\mathbf{rt_{t+1|t}}}\mathbf{w}_t - \delta\mathbf{w}_t^{'}\boldsymbol{\mu}_{\boldsymbol{rt_{t+1|t}}} \\ \text{subject to} \quad & \mathbf{w}_t^{'}\mathbf{1} = \mathbf{1} \\ & \mathbf{w}_t \geq \mathbf{0} \\ & \tau_{\mathbf{d}} = \mathbf{w}_t^{'}\tau \end{aligned} \tag{4.4.2}$$

where $\boldsymbol{\tau}$ is the vector of individual bond durations and τ_d is the target portfolio duration. Alternatively, the mean-variance problem can be stated as a myopic single-period problem where portfolio weights are calculated based on one-step-ahead bond return forecasts. In addition, when an investor changes the composition of its portfolio over time, then faces with transaction costs and these costs are a function of frequency and magnitude of asset allocation changes in the portfolio. The portfolio turnover is estimated as

$$T_r = \frac{1}{T-1}\sum_{t=1}^{T-1}\sum_{i=1}^{N}(|\mathbf{w}_{i,t-1} - \mathbf{w}_{i,t}|). \tag{4.4.3}$$

The transaction costs is set to 3 basis points (bps) per transaction. Then, the cost of a trade over all assets is

$$T_c = 0.003 \sum_{t=1}^{T-1} \sum_{i=1}^{N} (|\mathbf{w}_{i,t-1} - \mathbf{w}_{i,t}|). \tag{4.4.4}$$

4.4.2 Global Minimum Variance Portfolio

The GMVP is the portfolio with the the smallest variance for a given covariance matrix (Kempf and Memmel (2006)). The optimal portfolio weights are determined independently from the expected asset returns. This has the advantage that the optimization depends completely on the covariance matrix of asset returns. The covariance matrix can be estimated with more reliability than expected returns (Golosnoy et al. (2011)). The GMVP is given from the following minimization

$$\begin{aligned} \underset{w_t}{\text{minimize}} \quad & \mathbf{w}_t^{'} \boldsymbol{\Sigma} \mathbf{w}_t \\ \text{subject to} \quad & \mathbf{w}_t^{'} \mathbf{1} = \mathbf{1} \\ & \mathbf{w}_t \geq \mathbf{0} \end{aligned} \tag{4.4.5}$$

where the last inequality is valid when short selling is not allowed. The optimal weights for the GMV portfolio when short selling is allowed are given by

$$\mathbf{w} = \frac{\boldsymbol{\Sigma}^{-1}\mathbf{1}}{\mathbf{1}'\boldsymbol{\Sigma}^{-1}\mathbf{1}}.$$

The GMV portfolio is the only portfolio of the efficient frontier that does not depend on the expected returns. In our work also we estimate the GMV portfolio under the assumption of allowing short selling on assets. This has as a result a better portfolio performance in terms of expected return and volatility compared to the case of constrained GMVP.

4.4.3 Benchmark portfolio strategies and Portfolio evaluation performance

The relative performance of the proposed bond portfolio strategy based on the Markowitz's portfolio theory is compared with a set of yield curve strategies (for more information about traditional yield curve strategies see Fabozzi and Fong (1994) and

Fabozzi (2018)). We consider the following yield curve strategies: barbell strategy, bullet strategy and ladder or equally weighted portfolio strategy. The main purpose of these strategies is to reduce yield volatility and risk. Also, we assume that the investor invests either in a 48-month or either in a 60-month bond. In the barbell portfolio strategy, the maturity of the bonds included in the portfolio is equally-weighted in the two extreme maturities, the 3-month and the 10-year bond. In the bullet strategy, the maturity of the bonds in the portfolio is concentrated at one point on the bond yield curve. This strategy has means that we can invest either to 48-month or 60-month or 72-month or 84-month bond, totally four alternative portfolios. Finally, in the equally weighted portfolio strategy the portfolio is constructed so as to has equal amount of each yield maturity.

Even if the tangency portfolio offers the best possible combinations of portfolio risk and expected return, the GMVP often yields better out-of-sample results than does an investment in the tangency portfolio (Kempf and Memmel (2006)). The empirical implementation of the mean-variance optimization problem defined by (4.4.1) is performed by using one- step-ahead estimates of the vector of expected returns and its covariance matrix, considering alternative values for the risk aversion coefficient δ, 0.0001, 0.01, 0.1 ,0.5,1,2 and 4.

The performance of optimal MV and GMVPs is evaluated using the average portfolio return ($\boldsymbol{\mu_r}$), the average excess return with respect to the risk-free rate ($\boldsymbol{\mu_{ex}}$) and the Sharpe Ratio (SR). We consider the risk-free rate to be the Federal Funds rate. These statistics are calculated as

$$\hat{\boldsymbol{\mu}} = \frac{1}{T-1}\sum_{t=1}^{T-1} \mathbf{w}_{\mathbf{i,t}}^{'}\mathbf{R_{t+1}}, \tag{4.4.6}$$

$$\hat{\mu}_{ex} = \frac{1}{T-1}\sum_{t=\tau}^{T-1} (\mathbf{w}_{t}^{'}\mathbf{R_{t+1}} - r_{t+1}^{f}), \tag{4.4.7}$$

$$SR = \frac{\hat{\mu}_{ex}}{\hat{\sigma}}, \tag{4.4.8}$$

where r^f is the risk-free rate which in our case is the federal feds rate, $\mathbf{w}_t$ is the vector of weights in the portfolio in period t. $\mathbf{R_t} = [r_{1,t}, \ldots, r_{N,t}]^{'}$ is a vector with the bond returns of all maturities and $\boldsymbol{\sigma}$ is the standard deviation of the portfolio's excess return.

4.4.4 Results for MV and GMV portfolios

We now present the optimal MV portfolios for the out-of-sample period, totally 120 months, for the JKV data set and for different levels of the risk aversion coefficient δ. Optimal portfolio compositions are rebalanced on a 3-month basis. First, we estimate the optimal weights under the mean-variance framework for both allowing or not short selling and subsequently the optimal weights for the GMVP. The excess return is calculated using the Federal Funds rate as the risk-free asset and the level of transaction costs is set to 3 bps. The results presented here for the mean-variance portfolio are for risk aversion $\delta = 0.001$. The excess return is calculated using the Federal Feds rate as a risk free rate.

Table 4.4.1 reports the following monthly performance measures: mean gross return, mean net excess return, portfolio standard deviation and the Sharpe ratio of the proposed portfolio strategy for both the cases allowing short selling or not. The table includes the results for the barbell strategy, the portfolio strategy of investing in the maturities remaining after excluding the 3-month and the 10-year bond (portfolio strategy A). Table 4.4.2 reports the performance measures for the ladder portfolio strategy and a bullet strategy investing either in a 4-year, 5-year, 6-year or 7-year bond. The results show that our portfolio strategy (MV) based on the ATSM produces returns and Sharpe ratios higher from many of the other benchmark strategies. Table 4.4.1 shows that the optimal mean-variance portfolio of U.S. Treasury bonds achieved a mean monthly average gross return of 9.83% for unconstrained portfolio and 5.36% when short selling is not allowed. The monthly standard deviation is 0.3602% and 0.3610% respectively. The risk-adjusted performance is measured by the Sharpe ratio which is equal to 5.88% and 2.90% for unconstrained and constrained portfolio respectively. The results indicate that the mean-variance bond portfolios can be very good alternatives to many traditional portfolio strategies.

Figure C.0.20 presents the evolution of optimal mean variance portfolio weights for the out-of-sample period under the assumption that short selling is not allowed and figure C.0.19 the evolution of optimal weights for each bond when short selling is allowed. In both cases the investor's position is concentrated in levels higher than 55% holding a 48-month bond at time t and a 3-month bond at time $t+1$. Figure 4.4.1 illustrates for the case of no short selling the cumulative returns of optimal portfolios estimated through our term structure model in comparison with some basic benchmark portfolio strategies. Specifically we have estimated the cumulative returns following the Barbell, A and Ladder portfolio strategy. The cumulative returns of the mean variance portfolios obtained from the term structure model using the minimum

chi-square method outperforms the other strategies for the out-of-sample period. In case of short selling (see figure 4.4.2) again our method outperforms the others.

Portfolio	Mean monthly return	Mean net excess return	Std (%)	Sharpe ratio (%)
MV	0.0983	0.0959	0.3602	5.8861
Barbell	0.1658	0.1634	0.3931	5.3485
A	0.0741	0.0717	0.5171	4.2990
MV^*	0.0989	0.0965	0.3610	2.9036
$Barbell^*$	0.1658	0.1634	0.3931	3.6206
A^*	0.0536	0.0512	0.2946	1.9334

Table 4.4.1: Performance of MV yield curve strategies for both allowing and not short selling (with * are denoted the results when short selling is not allowed).

Portfolio	Mean monthly return	Mean net excess return	Std (%)	Sharpe ratio (%)
Ladder	0.0764	0.0740	0.1228	5.4280
4-year Bond	0.0342	0.0317	0.1032	3.3209
5-year Bond	0.0131	0.0107	0.1325	0.8870
6-year Bond	0.0531	0.0507	0.1159	4.7890
7-year Bond	0.1415	0.1390	0.1971	7.7157

Table 4.4.2: Performance of benchmark portfolio strategies

The evolution of MV optimal portfolio weights in the out of sample period for the case of unconstrained and constrained portfolio for risk aversion δ equal to 0.001 is presented in figures C.0.19 and C.0.20 respectively. In the constrained case the weights are concentrated in investing in the first three maturities at time t and moving to a bond of the next maturity at time $t+1$. The portfolio turnover in both case shows a large increase at the end of 2008 during the global financial crisis (figure C.0.21 and figure C.0.22). The realized returns net of transaction costs for unconstrained and constrained MV portfolios, figures C.0.23 and C.0.24 respectively, show the same pattern for the out-of-sample period 2000:01 to 2009:12.

In table 4.4.3 the performance measures are presented for the unconstrained and constrained GMVP. The results show that our portfolio strategy based on the ATSM performs quite well in terms of mean returns, since only the barbell portfolio outperforms our strategy but with higher portfolio standard deviation.

Portfolio	Mean monthly return	Mean net excess return	Std (%)	Sharpe ratio (%)
GMV	0.0858	0.0833	0.3481	4.5956
Barbell	0.1404	0.1380	0.4114	3.6206
A	0.0255	0.0230	0.1296	1.9334
$GMV*$	0.0917	0.0893	0.2124	2.8861
$Barbell*$	0.1404	0.1380	0.2564	3.6206
$A*$	0.0287	0.0263	0.3136	2.6072

Table 4.4.3: Performance of GMVP yield curve strategies for both allowing and not short selling (with * are denoted the results when short selling is not allowed).

The performance of the portfolio constructed via an ATSM is compared in terms of cumulative returns, for the entire out-of-sample period, with other benchmark portfolio strategies (see figures 4.4.3 and 4.4.4). The results favor our method for case of mean-variance optimal portfolios either with short selling or not. In the GMV portfolio strategy the term structure based method performs quite satisfactory and only the barbell strategy outperforms ours.

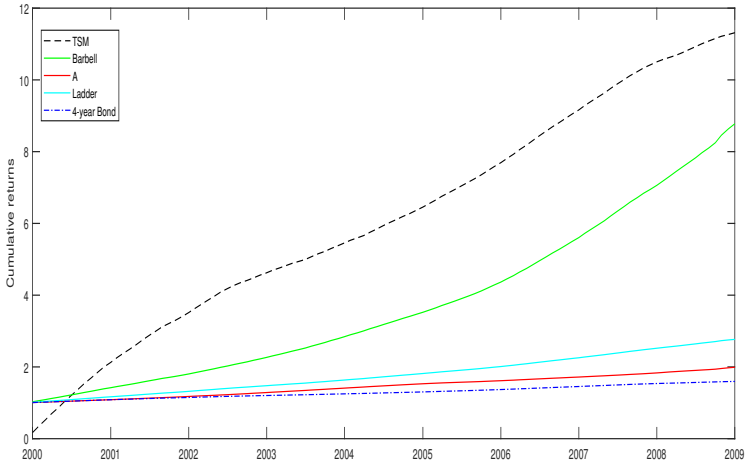

Figure 4.4.1: Cumulative MV portfolio returns for the out-of-sample period 2000:1 to 2009:12. Short selling is not allowed.

The results for the GMVP show that in terms of Sharpe ratio, mean gross and excess returns only the barbel strategy performs better than our strategy. A comparative

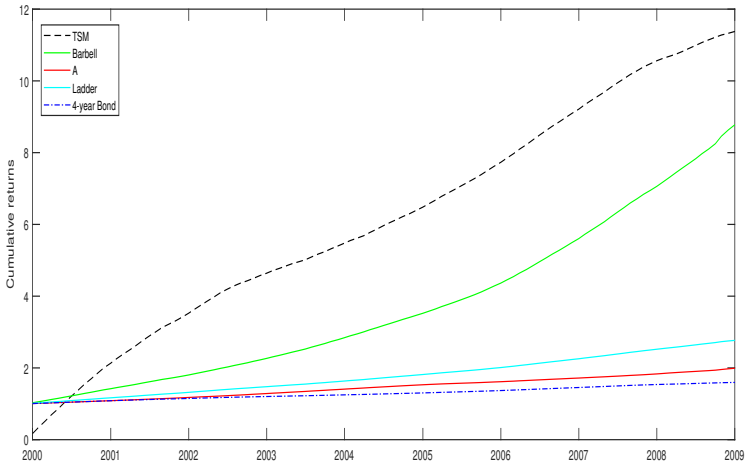

Figure 4.4.2: Cumulative MV portfolio returns for the out-of-sample period 2000:1 to 2009:12. Short selling is allowed.

analysis of the performance of mean-variance and GMVPs shows that the first generates higher Sharpe ratios but the latter exhibit lower standard deviation. The evolution of portfolio allocation (see figures C.0.15 and C.0.14) shows that as in the MV portfolio optimization the position of the investor is concentrated in in holding a 48-month bond at time t and a 3-month bond at time $t+1$ but now in lower levels. Also, our portfolio strategy for the entire out-of-sample period produce lower standard deviation from the barbell, bullet and ladder portfolio strategy (see figures C.0.16 and C.0.17).

In conclusion, the results obtained from the construction of optimal portfolios from the affine term structure presented in section 4 can be summarized as follows. The proposed bond portfolio strategies for the MV potfolio (ATSM-MV) and the GMV portfolio (ATSM-GMV) in most of the cases produce better mean returns and Sharpe ratios with lower risk, in comparison with traditional bond portfolio strategies. The results are valid regardless or not of the choice of allowing short selling.

4.5 Control charts and optimal weights monitoring

In this section, we construct control chart procedures for monitoring optimal portfolio weights obtained from the method described in the previous section. Our sequential

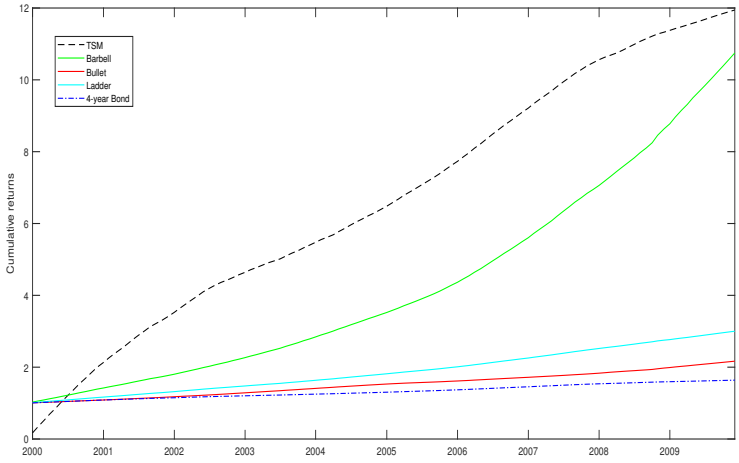

Figure 4.4.3: Cumulative GMV portfolio returns for the out-of-sample period 2000:1 to 2009:12. Short selling is not allowed.

monitoring analysis is restricted to GMV optimal portfolio weights. In contrast with the MV portfolio, the GMVP weights depend only on the covariance matrix of yield returns but not on the mean yield returns which increases the estimation risk of the portfolio. Since the investment decisions are mainly made in terms of portfolio weights we choose to monitor the vector of optimal weights each time period. Also, monitoring optimal weights in government bond portfolios can be very helpful in cases of liquidity problems.

4.5.1 Sequential Monitoring of optimal portfolio weights

Structural changes in the distribution of assets returns may have as a result changes is the optimal asset portfolio allocation. A very common assumption in the finance literature is that asset returns follow an independent and identically distribution which is usually normal. In our case bond expected returns due to their construction from the same dynamic term structure model exhibit correlation. Table B.0.3 presents the correlation coefficients for the bond expected returns. The results show that expected returns in most of the cases show correlation greater than 0.68. Okhrin and Schmid (2006) following the normality assumption for asset returns, examined the distribution and the asymptotic distribution properties of optimal weights in a GMV portfolio . They find that the optimal portfolio weights $\mathbf{w}_t$ follow an elliptical multivariate t-distribution with mean and variance:

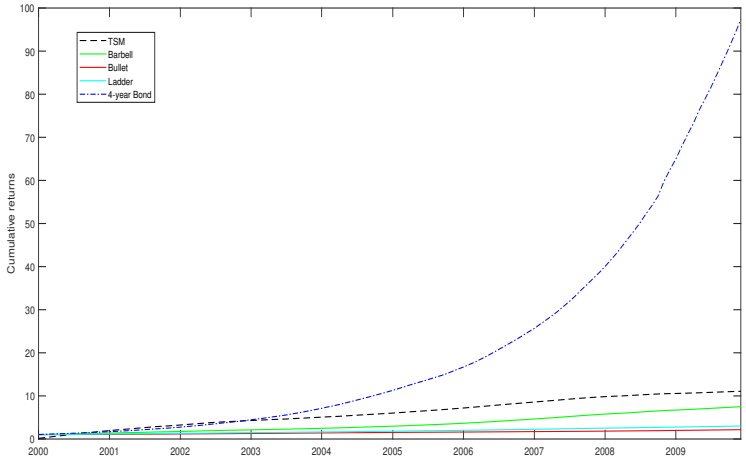

Figure 4.4.4: Cumulative GMV portfolio returns for the out-of-sample period 2000:1 to 2009:12. Short selling is allowed.

$$E(\hat{\mathbf{w}}) = \mathbf{w} \text{ and } \mathbf{\Omega} = Var(\hat{\mathbf{w}}) = \frac{1}{n-k-1} \cdot \frac{\mathbf{Q}}{\mathbf{1'\Sigma^{-1}1}},$$

respectively, where

$$\mathbf{Q} = \mathbf{\Sigma^{-1}} - \frac{\mathbf{\Sigma^{-1}11'\Sigma'}}{\mathbf{1'\Sigma^{-1}1}}.$$

The observed monitoring process of optimal portfolio weights is considered to be in control if $E(\hat{\mathbf{w}}_{t,n}) = \mathbf{w}$ holds for all $t \geq 1$, n is the size of the estimation window, otherwise the observed process is denoted to be out-of-control. We assume that the covariance matrix $\mathbf{\Sigma}$ remains unchanged between two consecutive change points.

Golosnoy and Schmid (2007) applied sequential control procedures for monitoring the optimal GMV portfolio weights. Specifically these procedures are applied to the random vector $\hat{\mathbf{w}}^*_{t,n}$ that contains the first *k-1* components of $\hat{\mathbf{w}}_{t,n}$. $\mathbf{\Omega}^*$ denotes the $(k-1) \times (k-1)$ matrix obtained by dropping the k-th row and the k-th column of the matrix $\mathbf{\Omega}$. The proposed control charts are based either on the estimated sample optimal weights $\hat{\mathbf{w}}_{t,n}$ or either on the first differences of the optimal weights $\mathbf{D_{t,n}} = \mathbf{\hat{w}_{t,n}} - \mathbf{\hat{w}_{t-1,n}}$. Portfolio weights are highly correlated and the use of differences has as a result the reduction of the correlation. The variables $\mathbf{w^*_t} - \mathbf{w^*_{t-1}}$

are asymptotically independent. A possibly disadvantage is that it depends on the estimation window length n (Golosnoy and Schmid (2007)). The control charts on sample weights are based on the univariate EWMA recursion applied on Mahalanobis distance and the MEWMA statistic. The Mahalanobis distance is referred to be the distance of optimal weight to its in-control (when there in no change) mean $\mathbf{w}^* = E_0(\hat{\mathbf{w}}^*_{t,n})$ and is measured by

$$T_{t,n} = (\hat{\mathbf{w}}^*_{t,n} - \mathbf{w}^*)' \mathbf{\Omega}^{*-1} (\hat{\mathbf{w}}^*_{t,n} - \mathbf{w}^*), t \geq 1. \tag{4.5.1}$$

The univariate EWMA recursion is given by

$$Z_{t,n} = (1 - \lambda) Z_{t-1,n} + \lambda T_{t,n}, \tag{4.5.2}$$

for $t \geq 1$. The starting value $Z_{0,n}$ is set equal to $E_0(T_{t,n}) = k - 1$. A signal is given if $Z_{t,n} > c_1$. The control limit c_1, which determines the rejection area, is estimated for a predetermined value of the ARL_0.

The multivariate EWMA recursion can be written as

$$\mathbf{Z}_{t,n} = (\mathbf{I} - \mathbf{R})^t \mathbf{Z}_{t-1,n} + \mathbf{R} \hat{\mathbf{w}}^*_{t-,n}, t \geq 1,$$

or

$$\mathbf{Z}_{t,n} = (\mathbf{I} - \mathbf{R})^t \mathbf{Z}_{0,n} + \mathbf{R} \sum_{\upsilon=0}^{t-1} (\mathbf{I} - \mathbf{R})^\upsilon \hat{\mathbf{w}}^*_{t-\upsilon,n}, \tag{4.5.3}$$

where $\mathbf{I}$ is the $(k-1) \times (k-1)$ identity matrix and $\mathbf{R} = diag(r_1, r_2, \ldots, r_{k-1})$ is $(k-1) \times (k-1)$ diagonal matrix with diagonal elements $0 < r_i \leq 1$, $i \in \{1, 2, \ldots, k-1\}$. The starting value $\mathbf{Z}_{0,n}$ is $E_0(\mathbf{Z}_{t,n}) = \mathbf{w}^*$, with E_0 is denoted the mean value when the monitoring process is in-control. The covariance matrix of the multivariate EWMA statistic $\mathbf{Z}_{t,n}$ in the in-control state is given by

$$Cov_0(\mathbf{Z_{t,n}}) = \mathbf{R} \left(\sum_{i,j=0}^{t-1} (\mathbf{I} - \mathbf{R})^i Cov_0(\hat{\mathbf{w}}^*_{t-i,n}, \hat{\mathbf{w}}^*_{t-j,n}) (\mathbf{I} - \mathbf{R})^J \right) \mathbf{R}. \tag{4.5.4}$$

A signal is given if

$$(\mathbf{Z}_{t,n} - E_0(\mathbf{Z}_{t,n}))' Cov_0(\mathbf{Z}_t)^{-1} (\mathbf{Z}_{t,n} - E_0(\mathbf{Z}_{t,n})) > c.$$

Golosnoy and Schmid (2007) constructed analogously the control charts based on the first differences of optimal portfolio weights. The Mahalanobis distance of the first differences from the mean when the process is in control, is defined as

$$T_{t,n}^{d} = (\mathbf{D_{t,n}} - E_0(\mathbf{D_{t,n}}))' \Omega_d^{*-1} (\mathbf{D_{t,n}} - E_0(\mathbf{D_{t,n}})), \tag{4.5.5}$$

with $\Omega_d^* = Cov_0(\mathbf{D_{t,n}})$. When the process is in-control we have $E_o(\mathbf{D_{t,n}}) = 0$, then the Malanobis distance takes the following form

$$T_{t,n}^{d} = \mathbf{D_{t,n}} \Omega_d^{*-1} \mathbf{D_{t,n}}. \tag{4.5.6}$$

The univariate EWMA recursion is given by

$$Z_{t,n}^{d} = (1-\lambda) Z_{t-1,n}^{d} + \lambda T_{t,n}^{d}, \tag{4.5.7}$$

where $t \geq 1$ and $\lambda \in (0,1]$. The starting value is

$$Z_{0,n}^{d} = E_0(\mathbf{D_{t,n}}' Cov_0(\mathbf{D_{t,n}})^{-1} \mathbf{D_{t,n}}) = E_0(T_{t,n}^{d}) = k - 1.$$

The monitoring process is out of control if $Z_{t,n}^{d} > c_d$, c_d is a chosen control limit. For the difference control charts based on the multivariate EWMA recursion the control statistic is

$$\mathbf{Z_{t,n}^{d}} = \mathbf{(I\text{-}R)}\ \mathbf{Z_{t-1,n}^{d}} + \mathbf{R}\ D_{t,n}, t \geq 1, \tag{4.5.8}$$

with starting value $\mathbf{Z_{0,n}^{d}} = E_0(\mathbf{D_{t,n}}) = 0$. The process is out of control if

$$\mathbf{Z_{t,n}^{d'}} Cov_0(\mathbf{Z_{t,n}^{d}})^{-1} \mathbf{Z_{t,n}^{d}} > c_d.$$

The control limit of a control chart defines the rejection area in every control scheme and is estimated through a simulation study for a predetermined value of the ARL (usually in financial applications is equal to 120 days or 1/2 year of daily observations Golosnoy and Schmid (2007)). After a signal is given the financial analyst should examine it and decide for further actions about the portfolio allocation. The control limit of each control chart is determined through a simulation study for a prespecified value c for ARL_0. Because of the monthly sequence of our data, we chose in-control average run length to be equal to 6 months. This means that on average the first false signal comes after six months of observations. The critical value c_d is the solution of the equation (1.2.1). After a starting value of the control limit is chosen, 5×10^4 values of the difference process are simulated. These simulated values are applied to the control chart procedure and the stopping times of the control charts are simulated. Again, 5×10^4 values of the difference process are simulated and the stopping times

are recorded. This simulation procedure is iterated 5×10^4 times. The estimated ARL in the in-control state is the average of simulated stopping times. The iterations are stopped if the absolute deviation from the prespecified ARL_0 is less than 0.002. For the estimation of the control limit using the MRL we follow the same technique as described with the ARL and the MRL_0 is chosen equal to 6 months.

4.5.2 Estimation of the covariance matrix

The optimal portfolio weights depend on the unknown parameters of the asset returns distribution which are subject to unknown structural breaks. In the GMVP framework the expected portfolio return and the portfolio risk depends through the optimal weights composition on the variance of asset returns. Because the variance of asset return is unknown in practice, it has to be estimated. The parameter estimation causes estimation risk in the optimal portfolio selection and ignoring it may have negative consequences in optimal portfolio selection (Frisén (2008)). Various methods have been applied in order to reduce the estimation risk (see for example Brandt (2010) and DeMiguel et al. (2009)). A very common estimator of the covariance matrix of asset returns is the sample covariance matrix. In our work the covariance matrix of asset returns is estimated through the affine term structure model.

The main problem in order to estimate the control statistics for the difference charts we presented in the previous section, is the estimation of the covariances when the process is in control of the differences of the optimal weights. Suppose a portfolio consisting of risky assets under the assumption of independent and normally distributed returns. Since the exact estimation of these autocovariances we previously mentioned is difficult, Golosnoy and Schmid (2007) based on the work of Okhrin and Schmid (2006) proposed an approximation for large n. However, in our case due the high correlation of the asset returns we have we choose to estimate these quantities through a simulation study. Golosnoy et al. (2010) mentioned as an alternative method for the covariance estimation could be a Monte Carlo approach. In our work we try to approximate the covariance matrix through a simulation study. The estimation of the covariance of the control statistic $\mathbf{Z}_{t,n}^d$, when the process is in control, requires the estimation of the covariance matrix between the weights. Golosnoy and Schmid (2007) studied and approximated the limit behavior of $Cov_0(\mathbf{Z}_{t,n}^d)$ as n tends to infinity.

For the estimation of the autocovariance matrix of the first differences of optimal weights we use the following iterative procedure:

1) Generate data from the state evolution process $\mathbf{X_t} \sim N(\boldsymbol{\mu}, \boldsymbol{\Sigma}\boldsymbol{\Sigma}')$ when the process is in-control.
2) Generate residual data for the state evolution process $U \sim N(\mathbf{0}, \mathbf{I})$.
3) Estimate the covariance matrix of the filtered states $\mathbf{X_{t|t+1}}$.
4) Estimate the covariance matrix of one-period ahead bond yields $\mathbf{Y_{t|t+1}}$.
5) Estimate one-period ahead realized returns according to section 4.5.
6) Estimate optimal global minimum variance portfolio weights.
7) Estimate the first differences of optimal weights.
8) Estimate variance of first differences of optimal weights.
9) Repeat the above procedure for 5×10^4 iterations.
After the estimation of the autocovariances of optimal weights from equations (4.5.7) and (4.5.8) we can estimate the control statistics for the first difference procedures of the univariate EWMA based on the Mahalanobis distance and the multivariate EWMA.

4.6 Simulation study

The proposed difference control schemes for correlated data along with their detection ability are analyzed within a simulation study. At first, the control limits for all charts are determined in such a way that the control charts provide the same in-control average run lengths, here assumed to be equal to a period of six months. After obtaining the control limits through simulation as described previously, the performance of control charts assuming that a change point happens at the beginning the performance is evaluated by computing the ARL_1 and the MRL_1.

4.6.1 Modeling the out-of-control state

In our simulation study we follow the approach of Golosnoy et al. (2011) for modelling the asset variance. We suppose that we have k=6 assets, government bond yields, that follow the normal distribution with mean $\boldsymbol{\mu}$ and variance $\boldsymbol{\Sigma}$ which has the following form

$$\boldsymbol{\Sigma} = \mathbf{S} \cdot \mathbf{C} \cdot \mathbf{S},$$

or else

$$\mathbf{\Sigma} = \begin{pmatrix} \sigma_1 & 0 & 0 & 0 & 0 & 0 \\ 0 & \sigma_2 & 0 & 0 & 0 & 0 \\ 0 & 0 & \sigma_3 & 0 & 0 & 0 \\ 0 & 0 & 0 & \sigma_4 & 0 & 0 \\ 0 & 0 & 0 & 0 & \sigma_5 & 0 \\ 0 & 0 & 0 & 0 & 0 & \sigma_6 \end{pmatrix} \begin{pmatrix} 1 & a_{12} & a_{13} & a_{14} & a_{15} & a_{16} \\ a_{21} & 1 & a_{23} & a_{24} & a_{25} & a_{26} \\ a_{31} & a_{32} & 1 & a_{34} & a_{35} & a_{36} \\ a_{41} & a_{42} & a_{43} & 1 & a_{45} & a_{46} \\ a_{52} & a_{52} & a_{53} & a_{54} & 1 & a_{56} \\ a_{61} & a_{62} & a_{63} & a_{64} & a_{65} & 1 \end{pmatrix} \begin{pmatrix} \sigma_1 & 0 & 0 & 0 & 0 & 0 \\ 0 & \sigma_2 & 0 & 0 & 0 & 0 \\ 0 & 0 & \sigma_3 & 0 & 0 & 0 \\ 0 & 0 & 0 & \sigma_4 & 0 & 0 \\ 0 & 0 & 0 & 0 & \sigma_5 & 0 \\ 0 & 0 & 0 & 0 & 0 & \sigma_6 \end{pmatrix},$$

where $\mathbf{S}$ is a diagonal matrix that contains the standard deviations and $\mathbf{C}$ is the correlation matrix. In our study we assume that the in-control variance is

$$\mathbf{\Sigma_0} = \begin{pmatrix} 0.7 & 0 & 0 & 0 & 0 & 0 \\ 0 & 0.8 & 0 & 0 & 0 & 0 \\ 0 & 0 & 0.85 & 0 & 0 & 0 \\ 0 & 0 & 0 & 0.9 & 0 & 0 \\ 0 & 0 & 0 & 0 & 0.95 & 0 \\ 0 & 0 & 0 & 0 & 0 & 0.99 \end{pmatrix} \cdot \begin{pmatrix} 1 & 0.403 & 0.421 & 0.433 & 0.331 \\ 0.403 & 1 & 0.8030 & 0.8319 & 0.6757 \\ 0.421 & 0.8030 & 1 & 0.8570 & 0.7015 \\ 0.433 & 0.8319 & 0.8570 & 1 & 0.7287 \\ 0.331 & 0.6757 & 0.7015 & 0.7287 & 1 \end{pmatrix} \cdot \begin{pmatrix} 0.7 & 0 & 0 & 0 & 0 & 0 \\ 0 & 0.8 & 0 & 0 & 0 & 0 \\ 0 & 0 & 0.85 & 0 & 0 & 0 \\ 0 & 0 & 0 & 0.9 & 0 & 0 \\ 0 & 0 & 0 & 0 & 0.95 & 0 \\ 0 & 0 & 0 & 0 & 0 & 0.99 \end{pmatrix},$$

Also, the variance of the out-of-control state has the following form

$$\mathbf{\Sigma_1} = \mathbf{S_1} \cdot \mathbf{C_1} \cdot \mathbf{S_1},$$

or

$$\mathbf{\Sigma_1} = \begin{pmatrix} 0.7h & 0 & 0 & 0 & 0 & 0 \\ 0 & 0.8h & 0 & 0 & 0 & 0 \\ 0 & 0 & 0.85h & 0 & 0 & 0 \\ 0 & 0 & 0 & 0.9h & 0 & 0 \\ 0 & 0 & 0 & 0 & 0.95h & 0 \\ 0 & 0 & 0 & 0 & 0 & 0.99h \end{pmatrix} \cdot \begin{pmatrix} 1 & 0.403v & 0.421v & 0.433v & 0.331v \\ 0.0403v & 1 & 0.8030v & 0.8319v & 0.6757v \\ 0.421v & 0.8030v & 1 & 0.8570v & 0.7015v \\ 0.433v & 0.8319v & 0.8570v & 1 & 0.7287v \\ 0.331v & 0.6757v & 0.7015v & 0.7287v & 1 \end{pmatrix} \cdot \begin{pmatrix} 0.7h & 0 & 0 & 0 & 0 & 0 \\ 0 & 0.8h & 0 & 0 & 0 & 0 \\ 0 & 0 & 0.85h & 0 & 0 & 0 \\ 0 & 0 & 0 & 0.9h & 0 & 0 \\ 0 & 0 & 0 & 0 & 0.95h & 0 \\ 0 & 0 & 0 & 0 & 0 & 0.99h \end{pmatrix}.$$

Here we assume changes only in the variance of the bond yield returns, so $v = 1$. The standard deviation parameter h can take values from the set $\{1.5, 2, 2.5, 3, 3.5, 4, 4.5\}$. The estimation window n is equal to 25 and the smoothing parameter in the univariate EMWA based on the Mahalanobis distance is $\lambda \in \{0.05, 0.1, 0.15, 0.2, 0.25, 0.3, 0.35, 0.4, 0.45, 0.5, 0.75, 0.9\}$. The MEWMA control charts are constructed with all smoothing parameters in the main diagonal equal, $r = r_1 = \cdots = r_{k-1} = \lambda I$. In our simulation study there are totally 84 different out-of-control cases. We mention that ARL_1 is calculated under the restrictive assumption that the change happens at time $t = 1$.

4.6.2 Simulation study results

Okhrin and Schmid (2006) under the assumption that the asset returns are independent and identically normally distributed, they derived the exact distribution of optimal weights $\hat{\mathbf{w}}_\mathbf{t}$ and prove they are asymptotically normal. In our work the independence of asset returns is not valid because bond yields are estimated via a common dynamic factor model. In order to overcome this problem we choose to follow a simulation approach for estimating the necessary moments of optimal weights. We mention that for the distribution of optimal weights in a GMVP when asset returns are dependent and identically distributed a possible approach could be the logistic distribution but with larger kyrtosis (see figure C.0.18) and this topic remains for further research. We remind that the logistic distribution is very similar in shape to the normal distribution and has roughly the same shape as the Student's t-distribution.

The simulation study compares the results for the out-of-sample period of four control chart cases: the univariate EWMA control charts based on Mahalanobis distance for unconstrained (Mahalu) and constrained portfolio (Mahalc), the control charts based on the MEWMA statistic for unconstrained (MEWMAu) and constrained portfolio (MEWMAc). We remind that small values of the smoothing parameter λ give more weight to older data and for $\lambda = 1$ the EWMA chart is a Shewhart chart. For the first case (Mahalu) (table B.0.4) the ARL_1 is reduced for each certain level of the smoothing parameter λ as the variance increases. For values $\lambda = \{0.05, 1\}$ and $\lambda = \{0.75, 9\}$ we observe large values for the ARL_1. In parentheses we present the MRL_1s which they follow the same pattern as the $ARLs_1$. The results for the second case (table B.0.6) show that the strategy of not allowing short selling gives smaller out-of-sample ARL_1s. Again for a given value of the smoothing parameter as the shock in variance increases the ARL_1 decreases. Control charts based on the MEWMA statistic for unconstrained portfolio (table B.0.5) exhibit lower values of ARL_1 for the Mahalanobis distance case. Finally, the fourth case (table B.0.7) gives the lowest ARL_1s except in the cases with smoothing parameters $\lambda = \{0.75, 0.9\}$. Generally, the examples with portfolios not allowing short selling perform better in terms of ARL_1 than allowing short selling. The MRL_1s for the constrained portfolios indicate that our method gives signal at the next time period when the monitoring process of portfolio weights is already in the out-of-control state. The fact that the MRL_1 is smaller in some cases from the ARL_1 indicate that the distribution of the run length may be extremely right-skewed (Golosnoy and Schmid (2007)).

Table 4.6.1 presents the best ARL_1 values for each control chart case and the cor-

responding value of smoothing parameter λ for each shock in the variance matrix. For the Mahalu case the control chart with smoothing parameter $\lambda = 0.35$ performs better and gives the smallest out-of-sample ARL. In Mahac this happens for smoothing parameter $\lambda = 0.1$. On the contrary in MEWMAu and MEWMAc occasion there is no unique smoothing parameter value that outperforms the others. In the first case small shocks are detected faster from large values of λ in contrast to larger shocks where more appropriate are small values of the smoothing parameter. In the latter, for all shocks in the variance the best results are given for small values of the smoothing parameter. Table 4.6.2 exhibits the best MRL_1 values for the two cases for unconstrained portfolio, Mahalu and MEWMAu, along with the corresponding smoothing parameter values. In both cases there is no specific value for the smoothing parameter that outperforms the others.

The difference control charts based on the Mahalanobis distance perform better that these based on the multivariate EMWA recursion in the case of unconstrained portfolios. This not always happens when short selling in not allowed since in many cases the control schemes based on MEWMA recursion have slightly better results in terms of out-of-sample ARL. As a portfolio strategy the prohibition of short selling has as result lower out-of-sample ARL_1s and MRL_1s. The smallest out-of-sample ARL_1s obtained for the Mahalu charts are comparable with the results from the MEWMAu charts. With some exceptions the proposed difference control schemes for monitoring optimal weights from a government bond portfolio favour small values of the smoothing parameter. This is in accordance with the results for the case of portfolios constructed from risk assets (Golosnoy and Schmid (2007)). Additionally, the difference control schemes appear to react slowly in small changes in the variance of asset returns and the out-of-sample ARL_1s takes large values except in the case of MEWMAc.

4.7 Empirical example

The control charts based on the first differences of optimal portfolio weights are applied in the out-of-sample period from January, 2000 to December, 2009 in total 120 months. We assume an investor who holds a portfolio consisted of $k = 6$ U.S. Treasury bonds. Before we construct the control charts it is necessary to determine the target process or else the in-control process. This may be quite challenging for real data in financial applications specially in our example where we have lees frequently data than daily, monthly. When the monitoring process is in control, it is assumed there is no change point and the target process is estimated.

u	Malalu	Mahalc	MEWMAu	MEWMAc
1.5	4.2689 (0.35)	1.1212 (0.1)	5.4578 (0.75)	1.3646 (0.05)
2	4.1450 (0.35)	1.0668 (0.1)	5.3463 (0.75)	1.1986 (0.1)
2.5	4.0805 (0.35)	1.0320 (0.1)	2.2036 (0.5)	1.0656 (0.1)
3	3.9716 (0.35)	1.0252 (0.1)	4.9013 (0.05)	1.0168 (0.05)
3.5	3.7859 (0.35)	1.0178 (0.1)	4.5306 (0.25)	1.0136 (0.05)
4	3.6668 (0.35)	1.0106 (0.1)	3.9979 (0.05)	1.0102 (0.1)
4.5	3.4719 (0.35)	1.0050 (0.1)	3.7748 (0.15)	1.0106 (0.1)

Table 4.6.1: Best out-of-control ARLs values for each shock in variance of asset returns, for n=40 and in-control ARL=6. The corresponding smoothing parameter values are given in parentheses.

u	1.5	2	2.5	3	3.5	4	4.5
Malalu	5 (0.5)	5 (0.5)	5 (0.15)	4 (0.5)	4 (0.5)	5 (*)	4 (0.05)
MEWMAu	4 (*)	3 (0.3)	4 (*)	4 (*)	3 (*)	3 (*)	3 (*)

Table 4.6.2: Best out-of-control MRLs values for n=40 and in-control MRL=6 for unconstrained portfolios.The corresponding smoothing parameter values are given in parentheses.The notation (*) means that more than on value of λ is appropriate.

We choose the period from September 1996 to December 1999, in total 40 months, as the prerun period where the process is in-control. In this period the U.S. Treasury bond returns are assumed to be in the in-control state. Using the observations from this period we estimate the in-control one period ahead log- realized returns, the one-period ahead expected returns, the covariance matrix of bond returns and the target optimal GMVP weights. The control charts are constructed for the out-of-sample period and there is no-reestimation of the target process. After the control chart gives a signal and is confirmed from the financial analyst that this is a structural break, normally the target process should be reevaluated (see for example Golosnoy and Schmid (2007) and Golosnoy et al. 2011). Since, in our case we have less frequently data a possible solution to this problem may be via simulation. The control limits are chosen for a prespecified value h of the in-control ARL equal to 6 months, this means that on average each control chart should give the first false alarm after six months. The control charts are estimated for the following set of smoothing parameters $\lambda \in \{0.05, 0.1, 0.15, 0.2, 0.25, 0.3, 0.35, 0.4, 0.45, 0.5, 0.75, 0.9\}$. Golosnoy and Schmid (2007) mentioned that a benefit of the first difference control charts is that give an alarm almost immediately with high probability if the change in the

parameters we monitor is large.

Longerstaey and Spencer (1996) supported the choice of large values of the smoothing parameters in the EWMA model in financial applications, specifically equal to 0.97. In contrast Bollen (2015) is in favor of lower values values and found that the optimal value of λ is time varying and clusters in high and low periods. In our empirical example we find that in the case of control schemes based on the Mahalanobis distance for constrained and unconstrained GMVP values equal or lower than 0.15 and 0.3 respectively, are appropriate. In addition, for control schemes based on multivariate EWMA recursion for both cases smoothing parameter values equal or lower than 0.3 are preferred.

The behavior of the control statistics based on the Mahalanobis distance for smoothing parameter values $r = \lambda I, \lambda \in \{0.05, 0.1, 0.15, 0.2, 0.25, 0.3\}$. is shown in figures 4.7.1 and 4.7.2 for constrained and unconstrained portfolio respectively. Results for the rest of the smoothing parameter values are presented in the Appendix B. Figures 4.7.3 and 4.7.4 present analogously the control statistics based on the MEWMA recursion. We remind that for the MEWMA charts the smoothing matrix is taken as a diagonal matrix with diagonal elements equal to λ, $r = \lambda I$. In the control schemes based on the Mahalanobis distance the control statistics show large oscillations in contrast with those of MEWMA recursion that exhibit a very smoother behavior. As a consequence, control statistics based on Mahalanobis distance are more often lying above the control limit from those based on MEWMA recursion.

Control scheme	Smth parameter.	Control limit
Mahal. dist. (constrained)	0.15	29.8
Mahal. dist. (unconstrained)	0.15	31.8
MEMWA (constrained)	0.2	1809.8
MEMWA (unconstrained)	0.2	12.9

Table 4.7.1: Control limits for the out-of-sample period for the various control schemes and fixed ARL equal to 6. The control schemes are applied to constrained or unconstrained portfolios.

The main purpose of an investor is to minimize the one period ahead out-of-sample portfolio variance. The proposed control charts give a signal when a structural break in the optimal portfolio weights is likely to happen. Table 4.7.1 presents for the two control chart procedures and constrained and unconstrained portfolio optimization,

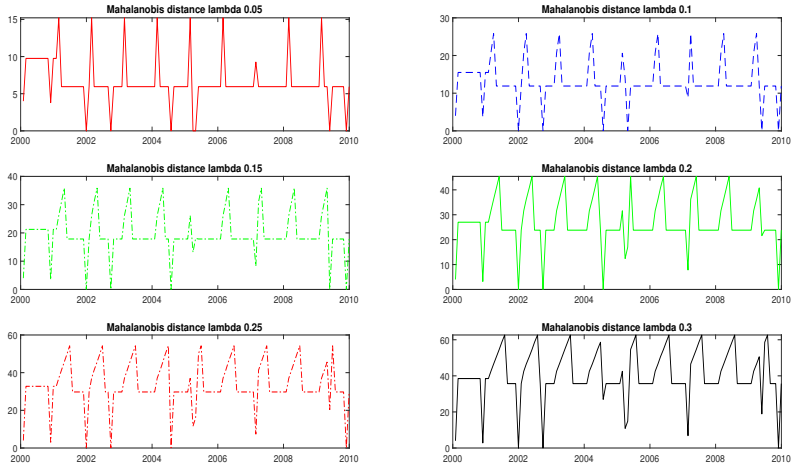

Figure 4.7.1: Control Statistics for constrained GMVP based on Mahalanobis distance for $\lambda = \{0.05, 0.1, 0.15, 0.2, 0.25, 0.3\}$. The out-of-sample period is 2000:01 to 2009:12.

the control limits and the corresponding smoothing parameters. The smoothing parameters for the procedures based on the Mahalanobis distance are set equal to 0.15 and for the MEWMA statistic are for both optimization cases equal to 0.2. Additional results for other values of the smoothing parameter are available upon request. Figure 4.7.5 illustrates the change points for the control schemes based on the MEWMA. We remind that when a signal is given and a change point is identified the process should be re-estimated as Golosnoy and Schmid (2007) mentioned.

Figures 4.7.6 and 4.7.5 present the control charts for the two portfolio strategies based on the Mahalanobis distance and the multivariate EWMA recursion, respectively. The difference control charts using the Mahalanobis distance for both constrained and unconstrained portfolios give more signals than the charts using the MEWMA statistic. The latter control schemes behave better which is a results in contradiction with the results for risk assets and daily data that Golosnoy and Schmid (2007) found. A possible explanation could be the difference in the risk characteristics of the data since here we have less risky assets than stocks, government bonds. A possibly advantage of using less frequently data than daily could be the reduction of large number of signals specially in term structure models. A distinction between real and false alarm is difficult and each signal obtained should be evaluated for further actions by a financial analyst. In our work we attempt to give, if it is possible, to

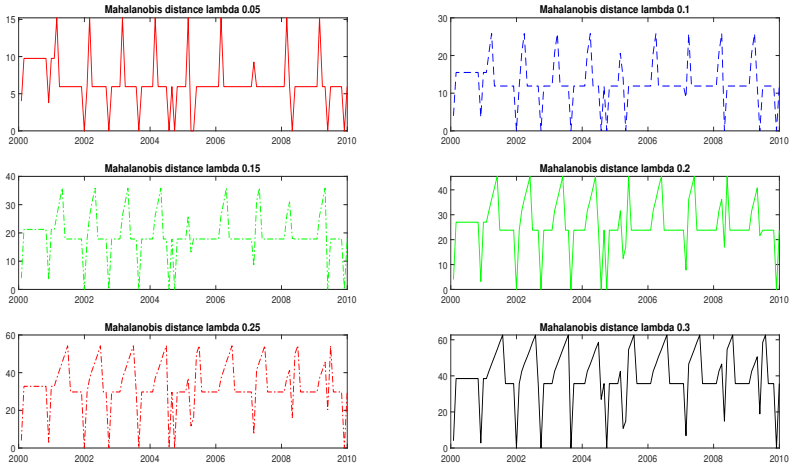

Figure 4.7.2: Control Statistics for unconstrained GMVP based on Mahalanobis distance for $\lambda = \{0.05, 0.1, 0.15, 0.2, 0.25, 0.3\}$. The out-of-sample period is 2000:01 to 2009:12.

the signals obtained from the control charts an economic interpretation. The use of difference MEWMA control chart for unconstrained portfolio gives in the out-of-sample period four signals (without reestimation). The dates of the signals are: 2005:09, 2007:10, 2008:10 and 2008:11. The difference MEWMA control chart for constrained portfolio gives signals at the following dates: 2005:09, 2005:11, 2007:09 and 2008:10. The economic evaluation of all given signals is of great importance in finance. At December 2007 started the global financial crisis which led to the Great Recession until June 2009 according to the National Bureau of Economic Research (NBER). Both control schemes detect the structural break due to the financial crisis of 2007. However, the MEWMA chart for constrained portfolio gives a signal a month earlier than the chart in unconstrained case. The signals that both charts give at September of 2005 could be associated with the housing market correction during the period 2005-2006 that started the June of 2005.

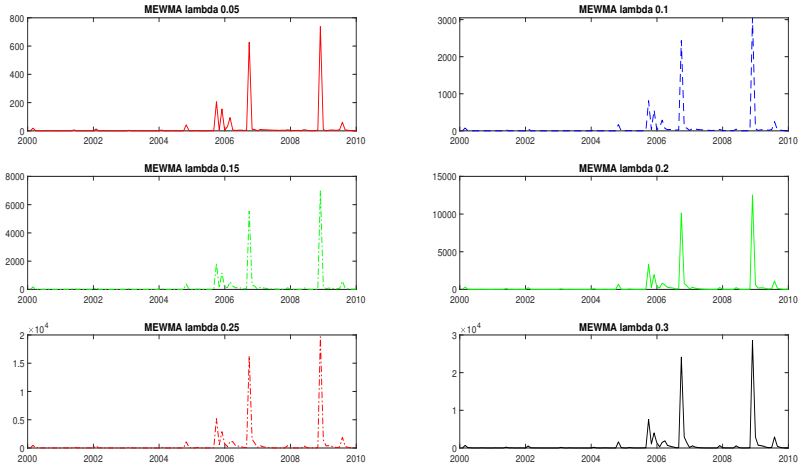

Figure 4.7.3: MEWMA Control Statistics for constrained GMVP for $\lambda = \{0.05, 0.1, 0.15, 0.2, 0.25, 0.3\}$. The out-of-sample period is 2000:01 to 2009:12.

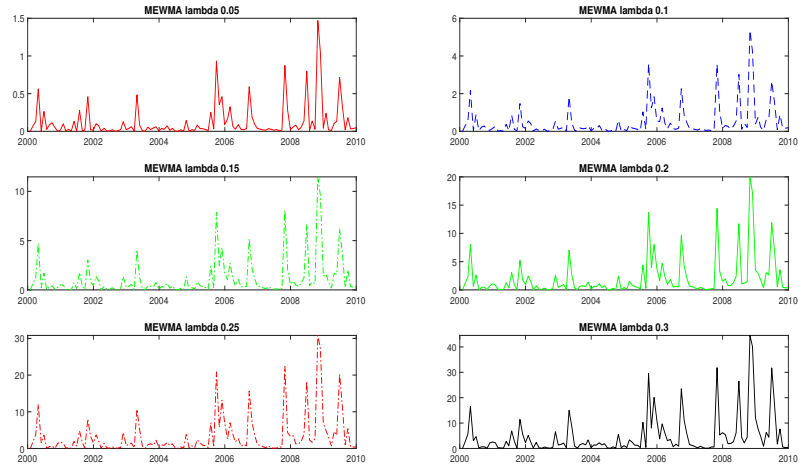

Figure 4.7.4: MEWMA Control Statistics for unconstrained GMVP for $\lambda = \{0.05, 0.1, 0.15, 0.2, 0.25, 0.3\}$. The out-of-sample period is 2000:01 to 2009:12.

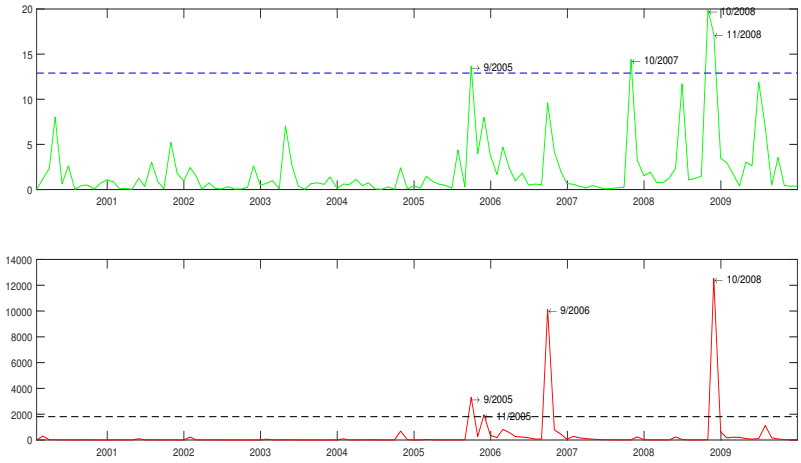

Figure 4.7.5: Control charts based on MEWMA statistic for smoothing parameter equal to 0.2. The out-of-sample period is 2000:01 to 2009:12.

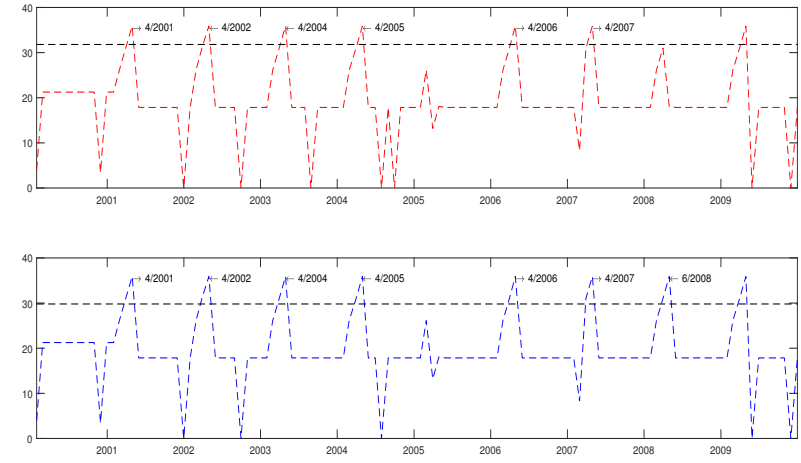

Figure 4.7.6: Control charts based on Mahalanobis distance for smoothing parameter equal to 0.15. The out-of-sample period is 2000:01 to 2009:12.

Chapter 5

Change points and VARMA Affine Term Structure Models

5.1 Introduction

In this chapter we monitoring the parameters of an arbitrage-free VARMA ATSM where the vector of state variables is observable and the estimation procedure following Ang et al. (2006) is a two-step process. In the first step we estimate parameters of the VARMA model and in the second step the market prices of risk given the estimates from the first step. This research in addition to standard estimation techniques for the first step of the estimation procedure is focused in a numerical robust estimation technique that so far as we know is the first time that is applied in an ATSM for interest rates, which is called projection minimum distance (PMD) estimation approach (Jordà and Kozicki (2011)). This method is previously applied in the estimation of DSGE models. In this method the restrictions of the model are opposed to a semi-parametric representation of the data based on its Wold representation (or impulse responses). Jordà and Kozicki (2011) proposed this two step estimation procedure where the mapping between Wold coefficients and parameters is linear and the likelihood score function is nonlinear in the parameters. PMD belongs to the class of limited-information, minimum distance estimators. In the first step for the estimation of the Wold representation coefficients is used the local projections method (Jordà (2005)). The second step of the estimator consists in minimizing the distance resulting from the mapping between the Wold coefficients and the coefficients of our model.

The estimation of impulse responses with the local projections method is robust to potential misspecification of the data generating process. However, a disadvantage of this method is an efficiency loss in the estimation of impulse response functions. Teulings and Zubanov (2014) addressed this issue and propose an extension of the local projections method for the estimation of the impulse response function (IRF) of GDP taking into consideration banking crisis.

We mention that affine models are usually used to describe the term structure between yields and interest rates and for the modeling of the state evolution process the majority of the literate is based on linear models such as VARs. The advantage of VAR models is the fact they have the ability of reproducing the complex dynamics of the term structure quite well. In recent years VARMA models are introduced to macroeconomic applications and their theoretical advantages have been examined (Kascha (2012)). However, estimation problems are a possible drawback that discourage its application very often.

Metaxoglou and Smith (2007) dealt with the computational problems of ML estimation of VARMA models and introduced a state-space representation for VARMA that enables ML estimation using the expectation–maximization (EM) algorithm. Dufour and Pelletier (2008) proposed a modeling and estimation method for weak VARMA processes simpler than the usual echelon form of VARMA model. The estimation method is a three-step generalization of the regression-based estimation method proposed by Hannan and Rissanen (1982) for univariate ARMA models. Kascha and Mertens (2009) used structural VARMA and state space models in DSGE models. Feunou and Fontaine (2009) studied VARMA ATSMs and presented the benefits of using VARMA process for the term structure. Kascha (2012) presented a comparison of the main estimation methods for VARMA models such as the Hannan-Rissanen Method (HR) (Hannan and Rissanen (1982)), the Hannan-Kavalieris-Procedure (HK) Hannan and Kavalieris (1984) and Hannan and Deistler (2012), Generalized Least Squares (KP) (Koreisha and Pukkila (1990) Kavalieris et al. (2003)), the Iterative Least Squares (IHR) proposed by Kapetanios (2003), and finally the MLE method. The results showed advantages in the use of VARMA instead of VAR modeling and the best performance is made from the algorithm of Hannan and Kavalieris (1984). Also the results favored the opinion that for a VARMA model the preferred estimation method should be close to a robust maximum likelihood method.

Mainassara and Francq (2011) examined the asymptotic properties of the quasi-maximum likelihood estimator (QMLE) of VARMA models assuming that the errors are uncorrelated but not necessarily independent martingale differences. Maïnassara

et al. (2014) estimated the asymptotic variance matrix of the least squares (LS) and the quasi-maximum likelihood (QML) estimators of VARMA models in terms of the VAR and MA polynomials and the second and fourth-order structure of the noise. The main assumption is that the errors are uncorrelated but not necessarily independent. Chan et al. (2016) developed a Bayesian approach for inference in VARMA models and to deal up with potential problems of over-parameterization and computation. Chan and Eisenstat (2017) proposed Bayesian approach for the estimation of VARMA models. Wilms et al. (2021) presented a sparse identification and estimation approach for Gaussian VARMA models.

Kascha and Trenkler (2011) proposed an estimation strategy for the cointegrated VARMA models applied to U.S. term structure of interest rates. Simionescu (2013) applied a VARMA model for the U.S. economy and compared its forecasts with these from a VAR model. For small time horizons the forecasts based on VARMA models are better than others for variables unaffected by structural shocks. For the evaluation of the relative forecasting accuracy is introduced the the generalized forecast error of second moment (GFESM). Dufour and Stevanović (2013) studied the relationship between VARMA and factor representations of a vector stochastic process and combined factor and VARMA modeling by using factor-augmented VARMA (FAVARMA) models.

Śliwa and Schmid (2005) proposed EWMA control charts, for jointly monitoring all elements of the covariance matrix at lag 0 of a multivariate time series. The underlying target process is assumed to be a stationary Gaussian process especially a VARMA(1,1) process. Śliwa and Schmid (2005) applied control charts for the surveillance of the covariance matrices of multivariate nonlinear time series. The target process is assumed to be a multivariate GARCH(1,1) model. Bodnar and Schmid (2007) proposed several CUSUM charts, modified and residual charts, for the mean of stationary multivariate time series by taking into account the structure of the underlying stochastic process. The target process is always assumed to be a multivariate stationary Gaussian process such as a VARMA(1,1) model. The proposed charts are in general not directionally invariant in contrast to CUSUM charts for i.i.d. variables. However, the authors derived a sufficient condition under which the introduced CUSUM charts fulfill this property.

Bodnar and Schmid (2011) introduced various CUSUM type control chart procedures for monitoring the mean of a multivariate Gaussian process. In a simulation study the introduced CUSUM charts are compared with other control chart procedures. The in-control process is assumed to be either a 10-dimensional VAR(1) process or a two-dimensional VARMA(1,1) process. The 10-dimensional VAR(1) process satisfies the

invariance condition but not the VARMA(1,1) process. The out-of-control condition assumed a constant shift in the mean vector. The results showed that there is no overall best chart procedure and the performance of the charts depends on the underlying in-control process.

Vanhatalo and Kulahci (2015) studied how the autocorrelation in data affects the Hotelling T^2 control chart. The detection ability of the control chart is evaluated for various shifts in the mean vector for simulated data from a VAR model. Among the approaches constructing the Hotelling T^2 chart for a comparison study Vanhatalo and Kulahci (2015) used the residuals from a VARMA(1,1) model fitted to the raw data.

The chapter is organized as follows. In Section 2, we summarize and analyze our data. Next, in Section 3 we introduce the framework of the ATSM. Also, in this section we present the basic estimation techniques of the model and the adaptation of the PMD estimation technique for our case. In Section 4 the results for the model estimation and a comparison study is presented. In Section 5 we introduce the control chart procedures for the sequential monitoring of the affine model. In Section 6 a simulation study for all proposed control charts compared with each other is displayed. An empirical example is presented in Section 7.

5.2 Data

We use monthly data on continuously compounded nominal spot yields for the U.S. yield curve from the FED St. Louis dataset with maturities 1,12, 24, 36, 48, 60, 120 months with the 1-month Treasury bill to be the short rate and assuming them to be default-risk-free. Also we use two macroeconomic factors, the IP index growth rate which measures the economic activity and as a proxy for the inflation the CPI. The inclusion of inflation is necessary for recovering the canonical decomposition of nominal yields into the term structure of real yields, inflation expectation and inflation risk premia. All data are in monthly frequency from 1983:01 to 2003:12, in total 252 observations. The out-of-sample period is from 2004:01 to 2011:12, 96 monthly observations. We denote the yield at time t with maturity in n-months as y_t^n.Summary statistics for yields and macroeconomic factors are presented in tables 5.2.1 and 5.2.2 respectively.

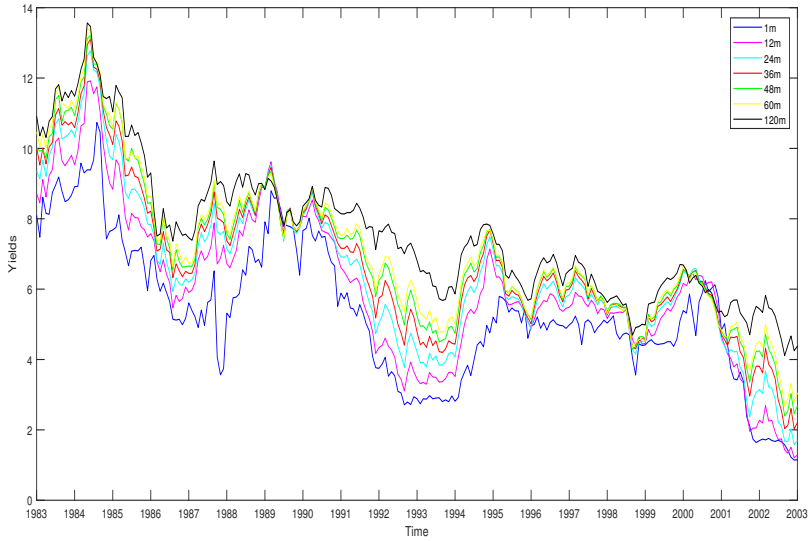

Figure 5.2.1: U.S. Treasury Yields. The sample period is 1983:01 to 2003:12.

Yields	Mean	Std deviation	Kurtosis	Skewness
1 months	5.1591	2.141	2.6663	0.0262
12 months	5.887	2.3748	2.8104	0.0120
24 months	6.2732	2.3830	2.9762	0.1837
36 months	6.5507	2.3211	3.0306	0.3026
48 months	6.7778	2.2884	3.0414	0.4161
60 months	6.9083	2.2569	3.0746	0.52367
120 months	7.4559	2.0687	3.0202	0.7019

Table 5.2.1: Summary Statistics of U.S. Treasury yields from 1983:01 to 2003:12.

Summary Statistics of Macroeconomic factors		
	IP growth	CPI
Mean	3.1217	3.1257
Median	3.1953	3.0143
Mode	-5.1737	1.6667
Std deviation	3.3294	1.111
Kurtosis	3.0887	2.8284
Skewness	-0.0289	0.4410
Range	17.382	5.3104
Minimum	-5.1737	1.0692
Maximum	12.209	6.3796

Table 5.2.2: Summary Statistics of macroeconomic factors.

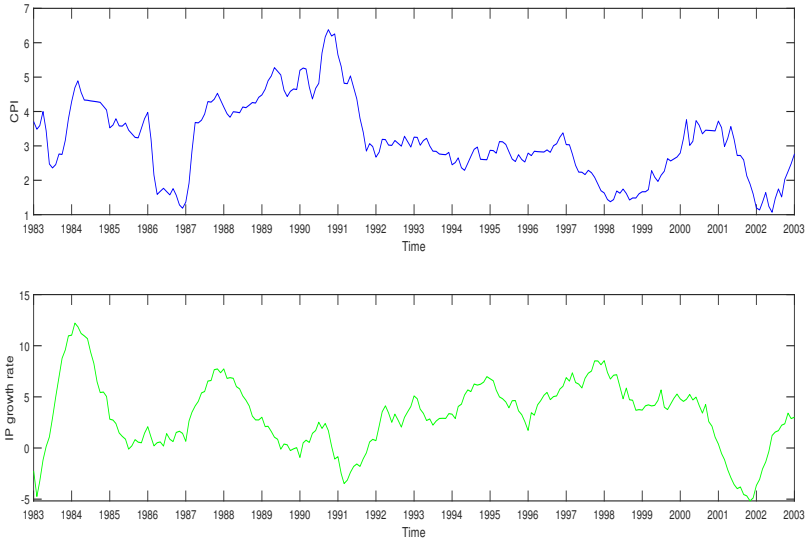

Figure 5.2.2: Macroeconomic factors. The sample period is 1983:01 to 2003:12.

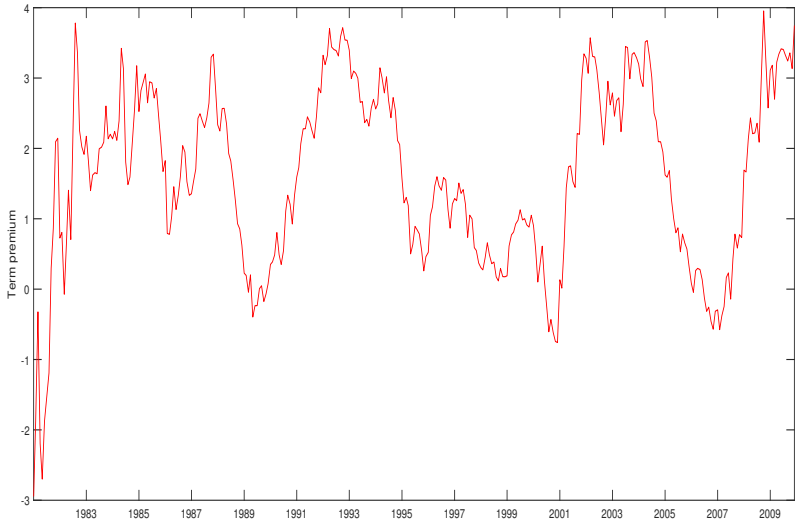

Figure 5.2.3: Term Premia. The sample period is 1983:01 to 2003:12.

Figure 5.2.1 plots the time series of U.S. government yields and figure 5.2.2 presents the two macroeconomic factors, CPI and IP growth rate for the in-sample period from 1983:01 to 2003:12. Specifically, figure 5.2.1 illustrates the time series of US government bond yields that start from a high level due to early 1980's recession they reach at a peak in the mid of 1984 and subsequently they exhibit a downward trend until they reach the lowest levels at the end of our sampling period.

From figure 5.2.2 we see that CPI starts from a high level due to early 1980s recession and in the subsequent period moves generally in lower levels before the increase in the first semester of 1984 and shows a downward trend until the end of 1986 where reaches at the lowest level. This is followed by a long period of upward trend until the end of 1991 where reaches the highest level of the entire sampling period. Next, CPI with the exception of two periods remains at the same level. The IP growth rates with the exceptions at the very beginning and the end of the in-sample period show movements generally opposite with those of the CPI. The movements of IP growth rates follow most of the time that of the government yields in contrast with the time series of CPI. The yields and macroeconomic factors exhibit mild excess kurtosis and right-skewness.

Before we present and estimate our model it is useful to highlight some characteris-

tics of the data. In table 5.2.3 we present the autocorrelations of the time series of nominal yields for up to five lags.The time series of all bond yields are highly autocorrelated showing high degree of persistence and the autocorrelations increase for longer maturity. Also, in table 5.2.4 we present the autocorrelations for the macroeconomic factors. IP growth rate and CPI show medium to strong autocorrelation.

The term spread is defined as the difference between the long-end and the short-end bond yield: $y_t^{(120)} - y_t^{(1)}$. Figures 5.2.3 and C.0.76 present the term spread for the in-sample and out-of-sample period respectively. For the in-sample period the plot indicates that periods with high (or low) term spreads are followed by periods of high (or low) IP growth rate. In the out-of-sample period we observe that the term spread exhibits the lowest position before the outbreak of the global financial crisis of 2007-09. Finally, the curvature of the yield curve for the in-sample period, estimated as

$$curv = 2 * y_t^{(48)} - y^{(120)} - y_t^{(36)}$$

is displayed in figure C.0.71.

Yields	Lag 1	Lag 2	Lag 3	Lag 4	Lag 5
1 month	0.96708	0.93836	0.90711	0.88467	0.85865
12 months	0.97967	0.9569	0.93096	0.90392	0.87614
24 months	0.97944	0.95521	0.92883	0.9016	0.87481
36 months	0.9777	0.95345	0.92746	0.90072	0.87471
48 months	0.97802	0.95334	0.92961	0.90441	0.87987
60 months	0.97773	0.97773	0.97773	0.97773	0.97773
120 months	0.97845	0.95761	0.93693	0.91579	0.89322

Table 5.2.3: Autocorrelations of U.S. Treasury Yields.

Factors	Lag 1	Lag 2	Lag 3	Lag 4	Lag 5
CPI	0.96475	0.90738	0.85313	0.79845	0.74463
IP growth	0.96626	0.91183	0.84575	0.76689	0.67817
Term spread	0.9175	0.8479	0.7858	0.7534	0.7112

Table 5.2.4: Autocorrelations of macroeconomic factors.

5.3 VARMA Affine Term Structure Model

In recent decades, there has been a interest in modeling economic time series by VARMA models. However, this class of models has been unpopular in practice because of estimation problems and the complexity of the identification stage. These disadvantages have led to the dominant use of VAR models in macroeconomic applications. In this paper, we apply several simple estimation methods for VARMA models are compared among each other and with pure vector autoregressive modeling using ordinary least squares. For the evaluation of the estimation methods we use the RMSE not only for the in-sample period but also for an out-of-sample horizon up to 24 months.

5.3.1 The Model

The Vector Autoregressive Moving Average process VARMA(p,q) is generally defined as

$$\boldsymbol{X}_t = \boldsymbol{\mu} + \sum_{i=1}^{p} \boldsymbol{\phi}_i \boldsymbol{X}_{t-i} - \sum_{j=1}^{q} \boldsymbol{\theta}_j \boldsymbol{\epsilon}_{t-j} + \boldsymbol{\epsilon}_t,\ \boldsymbol{\epsilon}_t \sim N(\mathbf{0}, \boldsymbol{\Sigma}), \tag{5.3.1}$$

where $t = 0, 1, 2, \ldots$. In terms of matrix polynomial lag operators the process can be written as

$$\Phi(L)\boldsymbol{X}_t = \Theta(L)\boldsymbol{\epsilon}_t, \tag{5.3.2}$$

where
$\Phi(L) = I - \Phi_1 L - \cdots - \Phi_p L^p,\ \Theta(L) = I - \Theta_1 L - \cdots - \Theta_p L^p$ and $L^p \boldsymbol{X}_t = \boldsymbol{X}_{t-p}$.
In our case the process that describes the evolution of the state variables in the economy is a reduced-form VARMA(1,1) process which under the historical probability measure P is defined as

$$\boldsymbol{X}_t = \boldsymbol{\mu} + \boldsymbol{\Phi}_1 \boldsymbol{X}_{t-1} + \boldsymbol{\epsilon}_t - \boldsymbol{\Theta}_1 \boldsymbol{\epsilon}_{t-1},\ \boldsymbol{\epsilon}_t \sim N(\mathbf{0}, \boldsymbol{\Sigma}), \tag{5.3.3}$$

where $\boldsymbol{\mu}$ is a $k \times 1$ vector and $\boldsymbol{\Phi}_1, \boldsymbol{\Theta}_1$ are $k \times k$ matrices. The log-normal pricing kernel is

$$M_{t+1} = exp(-y_t^{(1)} - \frac{1}{2}\boldsymbol{\lambda}_t^{'}\boldsymbol{\lambda}_t - \boldsymbol{\lambda}_t^{'}\boldsymbol{\epsilon}_{t+1}), \tag{5.3.4}$$

where $\boldsymbol{\lambda}_t$ is the $k \times 1$ vector market price of risk and $y^{(1)}$ is the 1-month U.S. Treasury bond yield. We assume that the short rate is the 1-month Treasury bill.

The conditional expectation of the state evolution process $\boldsymbol{X}_{t+1}$ is given by

$$\boldsymbol{m}_t = \boldsymbol{\mu} + \boldsymbol{\Phi}_1 \boldsymbol{X}_t - \boldsymbol{\Theta}_1 \boldsymbol{\epsilon}_{t-1}, \tag{5.3.5}$$

then from equation (5.3.3) we have that

$$\boldsymbol{X}_{t+1} = \boldsymbol{m}_t + \boldsymbol{\epsilon}_t. \tag{5.3.6}$$

The conditional mean $\boldsymbol{m}_t = E_t(\boldsymbol{X}_{t+1})$ evolves recursively as follows:

$$\begin{aligned} \boldsymbol{m}_{t+1} &= \boldsymbol{\mu} + \boldsymbol{\Phi}_1 \boldsymbol{X}_{t+1} - \boldsymbol{\Theta}_1 \boldsymbol{X}_{t+1} \\ &= \boldsymbol{\mu} + \boldsymbol{\Phi}_1 \boldsymbol{X}_{t+1} - \boldsymbol{\Theta}_1 (\boldsymbol{X}_{t+1} - \boldsymbol{m}_t) \\ &= \boldsymbol{\mu} + \boldsymbol{\Phi}_1 \boldsymbol{X}_{t+1} - \boldsymbol{\Theta}_1 \boldsymbol{X}_{t+1} + \boldsymbol{\Phi}_1 \boldsymbol{m}_t. \end{aligned}$$

The moment generating function of the vector of the state variables $\boldsymbol{X}_t$ under the risk-neutral probability measure Q is

$$E_t^Q[exp(\boldsymbol{u}^{'} \boldsymbol{z}_{t+1})] = exp(\boldsymbol{u}_t(\boldsymbol{m}_t - \boldsymbol{\Sigma}\boldsymbol{\lambda}_t + \frac{1}{2}\boldsymbol{u}^{'}\boldsymbol{\Sigma}\boldsymbol{\Sigma}^{'}\boldsymbol{u}). \tag{5.3.7}$$

In our case we assume that the variance matrix Σ is lower triangular and in contrast with the work of Feunou and Fontaine (2009) we do not impose any restriction to the matrix Θ_1.
The market price of risk vector λ_t is linear in the state variables and the conditional expectations μ_t under the risk-neutral probability measure in order the model dynamics to keep their VARMA properties. The market prices of risk have the following form

$$\boldsymbol{\lambda}_t = \boldsymbol{\lambda}_0 + \boldsymbol{\lambda}_1 \boldsymbol{X}_t + \boldsymbol{\lambda}_2 \boldsymbol{m}_t, \tag{5.3.8}$$

where $\boldsymbol{\lambda}_0$ is a $k \times 1$ vector and $\boldsymbol{\lambda}_1$ and$\boldsymbol{\lambda}_2$ are $k \times k$ matrices. This framework of the market prices of risk is an extension of that of Ang and Piazzesi (2003) . For $\boldsymbol{\lambda}_2 = 0$ we have the market price structure of Ang and Piazzesi (2003). The bond prices under the affine framework are exponential affine functions of the state variables and their conditional mean. The price at time t of a zero-coupon bond with maturity n is

$$P_t^n = E_t^Q\left(- \sum_{t=0}^{n-1} r_t \right) = exp(y_t^{(1)} + A_n + \boldsymbol{B}_{1,n}^{'} \boldsymbol{X}_t + \boldsymbol{B}_{2,n}^{'} \boldsymbol{m}_t). \tag{5.3.9}$$

The yields of a n-period zero coupon bond are affine in the state factors $\boldsymbol{X}_t$ and their conditional expectations $\boldsymbol{m}_t$:

$$y_t^{(n)} = \alpha_n + \boldsymbol{b}_{1,n}^{'} \boldsymbol{X}_t + \boldsymbol{X} b_{2,n}^{'} \boldsymbol{m}_t. \tag{5.3.10}$$

5.3.1.1 Model dynamics under the Risk-neutral measure

According to Feunou and Fontaine (2009) the state evolution process under the risk-neutral probability measure follows a Gaussian VARMA(2,1) process if under the historical probability measure follows a VARMA(1,1) process. Specifically

$$\boldsymbol{X}_t = \boldsymbol{\mu}^Q + \boldsymbol{\Phi}_1^Q \boldsymbol{X}_{t-1} + \boldsymbol{\epsilon}_t^Q - \boldsymbol{\Theta}_1^Q \boldsymbol{\epsilon}_{t-1}^Q. \tag{5.3.11}$$

Under the risk-neutral probability measure we have that

$$\begin{aligned} \boldsymbol{m}_t^Q &= \boldsymbol{m}_t - \boldsymbol{\Sigma}\boldsymbol{\lambda}_t \\ &= \boldsymbol{m}_t - \boldsymbol{\Sigma}(\boldsymbol{\lambda}_0 + \boldsymbol{\lambda}_1 \boldsymbol{X}_t + \boldsymbol{\lambda}_2 \boldsymbol{m}_t) \\ &= \boldsymbol{m}_t - \boldsymbol{\Sigma}\boldsymbol{\lambda}_0 - \boldsymbol{\Sigma}\boldsymbol{\lambda}_1 \boldsymbol{X}_t - \boldsymbol{\Sigma}\boldsymbol{\lambda}_2 \boldsymbol{m}_t \\ &= (\boldsymbol{I} - \boldsymbol{\Sigma}\boldsymbol{\lambda}_2)\boldsymbol{m}_t - \boldsymbol{\Sigma}(\boldsymbol{\lambda}_0 + \boldsymbol{\lambda}_1 \boldsymbol{X}_t). \end{aligned}$$

This means that

$$\boldsymbol{m}_t = (\boldsymbol{I} - \boldsymbol{\Sigma}\boldsymbol{\lambda}_2)^{-1} \boldsymbol{m}_t^Q + (\boldsymbol{I} - \boldsymbol{\Sigma}\boldsymbol{\lambda}_2)^{-1} \boldsymbol{\Sigma}(\boldsymbol{\lambda}_0 + \boldsymbol{\lambda}_1 \boldsymbol{X}_t). \tag{5.3.12}$$

According to Feunou and Fontaine (2009) when the state evolution process under the historical probability measure follows a VARMA(1,1) process then under the risk-neutral measure follows a VARMA(2,1) process:

$$\boldsymbol{m}_t = (\boldsymbol{I} - \boldsymbol{\Sigma}\boldsymbol{\lambda}_2)^{-1} \boldsymbol{m}_t^Q + (\boldsymbol{I} - \boldsymbol{\Sigma}\boldsymbol{\lambda}_2)^{-1} \boldsymbol{\Sigma}(\boldsymbol{\lambda}_0 + \boldsymbol{\lambda}_1 \boldsymbol{X}_t). \tag{5.3.13}$$

Feunou and Fontaine (2009) stated that adding a MA component to a standard VAR process improvements the forecasting of bond yields, inflation, real activity and future interest rate risk premia in contrast to a standard VAR model or to the Nelson-Siegel model.

5.3.2 Estimation Method

In our Gaussian ATSM we use two factors from the yield curve, the first is the one-month bond yield ($y_t^{(1)}$) assumed to be the short rate process and used as a proxy for the level of the yield curve. The second is the term premia (Ytp_t), defined as the differnce between the 10-year and the one-month bond yield taken as a proxy for the slope of the yield curve. The vector of state-variables can be expressed as $\boldsymbol{X} = \{CPI_t, IP_t, Ytp_t, y_t^{(1)}\} = \{CPI_t, IP_t, y_t^{(120)} - y_t^{(1)}, y_t^{(1)}\}$ where $Ytp_t = y_t^{120} - y_t^1$ is the yields term premia, CPI_t and IP_t are the time series for CPI and the IP growth

rate, respectively. The VARMA(1,1) state factor process described in the section 4.1 can now be expressed in the following matrix form

$$\begin{bmatrix} CPI_t \\ IP_t \\ Ytp_t \\ Y_t^{(1)} \end{bmatrix} = \begin{bmatrix} \mu_1 \\ \mu_3 \\ \mu_4 \\ \mu_2 \end{bmatrix} + \begin{bmatrix} \Phi_{11} \\ \Phi_{12} \\ \Phi_{13} \\ \Phi_{14} \end{bmatrix} \begin{bmatrix} CPI_{t-1} \\ IP_{t-1} \\ Ytp_{t-1} \\ Y_{t-1}^{(1)} \end{bmatrix} + \begin{bmatrix} \epsilon_{1,t} \\ \epsilon_{2,t} \\ \epsilon_{3,t} \\ \epsilon_{4,t} \end{bmatrix} - \begin{bmatrix} \Theta_{11} \\ \Theta_{12} \\ \Theta_{13} \\ \Theta_{14} \end{bmatrix} \begin{bmatrix} \epsilon_{1,t-1} \\ \epsilon_{2,t-1} \\ \epsilon_{3,t-1} \\ \epsilon_{4,t-1} \end{bmatrix}. \tag{5.3.14}$$

Since our model contains only observable factors, similar to the method of Ang et al. (2006) we use a two-step procedure to estimate the term structure model. In the first step the set of the parameters $\boldsymbol{\xi}_1 = \{\boldsymbol{\mu}, \boldsymbol{\Phi}_1, \boldsymbol{\Theta}_1, \boldsymbol{\Sigma}\}$ of the VARMA(1,1) process under the historical probability measure is estimated. For the estimation we choose the approach of Hannan and Rissanen (1982) . A comparison review of the main methods for the estimation of VARMA processes is presented in Kascha (2012). In the second step, we minimize the sum of squared fitting errors for the zero-coupon bond yields, given the estimates of the first step:

$$min \sum_{t=1}^{T} \sum_{n=1}^{N} (\hat{y}_t^{(n)} - y_t^{(n)})^2, \tag{5.3.15}$$

for the n yields we use in our model and estimate risk premia parameters $\boldsymbol{\xi}_2 = \{\boldsymbol{\lambda}_0, \boldsymbol{\lambda}_1, \boldsymbol{\lambda}_2\}$. We mention that all our term structure factors are observable and the data used for our analysis are demeaned. Ang et al. (2006) noted that the two-step estimation procedure may be not as efficient as the one-step maximum likelihood procedure but this does not affect the forecasting procedure. According to equation (5.3.10) the 120-month (10-year) yield ($y_t^{(120)}$) is estimated as follows

$$y_t^{(120)} = \alpha_{(120)} + \boldsymbol{b}_{1,120}^{'} \boldsymbol{X}_t + \boldsymbol{X} b_{2,120}^{'} \boldsymbol{m}_t, \tag{5.3.16}$$

and for the yield term premia ($Ytp_t = y_t^{(120)} - y_t^{(1)}$) we have that

$$Ytp_t = y_t^{(120)} - y_t^{(1)} = \alpha_{(120)} + (\boldsymbol{b}_{1,120}^{'} - e_3)^{'} \boldsymbol{X}_t + b_{2,120}^{'} \boldsymbol{m}_t. \tag{5.3.17}$$

For the model estimation we need to impose the following restrictions in order the results from the yields pricing equation to be consistent with those from the results from the yields under the historical dynamics.

$$a_1 = 0, b_{1,1} = e3, b_{2,1} = 0, a_{120} = 0, b_{1,120} = e3 + e4, b_{2,120} = 0,$$

where $e_3 = [0\ 0\ 1\ 0]'$, $e_4 = [0\ 0\ 0\ 1]'$. This approach indicates that $y_t^{(1)}$ and $y_t^{(120)}$ yields are measured without errors. Also, for the constant factor of the VARMA(1,1) process we assume that $\mu_1 = \mu_2 = \mu_3 = \mu_4 = 0$.

Another estimation technique for the estimation of the parameters of the first step we previously described, we use so far as we know for the first time in Gaussian ATSMs the the PMD method introduced by Jordà and Kozicki (2011). This approach has been applied until now in macroeconomic applications such as DSGE models (see e.g. Giraitis et al. (2014)) and models that described by a VAR process. The authors mentioned that this method could be applied among others to VARMA models. In our work we apply it to an empirical example modeled by a VARMA(1,1) process. The PMD method introduced by Jordà and Kozicki (2011) is a limited-information estimation method. The approach is based on the fact that a covariance-stationary process has a Wold representation. The VARMA process of equation (5.3.1) assuming that it is covariance-stationary, according to the Wold representation and omitting for simplicity the constant factor, can be expressed as follows

$$\boldsymbol{X}_t = \sum_{h=0}^{\infty} \boldsymbol{b}_h \boldsymbol{u}_{t-j}, \tag{5.3.18}$$

with the restriction

$$\sum_{h=0}^{\infty} |\boldsymbol{b}_h| < \infty,$$

where $\boldsymbol{b}_h$ are the Wold coefficients with the restriction $\boldsymbol{b}_0 = I$ and $\boldsymbol{u}_t$ is an i.i.d. sequence with mean zero and finite second-order moment. In practice h is set to a finite number usually estimated from an information criterion. The vector of coefficients of the Wold representation can be semi-parametrically estimated by local projections (see Jordà (2005)). Next, the parameters of the model can be estimated from the restrictions the model imposes on the Wold coefficients by the PMD method. This method in many cases is asymptotically equivalent to maximum likelihood estimation (MLE) as the sample grows to infinity and can be useful when the true data generating process is unknown. PMD is appropriate for estimation of models whose likelihood require numerical optimization routines such as VARMA models. The first step of the PMD method is the estimation of the Wold coefficients based on local projections which is is consistent and asymptotically normal under some general assumptions. According to Jordà (2005) local projections have the advantage of providing a closed-form and analytic expression for the covariance matrix of impulse response coefficients across time and across variables. The mapping between Wold

coefficients and the parameters of interest in the VARMA model of equation (5.3.1) is linear. From equation (5.3.18) and

$$\boldsymbol{X}_t = \boldsymbol{\Phi}_1^Q \boldsymbol{X}_{t-1} + \boldsymbol{\epsilon}_t^Q - \boldsymbol{\Theta}_1^Q \boldsymbol{\epsilon}_{t-1}^Q, \tag{5.3.19}$$

after we equating terms we have that

$$\boldsymbol{b}_h = \boldsymbol{\Phi}_1 \boldsymbol{b}_{h-1} - \boldsymbol{\Theta}_1 d_h, h \geq 1, \tag{5.3.20}$$

where $d_h = 1$ if $h = 1$. Suppose now that the $n \times k$ vector of parameters of interest is $\boldsymbol{\pi}$, k regressors in n equations, then the mapping between the Wold coefficients and the parameters of interest in our model is

$$\boldsymbol{SB'} = \boldsymbol{S_1 B \Phi} + \boldsymbol{S_2 B \Theta}, \tag{5.3.21}$$

where $\boldsymbol{B}$ $nh \times n$ matrix with $b = vec(\boldsymbol{B})$, h the truncated horizon for equation (5.3.18). Also, the matrices $\boldsymbol{S}, \boldsymbol{S}_1, \boldsymbol{S}_2$ are selector matrices so as to pick the appropriate elements in matrix B in order to describe the mapping of the model of interest. As a result the minimum-distance function that corresponds to our problem is

$$\boldsymbol{S}^* \hat{\boldsymbol{b}_T} - g(\hat{\boldsymbol{b}_T}; \boldsymbol{\pi}) = (\boldsymbol{I}_r \otimes \boldsymbol{S}) \hat{b_T} - (\boldsymbol{I}_r \otimes (\boldsymbol{S}_1 \boldsymbol{B}_T \ \boldsymbol{S}_2 \boldsymbol{B}_T)) \boldsymbol{\pi}, \tag{5.3.22}$$

where $\boldsymbol{\pi} = vec(\boldsymbol{\phi\theta})$ and the estimation of the parameters of the VARMA model is the solution to the following problem

$$[\boldsymbol{S}^* \hat{\boldsymbol{b}}_T - g(\hat{\boldsymbol{b}}_{\boldsymbol{T}}; \boldsymbol{\pi})]' \boldsymbol{W} [\boldsymbol{S}^* \hat{\boldsymbol{b}}_{\boldsymbol{T}} - g(\hat{\boldsymbol{b}}_{\boldsymbol{T}}; \boldsymbol{\pi})]. \tag{5.3.23}$$

The optimal covariance matrix for the vector of estimated coefficients v_t is

$$\Omega = (\boldsymbol{F}_b \boldsymbol{W} \boldsymbol{F}_b')^{-1}, \tag{5.3.24}$$

where

$$\boldsymbol{W} = (\boldsymbol{F}_b \boldsymbol{\Omega}_b \boldsymbol{F}_b')^{-1},$$

is the the optimal weighting matrix and

$$\boldsymbol{F}_b = (\boldsymbol{I}_r \otimes \boldsymbol{S}) - (\hat{\boldsymbol{\pi}} \otimes \boldsymbol{I}_{r*n})[\boldsymbol{I}_r \otimes \boldsymbol{S}_1; \boldsymbol{I}_r \otimes \boldsymbol{S}_2].$$

The lag length h for the Wold representation can be estimated via an information criterion.

5.4 Results for the Term Structure Model

In this section we present the results for the parameter estimation of the VARMA ATSM. Also, we compare VARMA and VAR term structure models estimated with standard techniques and the PMD approach in terms of their forecasting ability in the yield curve and the state factors of the model.

5.4.1 Comparison study

The results for the parameter estimates under the historical probability measure, of the first step for our VARMA term structure model along with the results for a standard Gaussian ATSM are provided in tables 5.4.1 and 5.4.2, respectively. Tables 5.4.3 and 5.4.4 present the results of the first step for the VARMA and VARM models but now using the PMD estimation approach. The covariance matrix Σ is lower triangular which implies that innovations to inflation are not correlated with innovations in IP and the short rate process and yields term premia. Also, innovations in IP are not correlated with innovations in yields term premia and the short rate. Comparing the autoregressive coefficients between VARMA and VARMA models the results from the VAR model indicate that that inflation, IP and the short rate process of are more persistent from those in the VARMA model but the yield spread is slightly less persistent in accordance with the findings of Feunou and Fontaine (2009). The results from the PMD-VAR model are for the autoregressive matrix are very similar with those in the standard VAR model but the results provided from the PMD-VARMA model exhibit, except from the inflation coefficient, much less persistence. The inclusion of a MA component in the standard model has as a result a slight reduction in the autocovariance matrix with the exception of the slope of the yield curve where we have an increase as we previously mentioned. Now for the PMD cases, VAR and VARMA, the result in a significant decline specially in the values of the term premia and short rate persistence.

The results for estimation of risk premia parameters for the four models are presented in tables 5.4.5, 5.4.6,5.4.7 and 5.4.8. The results indicate significant changes in the behavior of the price of risk not only between the VAR and VARMA specifications but also between the estimation approach, standard approach or PMD.

Figures C.0.77,C.0.79,C.0.81 and C.0.83 illustrate the path of the market price of risk for each variable in the case of VAR and the VARMA models under standard estimation methods. Figures C.0.78, C.0.80, C.0.82 and C.0.84 present the market prices of risk for each variable but not for VAR and VARMA models under the PMD

estimation approach.

	Φ_1				Θ_1			
CPI	0.9153	0.0088	0.0273	0.0012	0.4192	0.0181	0.0089	0.0500
IP growth	-0.3132	0.9342	0.1214	0.1600	0.4665	0.1674	0.2747	0.1696
Y1m	0.0132	0.0237	0.9765	0.0328	0.0681	0.0248	0.1489	0.2216
Term Premia	-0.0186	-0.0230	0.0125	0.9397	-0.0548	0.0254	-0.1367	-0.1604
Σ	0.2541	0	0	0				
	0.0748	0.6815	0	0				
	0.0004	-0.0087	0.4085	0				
	0.0322	0.0618	-0.3527	0.3026				

Table 5.4.1: Parameter estimates for VARMA-ATSM Model.

	μ	Φ_1			
CPI	-0.0067	0.9551	0.0131	0.0130	0.0033
IP growth	0.0170	-0.2586	0.9511	0.0953	0.1484
Y1m	-0.0285	0.0158	0.0222	0.9811	0.0560
Term Premia	0.0033	-0.0149	-0.0183	0.0043	0.9235
Σ	-0.0647	0	0	0	
	0.0395	0.2759	0	0	
	0.0426	-0.0052	0.1017	0	
	-0.0329	-0.0072	-0.1008	0.0371	

Table 5.4.2: Parameter estimates for VAR ATSM Model.

	Φ_1				Θ_1			
CPI	0.9156	0.4480	-0.0035	0.0260	0.0603	-0.0780	0.0554	-0.0111
IP growth	-0.3509	0.7465	1.0867	-0.0294	0.0966	-0.0284	0.3053	-0.0008
Y1m	-0.0762	0.2442	0.0428	0.0206	0.8873	0.0202	-0.0282	0.2655
Term Premia	-0.0020	0.0020	0.0109	0.0797	-0.0077	-0.7761	0.8728	-0.0787
Σ	0.5270	0	0	0				
	0.6277	0.6193	0	0				
	0.5579	0.2524	0.2626	0				
	0.5246	-0.2258	0.6456	0.1327				

Table 5.4.3: Parameter estimates for PMD-VARMA ATSM Model.

	Φ_1			
CPI	0.9551	0.0131	0.0130	0.0033
IP growth	-0.2586	0.9511	0.0953	0.1484
Y1m	0.0158	0.0222	0.9811	0.0560
Term Premia	-0.0149	-0.0183	0.0043	0.9235
Σ	-0.0646	0	0	0
	0.0394	0.2753	0	0
	0.0425	-0.0052	0.1015	0
	-0.0328	-0.0072	-0.1006	0.0370

Table 5.4.4: Parameter estimates for PMD-VAR ATSM Model.

	VARMA Risk premia parameters			
λ_0	1.1296	2.1468	-1.7722	-0.0285
λ_1	5.8268	0.2033	2.4117	6.4030
	(0.105)	(0.0151)	(0.03)	(0.017)
	-2.6392	0.3186	-1.8522	-10.0501
	(0.018)	(0.002)	(0.019)	(0.48)
	1.1895	0.3739	-4.7565	3.5196
	(0.0018)	(0.0034)	(0.0012)	(0.756)
	-1.2833	-0.3105	-1.7404	-2.0460
	(0.0016)	(0.0004)	(0.0010)	(0.0003)
λ_2	10.4848	3.8771	1.2375	8.6610
	(0.05)	(0.38)	(0.0279)	(0.34)
	-4.2940	-1.1470	-2.3012	-7.5446
	(0.178)	(0.068)	(0.0485)	(0.0318)
	0.0385	-0.1405	5.1830	-2.5266
	(0.089)	(0.0048)	(0.0182)	(0.410)
	-0.5308	-0.3293	1.8274	2.5444
	(0.0016)	(0.0004)	(0.0010)	(0.0003)

Table 5.4.5: Risk premia parameter estimates for the VARMA model under historical probability measure. The asymptotic standard errors are in parentheses.

	VAR Risk premia parameters			
λ_0	0.0744	-0.8410	-6.6192	0.2575
λ_1	7.7520	-4.1785	7.7632	-4.9087
	(0.0215)	(0.138)	(0.0289)	(0.585)
	6.7696	2.3050	-7.0524	-32.3220
	(1.018)	(0.0728)	(0.719)	(3.38)
	-4.9236	2.1397	-3.6489	6.0810
	(0.048)	(0.0434)	(0.412)	(0.54)
	1.4220	1.0570	-2.8516	-9.1001
	(0.0217)	(0.014)	(0.051)	(0.913)

Table 5.4.6: Risk premia parameter estimates for the VAR model under historical probability measure. The asymptotic standard errors are in parentheses.

	PMD-VARMA Risk premia parameters			
λ_0	5.3328	-0.8359	-2.7418	2.3620
λ_1	7.0249	-3.2263	-3.2039	19.3562
	(1.015)	(0.485)	(0.6029)	(2.19)
	0.7148	1.6741	-1.5818	-9.7660
	(0.0819)	(0.38)	(0.0169)	(0.98)
	-0.0013	0.6471	-1.7451	0.9442
	(0.00008)	(0.004)	(0.082)	(0.043)
	-0.2214	-0.1692	-2.4969	-2.2541
	(0.0056)	(0.0018)	(0.22)	(0.448)
λ_2	7.5959	-4.5877	12.4222	12.7802
	(1.77)	(0.88)	(2.110)	(1.449)
	1.0893	-0.5635	1.2528	0.0719
	(0.140)	(0.008)	(0.0229)	(0.0078)
	-1.3440	-0.0002	1.6016	-0.5260
	(0.07)	(0.00004)	(0.12)	(0.009)
	-0.8288	0.2961	2.2140	2.5027
	(0.0076)	(0.04)	(0.11)	(0.39)

Table 5.4.7: Risk premia parameter estimates for the VARMA-PMD model under historical probability measure. The asymptotic standard errors are in parentheses.

	PMD-VAR Risk premia parameters			
λ_0	-8.1537	-4.6053	-3.1419	6.2122
λ_1	-0.0345	1.4113	-3.3751	1.3897
	(0.05)	(0.041)	(0.859)	(0.103)
	1.3802	-1.1069	1.1160	-1.0325
	(0.168)	(0.288)	(0.55)	(0.138)
	-0.3057	0.6188	-0.7878	0.6241
	(0.028)	(0.0064)	(0.052)	(0.099)
	-0.5496	-0.2355	0.5379	-0.0709
	(0.0076)	(0.0504)	(0.0410)	(0.009)

Table 5.4.8: Risk premia parameter estimates for the VAR-PMD model under historical probability measure. The asymptotic standard errors are in parentheses.

The market price of inflation risk is on average positive for both VARMA models but for the PMD-VAR the price of risk is mostly negative. The price of risk for inflation in the PMD-VAR exhibits less fluctuations compared to the other models. The price of inflation risk becomes more negative in the VARMA model when current inflation is higher. The price of real activity risk is negative on average. The market price of short rate risk is negative on average, implying higher valuations for assets that have higher payoffs in states of the economy with a higher short rate. The market price of yields term premia for VARMA, PMD-VARMA and PMD-VAR is mostly positive with the results from VAR model to include and negative periods of premia.

5.4.2 Forecasting

In this section, we focus on forecasting performance of the four models and compare their relative performance on forecasting the state factor process and the future yields. We remind the four models are the VARMA-ATSM, the VAR-ATSM, the PMD-VARMA-ATSM and the PMD-VAR-ATSM. After the parameter estimation we try to test the forecasting ability of our yield curve model. The yield curve could provide information about the future path of the economy (Cochrane and M. Piazzesi (2009)). The estimation of forecasts for the model is a crucial procedure for the performance evaluation of the term structure model. First, we evaluate the in-sample performance of the four models for the state factors used in the models and the bond yields. We remind that according our estimation procedure the 1-month and the 10-year yields are estimated without error. Second, we evaluate and compare the out-of-sample performance of the four models in terms of the yield curve but also for the forecasting of the state factors. The performance measure is the RMSE.

RMSEs e.g. for the bond yields are estimated according to the following equation

$$RMSE = \sqrt{\frac{1}{T}\sum_{t=1}^{T}(\hat{y}_t^{(n)} - y_t^{(n)})^2}, \tag{5.4.1}$$

where $\hat{y}_t^{(n)}$ and $y_t^{(n)}$ are the predicted and the actual yields respectively of a bond with maturity n months and T indicates the total length of the forecasting period. Lower values of root mean square error denote better forecasts. The length of the in-sample period is 252 months and the length of the out-of-sample period is 96 months.

Tables 5.4.9 and 5.4.10 illustrate the RMSEs for the state factors and the 12-,24-,36-,48-,60- months bond yields, respectively. For the inflation factor the VAR and PMD-VAR perform better than the VARMA models. Also, this happens for the IP factor and the short rate process. However, the VARMA model performs better for the yield premia factor. The best overall performance for the bond yields in general has the VARMA model and the worst the PMD-VAR model. The VARMA models perform better that their correspondent VAR model. In figures C.0.72, C.0.73, C.0.74 and C.0.75 we present for every bond yield we used in our models the theoretical estimated values versus the actual values for the entire in-sample period. With the exception of the PMD-VAR the results in the other three models perform close enough to each other in predicting the actual bond yield values estimated from the various theoretical models.

We implement an out-of sample forecast study for a period of 96 monthly time series of the state factors described in section 5.3 and yields, from 2004:01 to 2011:12, for various forecast horizons in order to examine whether our model provides a good forecast of the factor evolution process and the yield curve dynamics. The forecasting horizons are 1,3,9,12 and 24 months. Table 5.4.11 summarizes the out-of-sample forecasting errors for the VAR models and table 5.4.12 for the VARMA models. For the two macroeconomic factors the PMD-VAR model outperforms the standard VAR model but for the yield curve factors the standard VAR model has smaller forecasting errors. The standard VARMA model has smaller RMSEs than the PMD-VARMA model for the macroeconomic factors. Comparing now the VARMA models for the yield curve factors the standard VARMA model performs better for short-term horizons. However, for long term horizons the PMD-VARMA model exhibit better results. Generally, in most of the cases the models estimated with standard methods outperform the models estimated with the PMD approach.

	RMSE (in-sample)			
Factor	VAR	PMD-VAR	VARMA	PMD-VARMA
CPI	0.0647	0.0606	0.2272	0.2506
IP change	0.2787	0.3247	0.3969	0.6235
Y1m	0.1103	0.1017	0.1604	0.3967
Term premia	0.1126	1.5972	0.1053	0.4586

Table 5.4.9: Forecast comparisons. The table presents the comparisons of the in-sample forecasts for the state factors. The in-sample forecasting period is 1983:01 to 2003:12, a total of 252 months. The root mean square error (RMSE) for annualized data is calculated.

	RMSE (in-sample)			
Yields	VAR	PMD-VAR	VARMA	PMD-VARMA
12-months	0.3884	0.6781	0.3832	0.3875
24-months	0.3502	0.6223	0.3451	0.3485
36-months	0.2954	0.7071	0.2940	0.2931
48-months	0.2404	0.7960	0.2351	0.2346
60-months	0.1913	0.8688	0.1932	0.1876

Table 5.4.10: Forecast comparisons. The table presents the comparisons of the in-sample forecasts for the yield curve. The in-sample forecasting period is 1983:01 to 2003:12, a total of 252 months. The root mean square error (RMSE) for annualized data is calculated.

Next, table 5.4.13 and table 5.4.14 illustrate the forecasting errors for the zero-coupon bond yields in the VAR and VARMA models, respectively. In the VAR models for the 24-,36-,48- and 60-month yield the standard VAR model performs better than the PMD-VAR except for the 9-,12- and 24-month horizon of the 12-months bond yield. The standard VARMA model outperforms the PMD-VARMA model by producing lower forecasting error. The forecasting study confirms the findings of Feunou and Fontaine (2009) that the VARMA model improves the forecasting ability of the VAR model. The PMD-VARMA could be an possible alternative if someone wants good forecasting for horizons greater than 12 months.

In conclusion, in terms of forecasting performance the VARMA models provides the best results for the yield curve. However, for the state factors the standard models perform better. In the out-of-sample study concerning the state factors, the VAR

models produce smaller forecasting errors with many case the PMD-VAR to improve the forecasting. Finally, for the yield curve the VARMA model is the dominant model with the PMD-VARMA more suitable for longer than 12 months horizons.

		VAR model			
	1m horizon	3m horizon	9m horizon	12m horizon	24m horizon
CPI	0.0182	0.0028	0.0197	0.0371	0.0300
IP growth	0.1855	0.1988	0.0506	0.3295	0.3828
Y1m	0.0734	0.0487	0.0563	0.0616	0.1113
Term premia	0.0809	0.0488	0.0535	0.0520	0.1281
		PMD VAR model			
	1m horizon	3m horizon	9m horizon	12m horizon	24m horizon
CPI	0.0095	0.0035	0.0084	0.0204	0.0195
IP growth	0.1356	0.0007	0.0812	0.1463	0.1797
Y1m	0.1598	0.1106	0.1850	0.2637	0.0309
Term premia	2.5069	2.4602	2.1344	1.8892	0.3962

Table 5.4.11: RMSE: Forecasting errors for state variables. The out-of-sample period is 2004:01 to 2011:12.

		VARMA model			
	1m horizon	3m horizon	9m horizon	12m horizon	24m horizon
CPI	0.3059	0.0529	0.8419	1.6001	1.3302
IP growth	0.4242	0.2324	0.3021	1.0762	0.3283
Y1m	0.7509	0.6651	0.6661	0.8599	2.0371
Term premia	0.0164	0.2688	0.1524	0.3775	1.8497
		PMD-VARMA model			
	1m horizon	3m horizon	9m horizon	12m horizon	24m horizon
CPI	1.3410	4.6405	3.7988	8.4746	2.0162
IP growth	4.4702	0.7736	6.9449	0.2368	12.2833
Y1m	1.7390	0.7507	2.3647	0.5767	1.1726
Term premia	0.9706	0.9551	0.6225	0.2426	1.8187

Table 5.4.12: RMSE: Forecasting errors for state variables. The out-of-sample period is 2004:01 to 2011:12.

		VAR model			
	1m horizon	3m horizon	9m horizon	12m horizon	24m horizon
12-months	1.2613	1.3025	0.9035	0.8033	0.5681
24-months	1.3557	1.4655	0.9398	0.8313	0.5907
36-months	1.2146	1.3963	0.9591	0.8583	0.6020
48-months	1.1482	1.3007	0.9577	0.8561	0.6575
60-months	1.1141	1.2703	1.0159	0.9284	0.7841
		PMD VAR model			
	1m horizon	3m horizon	9m horizon	12m horizon	24m horizon
12-months	1.0821	1.2237	0.7504	0.5974	0.4193
24-months	1.9944	2.2021	1.8141	1.9191	1.5241
36-months	1.5881	1.8641	1.7074	1.9881	1.5942
48-months	1.5774	1.8364	1.8678	2.2535	2.0212
60-months	1.4209	1.6836	1.8747	2.3567	2.1852

Table 5.4.13: RMSE: Forecasting errors for bond yields for the VAR and PMD-VAR model. The out-of-sample period is 2004:01 to 2011:12.

		VARMA model			
	1m horizon	3m horizon	9m horizon	12m horizon	24m horizon
12-months	0.5476	0.7807	0.2239	0.1495	1.0505
24-months	0.3781	0.7610	0.1745	0.0663	0.6104
36-months	0.2010	0.6782	0.1991	0.0281	0.3754
48-months	0.2105	0.6621	0.2632	0.1266	0.1347
60-months	0.3582	0.8092	0.4694	0.3614	0.1694
		PMD-VARMA model			
	1m horizon	3m horizon	9m horizon	12m horizon	24m horizon
12-months	2.9868	2.6347	2.1013	0.1367	1.0488
24-months	0.9026	2.3513	2.1475	0.0658	0.5626
36-months	0.6665	2.9455	2.2482	0.8477	0.1098
48-months	2.3395	2.4319	2.2719	0.1815	0.2845
60-months	2.4299	2.4036	2.1956	0.3234	0.1588

Table 5.4.14: RMSE: Forecasting errors for bond yields for the VARMA nad PMD-VARMA model. The out-of-sample period is 2004:01 to 2011:12.

5.5 Sequential monitoring

The basic aim of MSPC is the simultaneous detection of changes in a process characteristics. These changes may be caused at unknown times with unpredictable origins.

The most important tool of SPC is the control chart. In our work we use control charts so as to sequentially detect a change in the parameters of a VARMA ATSM. Specially, a change in the parameters of the state evolution process of the term structure model of equation (5.3.3). We propose several types of MEWMA control charts for sequential detection of changes in the VARMA(1,1) state evolution process of the term structure model. Specifically, we propose modified EWMA control charts based on the Mahalanobis distance and the multivariate EWMA statistic and the correspondent residual based EWMA charts. The EWMA control chart was introduced by Roberts (1959) where the control statistic is the exponentially weighted average of the previous and current observations. Lowry et al. (1992) extended the univariate EWMA control chart procedure for the multivariate case and Kramer and Schmid (1997) generalized the MEWMA control chart of Lowry et al. (1992) to correlated observations. Additionally, we construct a multivariate EWMA control chart which is an extension of the simple MEWMA chart by adding to the control statistic the difference of the current with the previous value of the monitoring process, first introduced in the univariate case by Patel and Divecha (2011) and for the multivariate by Patel and Divecha (2013), for industrial applications.

5.5.1 Modeling out-of-control situation

We monitor directly the vector of parameters $\boldsymbol{\xi} = (\boldsymbol{\Phi_1}, \boldsymbol{\Theta_1})$ assuming homoscedasticity for the covariance matrix of the residuals. We mention that a change in the vector of parameters $\boldsymbol{\xi}$ or in a part of it could affect the yield curve as we see from the set of equations that describe the term structure model in section 4.1. When the process is in-control we assume that there is no change in the vector of the model parameters $\boldsymbol{\xi}$. The observed process, which in our case in the VARMA state evolution process, is given by

$$\mathbf{Q}_{1t} = \begin{cases} \boldsymbol{X_t}, & \text{if} \quad t \leq 0 \\ (\boldsymbol{I} + \boldsymbol{D}_1)\boldsymbol{\Phi}_1 \boldsymbol{X}_{t-1} + \boldsymbol{\epsilon}_t - (\boldsymbol{I} + \boldsymbol{D}_2)\boldsymbol{\Theta}_1 \boldsymbol{\epsilon}_{t-1}, & \text{if} \quad t > 1 \end{cases}$$

where $\boldsymbol{D}_1, \boldsymbol{D}_2$ are the diagonal matrices that contain the shocks to the model parameters. Their diagonal elements are $\boldsymbol{d}_1^{(1)}, \ldots, \boldsymbol{d}_1^{(k)}$ and $\boldsymbol{d}_2^{(1)}, \ldots, \boldsymbol{d}_2^{(k)}$ respectively. If $\boldsymbol{D}_1 = \boldsymbol{D}_2 = 0$ then the monitoring process is in-control, else it is out-of-control. The multivariate control chart we examine are based on the distance between the vector of the observed values of the monitoring process and the vector of the mean values of the target process. In our model as the mean of the target values we take the conditional expectations of the state factor process defined in equation (5.3.5). At every time point t a control statistic is appropriately constructed and in order

to decide if the process is out-of-control at time t, it is necessary the determination of a control limit h_1 that defines the rejection area. If the value of the control statistic lies within the acceptance area then the monitoring process is considered to be in-control. We determine the critical value h_1 in such a way that the ARL is equal to a predetermined value k_1 through a simulation study. When the process is in the in-control state, the average run length (ARL_0) denotes the average number of observations or samples until a signal is obtained. In our work we assume that the value of the ARL_0 is equal to 12 months. For the determination of the control limit first a starting value of the control limit is chosen. Next, under the assumption that the process is in-control and the target values are identified, the data for the state evolution process $\boldsymbol{X_t}$ are generated from equations described at section 4.1. These simulated values are applied to each control chart procedure and the stopping times, when the control statistic exceeds the control limit, of the control chart are recorded. Finally, the estimated run length in the in-control state is the average of the simulated stopping times. If now the estimated ARL_0 is greater or lower from its prespecified by an error equal to 1% a new value for the control limit is chosen. Using this new control limit a new iteration procedure is performed so as to estimate the stopping times and the ARL_0. The control limits that fulfill the error condition are chosen as the appropriate control limits. The number of iterations for the above procedure is 10^5 times.

The detection ability of a control chart can be evaluated and compared with other control charts from the ARL_1. The ARL_1 indicates the average number of observations (or samples) that is required until the control chart provides a signal that there is a change in the target process. We desire the value of ARL_1 to be as small as it can be and the opposite for the ARL_0.

Bodnar and Schmid (2011) chose as the in-control process a 10-dimensional VAR(1) process and a two- dimensional VARMA(1,1) process.The first process satisfies the invariance condition but not the latter process. Their out-of-control modeling is restricted to the case of a constant shift in the covariance matrix. The measure for the performance of a control chart is the maximum expected delay (MED). Bodnar and Schmid (2017) mentioned that the changes of interest in a VARMA process can be shifts in the mean value of the time series, changes in the variance of the error terms, changes in the process scaling and changes in the correlation structure such as changes in the coefficients of a VARMA process. In their work they dealt with the detection of changes in the mean and in the scaling of (V)ARMA processes. In contrast we are interested for detecting changes in the coefficients of a VARMA process.

5.5.2 Control chart procedures

For the sequential monitoring we use five categories of control chart procedures: Modified EWMA control chart based on the Mahalanobis distance (ModMah), modified chart based on the Multivariate EWMA Statistic (ModMEWMA), EWMA Residual chart based on the Mahalanobis Distance (ResMah), Residual chart Based on the multivariate EWMA Statistic (ResMEWMA) and Multivariate Modified EWMA control chart (MMOEWMA). The monitoring process for the modified control schemes is a stationary VARMA(1,1) process. In the residual based charts instead of the original observations for the state factor process, the residual process is monitored.

5.5.2.1 Modified EWMA control charts

The EWMA control charts are very effective for the detection of small shifts in the monitoring process (Montgomery (2013)). Lowry et al. (1992) generalized the univariate EWMA control chart procedure for the multivariate case. The EWMA is used extensively in time series modeling and since it can be viewed as a weighted average of all past and current observations, it is very insensitive to the normality assumption of the monitoring process. Small values of the smoothing parameter give more weight to recent values.

Suppose that $\mathbf{X_t^n} = [\boldsymbol{X}_t^1, \ldots, \boldsymbol{X}_t^K]$ is the vector of observed state factors of the economy at time t. Also, under the assumption that $E(\boldsymbol{\epsilon_t}) = \mathbf{0}$ for all $t \geq 1$ and the underlying process is weak stationary we have that $E(\boldsymbol{X}_t) = E(\boldsymbol{X}_{t-1})$ and $V(\boldsymbol{X}_t) = V(\boldsymbol{X}_{t-1})$. The in-control expected value for the state evolution process is

$$E_0(\mathbf{X}_t^n) = \boldsymbol{\Phi}_1 E_0(\mathbf{X_t}). \tag{5.5.1}$$

Under the assumption that $Cov_0(\boldsymbol{X}_t, \epsilon_\mathbf{t}) = \mathbf{0}$, $E(\epsilon_\mathbf{t}) = \mathbf{0}$, $E(\epsilon_\mathbf{t}\epsilon_\mathbf{t})' = \mathbf{U}$, the covariance matrix of the vector of the state evolution process is

$$Cov_0(\mathbf{X_t}) = \boldsymbol{\Phi}_1 V_0(\boldsymbol{X_{t-1}})\boldsymbol{\Phi}_1' + \boldsymbol{\Sigma_\epsilon} + \boldsymbol{\Theta}_1\boldsymbol{\Sigma_\epsilon}\boldsymbol{\Theta}_1'. \tag{5.5.2}$$

The univariate EWMA control chart is based on the EWMA recursion applied on the Mahalanobis distance. The Mahalanobis distance is referred to be the distance of observed state factors from its in-control conditional expectation $\mathbf{m_{0,t}} = \mathbf{E_{0,t}}(\mathbf{X_{t+1}^{n,*}})$ and is measured by

$$T_{t,n} = (\mathbf{X_t^{n,*}} - \boldsymbol{m_{0,t}})' \mathbf{Cov_0}(\mathbf{X_t^{n,*}})^{-1}(\mathbf{X_t^{n,*}} - \boldsymbol{m_{0,t}}), t \geq 1. \tag{5.5.3}$$

The univariate EWMA statistic based on the Mahalanobis distance is given by

$$Z_{t,n} = (1-\lambda)Z_{t-1,n} + \lambda T_{t,n}, \tag{5.5.4}$$

for $t \geq 1$. The starting value $Z_{0,n}$ is set equal to $E_0(T_{t,n}) = k$. A signal is given if $Z_{t,n} > h_1$. The control limit $h_1 > 0$ that determines the rejection area, is estimated through simulation for a predetermined value of the in-control average run length (ARL_0).

Multivariate EWMA control charts are constructed by applying a multivariate EWMA recursion directly to the components of the monitoring characteristic $\mathbf{X_t^n}$. The advantage of this approach is that each characteristic element obtains its own smoothing factor and as a result allows for more flexibility compared to the univariate EWMA (Golosnoy and Schmid (2007)). Suppose that $Cov_0(X_t, u_t) = 0$, $E(\epsilon_t) = 0$, $E(\epsilon_t \epsilon_t)^{'} = U$ and $E(\epsilon_t \epsilon_s)^{'} = \mathbf{0}$ $t \neq s$. The multivariate EWMA statistic has the following form

$$\mathbf{Z}_{t,n} = (\mathbf{I} - \mathbf{R})^t \mathbf{Z}_{t-1,n} + \mathbf{R}\mathbf{X_t^{n,*}}, t \geq 1, \tag{5.5.5}$$

or else

$$\mathbf{Z}_{t,n} = (\mathbf{I} - \mathbf{R})^t \mathbf{Z}_{0,n} + \mathbf{R} \sum_{\upsilon=0}^{t-1} (\mathbf{I} - \mathbf{R})^\upsilon \mathbf{X_{t-\upsilon}^{n,*}}, \tag{5.5.6}$$

where $\mathbf{I}$ is the $k \times k$ identity matrix and $\mathbf{R} = diag(r_1, r_2, \ldots, r_k)$ is $k \times k$ diagonal matrix with diagonal elements $0 < r_i \leq 1$, $i \in \{1, 2, \ldots, k\}$, k is the total number of observable state factors at each time t. The starting value $\mathbf{Z}_{0,n}$ is $E_0(\mathbf{T}_{t,n}) = A_n + \mathbf{B_n} E_0(\mathbf{X_t})$, with E_0 is denoted the mean value when the monitoring process is in-control. The covariance matrix of the multivariate EWMA statistic $\mathbf{Z}_{t,n}$ in the in-control state is given by

$$Cov_0(\mathbf{Z_{t,n}}) = \mathbf{R}\left(\sum_{i,j=0}^{t-1} (\mathbf{I} - \mathbf{R})^i Cov_0(\mathbf{X_t^{n,*}})(\mathbf{I} - \mathbf{R})^J \right)\mathbf{R}. \tag{5.5.7}$$

A signal is given if

$$(\mathbf{Z}_{t,n} - E_0(\mathbf{Z}_{t,n}))^{'} Cov_0(\mathbf{Z}_t)^{-1} (\mathbf{Z}_{t,n} - E_0(\mathbf{Z}_{t,n})) > h_1,$$

where the expected value of the control statistic when the process is in-control is

$$E_0(\mathbf{Z}_t) = (\mathbf{I} - \mathbf{R})^\mathbf{t} \mathbf{Z_0} + (\mathbf{I} - (\mathbf{I} - \mathbf{R})^\mathbf{t} \boldsymbol{\mu_{0,X}}. \tag{5.5.8}$$

where $\boldsymbol{\mu_{0,X}} = E_0(\mathbf{X_t})$. The covariance matrix for the Modified MEWMA statistic is

$$Cov_0(\mathbf{Z_t}) = \mathbf{R}\left(2 * \boldsymbol{\Phi}_1 Cov_0(\mathbf{X_{t-i-1}} \mathbf{X_{t-j-1}}^{'}) \boldsymbol{\Phi}_1^{'} + \Sigma_0(\boldsymbol{\epsilon_t}) + 2 * \boldsymbol{\Theta}_1 \Sigma_0(\boldsymbol{\epsilon_t}) \boldsymbol{\Theta}_1^{'} \right)$$

$$\frac{\boldsymbol{I}}{\boldsymbol{I}-(\boldsymbol{I}-\boldsymbol{R})^2}\mathbf{R},$$

where

$$Cov_0(\boldsymbol{m}_{t-i}\boldsymbol{m}_{t-j}^{'}) = \boldsymbol{\Phi}_1 E_0([\mathbf{X_{t-i}}\mathbf{X_{t-j}}^{'}]\boldsymbol{\Phi}_1^{'} + \boldsymbol{\Theta}_1 E_0[\boldsymbol{\epsilon}_{\boldsymbol{t-i}}\boldsymbol{\epsilon}_{\boldsymbol{t-j}}^{'}]\boldsymbol{\Theta}_1^{'}.$$

Also, $\boldsymbol{\mu_{0,X}} = E_0(\mathbf{X_t})$ and $\boldsymbol{\sigma^2_{0,X}} = V_0(\mathbf{X_t})$. For the proof of the previous equations see appendix A.3.1.

5.5.2.2 Residual based control charts

For the residual control charts the procedures based on the Mahalanobis distance and the multivariate EWMA statistic for the series of the observed state factors are now replaced by the residuals. We assume that the vector of residuals is defined as the deviations of the observed factors at time t from their conditional expectations when the process is in-control, $E_0(\mathbf{X_t^{n,*}}/\mathbf{X_{t-1}^{n,*}})$. We suppose that the vector of the residuals is $\mathbf{d_t} = \boldsymbol{X}_t^{n,*} - E_0(\mathbf{X_t^{n,*}}/\mathbf{X_{t-1}^{n,*}})$. Suppose that $Cov_0(\mathbf{X_t}, \epsilon_\mathbf{t}) = \mathbf{0}$, $Cov_0(\epsilon_\mathbf{t}, \mathbf{X_t}) = \mathbf{0}$, $E(\mathbf{d_t}) = \mathbf{0}$, $E(\epsilon_\mathbf{t}) = \mathbf{0}$, $E(\epsilon_\mathbf{t}\epsilon_\mathbf{t}^{'}) = \mathbf{U}, E(\epsilon_\mathbf{t}\epsilon_\mathbf{s}^{'}) = \mathbf{0}, t \neq s$, The control statistic for the Residual chart based on the Mahalanobis distance is

$$Z_t = (1-\lambda)^t Z_0 + \lambda T_{d,t},\ t \geq 1,$$

with the Mahalanobis distance between the observed state factors and the target mean vector given as

$$T_{d,t} = \mathbf{d_t^{'}}\boldsymbol{\Sigma}_\mathbf{d}^{-1}\mathbf{d_t}.$$

The in-control covariance matrix of the vector of the residuals is

$$Cov_0(\mathbf{d_t}) = \boldsymbol{\Phi}_1 V_0(\mathbf{X_{T-1}})\boldsymbol{\Phi}_1^{'} + \boldsymbol{\Sigma}_\epsilon - \boldsymbol{\Theta}_1\boldsymbol{\Sigma}_\epsilon\boldsymbol{\Theta}_1^{'}.$$

For the multivariate case we assume that $Cov_0(\mathbf{X_t}, \epsilon_\mathbf{t}) = \mathbf{0}$, $Cov_0(\epsilon_\mathbf{t}, \mathbf{X_t}) = \mathbf{0}$, $E(\mathbf{d_t}) = \mathbf{0}$, $E(\epsilon_\mathbf{t}) = \mathbf{0}$, $E(\epsilon_\mathbf{t}\epsilon_\mathbf{t}^{'}) = \mathbf{U}, E(\epsilon_\mathbf{t}\epsilon_\mathbf{s}^{'}) = \mathbf{0}, t \neq s$, then the covariance matrix of the statistic $\mathbf{Z_t}$ is

$$Cov_0(\mathbf{Z_t}) = \mathbf{R}\Big(2 * \boldsymbol{\Phi}_1\mathbf{X_{t-i-1}}\mathbf{X_{t-j-1}}^{'}\boldsymbol{\Phi}_1^{'} + \boldsymbol{\Sigma}_\boldsymbol{\epsilon} - \boldsymbol{\Sigma}_\boldsymbol{\epsilon}\boldsymbol{\Theta}_1^{'} - \boldsymbol{\Theta}_1\boldsymbol{\Sigma}_\boldsymbol{\epsilon}\Big)\frac{\boldsymbol{I}}{\boldsymbol{I}-(\boldsymbol{I}-\boldsymbol{R})^2}\mathbf{R}.$$

For the proof of the previous equations see appendix A.3.2 and appendix A.3.3.

5.5.2.3 MMOEWMA control charts

Patel and Divecha (2013) introduced the MMOEWMA control chart for detecting both large and small shifts in a VAR(1) process. Their approach is an extension of their univariate Modified EWMA chart (Patel and Divecha (2011)). The MMOEWMA control chart statistic is a correction of the MEWMA chart statistic by adding the sum of the last change in the monitoring process. The authors mentioned that the use of the Modified MEWMA chart corrects the MEWMA statistic from the inertia problem. The MMOEWMA control statistic takes into consideration each current change in the monitoring process by giving full weight in addition to the past observations. In our work we adapt their approach appropriately and estimate the expected value and the covariance of the control statistic.

The control statistic for the modified MEWMA (MMOEWMA) control chart based on the multivariate EWMA recursion is

$$\mathbf{Z_t} = (\mathbf{I} - \mathbf{R})\mathbf{Z_{t-1}} + \mathbf{R}\mathbf{X_{t-1}} + (\mathbf{X_t} - \mathbf{X_{t-1}}),\ t \geq 1 \tag{5.5.9}$$

It can be proved by repeated substitution in equation (5.5.9) that

$$\mathbf{Z_t} = (\mathbf{I} - \mathbf{R})^{\mathbf{t}}\mathbf{Z_0} + \mathbf{R}\sum_{j=0}^{t-1}(\mathbf{I} - \mathbf{R})^{\mathbf{j}}\mathbf{X_{t-j}} + \sum_{j=0}^{t-1}(I - R)^j(\mathbf{X_{t-j}} - \mathbf{X_{t-j-1}}). \tag{5.5.10}$$

The MMOEWMA control chart gives an out-of-control signal when

$$(\mathbf{Z_t} - E_0(\mathbf{Z}_t))^{'}(Cov_0(\mathbf{Z_t}))^{-1}(\mathbf{Z_t} - E_0(\mathbf{Z}_t)) > h_1,$$

where $h_1 > 0$ is estimated for a determined value of ARL through a simulation study.

The expected value of the control statistic is given by

$$\begin{aligned} E_0(\mathbf{Z}_t) &= E_0((\mathbf{I} - \mathbf{R})^t\mathbf{Z_0} + \mathbf{R}\sum_{j=0}^{t-1}(\mathbf{I} - \mathbf{R})^j\mathbf{X_t} + \sum_{j=0}^{t-1}(\mathbf{I} - \mathbf{R})^j(\mathbf{X_{t-j}} - \mathbf{X_{t-j-1}}) \\ &= (\mathbf{I} - \mathbf{R})^{\mathbf{t}}\mathbf{Z_0} + (\mathbf{I} - (\mathbf{I} - \mathbf{R})^{\mathbf{t}}\boldsymbol{\mu_{0,X}}. \end{aligned}$$

Suppose that $Cov_0(\mathbf{X_t}, \epsilon_\mathbf{t}) = \mathbf{0},\ E(\epsilon_\mathbf{t}) = \mathbf{0},\ E(\epsilon_\mathbf{t}\epsilon_\mathbf{t}^{'}) = \mathbf{U}$, then the in-control covariance matrix is

$$Cov_0(\mathbf{Z_t}) = \mathbf{R}\frac{\boldsymbol{I}}{\boldsymbol{I} - (\boldsymbol{I} - \boldsymbol{R})^2}\mathbf{R}V_0(\mathbf{X_t}).$$

For the proof of the previous equations see appendix A.3.4.

5.6 Simulation study results

In this section, we present the results for the Monte Carlo simulation for the comparison of detection ability of the control charts we introduced in the section 6 for the standard VARMA ATSM. We remind that in all our cases the normality assumption of the data is valid. The results are for a four-dimensional VARMA(1,1) state factor process where shifts are allowed to either the autoregressive matrix or the moving average matrix or in both of them. We mention that the introduced charts are not directionally invariant for this formulation of the monitoring process we use. The proportionate change in the parameters $\mathbf{\Phi}_1$ and $\mathbf{\Theta}_1$ varies between -40% and 40%, in total 16 cases.

In tables 5.7.1 and 5.7.2 we present the best results for the negative and positive values of the shift parameters $\boldsymbol{D_2}$ against all possible shifts in parameter $\boldsymbol{D_2}$, respectively. In our study we assume that $\boldsymbol{d}_1 = \boldsymbol{d}_1^{(1)} = \cdots = \boldsymbol{d}_1^{(k)}$ and $\boldsymbol{d}_2 = \boldsymbol{d}_2^{(1)} = \cdots = \boldsymbol{d}_2^{(k)}$. The tables illustrate the best ARL_1 and the correspondent smoothing parameter value, for every control chart procedure we use and every combination of shifts in the VARMA(1,1) process. The best value for each combination of shifts in denoted with bold font. For negative shifts in the moving average matrix regardless the sign of the change in the autoregressive matrix the MMOEWMA chart and next the modified chart based on the Mahalanobis distance turns out to have the smallest ARL_1. Now, for positive shocks in the moving average matrix the modified chart based on the Mahalanobis distance outperforms the other control charts.

In appendix B.4 we present the tables with the full results for every control chart procedure. For the modified EWMA control chart based on the Mahalanobis distance (see appendix B.4.1) all shifts are detected relatively fast, the $ARLs_1$ is lower than 7 months except for the case when $\lambda = 0.9$ and fails to detect fast the shift. The modified MEWMA chart (see appendix B.4.2) performs well only for values for the smoothing parameter greater than 0.5. The residual charts are the charts with the worst overall performance for both negative and positive shifts in the moving average parameter matrix. The residual based EWMA based on the Mahalanobis distance (see appendix B.4.3) detects the shifts in a period under 7 months only for $\lambda = \{0.1, 0.2\}$. The residual chart for the MEWMA statistic (see appendix B.4.4) performs well for value of the smoothing parameter greater or equal than 0.5. The MMOEWMA chart is the best performing chart for the case of negative shifts in the parameter matrix $\mathbf{\Theta}_1$. Also, for positive shifts in matrix $\mathbf{\Theta}_1$ gives the best results after the modified chart based on Mahalanobis distance. Generally, positive and negative shifts are detected with relative ease for the various values of λ. The

differences in the detection power between the modified control charts, including the MMOEWMA, and the residual based charts could be due to the estimation procedure for the residual of the VARMA term structure model. The residuals of the VARMA(1,1) process are independent and identically distributed when the process is in-control and the control limits of the residual based charts are the same as for the independent case. When the process is out-of-control, the residuals are independent but not identically distributed. According to Bodnar and Schmid (2017) the residual based control chart procedures are not directionally invariant.

An interesting fact is that in the modified MEWMA and the MMOEWMA chart the ARL_1 is always smaller than the ARL_0. We remind that all control charts are calibrated so as to have the same ARL_0, here is 12 months. Additionally, in most of the cases for each value of the smoothing parameter, the values of the ARL_1 show low to medium fluctuations. For the residual chart based on the MEWMA statistic for $\lambda \geq 0.3$ the ARL_1 is much larger than the ARL_0.

5.7 Empirical study

In this section, the control chart procedures that we previously proposed are applied to a Gaussian affine term structure model for the U.S. yield curve, whose state factor process is described by a VARMA(1,1) process. We assume that the in-control period of the term structure model is from January 1983 to December 2003. The results from this VARMA affine model estimated from historical data are obtained from section 5.4 under the no arbitrage assumption. Our aim is to monitor the process that describes the evolution of the observable factors in the economy. The out-of-sample period for the monitoring process is from January 2004 to December 2011 which contains the global financial crisis of 2007-08.

We perform the analysis by considering as the target process of the state factor equation $\boldsymbol{X}_t$ (see equation (5.3.3)) its conditional expectation $E_t(\boldsymbol{X}_{t+1})$. Furthermore, we use for monitoring in the out-of-sample period the modified and residual based control charts described in section 5.5.2.

However, here we present the results for the modified EWMA control chart based on the Mahalanobis distance with smoothing parameter $\lambda = 0.3$ and the MMOEWMA control chart with smoothing parameter $\lambda = 0.2$. The control limits are obtained from the Monte Carlo simulation study we described in previous section. The zero-coupon yield curve process is an affine function of the state factor process and its conditional expectations. As a result a shift is the state factor process may lead to

changes in the yield curve which is of crucial interest for the investors. The statistical monitoring processes we use for the detection of changes do not give us more insight to the causes of an out-of-control condition.

In figure 5.7.1 we present the control chart for the univariate EWMA based on the Mahalanobis distance for $\lambda = 0.3$ for the control limit obtained from a simulation study as described in section 5.5.2. From the control chart for the univariate EWMA based on the Mahalanobis distance we have two periods of significant changes in the parameters of the process that describes the evolution of the state factors in the economy. The first is from August,2005 to March, 2008 and the second from June, 2008 to August, 2011. The second period of changes contains the crisis on the US capital market, e.g. the failure of investment bank Lehman Brothers in September 2008, which led to the world financial crisis.

The MMOEWMA control chart for $\lambda = 0.2$ provides two signals, the first in January 2006 and the second in June 2008. We notice that the MMOEWMA chart in control with the univariate EWMA chart based on the Mahalanobis distance does not start from an out-of-control condition and after August 2010 the process returns to the in-control condition. Since the state factor evolution process contain two factors from the yield curve, the term premia and the 1-month yield, its dynamics is estimated directly from observed data. This fact affects the behavior and the fluctuations of the control statistics. We observe that in the period from the beginning of 2006 until the beginning of 2008 have more fluctuations of the control statistic in the MMOEWMA chart.

d_1 \ d_2		-0.4	-0.3	-0.2	-0.1
-0.4	ModMah	**2.1746(0.1)**	**2.0526(0.1)**	**2.1510(0.1)**	**2.1982(0.1)**
	ModMEWMA	2.8098 (0.9)	2.7753(0.9)	2.7923 (0.9)	2.8050 (0.9)
	ResMah	3.0125 (0.1)	3.3208 (0.1)	3.2167(0.1)	2.8625 (0.1)
	ResMEWMA	3.0032 (0.9)	3.0105(0.9)	3.0620 (0.9)	3.0100(0.9)
	MMOEWMA	2.2825 (0.1)	2.2908 (0.1)	2.2545 (0.1)	2.3325 (0.1)
-0.3	ModMah	2.1990 (0.2)	**2.1504(0.1)**	**2.0807(0.1)**	**2.0880(0.1)**
	ModMEWMA	2.7770 (0.9)	2.7440 (0.9)	2.8310 (0.9)	2.8330 (0.9)
	ResMah	3.3208 (0.1)	2.7917(0.1)	2.7000 (0.1)	2.8417 (0.1)
	ResMEWMA	3.0753 (0.9)	3.0507 (0.9)	3.0240 (0.9)	3.0473 (0.9)
	MMOEWMA	**2.0173(0.1)**	2.2447(0.1)	2.2803(0.1)	2.3035 (0.1)
-0.2	ModMah	2.1537(0.1)	**2.0230(0.1)**	**1.9936(0.1)**	**2.0330(0.1)**
	ModMEWMA	2.8218 (0.9)	2.7978(0.9)	2.8450 (0.9)	2.7948 (0.9)
	ResMah	2.6667(0.1)	3.4458 (0.1)	2.8500(0.1)	2.9083(0.1)
	ResMEWMA	2.9693 (0.9)	3.0930 (0.9)	3.0873 (0.9)	2.9733(0.9)
	MMOEWMA	**1.9910(0.1)**	2.2578 (0.1)	2.2327 (0.1)	2.2560 (0.1)
-0.1	ModMah	2.0720 (0.1)	2.4883 (0.3)	2.0830(0.1)	**2.1502(0.1)**
	ModMEWMA	2.8685 (0.9)	2.8255(0.9)	2.7445 (0.9)	2.8403(0.9)
	ResMah	3.3750(0.1)	3.0667(0.1)	2.9000 (0.1)	2.9625 (0.1)
	ResMEWMA	3.0315 (0.9)	2.9947 (0.9)	3.0177(0.9)	2.9595(0.9)
	MMOEWMA	**2.0232(0.1)**	**2.2700(0.1)**	**2.0383(0.1)**	2.3170 (0.1)
0.1	ModMah	2.0450(0.1)	**2.1527(0.2)**	2.09170.1)	2.2580(0.3)
	ModMEWMA	2.7690 (0.9)	2.8382 (0.9)	2.8312(0.9)	2.8592 (0.9)
	ResMah	3.0042 (0.1)	3.2208 (0.1)	2.9542(0.1)	2.9250 (0.1)
	ResMEWMA	3.0118 (0.9)	3.0048 (0.9)	3.0190 (0.9)	3.0975 (0.9)
	MMOEWMA	**1.9757(0.1)**	2.2668 (0.1)	**1.9932(0.1)**	**2.0562(0.1)**
0.2	ModMah	2.2350(0.1)	**2.0413(0.1)**	2.0647(0.1)	2.1943(0.1)
	ModMEWMA	2.8450 (0.9)	2.8093(0.9)	2.8555 (0.9)	2.8108(0.9)
	ResMah	3.0458 (0.1)	2.9833 (0.1)	2.9625(0.1)	3.2625 (0.1)
	ResMEWMA	3.0722(0.9)	2.9880 (0.9)	3.0332 (0.9)	3.0042 (0.9)
	MMOEWMA	**2.0558(0.1)**	.2942 (0.1)	**2.0055(0.1)**	**1.9880(0.1)**
0.3	ModMah	2.0240(0.1)	**2.1663(0.2)**	2.0907(0.1)	2.0680 (0.1)
	ModMEWMA	2.8180 (0.9)	2.7927 (0.9)	2.8683 (0.9)	2.8050 (0.9)
	ResMah	3.0708 (0.1)	2.6833(0.1)	2.8375(0.1)	3.5042 (0.1)
	ResMEWMA	2.9882 (0.9)	3.0097 (0.9)	3.0270 (0.9)	3.0528(0.9)
	MMOEWMA	**2.0190(0.1)**	2.2740 (0.1)	**2.0045(0.1)**	**2.0313(0.1)**
0.4	ModMah	2.1352(0.1)	**2.0506(0.1)**	2.1164(0.1)	2.1372 (0.1)
	ModMEWMA	2.8235 (0.9)	2.7877(0.9)	2.8080(0.9)	2.7920(0.9)
	ResMah	3.5625 (0.1)	2.8583 (0.1)	2.5542 (0.1)	2.8292 (0.1)
	ResMEWMA	3.0227 (0.9)	3.0303 (0.9)	3.0025(0.9)	2.9943 (0.9)
	MMOEWMA	**2.0135(0.1)**	2.2870 (0.1)	**1.9952(0.1)**	**2.0057(0.1)**

Table 5.7.1: Best out-of-control ARLs for negative shifts in the moving average component of the VARMA affine process.

d_1 \ d_2		0.1	0.2	0.3	0.4
-0.4	ModMah	**2.1106(0.1)**	**2.0124(0.1)**	**2.0454(0.1)**	**2.0960(0.1)**
	ModMEWMA	2.7492 (0.9)	2.8258 (0.9)	2.7942(0.9)	2.7793(0.9)
	ResMah	3.2625 (0.1)	2.7042(0.1)	2.9917(0.1)	2.8458 (0.1)
	ResMEWMA	3.0412 (0.9)	3.1012 (0.9)	2.9973(0.9)	3.0848 (0.9)
	MMOEWMA	2.2730 (0.1)	2.3160 (0.1)	2.2883 (0.1)	2.2675 (0.1)
-0.3	ModMah	**2.1467(0.1)**	**2.0113(0.1)**	**2.2723(0.1)**	**2.0563(0.1)**
	ModMEWMA	2.8105 (0.9)	2.7832(0.9)	2.8740 (0.9)	2.8150 (0.9)
	ResMah	3.0208 (0.1)	2.8833 (0.1)	3.1042(0.1)	3.1792 (0.1)
	ResMEWMA	2.9983 (0.9)	2.9600(0.9)	2.9870 (0.9)	2.9800 (0.9)
	MMOEWMA	2.2742 (0.1)	2.2828 (0.1)	2.2725 (0.1)	2.3148 (0.1)
-0.2	ModMah	**2.1913(0.1)**	**2.2877(0.1)**	**2.1020(0.1)**	**2.1507(0.2)**
	ModMEWMA	2.8070 (0.9)	2.7628(0.9)	2.7473 (0.9)	2.8392(0.9)
	ResMah	3.2375 (0.1)	2.6625(0.1)	2.9042(0.1)	3.6625 (0.1)
	ResMEWMA	2.9630 (0.9)	2.9663 (0.9)	3.0337 (0.9)	2.9882 (0.9)
	MMOEWMA	2.3395(0.1)	2.3100 (0.1)	2.2923 (0.1)	2.2535 (0.1)
-0.1	ModMah	**2.0177(0.1)**	**2.1707(0.1)**	**2.2343(0.2)**	**2.0917(0.1)**
	ModMEWMA	2.7520 (0.9)	2.7520 (0.9)	2.8390 (0.9)	2.7418(0.9)
	ResMah	3.0042 (0.1)	3.1833 (0.1)	3.1542(0.1)	3.1833 (0.1)
	ResMEWMA	3.0183 (0.9)	2.9278 (0.9)	3.0850 (0.9)	2.9848 (0.9)
	MMOEWMA	2.3080 (0.1)	2.3200 (0.1)	2.2982(0.1)	2.2677 (0.1)
0.1	ModMah	**2.1408(0.1)**	**2.1403(0.1)**	**2.1510(0.2)**	**2.1793(0.2)**
	ModMEWMA	2.7767 (0.9)	2.8502 (0.9)	2.8518 (0.9)	2.7830(0.9)
	ResMah	3.0792 (0.1)	2.8250 (0.1)	3.4750 (0.1)	2.6375(0.1)
	ResMEWMA	2.9080 (0.9)	3.0248(0.9)	3.0032 (0.9)	3.0090 (0.9)
	MMOEWMA	2.2670(0.1)	2.2738 (0.1)	2.2978 (0.1)	2.2510 (0.1)
0.2	ModMah	1.9867(0.1)	**2.0854(0.1)**	**2.0477(0.1)**	**2.1810(0.1)**
	ModMEWMA	2.8145 (0.9)	2.8045(0.9)	2.7938 (0.9)	2.8155(0.9)
	ResMah	2.6750 (0.1)	3.0542 (0.1)	2.8542(0.1)	3.1750(0.1)
	ResMEWMA	3.0120 (0.9)	3.0703(0.9)	3.0290(0.9)	3.0547 (0.9)
	MMOEWMA	**1.9770(0.1)**	2.3450 (0.1)	2.2810(0.1)	2.3055 (0.1)
0.3	ModMah	2.1320 (0.1)	2.0327 (0.1)	**2.1586(0.1)**	**2.0870(0.1)**
	ModMEWMA	2.8308 (0.9)	2.8255(0.9)	2.8400 (0.9)	2.7538(0.9)
	ResMah	3.1417 (0.1)	2.9375(0.1)	3.0875(0.1)	3.5792(0.1)
	ResMEWMA	3.0130 (0.9)	2.9562 (0.9)	3.0408(0.9)	2.9863(0.9)
	MMOEWMA	**1.9883(0.1)**	**2.0180(0.1)**	2.2515 (0.1)	2.3020 (0.1)
0.4	ModMah	2.1026 (0.1)	2.1062(0.1)	2.1598 (0.2)	**2.1264(0.1)**
	ModMEWMA	2.8105 (0.9)	2.8763(0.9)	2.8708(0.9)	2.8268 (0.9)
	ResMah	2.7708 (0.1)	2.7667 (0.1)	3.0250(0.1)	2.7792(0.1)
	ResMEWMA	3.0215 (0.9)	3.0515(0.9)	2.9482(0.9)	3.0082 (0.9)
	MMOEWMA	**2.0402(0.1)**	**2.0227(0.1)**	**2.0307(0.1)**	2.2917 (0.1)

Table 5.7.2: Best out-of-control ARLs for positive shifts in the moving average component of the VARMA affine process.

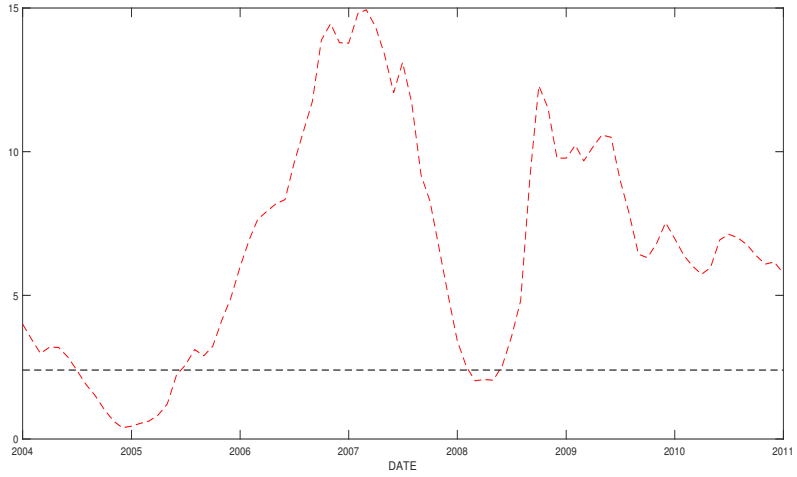

Figure 5.7.1: Modified EWMA chart based on Mahalanobis distance for $\lambda = 0.3$. The out-of-sample period is 2004:01 to 2011:12.

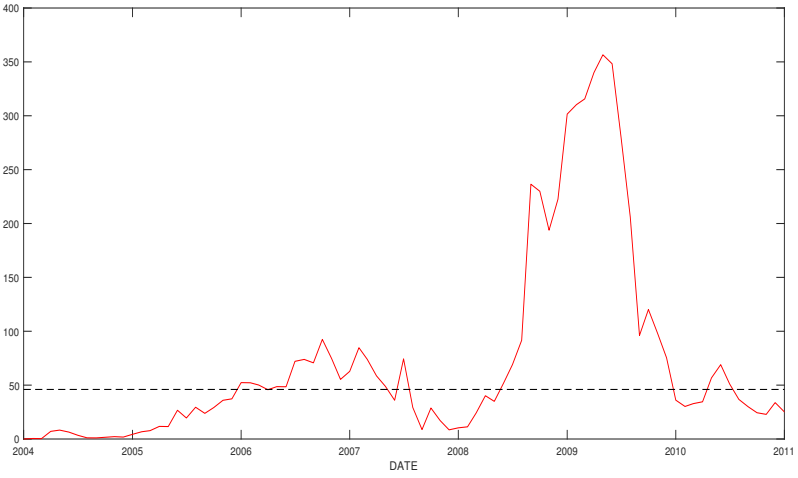

Figure 5.7.2: MMOEWMA chart for $\lambda = 0.2$. The out-of-sample period is 2004:01 to 2011:12.

Chapter 6

Conclusions and Discussion

In recent years SPC techniques such as control charts, originating from industrial production, have found application to various fields such as finance. Monitoring of a financial time series for detection of changes can be an important tool for decision making.

In this work first we apply control charts for the detection of structural breaks in a multifactor ATSM. The proposed control charts are the univariate EWMA based on the Mahalanobis distance, the MEWMA chart, their corresponding charts applied to the residual of the monitoring process, the MCUSUM and for the first time in a financial application a modification of the MEWMA control chart the MMOEWMA chart. The detection power of the control charts is tested through a simulation study. We simulate shifts in the factor loading of the state evolution process of the affine model and various parallel and non-parallel shifts in the yield curve process. The results indicate that the choice of the suitable control chart depends on the type of the shift, the size and the sign of the shift. The proposed control chart techniques have been applied empirically to the U.S. yield curve and various structural breaks have been documented. The main problem when the chart gives a signal is the reestimation of the target process and eventually the new control limits. Here we propose an estimation technique that is based on a estimation window that contains a small period after the signal is given.

Second, we apply the mean-variance portfolio approach introduced by Markowitz (1952) to obtain optimal portfolios composed of government bonds through an affine term structure model estimated using the minimum chi square approach. This portfolio optimization strategy is compared with other benchmark strategies and the

results are quite satisfactory. Next, we propose EWMA control charts based on the first differences for the surveillance of optimal GMVP weights. We apply this control schemes in two portfolio optimization cases, allowing or not short selling. The calculation of the control charts requires the knowledge of the moments of the estimated optimal weights. For the estimation of the covariance we use a simulation approach since our asset returns are correlated. For the out-of-sample period only changes in the variance of bond returns are considered. The MEWMA difference control chart performs better than the the Mahalanobis difference chart and for every control scheme the results for constrained portfolio outperform that for unconstrained. In the empirical study the results for the out-of-sample period favor the MEWMA difference control chart.

Finally, we study a no-arbitrage Gaussian VARMA model of the term structure estimated through a two-step procedure. For the first step additional to standard estimation approaches we apply an estimation procedure based on the impulse responses of the data process, the Projection Minimum Distance approach which is asymptotically equivalent to the maximum likelihood method. Next, we compare the forecasting ability for the state factor and theoretical bond yields not only for the VARMA models but also compared with VAR-based models. The comparison in terms of forecasting ability is done both for the in-sample and out-of-sample period. The results confirm mostly in the forecasting of zero-coupon bond yields the superiority of the VARMA models. The PMD estimation technique can be useful when we are interest in medium- and long-term forecasting of the yield curve. In addition, we apply control charts for detecting changes in the parameters of the VARMA model under the historical probability measure. The detection power of the control charts is tested through a simulation study for positive and negative shifts in the autoregressive and moving average component of the VARMA affine model. The results indicate the choice of the modified EWMA chart based on the Mahalanobis distance and the MMOEWMA control chart.

Future research in portfolio surveillance should concentrate on extending existing control schemes for the GMVP or establishing new techniques. This requires thorough study not only of SPC methods but also of modern portfolio theory. The majority of the work in monitoring portfolio weights is concentrated in GMVPs and should be extended for portfolio categories other than the GMVPs such as tangency or Sharpe ratio. This suggests exploring techniques in order to monitor simultaneously the mean and the variance of the portfolio weights. On a wider level the application of control charts in areas different from the Modern Portfolio Theory (MPT) such as the Post-Modern Portfolio Theory (PMPT) should be investigated.

Additionally the assumption of the distribution of the asset returns for cases other than the Normal distribution needs further work. Most of the literature in the Markowitz's portfolio theory is focused on the equity portfolios and less on the class of fixed-income portfolios. The monitoring of both mean and variance in a mean-variance portfolio framework points out the need for applying more advanced SPC techniques. One more possible application of control charts need to be considered is monitoring large-scale portfolio allocations. Control charts on portfolio based on realized covariance matrix is a new research area that future investigations are necessary in topics such as in high-dimensional portfolios using a parametric factor structure for the estimation of the covariance.

In many financial applications the sequence of the data is less frequent than daily data e.g monthly or quarterly data, specially in term structure models. Future studies should target on control schemes that take into consideration low frequency data and affect distributional properties of estimators. For example, the use of low frequency data for the asset returns may affect the estimation of the covariance matrix of the control statistic and the distributional properties of the optimal portfolio weights. In that case future work should aim at Monte Carlo simulation techniques. Additional investigation is needed for control charts that assist the decision-making process in stock trading for stocks that have low trading frequency. Future studies should target on control schemes that take into consideration low frequency data and affect distributional properties of estimators. Finally, further research should be focused on techniques for the estimation of the moments of optimal portfolio weights when the asset returns are identically and depended data under the normality assumption.

Bibliography

1. Abramowitz, Milton, Irene A Stegun, and Robert H Romer (1988). *Handbook of mathematical functions with formulas, graphs, and mathematical tables*.
2. Alexander, Sidney S (1961). "Price movements in speculative markets: Trends or random walks". In: *Industrial Management Review (pre-1986)* 2.2, p. 7.
3. — (1964). "Price Movements in Speculative Markets-Trends or Random Walks, Number 2". In: *IMR; Industrial Management Review (pre-1986)* 5.2, p. 25.
4. Alwan, Layth C and Harry V Roberts (1988). "Time-series modeling for statistical process control". In: *Journal of Business & Economic Statistics* 6.1, pp. 87–95.
5. Andreou, Elena and Eric Ghysels (2008). "Quality control for structural credit risk models". In: *Journal of Econometrics* 146.2, pp. 364–375.
6. Ang, Andrew, Geert Bekaert, and Min Wei (2008). "The term structure of real rates and expected inflation". In: *The Journal of Finance* 63.2, pp. 797–849.
7. Ang, Andrew, Jean Boivin, Sen Dong, and Rudy Loo-Kung (2011). "Monetary policy shifts and the term structure". In: *The Review of Economic Studies* 78.2, pp. 429–457.
8. Ang, Andrew and Monika Piazzesi (2003). "A no-arbitrage vector autoregression of term structure dynamics with macroeconomic and latent variables". In: *Journal of Monetary Economics* 50.4, pp. 745 –787. ISSN: 0304-3932.
9. Ang, Andrew, Monika Piazzesi, and Min Wei (2006). "What does the yield curve tell us about GDP growth?" In: *Journal of econometrics* 131.1-2, pp. 359–403.

10. Azevedo, Nuno, Diogo Pinheiro, and Gerhard-Wilhelm Weber (2014). "Dynamic programming for a Markov-switching jump–diffusion". In: *Journal of Computational and Applied Mathematics* 267, pp. 1–19.

11. Baker, Dean (2008). "The housing bubble and the financial crisis". In: *Real-world economics review* 46.20, pp. 73–81.

12. Baltas, Ioannis, Anastasios Xepapadeas, and Athanasios N Yannacopoulos (2018). "Robust portfolio decisions for financial institutions". In: *Journal of Dynamics & Games* 5.2, p. 61.

13. Baltas, Ioannis and Athanasios N Yannacopoulos (2019). "Portfolio management in a stochastic factor model under the existence of private information". In: *IMA Journal of Management Mathematics* 30.1, pp. 77–103.

14. Bansal, Ravi and Hao Zhou (2002). "Term structure of interest rates with regime shifts". In: *The Journal of Finance* 57.5, pp. 1997–2043.

15. Bauer, Michael D. (2009). *Term premia and the news*. Tech. rep.

16. Bech, Morten L and Yvan Lengwiler (2012). *The financial crisis and the changing dynamics of the yield curve*. Tech. rep. WWZ Discussion Paper.

17. Berlemann, Michael, Julia Freese, and Sven Knoth (2012). *Eyes Wide Shut? The U.S. House Market Bubble through the Lense of Statistical Process Control*. CESifo Working Paper Series 3962. CESifo.

18. Bersimis, Sotiris, Stelios Psarakis, and John Panaretos (2007). "Multivariate statistical process control charts: an overview". In: *Quality and Reliability Engineering International* 23.5, pp. 517–543.

19. Bersimis, Sotiris, Aggeliki Sgora, and Stelios Psarakis (2018). "The application of multivariate statistical process monitoring in non-industrial processes". In: *Quality Technology & Quantitative Management* 15.4, pp. 526–549.

20. Bilson, John FO, Andrew Kumiega, and Ben Van Vliet (2010). "Trading model uncertainty and statistical process control". In: *The Journal of Trading* 5.3, pp. 39–50.

21. Bock, David, Eva Andersson, and Marianne Frisén (2007). "The relation between statistical surveillance and technical analysis in finance". In: *Financial Surveillance*, pp. 69–92.

22. Bodnar, Olha and Wolfgang Schmid (2007). "Surveillance of the mean behavior of multivariate time series". In: *Statistica Neerlandica* 61.4, pp. 383–406.

23. — (2011). "CUSUM charts for monitoring the mean of a multivariate Gaussian process". In: *Journal of statistical planning and inference* 141.6, pp. 2055–2070.

24. — (2017). "CUSUM control schemes for monitoring the covariance matrix of multivariate time series". In: *Statistics* 51.4, pp. 722–744.

25. Bodnar, T and W Schmid (2008). "Mean–variance portfolio analysis under parameter uncertainty". In: *Statistics & Decisions* 26, pp. 179–201.

26. Bodnar, Taras and Wolfgang Schmid (2004). *A Test for the Weights of the Global Minimum Variance Portfolio in an Elliptical Model*. Univ., Department of Economics.

27. Bollen, Bernard (2015). "What should the value of lambda be in the exponentially weighted moving average volatility model?" In: *Applied Economics* 47.8, pp. 853–860.

28. Bradley, S.P. and D.B. Crane (Oct. 1972). "A Dynamic Model for Bond Portfolio Management". In: *Manage. Sci.* 19.2, pp. 139–151. ISSN: 0025-1909.

29. Brandt, Michael W (2010). "Portfolio choice problems". In: *Handbook of financial econometrics: Tools and techniques*. Elsevier, pp. 269–336.

30. Caldeira, João F., Guilherme V. Moura, and André A.P. Santos (2016). "Bond portfolio optimization using dynamic factor models". In: *Journal of Empirical Finance* 37, pp. 128 –158. ISSN: 0927-5398.

31. Chan, Joshua CC and Eric Eisenstat (2017). "Efficient estimation of Bayesian VARMAs with time-varying coefficients". In: *Journal of Applied Econometrics* 32.7, pp. 1277–1297.

32. Chan, Joshua CC, Eric Eisenstat, and Gary Koop (2016). "Large Bayesian VARMAs". In: *Journal of Econometrics* 192.2, pp. 374–390.

33. Chen, Ren-Raw and Louis Scott (1993). "Maximum likelihood estimation for a multifactor equilibrium model of the term structure of interest rates". In: *The Journal of Fixed Income* 3.3, pp. 14–31.

34. Chen, Ying and Linlin Niu (2014). "Adaptive dynamic Nelson–Siegel term structure model with applications". In: *Journal of Econometrics* 180.1, pp. 98–115.

35. Cheng, P. L. (July 1962). "Optimum Bond Portfolio Selection". In: *Management Science* 8, pp. 490–499.

36. Chib, Siddhartha and Kyu Ho Kang (2013). "Change-points in affine arbitrage-free term structure models". In: *Journal of Financial Econometrics* 11.2, pp. 302–334.

37. Christensen, Jens HE, Jose A Lopez, and Glenn D Rudebusch (2010). "Inflation expectations and risk premiums in an arbitrage-free model of nominal and real bond yields". In: *Journal of Money, Credit and Banking* 42, pp. 143–178.

38. Cochrane, J. H. and (2009) M. Piazzesi (2009). *Decomposing the Yield Curve*. Working Paper. AFA 2010 Atlanta Meetings Paper.

39. Cooper, Ricky A and Ben Van Vliet (2012). "Whole-distribution statistical process control in high-frequency trading". In: *The Journal of Trading* 7.2, pp. 57–68.

40. Cooper, Ricky, Michael Ong, and Ben Van Vliet (2015). "Multi-scale capability: A better approach to performance measurement for algorithmic trading". In: *Algorithmic Finance* 4.1-2, pp. 53–68.

41. Cox, John C, Jonathan E Ingersoll Jr, and Stephen A Ross (2005). "A theory of the term structure of interest rates". In: *Theory of valuation*. World Scientific, pp. 129–164.

42. Crosier, Ronald B. (1988). "Multivariate Generalizations of Cumulative Sum Quality-Control Schemes". In: *Technometrics* 30.3, pp. 291–303. ISSN: 00401706.

43. Cunha, Custodio Alves da, Elisa Henning, Robert Wayne Samohyl, Andrea Cristina Konrath, and Olga Maria Carvalho Formigoni Walter (2013). "Application of multivariate control charts for monitoring an industrial process". In: *Tecno-Lógica* 17.2, pp. 101–107.

44. Dai, Qiang and Kenneth J. Singleton (2000). "Specification Analysis of Affine Term Structure Models". In: *The Journal of Finance* 55.5, pp. 1943–1978. ISSN: 1540-6261.

45. Dai, Qiang, Kenneth J Singleton, and Wei Yang (2007). "Regime shifts in a dynamic term structure model of US treasury bond yields". In: *The Review of Financial Studies* 20.5, pp. 1669–1706.

46. DeMiguel, Victor, Lorenzo Garlappi, Francisco J. Nogales, and Raman Uppal (2009a). "A Generalized Approach to Portfolio Optimization: Improving Performance by Constraining Portfolio Norms". In: *Management Science* 55.5, pp. 798–812.

47. DeMiguel, Victor, Lorenzo Garlappi, and Raman Uppal (May 2009b). "Optimal Versus Naive Diversification: How Inefficient is the 1/N Portfolio Strategy?" In: *Review of Financial Studies* 22.

48. — (2009c). "Optimal versus naive diversification: How inefficient is the 1/N portfolio strategy?" In: *The review of Financial studies* 22.5, pp. 1915–1953.

49. Doroudyan, Mohammad Hadi, Mohammad Saleh Owlia, Hojatollah Sadeghi, and Amirhossein Amiri (2017). "Monitoring financial processes with ARMA-GARCH model based on shewhart control chart (case study: Tehran stock exchange)". In: *International Journal of Engineering* 30.2, pp. 270–280.

50. Duffee, Gregory R. (2002). "Term Premia and Interest Rate Forecasts in Affine Models". In: *The Journal of Finance* 57.1, pp. 405–443.

51. Duffie, D. and R. Kan (1996). "A yield-factor model of interest rates". In: *Mathematical Finance* 6, pp. 379–406.

52. Dufour, Jean-Marie and Denis Pelletier (2008). "Practical methods for modelling weak VARMA processes: Identification, estimation and specification with a macroeconomic application". In: *Manuscript, McGill University.*

53. Dufour, Jean-Marie and Dalibor Stevanović (2013). "Factor-augmented VARMA models with macroeconomic applications". In: *Journal of Business & Economic Statistics* 31.4, pp. 491–506.

54. Dumičić, Ksenija and Berislav Žmuk (2015). "Statistical control charts: performances of short term stock trading in Croatia". In: *Business Systems Research Journal: International journal of the Society for Advancing Business & Information Technology (BIT)* 6.1, pp. 22–35.

55. Erginel, Nihal (2008). "Fuzzy individual and moving range control charts with α-cuts". In: *Journal of Intelligent & Fuzzy Systems* 19.4, 5, pp. 373–383.

56. Estrella, Arturo and Gikas A Hardouvelis (1991). "The term structure as a predictor of real economic activity". In: *The journal of Finance* 46.2, pp. 555–576.

57. Estrella, Arturo and Frederic S Mishkin (1996). "The yield curve as a predictor of US recessions". In: *Current issues in economics and finance* 2.7.

58. Estrella, Arturo and Mary Trubin (2006). "The yield curve as a leading indicator: Some practical issues". In: *Current issues in Economics and Finance* 12.5.

59. Fabozzi, Frank J (2007). *Fixed income analysis*. Vol. 6. John Wiley & Sons.

60. — (2018). *The handbook of financial instruments*. John Wiley & Sons.

61. Fabozzi, Frank J. and Gifford Fong (1994). *Advanced fixed income portfolio management: the state of the art*. Probus.

62. Fama, Eugene F and Marshall E Blume (1966). "Filter rules and stock-market trading". In: *The Journal of Business* 39.1, pp. 226–241.

63. Fama, Eugene and Robert R Bliss (1987). "The Information in Long-Maturity Forward Rates". In: *American Economic Review* 77.4, pp. 680–92.

64. Feunou, Bruno and J Fontaine (2009). *A no-arbitrage VARMA term structure model with macroeconomic variables*. Tech. rep. Working Paper, Duke University.

65. Freese, Julia (2015). "The Regional Pattern of the US House Price Bubble–An Application of SPC to City Level Data". In: *Review of Economics* 66.2, pp. 185–224.

66. Frisén, Marianne (2008). *Financial surveillance*. Vol. 71. Wiley Online Library.

67. — (2011). "Methods and evaluations for surveillance in industry, business, finance, and public health". In: *Quality and Reliability Engineering International* 27.5, pp. 611–621.

68. Gandy, Axel (2012). "Performance monitoring of credit portfolios using survival analysis". In: *International Journal of Forecasting* 28.1, pp. 139–144.

69. Garthoff, Robert, Iryna Okhrin, and Wolfgang Schmid (2014). "Statistical surveillance of the mean vector and the covariance matrix of nonlinear time series". In: *AStA Advances in Statistical Analysis* 98.3, pp. 225–255.

70. Garthoff, Robert and Wolfgang Schmid (2017). "Monitoring means and covariances of multivariate non linear time series with heavy tails". In: *Communications in Statistics-Theory and Methods* 46.21, pp. 10394–10415.

71. Giraitis, Liudas, George Kapetanios, Konstantinos Theodoridis, and Tony Yates (2014). "Estimating time-varying DSGE models using minimum distance methods". In: *Bank of England working paper*.

72. Golosnoy, Vasyl (2007). "Sequential monitoring of minimum variance portfolio". In: *AStA Advances in Statistical Analysis* 91.1, pp. 39–55. ISSN: 1863-818X.

73. — (2018). "Sequential monitoring of portfolio betas". In: *Statistical Papers* 59.2, pp. 663–684.

74. Golosnoy, Vasyl, Iryna Okhrin, Sergiy Ragulin, and Wolfgang Schmid (2010a). "On the Application of SPC in Finance". In: *Frontiers in Statistical Quality Control 9*. Springer, pp. 119–130.

75. Golosnoy, Vasyl, Iryna Okhrin, and Wolfgang Schmid (2010b). "New characteristics for portfolio surveillance". In: *Statistics* 44.3, pp. 303–321.

76. — (2012). "Statistical surveillance of volatility forecasting models". In: *Journal of Financial Econometrics* 10.3, pp. 513–543.

77. Golosnoy, Vasyl, Sergiy Ragulin, and Wolfgang Schmid (2011). "CUSUM control charts for monitoring optimal portfolio weights". In: *Computational Statistics & Data Analysis* 55.11, pp. 2991 –3009. ISSN: 0167-9473.

78. Golosnoy, Vasyl and Jan Roestel (2019). "Real Time Monitoring of the US Inflation Expectation Process". In: *Macroeconomic Dynamics* 23.6, pp. 2221–2249.

79. Golosnoy, Vasyl and Wolfgang Schmid (2007). "EWMA Control Charts for Monitoring Optimal Portfolio Weights". In: *Sequential Analysis* 26.2, pp. 195–224.

80. — (2009). "Statistical process control in asset management". In: *Applied Quantitative Finance*. Springer, pp. 399–416.

81. Golosnoy, Vasyl, Wolfgang Schmid, and Iryna Okhrin (2007). "Sequential monitoring of optimal portfolio weights". In: *Financial Surveillance. Chichester: Wiley*.

82. Golosnoy, Vasyl, Wolfgang Schmid, Miriam Isabel Seifert, and Taras Lazariv (2020). "Statistical inferences for realized portfolio weights". In: *Econometrics and Statistics* 14, pp. 49–62.

83. Govindaraju, K and AJ Godfrey (2011). "Analysis of stock market volatility using Shewhart methodology". In: *Total Quality Management* 22.4, pp. 425–432.

84. Gülbay, Murat and Cengiz Kahraman (2006). "Development of fuzzy process control charts and fuzzy unnatural pattern analyses". In: *Computational statistics & data analysis* 51.1, pp. 434–451.

85. Hamilton, James D (1988). "Rational-expectations econometric analysis of changes in regime: An investigation of the term structure of interest rates". In: *Journal of Economic Dynamics and Control* 12.2-3, pp. 385–423.

86. Hamilton, James D. and Jing Cynthia Wu (2012). "Identification and estimation of Gaussian affine term structure models". In: *Journal of Econometrics* 168.2, pp. 315 –331. ISSN: 0304-4076.

87. Hannan, Edward J and Laimonis Kavalieris (1984). "Multivariate linear time series models". In: *Advances in Applied Probability*, pp. 492–561.

88. Hannan, Edward J and Jorma Rissanen (1982). "Recursive estimation of mixed autoregressive-moving average order". In: *Biometrika* 69.1, pp. 81–94.

89. Hannan, Edward James and Manfred Deistler (2012). *The statistical theory of linear systems*. SIAM.

90. Harris, Thomas J and William H Ross (1991). "Statistical process control procedures for correlated observations". In: *The Canadian Journal of Chemical Engineering* 69.1, pp. 48–57.

91. Harvey, Campbell R (1988). "The real term structure and consumption growth". In: *Journal of Financial Economics* 22.2, pp. 305–333.

92. Hassan, M Zia, Andrew Kumiega, and Ben Van Vliet (2010). "Trading machines: Using SPC to assess performance of financial trading systems". In: *Quality Management Journal* 17.2, pp. 42–53.

93. Horváth, Lajos, Piotr Kokoszka, and Aonan Zhang (2006). "Monitoring constancy of variance in conditionally heteroskedastic time series". In: *Econometric Theory*, pp. 373–402.

94. Hotelling, H (1947). "Multivariate quality control, illustrated by the air testing of sample bombsights". In: *Techniques of Statistical Analysis*, pp. 111–184.

95. Hsu, Der-Ann, Robert B. Miller, and Dean W. Wichern (1974). "On the Stable Paretian Behavior of Stock-Market Prices". In: *Journal of the American Statistical Association* 69.345, pp. 108–113. ISSN: 01621459.

96. Hubbard, Charles L (1967). "A control chart for postwar stock price levels". In: *Financial Analysts Journal* 23.6, pp. 139–145.

97. Jordà, Òscar and Sharon Kozicki (2011). "Estimation and Inference by the Method of Projection Minimum Distance: An Application to the New Keynesian Hybrid Phillips Curve". In: *International Economic Review* 52.2, pp. 461–487. ISSN: 1468-2354.

98. Jordà, Òscar (2005). "Estimation and inference of impulse responses by local projections". In: *American economic review* 95.1, pp. 161–182.

99. Jumah, Jawaher A Bin, René P Burt, and Benjamin Buttram (2012). "An exploration of quality control in banking and finance". In: *International Journal of Business and Social Science* 3.6.

100. Jungbacker, Borus, Siem Jan Koopman, and Michel Wel (2012). "Smooth Dynamic Factor Analysis with Application to the U.S. Term Structure of Interest Rates". In: *Journal of Applied Econometrics* 29.1, pp. 65–90.

101. Kapetanios, George (2003). "A note on an iterative least-squares estimation method for ARMA and VARMA models". In: *Economics Letters* 79.3, pp. 305–312.

102. Kascha, Christian (2012). "A comparison of estimation methods for vector Autoregressive Moving-Average Models". In: *Econometric Reviews* 31.3, pp. 297–324.

103. Kascha, Christian and Karel Mertens (2009). "Business cycle analysis and VARMA models". In: *Journal of Economic Dynamics and Control* 33.2, pp. 267–282.

104. Kascha, Christian and Carsten Trenkler (2011). "Cointegrated VARMA models and forecasting US interest rates". In: *Available at SSRN 1957103*.

105. Kavalieris, L, EJ Hannan, and M Salau (2003). "Generalized least squares estimation of ARMA models". In: *Journal of Time Series Analysis* 24.2, pp. 165–172.

106. Kaya, Ihsan, Melike Erdoğan, and Cansın Yıldız (2017). "Analysis and control of variability by using fuzzy individual control charts". In: *Applied Soft Computing* 51, pp. 370–381.

107. Kempf, Alexander and Christoph Memmel (2006). "Estimating the global minimum variance portfolio". In: *Schmalenbach Business Review* 58.4, pp. 332–348.

108. Khan, Nasrullah, Muhammad Aslam, and Chi-Hyuck Jun (2017). "Design of a control chart using a modified EWMA statistic". In: *Quality and Reliability Engineering International* 33.5, pp. 1095–1104.

109. Knoth, Sven and Wolfgang Schmid (2004). "Control charts for time series: A review". In: *Frontiers in Statistical Quality Control 7*. Springer, pp. 210–236.

110. Koreisha, Sergio and Tarmo Pukkila (1990). "A generalized least-squares approach for estimation of autoregressive moving-average models". In: *Journal of Time Series Analysis* 11.2, pp. 139–151.

111. Korn, Olaf and Christian Koziol (Jan. 2006). "Bond portfolio optimization: A risk-return approach". In: *The Journal of Fixed Income* 15, pp. 48–60.

112. Korn, Ralf and Elke Korn (2001). *Option pricing and portfolio optimization: modern methods of financial mathematics*. Vol. 31. American Mathematical Soc.

113. Kramer, Holger G and LV Schmid (1997). "EWMA charts for multivariate time series". In: *Sequential Analysis* 16.2, pp. 131–154.

114. Kumiega, Andrew, Thaddeus Neururer, and Ben Van Vliet (2014). "Trading system capability". In: *Quantitative Finance* 14.3, pp. 383–392.

115. Lam, Kin and HC Yam (1997). "Cusum techniques for technical trading in financial markets". In: *Financial Engineering and the Japanese Markets* 4.3, pp. 257–274.

116. Li, Shanshan (2016). "Estimation and Detection of Network Variation in Intraday Stock Market". PhD thesis. The Graduate School, Stony Brook University: Stony Brook, NY.

117. Litterman, Robert and Jose Scheinkman (1991). "Common factors affecting bond returns". In: *Journal of fixed income* 1.1, pp. 54–61.

118. Longerstaey, Jacques and Martin Spencer (1996). "Riskmetrics—technical document". In: *Morgan Guaranty Trust Company of New York: New York* 51, p. 54.

119. Lowry, Cynthia A., William H. Woodall, Charles W. Champ, and Steven E. Rigdon (1992). "A Multivariate Exponentially Weighted Moving Average Control Chart". In: *Technometrics* 34.1, pp. 46–53. ISSN: 00401706.

120. Mainassara, Y Boubacar and Christian Francq (2011). "Estimating structural VARMA models with uncorrelated but non-independent error terms". In: *Journal of Multivariate Analysis* 102.3, pp. 496–505.

121. Maïnassara, Yacouba Boubacar et al. (2014). "Estimation of the variance of the quasi-maximum likelihood estimator of weak VARMA models". In: *Electronic Journal of Statistics* 8.2, pp. 2701–2740.

122. Markowitz, Harry (1952). "Portfolio Selection". In: *The Journal of Finance* 7.1, pp. 77–91. ISSN: 00221082, 15406261.

123. Metaxoglou, Konstantinos and Aaron Smith (2007). "Maximum Likelihood Estimation of VARMA Models Using a State-Space EM Algorithm". In: *Journal of Time Series Analysis* 28.5, pp. 666–685.

124. Meucci, Attilio (Apr. 2010). "Managing Diversification". In: *Risk* 22.

125. Mishkin, Frederic S (1990). "What does the term structure tell us about future inflation?" In: *Journal of monetary economics* 25.1, pp. 77–95.

126. Montgomery, Douglas C. (2013). *Introduction to statistical quality control*. 7th ed. Previous ed.: 2005. Hoboken, N.J. : John Wiley & Sons Inc.

127. Morabi, Zahra Sorayanezhad, Mohammad Saleh Owlia, Mahdi Bashiri, and Mohammad Hadi Doroudyan (2015). "Multi-objective design of X control charts with fuzzy process parameters using the hybrid epsilon constraint PSO". In: *Applied Soft Computing* 30, pp. 390–399.

128. Ncube, Matoteng M. and William H. Woodall (1985). "Multivariate CUSUM Quality-Control Procedures". In: *Technometrics* 27.3, pp. 285–292. ISSN: 00401706.

129. Ngai, Hung-Man and Jian Zhang (2001). "Multitivariate cumulative sum control charts based on projection pursuit". In: *Statistica Sinica* 11.3, pp. 747–766. ISSN: 10170405, 19968507.

130. Okhrin, Yarema and Wolfgang Schmid (2006). "Distributional properties of portfolio weights". In: *Journal of Econometrics* 134.1, pp. 235 –256. ISSN: 0304-4076.

131. Okhrin, Yarema and Wolfgang Schmid (2007a). "Surveillance of Univariate and Multivariate Linear Time Series". In: *Financial Surveillance*. John Wiley & Sons, Ltd. Chap. 5, pp. 115–152. ISBN: 9780470987179.

132. — (2007b). "Surveillance of Univariate and Multivariate Nonlinear Time Series". In: *Financial Surveillance*. John Wiley & Sons, Ltd. Chap. 6, pp. 153–177. ISBN: 9780470987179.

133. Olha, Bodnar (2007). "Sequential Procedures for Monitoring Covariances of Asset Returns". In: *Advances in Risk Management*. Ed. by Greg N. Gregoriou. London: Palgrave Macmillan UK, pp. 241–264. ISBN: 978-0-230-62584-6.

134. Owlia, Mohammad Salleh, Mohammad Hadi Doroudyan, Amirhossein Amiri, and Hojatollah Sadeghi (2017). "The effect of parameter estimation on phase II control chart performance in monitoring financial GARCH processes with contaminated data". In: *Journal of Industrial and Systems Engineering* 10.Special issue on Quality Control and Reliability, pp. 93–108.

135. Page, E. S. (1954). "Continuous Inspection Schemes". In: *Biometrika* 41.1-2, pp. 100–115.

136. Pan, Xia and Jeffrey Jarrett (2007). "Using vector autoregressive residuals to monitor multivariate processes in the presence of serial correlation". In: *International Journal of Production Economics* 106.1, pp. 204–216.

137. Papayiannis, GI and AN Yannacopoulos (2018). "Convex risk measures for the aggregation of multiple information sources and applications in insurance". In: *Scandinavian Actuarial Journal* 2018.9, pp. 792–822.

138. Patel, Alpaben K and Jyoti Divecha (2011). "Modified exponentially weighted moving average (EWMA) control chart for an analytical process data". In: *Journal of Chemical Engineering and Materials Science* 2.1, pp. 12–20.

139. — (2013). "Modified MEWMA control scheme for an analytical process data". In: *Global Journal of Computer Science and Technology*.

140. Pericoli, Marcello and Marco Taboga (2008). "Canonical Term-Structure Models with Observable Factors and the Dynamics of Bond Risk Premia". In: *Journal of Money, Credit and Banking* 40.7, pp. 1471–1488.

141. Pignatiello, Joseph J. Jr. and George C. Runger (1990). "Comparisons of Multivariate CUSUM Charts". In: *Journal of Quality Technology* 22.3, pp. 173–186.

142. Pollock, D (Apr. 1989). "Matrix Differential Calculus Jan R. Magnus and Heinz Neudecker John Wiley and Sons, 1988Linear Structures Jan R. Magnus Charles Griffin and Co., 1988". In: *Econometric Theory* 5, pp. 161–165.

143. Premarathna, Nadeeka, A Jonathan R Godfrey, and K Govindaraju (2016). "Decomposition of stock market trade-offs using Shewhart methodology". In: *International Journal of Quality & Reliability Management*.

144. Puhle, Michael (Jan. 2008). *Bond Portfolio Optimization*. Vol. 605. ISBN: 978-3-540-76592-9.

145. Raz, Tzvi and Jyh-Hone Wang (1990). "Probabilistic and membership approaches in the construction of control charts for linguistic data". In: *Production Planning & Control* 1.3, pp. 147–157.

146. Rębisz, Beata (2015). "Appliance of quality control charts for sovereign risk modelling." In: *Journal of Applied Economics & Business Research* 5.3.

147. Riegel Sant'Anna, Leonardo, Tiago Pascoal Filomena, João Frois Caldeira, and Denis Borenstein (2019). "Investigating the use of statistical process control charts for index tracking portfolios". In: *Journal of the Operational Research Society* 70.10, pp. 1622–1638.

148. Roberts, Harry V (1959a). "Stock-market "patterns" and financial analysis: methodological suggestions". In: *The Journal of Finance* 14.1, pp. 1–10.

149. Roberts, SW (1959b). "Control Chart Tests Based on Geometric Moving Averages". In: *Technometrics* 1.3, pp. 239–250.

150. — (1966). "A comparison of some control chart procedures". In: *Technometrics* 8.3, pp. 411–430.

151. Rosołowski, Maciej and Wolfgang Schmid (2003). "EWMA charts for monitoring the mean and the autocovariances of stationary Gaussian processes". In: *Sequential Analysis* 22.4, pp. 257–285.

152. Rothenberg, Thomas J. (1973). *Efficient estimation with a priori information [by] Thomas J. Rothenberg*. English. Yale University Press New Haven, viii, 180 p. ISBN: 0300016077.

153. Saghir, Aamir, Muhammad Aslam, Alireza Faraz, Liaquat Ahmad, and Cedric Heuchenne (2020). "Monitoring process variation using modified EWMA". In: *Quality and Reliability Engineering International* 36.1, pp. 328–339.

154. Savku, E and G-W Weber (2021). "A Regime-Switching Model with Applications to Finance: Markovian and Non-Markovian Cases". In: *Dynamic Economic Problems with Regime Switches*. Springer, pp. 287–309.

155. Savku, Emel and Gerhard-Wilhelm Weber (2018). "A stochastic maximum principle for a markov regime-switching jump-diffusion model with delay and an application to finance". In: *Journal of Optimization Theory and Applications* 179.2, pp. 696–721.

156. Schipper, Stefan and Wolfgang Schmid (2001). "Sequential methods for detecting changes in the variance of economic time series". In: *Sequential Analysis* 20.4, pp. 235–262.

157. Schmid, Wolfgang (1995). "On the run length of a Shewhart chart for correlated data". In: *Statistical Papers* 36.1, p. 111.

158. Schmid, Wolfgang and Dobromir Tzotchev (2004). "Statistical surveillance of the parameters of a one-factor Cox–Ingersoll–Ross model". In: *Sequential Analysis* 23.3, pp. 379–412.

159. Severin, Thomas and Wolfgang Schmid (1996). *Monitoring changes in GARCH models*. Europa-Univ.

160. — (1998). "Statistical process control and its application in finance". In: *Risk Measurement, Econometrics and Neural Networks*. Springer, pp. 83–104.

161. Shewhart, WA (1931). "Statistical method from an engineering viewpoint". In: *Journal of the American Statistical Association* 26.175, pp. 262–269.

162. Simionescu, Mihaela (2013). "The use of VARMA models in forecasting macroeconomic indicators". In: *Economics & Sociology* 6.2, p. 94.

163. Śliwa, Przemysław and Wolfgang Schmid (2005a). "Monitoring the cross-covariances of a multivariate time series". In: *Metrika* 61.1, pp. 89–115.

164. — (2005b). "Surveillance of the covariance matrix of multivariate nonlinear time series". In: *Statistics* 39.3, pp. 221–246.

165. Teulings, Coen N. and Nikolay Zubanov (2014). "Is economic recovery a myth? Robust estimation of impulse responses". In: *Journal of Applied Econometrics* 29.3, pp. 497–514. ISSN: 1099-1255.

166. Tsui, Kwok-Leung, Wenchi Chiu, Peter Gierlich, David Goldsman, Xuyuan Liu, and Thomas Maschek (2008). "A review of healthcare, public health, and syndromic surveillance". In: *Quality Engineering* 20.4, pp. 435–450.

167. Vanhatalo, Erik and Murat Kulahci (2015). "The effect of autocorrelation on the Hotelling T2 control chart". In: *Quality and Reliability Engineering International* 31.8, pp. 1779–1796.

168. Vasicek, Oldrich (1977). "An equilibrium characterization of the term structure". In: *Journal of Financial Economics* 5.2, pp. 177 –188. ISSN: 0304-405X.

169. Vasilopoulos, Athanasios V and AP Stamboulis (1978). "Modification of control chart limits in the presence of data correlation". In: *Journal of Quality Technology* 10.1, pp. 20–30.

170. W. Brandt, Michael (Dec. 2010). "Portfolio Choice Problems". In: *Handbook of Financial Econometrics, Vol 1* 1.

171. Wang, Jyh-Hone and Tzvi Raz (1990). "On the construction of control charts using linguistic variables". In: *The International Journal of Production Research* 28.3, pp. 477–487.

172. Wilms, Ines, Sumanta Basu, Jacob Bien, and David S Matteson (2021). "Sparse identification and estimation of large-scale vector autoregressive moving averages". In: *Journal of the American Statistical Association* just-accepted, pp. 1–33.

173. Woodall, William H (2000). "Controversies and contradictions in statistical process control". In: *Journal of Quality Technology* 32.4, pp. 341–350.

174. Woodall, William H and Douglas C Montgomery (2014). "Some current directions in the theory and application of statistical process monitoring". In: *Journal of Quality Technology* 46.1, pp. 78–94.

175. Wu, Tao and Glenn Rudebusch (2004). *A Macro-Finance Model of the Term Structure, Monetary Policy, and the Economy*. 2004 Meeting Papers 104. Society for Economic Dynamics.

176. Xin, Ling, LH Philip, and Kin Lam (2013). "An Application of CUSUM Chart on Financial Trading". In: *2013 Ninth International Conference on Computational Intelligence and Security*. IEEE, pp. 178–181.

177. Yashchin, Emmanuel, Thomas K Philips, and David M Stein (1997). "Monitoring active portfolios using statistical process control". In: *Computational Approaches to Economic Problems*. Springer, pp. 193–205.

178. Yi, G, S Coleman, and Q Ren (2006). "CUSUM method in predicting regime shifts and its performance in different stock markets allowing for transaction fees". In: *Journal of Applied Statistics* 33.7, pp. 647–661.

179. Yousefi, Nooshin, Ahmad Sobhani, Leila Moslemi Naeni, and Kenneth R Currie (2019). "Using statistical control charts to monitor duration-based performance of project". In: *arXiv preprint arXiv:1902.02270*.

180. Zadeh, Lotfi A (1965). "Fuzzy sets". In: *Information and control* 8.3, pp. 338–353.

181. Žmuk, Berislav (2016). "Capabilities of Statistical Residual-Based Control Charts in Short-and Long-Term Stock Trading". In: *Naše gospodarstvo/Our economy* 62.1, pp. 12–26.

Appendix A

Appendix

A.1 ATSM-Moments for control chart procedures

A.1.1 Moments for EWMA based on Mahalanobis distance

Expected value for the Mahalanobis distance statistic
Suppose that $E(\mathbf{u_t}) = \mathbf{0}$ for all $t \geq 1$,then the in-control expected value for the vector of zero-coupon bond yields is

$$\begin{aligned} E_0(\mathbf{Y}_t^n) &= E_0(\mathbf{A_n} + \mathbf{B_n}^{'} X_t) \\ &= \mathbf{A_n} + \mathbf{B_n}^{'} E_0(X_t) \\ &= \mathbf{A_n} + \mathbf{B_n}^{'}(\boldsymbol{\mu}^Q + \boldsymbol{\phi}^Q E_0(\mathbf{X}_{t+1})). \end{aligned}$$

Covariance matrix for the Mahalanobis distance statistic
Suppose that $Cov_0(X_t, \mathbf{u_t}) = \mathbf{0}$, $E(\mathbf{u_t}) = \mathbf{0}$, $E(\mathbf{u_t}\mathbf{u_t})^{'} = \mathbf{U}$, then the covariance matrix of the vector of bond yields is

$$\begin{aligned} Cov_0(\mathbf{Y_t}) &= E_0[\mathbf{Y_t} - E_0(\mathbf{Y_t})][\mathbf{Y_t} - E_0(\mathbf{Y_t}]^{'} \\ &= E_0[A_n + \mathbf{B_n}^{'}\mathbf{X_t} + \mathbf{u_t} - A_n - \mathbf{B_n}^{'}E_0(\mathbf{X_t})][A_n + \mathbf{B_n}^{'}\mathbf{X_t} + \mathbf{u_t} - A_n - \mathbf{B_n}^{'}E_0(\mathbf{X_t})]^{'} \\ &= E_0[(\mathbf{B_n}^{'}\mathbf{X_t} + \mathbf{u_t} - \mathbf{B_n}^{'}\boldsymbol{\mu}^Q - \mathbf{B_n}\boldsymbol{\phi}^Q E_0(\mathbf{X_{t-1}}))(\mathbf{B_n}\mathbf{X_t} + \mathbf{u_t} - \mathbf{B_n}\boldsymbol{\mu}^Q - \mathbf{B_n}\boldsymbol{\phi}^Q E_0(\mathbf{X_{t-1}}))^{'}] \\ &= E_0[(\mathbf{B_n}^{'}(\mathbf{X_t} - \boldsymbol{\mu}^Q - \boldsymbol{\phi}^Q E_0(\mathbf{X_{t-1}})) + \mathbf{u_t})(\mathbf{B_n}^{'}(\mathbf{X_t} - \boldsymbol{\mu}^Q - \boldsymbol{\phi}^Q E_0(\mathbf{X_{t-1}})) + \mathbf{u_t})^{'}] \\ &= E_0[(\mathbf{B_n}^{'}(\mathbf{X_t} - E_0(\mathbf{X_t})) + \mathbf{u_t})(\mathbf{B_n}^{'}(\mathbf{X_t} - E_0(\mathbf{X_t})) + \mathbf{u_t})^{'}] \\ &= E_0[(\mathbf{B_n}^{'}(\mathbf{X_t} - E_0(\mathbf{X_t})) + \mathbf{u_t})((\mathbf{X_t} - E_0(\mathbf{X_t}))^{'}\mathbf{B_n} + \mathbf{u_t}^{'})] \end{aligned}$$

$$
\begin{aligned}
&= E_0[(\mathbf{B_n'}(\mathbf{X_t} - E_0(\mathbf{X_t}))((\mathbf{X_t} - E_0(\mathbf{X_t}))'\mathbf{B_n} + \mathbf{u_t}(\mathbf{X_t} - E_0(\mathbf{X_t}))'\mathbf{B_n} + \mathbf{B_n'}(\mathbf{X_t} \\
&\quad - E_0(\mathbf{X_t}))\mathbf{u_t}' + \mathbf{u_t}\mathbf{u_t'})] \\
&= E_0[\mathbf{B_n'}(\mathbf{X_t} - E_0(\mathbf{X_t}))(\mathbf{X_t} - E_0(\mathbf{X_t}))\mathbf{B_n}] + \mathbf{U} \\
&= \mathbf{B_n'}E_0[(\mathbf{X_t} - E_0(\mathbf{X_t}))(\mathbf{X_t} - E_0(\mathbf{X_t}))]\mathbf{B_n} + \mathbf{U} \\
&= \mathbf{B_n'}(\boldsymbol{\phi}^Q V_0(\mathbf{X_t})\boldsymbol{\phi}^{Q'} + \boldsymbol{\Sigma})\mathbf{B_n} + \mathbf{U}.
\end{aligned}
$$

A.1.2 Moments for Modified MEWMA control charts

Expected value for the Modified MEWMA statistic:
The control statistic for the modified control chart based on the multivariate EWMA recursion is

$$Z_t = (\mathbf{I} - \mathbf{R})^{\mathbf{t}}\mathbf{Z_0} + \mathbf{R}\sum_{j=0}^{t-1}(\mathbf{I} - \mathbf{R})^{\mathbf{j}}\mathbf{Y_t}.$$

The expected value of the statistic is

$$
\begin{aligned}
E_0(\mathbf{Z}_t) &= E_0((\mathbf{I} - \mathbf{R})^{\mathbf{t}}\mathbf{Z_0} + \mathbf{R}\sum_{j=0}^{t-1}(\mathbf{I} - \mathbf{R})^{\mathbf{j}}\mathbf{Y_t}) \\
&= (\mathbf{I} - \mathbf{R})^{\mathbf{t}}\mathbf{Z_0} + \mathbf{R}\sum_{j=0}^{t-1}(\mathbf{I} - \mathbf{R})^{\mathbf{j}}E_0(\mathbf{Y_t}) \\
&= (\mathbf{I} - \mathbf{R})^{\mathbf{t}}\mathbf{Z_0} + \mathbf{R}\sum_{j=0}^{t-1}(\mathbf{I} - \mathbf{R})^{\mathbf{j}}(A_n + \mathbf{B_n'}(\mathbf{X_{t-j}}) \\
&= (\mathbf{I} - \mathbf{R})^{\mathbf{t}}\mathbf{Z_0} + A_n + \mathbf{R}\mathbf{B_n'}\sum_{j=0}^{t-1}(\mathbf{I} - \mathbf{R})^{\mathbf{j}}E_0(\mathbf{X_{t-j}}) \\
&= (\mathbf{I} - \mathbf{R})^{\mathbf{t}}\mathbf{Z_0} + A_n + \mathbf{R}\mathbf{B_n'}\sum_{j=0}^{t-1}(\mathbf{I} - \mathbf{R})^{\mathbf{j}}\boldsymbol{\mu}_{\mathbf{0},\boldsymbol{X}} \\
&= (\mathbf{I} - \mathbf{R})^{\mathbf{t}}\mathbf{Z_0} + A_n + \mathbf{R}\mathbf{B_n'}\frac{(\mathbf{I} - (\mathbf{I} - \mathbf{R})^{\mathbf{t}}}{(\mathbf{I} - (\mathbf{I} - \mathbf{R})}\boldsymbol{\mu}_{\mathbf{0},\boldsymbol{X}} \\
&= (\mathbf{I} - \mathbf{R})^{\mathbf{t}}\mathbf{Z_0} + A_n + \mathbf{B_n'}(\mathbf{I} - (\mathbf{I} - \mathbf{R})^{\mathbf{t}}\boldsymbol{\mu}_{\mathbf{0},\boldsymbol{X}}.
\end{aligned}
$$

where $\boldsymbol{\mu}_{\mathbf{0},\boldsymbol{X}} = E_0(\mathbf{X_t})$.
Covariance matrix for the Modified MEWMA statistic:

Suppose that $Cov_0(X_t, u_t) = 0,\ E(u_t) = 0,\ E(u_t u_t)' = U$, then

$$
\begin{aligned}
Cov_0(\mathbf{Z_t}) &= Cov_0((\mathbf{I}-\mathbf{R})^{\mathbf{t}}\mathbf{Z_0} + \mathbf{R}\sum_{j=0}^{t-1}(\mathbf{I}-\mathbf{R})^{\mathbf{j}}\mathbf{Y_{t-j}}) \\
&= \mathbf{R}\Big(\sum_{i=0}^{t-1}\sum_{j=0}^{t-1}(\mathbf{I}-\mathbf{R})^{\mathbf{i}}Cov_0(\mathbf{Y_{t-i}Y_{t-j}})(\mathbf{I}-\mathbf{R})^{\mathbf{j}}\Big)\mathbf{R} \\
&= \mathbf{R}\Big(\sum_{i=0}^{t-1}\sum_{j=0}^{t-1}(\mathbf{I}-\mathbf{R})^{i}E_0[(\mathbf{Y_{t-i}} - E_0(\mathbf{Y_{t-i}}))(\mathbf{Y_{t-j}} - E_0(\mathbf{Y_{t-j}}))']({\mathbf{I}-\mathbf{R}})^{j}\Big)\mathbf{R} \\
&= \mathbf{R}\Big(\sum_{i=0}^{t-1}\sum_{j=0}^{t-1}(\mathbf{I}-\mathbf{R})^{i}E_0[(A_n + \mathbf{B_n}'\mathbf{X_{t-i}} + \mathbf{u_{t-i}} - A_n - \mathbf{B_n}'E_0(\mathbf{X_{t-i}})) \\
&\quad (A_n - \mathbf{B_n}'\mathbf{X_{t-j}} + \mathbf{u_{t-i}} - A_n - \mathbf{B_n}'E_0(\mathbf{X_{t-j}}))']({\mathbf{I}-\mathbf{R}})^{j}\Big)\mathbf{R} \\
&= \mathbf{R}\Big(\sum_{i=0}^{t-1}\sum_{j=0}^{t-1}(\mathbf{I}-\mathbf{R})^{i}E_0[(\mathbf{B_n}'\mathbf{X_{t-i}} + \mathbf{u_{t-i}} - \mathbf{B_n}'E_0(\mathbf{X_{t-i}})) \\
&\quad (\mathbf{B_n}'\mathbf{X_{t-j}} + \mathbf{u_{t-i}} - \mathbf{B_n}'E_0(\mathbf{X_{t-j}}))']({\mathbf{I}-\mathbf{R}})^{j}\Big)\mathbf{R} \\
&= \mathbf{R}\Big(\sum_{i=0}^{t-1}\sum_{j=0}^{t-1}(\mathbf{I}-\mathbf{R})^{i}E_0[(\mathbf{B_n}'(\mathbf{X_{t-i}} - E_0(\mathbf{X_{t-i}})) + \mathbf{u_{t-i}}) \\
&\quad (\mathbf{B_n}'(\mathbf{X_{t-j}} - E_0(\mathbf{X_{t-j}}) + \mathbf{u_{t-j}})'({\mathbf{I}-\mathbf{R}})^{j}\Big)\mathbf{R} \\
&= \mathbf{R}\Big(\sum_{i=0}^{t-1}\sum_{j=0}^{t-1}(\mathbf{I}-\mathbf{R})^{i}(\mathbf{B_n}'E_0[(\mathbf{X_{t-i}} - E_0(\mathbf{X_{t-i}}))(\mathbf{X_{t-j}} - E_0(\mathbf{X_{t-j}}))']\mathbf{B_n}' + \\
&\quad E_0(\mathbf{u_{t-i}u_{t-j}}'))({\mathbf{I}-\mathbf{R}})^{j}\Big)\mathbf{R} \\
&= \mathbf{R}\Big(\sum_{i=0}^{t-1}\sum_{j=0}^{t-1}(\mathbf{I}-\mathbf{R})^{i}(\mathbf{B_n}'Cov_0[((\mathbf{X_{t-i}}, \mathbf{X_{t-j}}))]\mathbf{B_n} + \mathbf{U})({\mathbf{I}-\mathbf{R}})^{j}\Big)\mathbf{R} \\
&= \mathbf{R}\Big(\sum_{i=0}^{t-1}\sum_{j=0}^{t-1}(\mathbf{I}-\mathbf{R})^{i}(\mathbf{B_n}'E_0[((\mathbf{X_{t-i}}E_0(\mathbf{X_{t-j}}/E_0(\mathbf{X_{t-i}}))]\mathbf{B_n} + \mathbf{U})({\mathbf{I}-\mathbf{R}})^{j}\Big)\mathbf{R}
\end{aligned}
$$

$$
\begin{aligned}
&= \mathbf{R}\Bigg(\sum_{i=0}^{t-1}\sum_{j=0}^{t-1}(\mathbf{I}-\mathbf{R})^i(\mathbf{B_n'}(\boldsymbol{\mu}^{\boldsymbol{Q}}E_0(\mathbf{X_{t-i}})+\boldsymbol{\phi}^{\boldsymbol{Q}})V_0(\mathbf{X_{t-i}})\mathbf{B_n}+\mathbf{U})(\mathbf{I}-\mathbf{R})^j\Bigg)\mathbf{R}\\
&= \mathbf{R}\Bigg(\sum_{i=0}^{t-1}\sum_{j=0}^{t-1}(\mathbf{I}-\mathbf{R})^i(\mathbf{B_n'}(\boldsymbol{\mu}^{\boldsymbol{Q}}E_0(\mathbf{X_{t-i}})+\boldsymbol{\phi}^{\boldsymbol{Q}})V_0(\mathbf{X_{t-i}})\mathbf{B_n}+\mathbf{U})(\mathbf{I}-\mathbf{R})^j\Bigg)\mathbf{R}\\
&= \mathbf{R}\Bigg(\sum_{i=0}^{t-1}\sum_{j=0}^{t-1}(\mathbf{I}-\mathbf{R})^i(\mathbf{B_n'}(\boldsymbol{\mu}^{\boldsymbol{Q}}E_0(\mathbf{X_{t-i}})+\boldsymbol{\phi}^{\boldsymbol{Q}})V_0(\mathbf{X_{t-i}})\mathbf{B_n})(\mathbf{I}-\mathbf{R})^j\Bigg)\mathbf{R}\\
&\quad \mathbf{R}\Bigg(\sum_{i=0}^{t-1}\sum_{j=0}^{t-1}(\mathbf{I}-\mathbf{R})^i\mathbf{U}(\mathbf{I}-\mathbf{R})^j\Bigg)\mathbf{R}\\
&= \mathbf{R}\Bigg(\sum_{i=0}^{t-1}\sum_{j=0}^{t-1}(\mathbf{I}-\mathbf{R})^i(\mathbf{B_n'}(\boldsymbol{\mu}^{\boldsymbol{Q}}E_0(\mathbf{X_{t-i}})+\boldsymbol{\phi}^{\boldsymbol{Q}}V_0(\mathbf{X_{t-i}})\mathbf{B_n}')(\mathbf{I}-\mathbf{R})^j+\\
&\quad \frac{\mathbf{I}-(\mathbf{I}-\mathbf{R})^{\mathbf{2t}}}{\mathbf{I}-(\mathbf{I}-\mathbf{R})^{\mathbf{2}}}\Bigg)\mathbf{R}\\
&= \mathbf{R}\Bigg(\sum_{i=0}^{t-1}\sum_{j=0}^{t-1}(\mathbf{I}-\mathbf{R})^i(\mathbf{B_n'}(\boldsymbol{\mu}^{\boldsymbol{Q}}\mu_{\mathbf{0,X}}+\boldsymbol{\phi}^{\boldsymbol{Q}}{\sigma_{\mathbf{0,X}}}^2\mathbf{B_n}')(\mathbf{I}-\mathbf{R})^j+\\
&\quad \frac{\mathbf{I}-(\mathbf{I}-\mathbf{R})^{\mathbf{2t}}}{\mathbf{I}-(\mathbf{I}-\mathbf{R})^{\mathbf{2}}}\mathbf{U}\Bigg)\mathbf{R}\\
&= \mathbf{R}\Bigg(\sum_{i=0}^{t-1}\sum_{j=0}^{t-1}(\mathbf{I}-\mathbf{R})^i(\mathbf{B_n'}\boldsymbol{\mu}^{\boldsymbol{Q}}\mu_{\mathbf{0,X}}\mathbf{B_n})(\mathbf{I}-\mathbf{R})^j+\sum_{i=0}^{t-1}\sum_{j=0}^{t-1}(\mathbf{I}-\mathbf{R})^i(\mathbf{B_n'}\boldsymbol{\phi}^{\boldsymbol{Q}}\boldsymbol{\sigma}^{\mathbf{2}}_{\mathbf{0,X}}\mathbf{B_n})\\
&\quad (\mathbf{I}-\mathbf{R})^j+\frac{\mathbf{I}-(\mathbf{I}-\mathbf{R})^{\mathbf{2t}}}{\mathbf{I}-(\mathbf{I}-\mathbf{R})^{\mathbf{2}}}\mathbf{U}\Bigg)\mathbf{R}.
\end{aligned}
$$

where $\boldsymbol{\mu}_{\mathbf{0},\boldsymbol{X}} = E_0(\mathbf{X_t})$ and $\boldsymbol{\sigma}^{\mathbf{2}}_{\mathbf{0},\boldsymbol{X}} = V_0(\mathbf{X_t})$. According to Abramowitz et al. (1988)

$$\sum_{j=0}^{t-1}(\mathbf{I}-\mathbf{R})^i(\mathbf{B_n'}\boldsymbol{\mu}^{\boldsymbol{Q}}\mu_{\mathbf{0,X}}\mathbf{B_n})(\mathbf{I}-\mathbf{R})^j = \mathbf{B_n'}\boldsymbol{\mu}^{\boldsymbol{Q}}\mu_{\mathbf{0,X}}\mathbf{B_n}\frac{\mathbf{I}}{\mathbf{I}-(\mathbf{I}-\mathbf{R})^{\mathbf{2}}}.$$

and

$$\sum_{i=0}^{t-1}\sum_{j=0}^{t-1}(\mathbf{I}-\mathbf{R})^i(\mathbf{B_n'}\boldsymbol{\phi}^{\boldsymbol{Q}}\sigma^{\mathbf{2}}_{\mathbf{0,X}}\mathbf{B_n})(\mathbf{I}-\mathbf{R})^j = \mathbf{B_n'}\boldsymbol{\phi}^{\boldsymbol{Q}}{\sigma_{\mathbf{0,X}}}^2\mathbf{B_n})\frac{\mathbf{I}}{\mathbf{I}-(\mathbf{I}-\mathbf{R})^{\mathbf{2}}}.$$

Also, we have that

$$\lim_{t\to\infty} \frac{\mathbf{I}-(\mathbf{I}-\mathbf{R})^{\mathbf{2t}}}{\mathbf{I}-(\mathbf{I}-\mathbf{R})^{\mathbf{2}}} = \frac{\mathbf{I}}{\mathbf{I}-(\mathbf{I}-\mathbf{R})^{\mathbf{2}}}.$$

Then, the in-control covariance of the statistic is

$$\begin{aligned} Cov_0(\mathbf{Z_{t,n}}) &= \mathbf{R}\big(\mathbf{B_n^{'}}\boldsymbol{\mu}^{\boldsymbol{Q}}\mu_{\mathbf{0,X}}\mathbf{B_n}\frac{\mathbf{I}}{\mathbf{I}-(\mathbf{I}-\mathbf{R})^{\mathbf{2}}} + \mathbf{B_n}\boldsymbol{\phi}^{\boldsymbol{Q}}\sigma^{\mathbf{2}}_{\mathbf{0,X}}\mathbf{B_n})\frac{\mathbf{I}}{\mathbf{I}-(\mathbf{I}-\mathbf{R})^{\mathbf{2}}}\mathbf{U}\big)\mathbf{R} \\ &= \mathbf{R}\big(\mathbf{B_n^{'}}(\boldsymbol{\mu}^{\boldsymbol{Q}}\mu_{\mathbf{0,X}} + \boldsymbol{\phi}^{\boldsymbol{Q}}\sigma^{\mathbf{2}}_{\mathbf{0,X}})\mathbf{B_n} + \mathbf{U}\big)\frac{\mathbf{I}}{\mathbf{I}-(\mathbf{I}-\mathbf{R})^{\mathbf{2}}}\mathbf{R}. \end{aligned}$$

A.1.3 Covariance matrix for Residual control chart statistic

Control chart based on Mahalanobis distance
Suppose that $Cov_0(\mathbf{X_t}, \mathbf{u_t}) = \mathbf{0}$, $E(\mathbf{u_t}) = \mathbf{0}$, $E(\mathbf{u_t u_t})^{'} = \mathbf{U}$. Since the control statistic for the Residual chart based on the Mahalanobis distance is

$$Z_t = (1-\lambda)^t Z_0 + \lambda T_{d,t},\ t \geq 1,$$

with

$$T_{d,t} = \mathbf{d_t^{'}}\boldsymbol{\Sigma}^{\mathbf{-1}}_{\mathbf{d}}\mathbf{d_t}.$$

The in-control covariance matrix of the vector of the residuals is

$$\begin{aligned} Cov_0(\mathbf{d_t}) &= E_0[(\mathbf{d_t} - E_0(\mathbf{d_t}))(\mathbf{d_t} - E_0(\mathbf{d_t}))]^{'} \\ &= E_0[A_n + \mathbf{B_n^{'}X_t} + \mathbf{u_t} - A_n - \mathbf{B_n^{'}}E_0(\mathbf{X_t})][A_n + \mathbf{B_n^{'}X_t} + \mathbf{u_t} - A_n - \mathbf{B_n^{'}}E_0(\mathbf{X_t})]^{'} \\ &= E_0[\mathbf{B_n^{'}X_t} - \mathbf{B_n^{'}}E_0(\mathbf{X_t}) + \mathbf{u_t}][\mathbf{B_n^{'}X_t} - \mathbf{B_n^{'}}E_0(X_t) + \epsilon_t]^{'} \\ &= E_0[(\mathbf{B_n^{'}}(\mathbf{X_t} - \mathbf{X_{t-1}}) + \mathbf{u_t})(\mathbf{B_n^{'}}(\mathbf{X_t} - \mathbf{X_{t-1}}) + \mathbf{u_t})^{'}] \\ &= \mathbf{B_n^{'}}E_0[V_0(\mathbf{X_t} - \mathbf{X_{t-1}})]\mathbf{B_n} + E_0(\mathbf{u_t u_t^{'}}) \\ &= \mathbf{B_n^{'}}E_0[V_0(\mathbf{X_t}/\mathbf{X_{t-1}})]\mathbf{B_n} + \mathbf{U} \\ &= \mathbf{B_n^{'}}(\boldsymbol{\phi}^{Q}V_0(\mathbf{X_{t-1}})\boldsymbol{\phi}^{Q'} + \boldsymbol{\Sigma_t})\mathbf{B_n} + \mathbf{U}. \end{aligned}$$

Control chart based on MEWMA statistic
Suppose that $Cov_0(\mathbf{X_t}, \mathbf{u_t}) = \mathbf{0}$, $Cov_0(\mathbf{u_t}, \mathbf{X_t}) = \mathbf{0}$, $E(\mathbf{d_t}) = \mathbf{0}$, $E(\mathbf{u_t}) = \mathbf{0}$, $E(\mathbf{u_t u_t})^{'} = \mathbf{U}$, then the covariance matrix of the statistic $\mathbf{Z_t}$ is

$$Cov_0(\mathbf{Z_t}) = Cov_0\left((\mathbf{I}-\mathbf{R})^{\mathbf{t}}\mathbf{Z_0} + \mathbf{R}\sum_{j=0}^{t-1}(\mathbf{I}-\mathbf{R})^{\mathbf{j}}\mathbf{d_{t-j}}\right)$$

$$
\begin{aligned}
&= \mathbf{R}\Bigg(\sum_{i=0}^{t-1}\sum_{j=0}^{t-1}(\mathbf{I}-\mathbf{R})^{\mathbf{i}}Cov_0(\mathbf{d_{t-i}},\mathbf{d_{t-j}})(\mathbf{I}-\mathbf{R})^{\mathbf{j}}\Bigg)\mathbf{R}\\
&= \mathbf{R}\Bigg(\sum_{i=0}^{t-1}\sum_{j=0}^{t-1}(\mathbf{I}-\mathbf{R})^{\mathbf{i}}E_0(\mathbf{d_{t-i}}\mathbf{d}'_{\mathbf{t-j}})(\mathbf{I}-\mathbf{R})^{\mathbf{j}}\Bigg)\mathbf{R}\\
&= \mathbf{R}\Bigg(\sum_{i=0}^{t-1}\sum_{j=0}^{t-1}(\mathbf{I}-\mathbf{R})^{\mathbf{i}}(\mathbf{B}'_{\mathbf{n}}((\boldsymbol{\phi}^{\boldsymbol{Q}})^2V_0(\mathbf{X_{t-1}})+\boldsymbol{\Sigma}_{\mathbf{t}})\mathbf{B_n}+\mathbf{U})(\mathbf{I}-\mathbf{R})^{j}\Bigg)\mathbf{R}\\
&= \mathbf{R}\Bigg(\sum_{i=0}^{t-1}\sum_{j=0}^{t-1}(\mathbf{I}-\mathbf{R})^{i}(\mathbf{B}'_{\mathbf{n}}((\boldsymbol{\phi}^{\boldsymbol{Q}})^2V_0(\mathbf{X_{t-1}})+\boldsymbol{\Sigma}_{\mathbf{t}})\mathbf{B_n})(\mathbf{I}-\mathbf{R})^{j}+\\
&\sum_{i=0}^{t-1}\sum_{j=0}^{t-1}(\mathbf{I}-\mathbf{R})^{i}\mathbf{B}'_{\mathbf{n}}\mathbf{U}\mathbf{B}'_{\mathbf{n}}(\mathbf{I}-\mathbf{R})^{j}\Bigg)\mathbf{R}.
\end{aligned}
$$

According to Abramowitz et al. (1988) we have that

$$
\sum_{j=0}^{t-1}(\mathbf{I}-\mathbf{R})^{i}(\mathbf{B}'_{\mathbf{n}}(\boldsymbol{\phi}^{\boldsymbol{Q}})^2V_0(\mathbf{X_{t-1}})+\boldsymbol{\Sigma}_{\mathbf{t}})\mathbf{B_n})(\mathbf{I}-\mathbf{R})^{j}=\mathbf{B}'_{\mathbf{n}}\boldsymbol{\Sigma}_{\mathbf{Y}}\mathbf{B_n}\frac{\mathbf{I}}{\mathbf{I}-(\mathbf{I}-\mathbf{R})^{\mathbf{2}}}.
$$

Also

$$
\lim_{t\to\infty}\frac{\mathbf{I}-(\mathbf{I}-\mathbf{R})^{\mathbf{2t}}}{\mathbf{I}-(\mathbf{I}-\mathbf{R})^{\mathbf{2}}}=\frac{\mathbf{I}}{\mathbf{I}-(\mathbf{I}-\mathbf{R})^{\mathbf{2}}}.
$$

Then the covariance matrix has the following form

$$
\begin{aligned}
Cov_0(\mathbf{Z_t}) &= \mathbf{R}\big(\mathbf{B}'_{\mathbf{n}}(\boldsymbol{\phi}^{\boldsymbol{Q}})^2V_0(\mathbf{X_{t-1}})+\boldsymbol{\Sigma}_{\mathbf{t}})\mathbf{B_n}\frac{\mathbf{I}}{\mathbf{I}-(\mathbf{I}-\mathbf{R})^{\mathbf{2}}}+\frac{\mathbf{I}}{\mathbf{I}-(\mathbf{I}-\mathbf{R})^{\mathbf{2}}}\mathbf{U}\big)\mathbf{R}\\
&= \mathbf{R}\big(\mathbf{B}'_{\mathbf{n}}\boldsymbol{\Sigma}_{\mathbf{Y}}\mathbf{B_n}+\mathbf{U}\big)\frac{\mathbf{I}}{\mathbf{I}-(\mathbf{I}-\mathbf{R})^{\mathbf{2}}}\mathbf{R}.
\end{aligned}
$$

A.1.4 Moments for MMOEWMA control chart statistic

Expected value for the control statistic
The statistic for the modified MEWMA (MMOEWMA) control chart based on the multivariate EWMA recursion is

$$
\mathbf{Z_t}=(\mathbf{I}-\mathbf{R})^{t}\mathbf{Z_0}+\mathbf{R}\sum_{j=0}^{t-1}(\mathbf{I}-\mathbf{R})^{j}\mathbf{Y_{t-j}}+\sum_{j=0}^{t-1}(\mathbf{I}-\mathbf{R})^{j}(\mathbf{Y_{t-j}}-\mathbf{Y_{t-j-1}}).
$$

The expected value of the control statistic is

$$
\begin{aligned}
E_0(\mathbf{Z}_t) &= E_0((\mathbf{I}-\mathbf{R})^t\mathbf{Z_0} + \mathbf{R}\sum_{j=0}^{t-1}(\mathbf{I}-\mathbf{R})^j\mathbf{Y_t} + \sum_{j=0}^{t-1}(\mathbf{I}-\mathbf{R})^j(\mathbf{Y_{t-j}} - \mathbf{Y_{t-j-1}}) \\
&= (\mathbf{I}-\mathbf{R})^t\mathbf{Z_0} + \mathbf{R}\sum_{j=0}^{t-1}(\mathbf{I}-\mathbf{R})^j E_0(\mathbf{Y_t} + \sum_{j=0}^{t-1}(\mathbf{I}-\mathbf{R})^j E_0(\mathbf{Y_{t-j}} - \mathbf{Y_{t-j-1}}) \\
&= (\mathbf{I}-\mathbf{R})^t\mathbf{Z_0} + \mathbf{R}\sum_{j=0}^{t-1}(\mathbf{I}-\mathbf{R})^j(A_n + \mathbf{B_n'}(\mathbf{X_{t-j}}) + \sum_{j=0}^{t-1}(\mathbf{I}-\mathbf{R})^j E_0(\mathbf{Y_{t-j}} - \mathbf{Y_{t-j-1}}) \\
&= (\mathbf{I}-\mathbf{R})^t\mathbf{Z_0} + A_n + \mathbf{R}\mathbf{B_n'}\sum_{j=0}^{t-1}(\mathbf{I}-\mathbf{R})^j E_0(\mathbf{X_{t-j}}) \\
&= (\mathbf{I}-\mathbf{R})^t\mathbf{Z_0} + A_n + \mathbf{R}\mathbf{B_n'}\sum_{j=0}^{t-1}(\mathbf{I}-\mathbf{R})^j \boldsymbol{\mu_{0,X}} \\
&= (\mathbf{I}-\mathbf{R})^t\mathbf{Z_0} + A_n + \mathbf{R}\mathbf{B_n'}\frac{(\mathbf{I}-(\mathbf{I}-\mathbf{R})^{\mathbf{t}}}{(\mathbf{I}-(\mathbf{I}-\mathbf{R})}\boldsymbol{\mu_{0,X}} \\
&= (\mathbf{I}-\mathbf{R})^{\mathbf{t}}\mathbf{Z_0} + A_n + \mathbf{B_n'}(\mathbf{I}-(\mathbf{I}-\mathbf{R})^{\mathbf{t}}\boldsymbol{\mu_{0,X}}.
\end{aligned}
$$

Covariance matrix for the control statistic

Suppose that $Cov_0(\mathbf{X_t}, \mathbf{u_t}) = \mathbf{0}$, $E(\mathbf{u_t}) = \mathbf{0}$, $E(\mathbf{u_t u_t})' = \mathbf{U}$, then the in-control covariance matrix is

$$
\begin{aligned}
Cov_0(\mathbf{Z_t}) &= Cov_0\Big((\mathbf{I}-\mathbf{R})^t\mathbf{Z_0} + \mathbf{R}\sum_{j=0}^{t-1}(\mathbf{I}-\mathbf{R})^j\mathbf{Y_{t-j}} + \sum_{j=0}^{t-1}(\mathbf{I}-\mathbf{R})^j(\mathbf{Y_{t-j}} - \mathbf{Y_{t-j-1}})\Big) \\
&= Cov_0\Big(\mathbf{R}\sum_{j=0}^{t-1}(I-R)^j\mathbf{Y_{t-j}}\Big) + Cov_0\Big(\sum_{j=0}^{t-1}(I-R)^j(\mathbf{Y_{t-j}} - \mathbf{Y_{t-j-1}})\Big) + \\
&\quad Cov_0\Big(\mathbf{R}\sum_{j=0}^{t-1}(\mathbf{I}-\mathbf{R})^j\mathbf{Y_{t-j}}, \sum_{j=0}^{t-1}(\mathbf{I}-\mathbf{R})^j(\mathbf{Y_{t-j}} - \mathbf{Y_{t-j-1}})\Big) \\
&= \mathbf{R}\big(\mathbf{B_n'}\boldsymbol{\Sigma_Y}\mathbf{B_n} + \mathbf{U}\big)\frac{\mathbf{I}}{\mathbf{I}-(\mathbf{I}-\mathbf{R})^{\mathbf{2}}}\mathbf{R} + \sum_{j=0}^{t-1}(\mathbf{I}-\mathbf{R})^j Cov_0(R\mathbf{Y_{t-j}}, \mathbf{Y_{t-j}} - \mathbf{Y_{t-j-1}})(\mathbf{I}-\mathbf{R})^j \\
&= \mathbf{R}\big(\mathbf{B_n'}\boldsymbol{\Sigma_Y}\mathbf{B_n} + \mathbf{U}\big)\frac{\mathbf{I}}{\mathbf{I}-(\mathbf{I}-\mathbf{R})^{\mathbf{2}}}\mathbf{R} + \sum_{j=0}^{t-1}(\mathbf{I}-\mathbf{R})^j(\mathbf{R}Var_0(\mathbf{Y_{t-j}})R)(\mathbf{I}-\mathbf{R})^j
\end{aligned}
$$

$$= \mathbf{R}\big(\mathbf{B_n^{'}\Sigma_Y B_n^{+}U}\big)\frac{\mathbf{I}}{\mathbf{I-(I-R)^2}}\mathbf{R} + \mathbf{R}\big(\sum_{j=0}^{t-1}(\mathbf{I-R})^j Var_0(\mathbf{Y_{t-j}})(\mathbf{I-R})^j\big)\mathbf{R}.$$

It can be proved that

$$\sum_{j=0}^{t-1}(\mathbf{I-R})^j Var_0(\mathbf{Y_{t-j}})(\mathbf{I-R})^j = \frac{\mathbf{I-(I-R)^{2t}}}{\mathbf{I-(I-R)^2}}\mathbf{\Sigma_Y}.$$

Also, we have that

$$\lim_{t\to\infty}\frac{\mathbf{I-(I-R)^{2t}}}{\mathbf{I-(I-R)^2}} = \frac{\mathbf{I}}{\mathbf{I-(I-R)^2}}.$$

Then, the covariance matrix is given as

$$\begin{aligned} Cov_0(\mathbf{Z_t}) &= \mathbf{R}\big(\mathbf{B_n^{'}\Sigma_Y B_n + U}\big)\frac{\mathbf{I}}{\mathbf{I-(I-R)^2}}\big)\mathbf{R} + \mathbf{R}\frac{\mathbf{I}}{\mathbf{I-(I-R)^2}}\mathbf{\Sigma_Y R} \\ &= \mathbf{R}\big(\big(\mathbf{B_n^{'}\Sigma_Y B_n + U}\big)\frac{\mathbf{I}}{\mathbf{I-(I-R)}}^{\mathbf{2}}\big)\mathbf{R} + \mathbf{R}\frac{\mathbf{I}}{\mathbf{I+R}}\mathbf{\Sigma_Y}. \end{aligned}$$

A.2 Moments of bond yields

Suppose that the yield of a n-period zero coupon bond is given by

$$Y_t^n = A_n + \boldsymbol{B}_n^{'}\boldsymbol{X}_t + \boldsymbol{\epsilon}_t, \boldsymbol{\epsilon}_t \sim N(\mathbf{0}, \boldsymbol{\Sigma}_Y).$$

The expected value is

$$E_{t-1}[Y_t] = A_n + \boldsymbol{B}_n^{'}E_{t-1}[\boldsymbol{X}_t] = A_n + \boldsymbol{B}_n^{'}\boldsymbol{X}_{t|t-1},$$

where $\boldsymbol{X}_{t|t-1}$ is the one-step-ahead predictions of the state factors.
The conditional covariance matrix of bond yields is given by

$$\begin{aligned} \Sigma_{Y_t} &= E_{t-1}[Y_t - E_{t-1}(Y_t)][Y_t - E_{t-1}(Y_t)] \\ &= E_{t-1}[A_n + \boldsymbol{B}_n^{'}\boldsymbol{X}_t + \boldsymbol{\epsilon}_t - A_n - \boldsymbol{B}_n^{'}E_{t-1}(\boldsymbol{X}_t)][A_n + \boldsymbol{B}_n^{'}\boldsymbol{X}_t + \boldsymbol{\epsilon}_t - A_n - \boldsymbol{B}_n^{'}E_{t-1}(\boldsymbol{X}_t)]^{'} \\ &= E_{t-1}[\boldsymbol{B}_n^{'}\boldsymbol{X}_t - \boldsymbol{B}_n^{'}E_{t-1}(\boldsymbol{X}_t) + \boldsymbol{\epsilon}_t][\boldsymbol{B}_n^{'}\boldsymbol{X}_t - \boldsymbol{B}_n^{'}E_{t-1}(\boldsymbol{X}_t) + \boldsymbol{\epsilon}_t]^{'} \\ &= E_{t-1}[\boldsymbol{B}_n^{'}\boldsymbol{X}_t - \boldsymbol{B}_n^{'}(\boldsymbol{\mu} + \boldsymbol{\rho}\boldsymbol{X}_{t-1})][\boldsymbol{B}_n^{'}\boldsymbol{X}_t - \boldsymbol{B}_n^{'}(\boldsymbol{\mu} + \boldsymbol{\rho}\boldsymbol{X}_{t-1})]^{'} \end{aligned}$$

$$
\begin{aligned}
&= E_{t-1}[(\boldsymbol{B}_n^{'}(\boldsymbol{X}_t - \boldsymbol{\mu} - \boldsymbol{\rho}\boldsymbol{X}_{t-1}) + \boldsymbol{\epsilon}_t)(\boldsymbol{B}_n^{'}(\boldsymbol{X}_t - \boldsymbol{\mu} - \boldsymbol{\rho}\boldsymbol{X}_{t-1}) + \boldsymbol{\epsilon}_t)^{'}] \\
&= E_{t-1}[(\boldsymbol{B}_n^{'}(\boldsymbol{\mu} + \boldsymbol{\rho}\boldsymbol{X}_{t-1} + \boldsymbol{u}_t - \boldsymbol{\mu} - \boldsymbol{\rho}\boldsymbol{X}_{t-1})(\boldsymbol{B}_n^{'}(\boldsymbol{\mu} + \boldsymbol{\rho}\boldsymbol{X}_{t-1} + \boldsymbol{u}_t - \boldsymbol{\mu} - \boldsymbol{\rho}\boldsymbol{X}_{t-1})^{'}] \\
&= E_{t-1}[(\boldsymbol{B}_n^{'}\boldsymbol{u}_t + \boldsymbol{\epsilon}_t)(\boldsymbol{B}_n^{'}\boldsymbol{u}_t + \boldsymbol{\epsilon}_t)^{'}] \\
&= E_{t-1}[\boldsymbol{B}_n^{'}\boldsymbol{u}_t\boldsymbol{u}_t^{'}\boldsymbol{B}_n + \boldsymbol{\epsilon}_t\boldsymbol{\epsilon}_t^{'}] \\
&= \boldsymbol{B}_n^{'}E_{t-1}[\boldsymbol{u}_t\boldsymbol{u}_t^{'}]\boldsymbol{B}_n + E_{t-1}[\boldsymbol{\epsilon}_t\boldsymbol{\epsilon}_t^{'}].
\end{aligned}
$$

A.3 VARMA ATSM-Moments for control chart procedures

A.3.1 Modified EWMA control charts

EWMA chart based on the Mahalanobis distance

Suppose that $E(\epsilon_\mathbf{t}) = \mathbf{0}$ for all $t \geq 1$ and under that the underlying process in weak stationary we have that $E(\boldsymbol{X}_t) = E(\boldsymbol{X}_{t-1})$ and $V(\boldsymbol{X}_t) = V(\boldsymbol{X}_{t-1})$. The in-control expected value for the state evolution process is

$$
\begin{aligned}
E_0(\mathbf{X}_t^n) &= E_0(\boldsymbol{\Phi_1}\boldsymbol{X_{t-1}} + \boldsymbol{\epsilon_t} - \boldsymbol{\Theta_1}\boldsymbol{\epsilon_{t-1}}) \\
&= \boldsymbol{\Phi}_1 E_0(\boldsymbol{X_{t-1}}) + E_0(\boldsymbol{\epsilon_t}) - \boldsymbol{\Theta}_1 E_0(\boldsymbol{\epsilon_{t-1}}) \\
&= \boldsymbol{\Phi}_1 E_0(\mathbf{X_t}).
\end{aligned}
$$

If we assume that $Cov_0(\boldsymbol{X}_t, \epsilon_\mathbf{t}) = \mathbf{0}$, $E(\epsilon_\mathbf{t}) = \mathbf{0}$, $E(\epsilon_\mathbf{t}\epsilon_\mathbf{t})^{'} = \mathbf{U}$, then the covariance matrix of the vector of the state evolution process is

$$
\begin{aligned}
Cov_0(\mathbf{X_t}) &= E_0[(\boldsymbol{\Phi_1}\boldsymbol{X_{t-1}} + \boldsymbol{\epsilon_t} - \boldsymbol{\Theta_1}\boldsymbol{\epsilon_{t-1}})][(\boldsymbol{\Phi_1}\boldsymbol{X_{t-1}} + \boldsymbol{\epsilon_t} - \boldsymbol{\Theta_1}\boldsymbol{\epsilon_{t-1}})]^{'} \\
&= E_0[(\boldsymbol{\Phi_1}\boldsymbol{X_{t-1}} + \boldsymbol{\epsilon_t} - \boldsymbol{\Theta_1}\boldsymbol{\epsilon_{t-1}})][\boldsymbol{X}_{t-1}^{\prime}\boldsymbol{\Phi}_1^{\prime} + \boldsymbol{\epsilon}_t^{\prime} - \boldsymbol{\epsilon}_{t-1}^{\prime}\boldsymbol{\Theta}_1^{\prime}] \\
&= E_0[\boldsymbol{\Phi_1}\boldsymbol{X_{t-1}}\boldsymbol{X}_{t-1}^{\prime}\boldsymbol{\Phi}_1^{\prime} + \boldsymbol{\Phi_1}\boldsymbol{X_{t-1}}\boldsymbol{\epsilon}_t^{\prime} - \boldsymbol{\Phi_1}\boldsymbol{X_{t-1}}\boldsymbol{\epsilon}_{t-1}^{\prime}\boldsymbol{\Theta}_1^{\prime} \\
&+ \boldsymbol{\epsilon_t}\boldsymbol{X}_{t-1}^{\prime}\boldsymbol{\phi}^{\prime} + \boldsymbol{\epsilon_t}\boldsymbol{\epsilon}_t^{'} - \boldsymbol{\epsilon_t}\boldsymbol{\epsilon}_{t-1}^{\prime}\boldsymbol{\theta}^{\prime} - \boldsymbol{\theta}\boldsymbol{\epsilon_{t-1}}\boldsymbol{X}_{t-1}^{\prime}\boldsymbol{\phi}^{\prime} - \boldsymbol{\theta}\boldsymbol{\epsilon_{t-1}}\boldsymbol{\epsilon}_t^{\prime} + \boldsymbol{\theta}\boldsymbol{\epsilon_{t-1}}\boldsymbol{\epsilon}_{t-1}^{'}\boldsymbol{\theta}^{'}] \\
&= E_0[\boldsymbol{\phi}\boldsymbol{X_{t-1}}\boldsymbol{X}_{t-1}^{\prime}\boldsymbol{\phi}^{\prime}] + E_0[\boldsymbol{\epsilon_t}\boldsymbol{\epsilon}_t^{'}] + E_0[\boldsymbol{\theta}\boldsymbol{\epsilon_{t-1}}\boldsymbol{\epsilon}_{t-1}^{'}\boldsymbol{\theta}^{'}] \\
&= \boldsymbol{\phi}V_0(\boldsymbol{X_{t-1}})\boldsymbol{\phi}^{'} + \boldsymbol{\Sigma_\epsilon} + \boldsymbol{\theta}\boldsymbol{\Sigma_\epsilon}\boldsymbol{\theta}^{'}.
\end{aligned}
$$

Chart Based on the Multivariate EWMA Statistic:

The control statistic for the modified control chart based on the multivariate EWMA recursion is

$$
Z_t = (\mathbf{I} - \mathbf{R})^{\mathbf{t}}\mathbf{Z_0} + \mathbf{R}\sum_{j=0}^{t-1}(\mathbf{I} - \mathbf{R})^{\mathbf{j}}\mathbf{X_{t-j}}.
$$

The expected value of the control statistic is

$$\begin{aligned}
E_0(\mathbf{Z}_t) &= E_0((\mathbf{I}-\mathbf{R})^{\mathbf{t}}\mathbf{Z_0} + \mathbf{R}\sum_{j=0}^{t-1}(\mathbf{I}-\mathbf{R})^{\mathbf{j}}\mathbf{X_{t-j}}) \\
&= (\mathbf{I}-\mathbf{R})^{\mathbf{t}}\mathbf{Z_0} + \mathbf{R}\sum_{j=0}^{t-1}(\mathbf{I}-\mathbf{R})^{\mathbf{j}}E_0(\mathbf{X_{t-j}}) \\
&= (\mathbf{I}-\mathbf{R})^{\mathbf{t}}\mathbf{Z_0} + \mathbf{R}\sum_{j=0}^{t-1}(\mathbf{I}-\mathbf{R})^{\mathbf{j}}E_0(\mathbf{X_t}) \\
&= (\mathbf{I}-\mathbf{R})^{\mathbf{t}}\mathbf{Z_0} + \mathbf{R}\sum_{j=0}^{t-1}(\mathbf{I}-\mathbf{R})^{\mathbf{j}}\boldsymbol{\mu_{0,X}} \\
&= (\mathbf{I}-\mathbf{R})^{\mathbf{t}}\mathbf{Z_0} + \mathbf{R}\frac{(\mathbf{I}-(\mathbf{I}-\mathbf{R})^{\mathbf{t}}}{(\mathbf{I}-(\mathbf{I}-\mathbf{R})}\boldsymbol{\mu_{0,X}} \\
&= (\mathbf{I}-\mathbf{R})^{\mathbf{t}}\mathbf{Z_0} + (\mathbf{I}-(\mathbf{I}-\mathbf{R})^{\mathbf{t}}\boldsymbol{\mu_{0,X}}.
\end{aligned}$$

where $\boldsymbol{\mu_{0,X}} = E_0(\mathbf{X_t})$.

Covariance matrix for the Modified MEWMA statistic

Suppose that $Cov_0(\boldsymbol{X}_t, \boldsymbol{\epsilon}_t) = 0,\ E(\boldsymbol{\epsilon}_t) = 0,\ E(\boldsymbol{\epsilon}_t\boldsymbol{\epsilon}_t)' = U$ and $E(\boldsymbol{\epsilon}_t\boldsymbol{\epsilon}_s)' = \mathbf{0}\ t \neq s$, then we have

$$\begin{aligned}
Cov_0(\mathbf{Z_t}) &= Cov_0((\mathbf{I}-\mathbf{R})^{\mathbf{t}}\mathbf{Z_0} + \mathbf{R}\sum_{j=0}^{t-1}(\mathbf{I}-\mathbf{R})^{\mathbf{j}}\mathbf{X_{t-j}}) \\
&= \mathbf{R}\Big(\sum_{i=0}^{t-1}\sum_{j=0}^{t-1}(\mathbf{I}-\mathbf{R})^{\mathbf{i}}Cov_0(\mathbf{X_{t-i}X_{t-j}})(\mathbf{I}-\mathbf{R})^{\mathbf{j}}\Big)\mathbf{R} \\
&= \mathbf{R}\Big(\sum_{i=0}^{t-1}\sum_{j=0}^{t-1}(\mathbf{I}-\mathbf{R})^{i}E_0[(\mathbf{X_{t-i}} - E_0(\mathbf{X_{t-i}}))(\mathbf{X_{t-j}} - E_0(\mathbf{X_{t-j}}))']({\mathbf{I}-\mathbf{R}})^{j}\Big)\mathbf{R} \\
&= \mathbf{R}\Big(\sum_{i=0}^{t-1}\sum_{j=0}^{t-1}(\mathbf{I}-\mathbf{R})^{i}E_0[(\boldsymbol{\Phi}_1\mathbf{X_{t-i-1}} + \boldsymbol{\epsilon_{t-i}} - \boldsymbol{\Theta}_1\boldsymbol{\epsilon_{t-i-1}} - E_0(\mathbf{X_{t-i}})) \\
&\quad (\boldsymbol{\Phi}_1\mathbf{X_{t-j-1}} + \boldsymbol{\epsilon_{t-j}} - \boldsymbol{\Theta}_1\boldsymbol{\epsilon_{t-j-1}} - E_0(\mathbf{X_{t-j}})')]({\mathbf{I}-\mathbf{R}})^{j}\Big)\mathbf{R} \\
&= \mathbf{R}\Big(\sum_{i=0}^{t-1}\sum_{j=0}^{t-1}(\mathbf{I}-\mathbf{R})^{i}E_0[(\boldsymbol{\Phi}_1\mathbf{X_{t-i-1}} + \boldsymbol{\epsilon_{t-i}} - \boldsymbol{\Theta}_1\boldsymbol{\epsilon_{t-i-1}} - \boldsymbol{m}_{t-i,0})
\end{aligned}$$

$$
\begin{aligned}
&(\mathbf{\Phi_1 X_{t-j-1}} + \boldsymbol{\epsilon_{t-j}} - \mathbf{\Theta_1}\boldsymbol{\epsilon_{t-j-1}} - -m_{t-j,0})^{'}](\mathbf{I}-\mathbf{R})^{j}\Big)\mathbf{R} \\
&= \mathbf{R}\Bigg(\sum_{i=0}^{t-1}\sum_{j=0}^{t-1}(\mathbf{I}-\mathbf{R})^{i}E_0[(\mathbf{\Phi_1 X_{t-i-1}} + \boldsymbol{\epsilon_{t-i}} - \mathbf{\Theta_1}\boldsymbol{\epsilon_{t-i-1}} - \boldsymbol{m}_{t-i,0}) \\
&(\mathbf{X}^{'}_{\mathbf{t-j-1}}\mathbf{\Phi}^{'}_{\mathbf{1}} + \boldsymbol{\epsilon}^{'}_{\boldsymbol{t-j}} - \boldsymbol{\epsilon}^{'}_{\boldsymbol{t-j-1}}\mathbf{\Theta}^{'}_{1} - -m^{'}_{t-j,0})](\mathbf{I}-\mathbf{R})^{j}\Bigg)\mathbf{R} \\
&= \mathbf{R}\Bigg(\sum_{i=0}^{t-1}\sum_{j=0}^{t-1}(\mathbf{I}-\mathbf{R})^{i}E_0[(\mathbf{\Phi_1 X_{t-i-1}X_{t-j-1}}^{'}\mathbf{\Phi}^{'}_{\mathbf{1}} + \boldsymbol{\epsilon_{t-i}}\boldsymbol{\epsilon}^{'}_{\boldsymbol{t-j}} + \mathbf{\Phi_1 X_{t-i-1}X_{t-j-1}}^{'}\mathbf{\Phi}^{'}_{\mathbf{1}} \\
&+ \mathbf{\Theta_1}\boldsymbol{\epsilon_{t-i}}\boldsymbol{\epsilon}^{'}_{\boldsymbol{t-j-1}}\mathbf{\Theta}^{'}_{1}](\mathbf{I}-\mathbf{R})^{j}\Bigg)\mathbf{R} \\
&= \mathbf{R}\Bigg(\sum_{i=0}^{t-1}\sum_{j=0}^{t-1}(\mathbf{I}-\mathbf{R})^{i}(\mathbf{\Phi}_1 E_0(\mathbf{X_{t-i-1}X_{t-j-1}}^{'})\mathbf{\Phi}^{'}_{\mathbf{1}} + E_0(\boldsymbol{\epsilon_{t-i}}\boldsymbol{\epsilon}^{'}_{\boldsymbol{t-j}}) + \mathbf{\Phi_1}E_0(\mathbf{X_{t-i-1}X_{t-j-1}}^{'})\mathbf{\Phi}^{'}_{\mathbf{1}} \\
&+ \mathbf{\Theta_1}E_0(\boldsymbol{\epsilon_{t-i}}\boldsymbol{\epsilon}^{'}_{\boldsymbol{t-j-1}})\mathbf{\Theta}^{'}_{1}](\mathbf{I}-\mathbf{R})^{j}\Bigg)\mathbf{R} \\
&= \mathbf{R}\Bigg(\sum_{i=0}^{t-1}\sum_{j=0}^{t-1}(\mathbf{I}-\mathbf{R})^{i}(\mathbf{\Phi}_1 Cov_0(\mathbf{X_{t-i-1}X_{t-j-1}}^{'})\mathbf{\Phi}^{'}_{\mathbf{1}} + \Sigma_0(\boldsymbol{\epsilon_t}) + \mathbf{\Phi}_1 Cov_0(\mathbf{X_{t-i-1}X_{t-j-1}}^{'}) \\
&\mathbf{\Phi}^{'}_{\mathbf{1}} + \mathbf{\Theta}_1\Sigma_0(\boldsymbol{\epsilon_t})\mathbf{\Theta}^{'}_{1}](\mathbf{I}-\mathbf{R})^{j}\Bigg)\mathbf{R} \\
&= \mathbf{R}\Bigg(2 * \mathbf{\Phi}_1 Cov_0(\mathbf{X_{t-i-1}X_{t-j-1}}^{'})\mathbf{\Phi}^{'}_{\mathbf{1}} + \Sigma_0(\boldsymbol{\epsilon_t}) + 2 * \mathbf{\Theta}_1\Sigma_0(\boldsymbol{\epsilon_t})\mathbf{\Theta}^{'}_{1}\Bigg)\frac{\boldsymbol{I}}{\boldsymbol{I}-(\boldsymbol{I}-\boldsymbol{R})^2}\mathbf{R}.
\end{aligned}
$$

where

$$
\begin{aligned}
Cov_0(m_{t-i}m^{'}_{t-j}) &= E_0([\mathbf{\Phi_1 X_{t-i}} - \mathbf{\Theta_1}\boldsymbol{\epsilon_{t-i}}][\mathbf{\Phi_1 X_{t-j}} - \mathbf{\Theta_1}\boldsymbol{\epsilon_{t-j}}]^{'}) \\
&= E_0([\mathbf{\Phi_1 X_{t-i}} - \mathbf{\Theta_1}\boldsymbol{\epsilon_{t-i}}][\mathbf{X_{t-j}}^{'}\mathbf{\Phi}^{'}_{1} - \boldsymbol{\epsilon}^{'}_{\boldsymbol{t-j}}\mathbf{\Theta}^{'}_{1}]) \\
&= \mathbf{\Phi}_1 E_0([\mathbf{X_{t-i}X_{t-j}}^{'}]\mathbf{\Phi}^{'}_{1} + \mathbf{\Theta}_1 E_0[\boldsymbol{\epsilon_{t-i}}\boldsymbol{\epsilon}^{'}_{\boldsymbol{t-j}}]\mathbf{\Theta}^{'}_{1}.
\end{aligned}
$$

Also, $\boldsymbol{\mu_{0,X}} = E_0(\mathbf{X_t})$ and $\boldsymbol{\sigma^2_{0,X}} = V_0(\mathbf{X_t})$. According to Abramowitz et al. 1988

$$
\sum_{i=0}^{t-1}\sum_{j=0}^{t-1}(\mathbf{I}-\mathbf{R})^{i}(\mathbf{I}-\mathbf{R})^{j} = \frac{\mathbf{I}-(\mathbf{I}-\mathbf{R})^{\mathbf{2t}}}{\mathbf{I}-(\mathbf{I}-\mathbf{R})^{\mathbf{2}}}.
$$

Also, we have that

$$\lim_{t\to\infty} \frac{\mathbf{I}-(\mathbf{I}-\mathbf{R})^{\mathbf{2t}}}{\mathbf{I}-(\mathbf{I}-\mathbf{R})^{\mathbf{2}}} = \frac{\mathbf{I}}{\mathbf{I}-(\mathbf{I}-\mathbf{R})^{\mathbf{2}}}.$$

A.3.2 Residual-based control charts

EWMA Residual Chart Based on the Mahalanobis Distance
Suppose that $Cov_0(\mathbf{X_t}, \epsilon_\mathbf{t}) = \mathbf{0},\ E(\epsilon_\mathbf{t}) = \mathbf{0},\ E(\epsilon_\mathbf{t}\epsilon_\mathbf{t}^{'}) = \mathbf{U}, E(\epsilon_\mathbf{t}\epsilon_\mathbf{s}^{'}) = \mathbf{0}, t \neq s$. Since the control statistic for the Residual chart based on the Mahalanobis distance is

$$Z_t = (1-\lambda)^t Z_0 + \lambda T_{d,t},\ t \geq 1,$$

with

$$T_{d,t} = \mathbf{d_t^{'}\Sigma_d^{-1}d_t}.$$

The in-control covariance matrix of the vector of the residuals is

$$\begin{aligned} Cov_0(\mathbf{d_t}) &= E_0[(\mathbf{d_t} - E_0(\mathbf{d_t}))(\mathbf{d_t} - E_0(\mathbf{d_t}))]^{'} \\ &= E_0[(\mathbf{X_t} - E_0(\mathbf{X_t}/\mathbf{X_{T-1}}))(\mathbf{X_t} - E_0(\mathbf{X_t}/\mathbf{X_{T-1}}))]^{'} \\ &= V_0(\mathbf{X_t}/\mathbf{X_{T-1}}) \\ &= V_0(\mathbf{\Phi}_1\mathbf{X_{T-1}} + \boldsymbol{\epsilon}_t - \mathbf{\Theta}_1\boldsymbol{\epsilon}_{t-1}) \\ &= \boldsymbol{\phi} V_0(\mathbf{X_{T-1}})\mathbf{\Phi}_1^{'} + \mathbf{\Sigma}_\epsilon - \mathbf{\Theta}_1\mathbf{\Sigma}_\epsilon\mathbf{\Theta}_1^{'}. \end{aligned}$$

A.3.3 Residual Chart Based on the Multivariate EWMA Statistic

Suppose that $Cov_0(\mathbf{X_t}, \epsilon_\mathbf{t}) = \mathbf{0},\ Cov_0(\epsilon_\mathbf{t}, \mathbf{X_t}) = \mathbf{0},\ E(\mathbf{d_t}) = \mathbf{0},\ E(\epsilon_\mathbf{t}) = \mathbf{0},\ E(\epsilon_\mathbf{t}\epsilon_\mathbf{t}^{'}) = \mathbf{U}, E(\epsilon_\mathbf{t}\epsilon_\mathbf{s}^{'}) = \mathbf{0}, t \neq s$, then the covariance matrix of the statistic $\mathbf{Z_t}$ is

$$\begin{aligned} Cov_0(\mathbf{Z_t}) &= Cov_0\left((\mathbf{I}-\mathbf{R})^{\mathbf{t}}\mathbf{Z_0} + \mathbf{R}\sum_{j=0}^{t-1}(\mathbf{I}-\mathbf{R})^{\mathbf{j}}\mathbf{d_{t-j}}\right) \\ &= \mathbf{R}\left(\sum_{i=0}^{t-1}\sum_{j=0}^{t-1}(\mathbf{I}-\mathbf{R})^{\mathbf{i}} Cov_0(\mathbf{d_{t-i}}, \mathbf{d_{t-j}})(\mathbf{I}-\mathbf{R})^{\mathbf{j}}\right)\mathbf{R} \\ &= \mathbf{R}\left(\sum_{i=0}^{t-1}\sum_{j=0}^{t-1}(\mathbf{I}-\mathbf{R})^{\mathbf{i}} E_0(\mathbf{d_{t-i}}\mathbf{d_{t-j}^{'}})(\mathbf{I}-\mathbf{R})^{\mathbf{j}}\right)\mathbf{R} \end{aligned}$$

$$
\begin{aligned}
&= \mathbf{R}\Bigg(\sum_{i=0}^{t-1}\sum_{j=0}^{t-1} (\mathbf{I}-\mathbf{R})^{\mathbf{i}} E_0[(\mathbf{X_{t-i}} \mathbf{m_{t-i}})(\mathbf{X_{t-i}} \mathbf{m_{t-j}})^{'})](\mathbf{I}-\mathbf{R})^{\mathbf{j}} \Bigg)\mathbf{R} \\
&= \mathbf{R}\Bigg(\sum_{i=0}^{t-1}\sum_{j=0}^{t-1} (\mathbf{I}-\mathbf{R})^{\mathbf{i}} E_0[(\mathbf{\Phi}_1 \mathbf{X_{t-i-1}} + \boldsymbol{\epsilon_{t-i}} \\
&- \mathbf{\Theta}_1 \boldsymbol{\epsilon_{t-i-1}} - m_{t-i})(\mathbf{\Phi}_1 \mathbf{X_{t-j-1}} + \boldsymbol{\epsilon_{t-j}} - \mathbf{\Theta}_1 \boldsymbol{\epsilon_{t-j-1}} - m_{t-j})^{'}](\mathbf{I}-\mathbf{R})^{j} \Bigg)\mathbf{R} \\
&= \mathbf{R}\Bigg(\sum_{i=0}^{t-1}\sum_{j=0}^{t-1} (\mathbf{I}-\mathbf{R})^{\mathbf{i}} E_0[(\mathbf{\Phi}_1 \mathbf{X_{t-i-1}} + \boldsymbol{\epsilon_{t-i}} \\
&- \mathbf{\Theta}_1 \boldsymbol{\epsilon_{t-i-1}} - m_{t-i})(\mathbf{X_{t-j-1}}^{'} \mathbf{\Phi}_1^{'} + \boldsymbol{\epsilon}_{\boldsymbol{t-j}}^{'} - \boldsymbol{\epsilon}_{\boldsymbol{t-j-1}}^{'} \mathbf{\Theta}_1^{'} - m_{t-j}^{'})](\mathbf{I}-\mathbf{R})^{j} \Bigg)\mathbf{R} \\
&= \mathbf{R}\Bigg(\sum_{i=0}^{t-1}\sum_{j=0}^{t-1} (\mathbf{I}-\mathbf{R})^{\mathbf{i}} E_0[(\mathbf{\Phi}_1 \mathbf{X_{t-i-1}} \mathbf{X_{t-j-1}}^{'} \\
&\mathbf{\Phi}_1^{'} + \mathbf{\Phi}_1 \mathbf{X_{t-i-1}} \boldsymbol{\epsilon}_{\boldsymbol{t-j}}^{'} - \mathbf{\Phi}_1 \mathbf{X_{t-i-1}} \boldsymbol{\epsilon}_{\boldsymbol{t-j-1}}^{'} \mathbf{\Theta}_1^{'} - \mathbf{\Phi}_1 \mathbf{X_{t-i-1}} m_{t-j}^{'} \\
&+ \boldsymbol{\epsilon_{t-i}} \mathbf{X_{t-j-1}}^{'} \mathbf{\Phi}_1^{'} + \boldsymbol{\epsilon_{t-i}} \boldsymbol{\epsilon}_{\boldsymbol{t-j}}^{'} \\
&- \boldsymbol{\epsilon_{t-i}} \boldsymbol{\epsilon}_{\boldsymbol{t-j-1}}^{'} \mathbf{\Theta}_1^{'} - \boldsymbol{\epsilon_{t-i}} m_{t-j}^{'} \\
&- \mathbf{\Theta}_1 \boldsymbol{\epsilon_{t-i-1}} \mathbf{X_{t-j-1}}^{'} \mathbf{\Phi}_1^{'} - \mathbf{\Theta}_1 \boldsymbol{\epsilon_{t-i-1}} \boldsymbol{\epsilon}_{\boldsymbol{t-j}}^{'} \\
&+ \mathbf{\Theta}_1 \boldsymbol{\epsilon_{t-i-1}} \boldsymbol{\epsilon}_{\boldsymbol{t-j-1}}^{'} \mathbf{\Theta}_1^{'} + \mathbf{\Theta}_1 \boldsymbol{\epsilon_{t-i-1}} m_{t-j}^{'} \\
&- m_{t-i} \mathbf{X_{t-j-1}}^{'} \mathbf{\Phi}_1^{'} - m_{t-i} \boldsymbol{\epsilon}_{\boldsymbol{t-j}}^{'} \\
&+ m_{t-i} \boldsymbol{\epsilon}_{\boldsymbol{t-j-1}}^{'} \mathbf{\Theta}_1^{'} + m_{t-i} m_{t-j}^{'})](\mathbf{I}-\mathbf{R})^{j} \Bigg)\mathbf{R} \\
&= \mathbf{R}\Bigg(2 * \mathbf{\Phi}_1 \mathbf{X_{t-i-1}} \mathbf{X_{t-j-1}}^{'} \mathbf{\Phi}_1^{'} + \mathbf{\Sigma}_{\boldsymbol{\epsilon}} \\
&- \mathbf{\Sigma}_{\boldsymbol{\epsilon}} \mathbf{\Theta}_1^{'} - \mathbf{\Theta}_1 \mathbf{\Sigma}_{\boldsymbol{\epsilon}} \Bigg) \frac{\boldsymbol{I}}{\boldsymbol{I}-(\boldsymbol{I}-\boldsymbol{R})^2} \mathbf{R}.
\end{aligned}
$$

According to Abramowitz et al. 1988 we have that

$$\sum_{j=0}^{t-1} (\mathbf{I}-\mathbf{R})^{i} (\mathbf{I}-\mathbf{R})^{j} = \frac{\mathbf{I}-(\mathbf{I}-\mathbf{R})^{\mathbf{2t}}}{\mathbf{I}-(\mathbf{I}-\mathbf{R})^{\mathbf{2}}}.$$

Also

$$\lim_{t\to\infty} \frac{\mathbf{I}-(\mathbf{I}-\mathbf{R})^{\mathbf{2t}}}{\mathbf{I}-(\mathbf{I}-\mathbf{R})^{\mathbf{2}}} = \frac{\mathbf{I}}{\mathbf{I}-(\mathbf{I}-\mathbf{R})^{\mathbf{2}}}.$$

Then the covariance matrix has the following form

$$Cov_0 = \mathbf{R}\Bigg(2 * \mathbf{\Phi}_1 \mathbf{X_{t-i-1}} \mathbf{X_{t-j-1}}' \mathbf{\Phi}_1' + \mathbf{\Sigma_\epsilon} - \mathbf{\Sigma_\epsilon}\mathbf{\Theta}_1' - \mathbf{\Theta}_1\mathbf{\Sigma_\epsilon}\Bigg)\frac{\boldsymbol{I}}{\boldsymbol{I}-(\boldsymbol{I}-\boldsymbol{R})^2}\mathbf{R}.$$

A.3.4 MMOEWMA control charts

Expected value for the control statistic
The control statistic for the modified MEWMA (MMOEWMA) chart based on the multivariate EWMA recursion is given by

$$\mathbf{Z_t} = (\mathbf{I}-\mathbf{R})^t\mathbf{Z_0} + \mathbf{R}\sum_{j=0}^{t-1}(\mathbf{I}-\mathbf{R})^j\mathbf{X_{t-j}} + \sum_{j=0}^{t-1}(\mathbf{I}-\mathbf{R})^j(\mathbf{X_{t-j}}-\mathbf{X_{t-j-1}}).$$

The expected value of the control statistic is

$$\begin{aligned}
E_0(\mathbf{Z}_t) &= E_0((\mathbf{I}-\mathbf{R})^t\mathbf{Z_0} + \mathbf{R}\sum_{j=0}^{t-1}(\mathbf{I}-\mathbf{R})^j\mathbf{X_t} + \sum_{j=0}^{t-1}(\mathbf{I}-\mathbf{R})^j(\mathbf{X_{t-j}}-\mathbf{X_{t-j-1}}) \\
&= (\mathbf{I}-\mathbf{R})^t\mathbf{Z_0} + \mathbf{R}\sum_{j=0}^{t-1}(\mathbf{I}-\mathbf{R})^j E_0(\mathbf{X_t}) + \sum_{j=0}^{t-1}(\mathbf{I}-\mathbf{R})^j E_0(\mathbf{X_{t-j}}-\mathbf{X_{t-j-1}}) \\
&= (\mathbf{I}-\mathbf{R})^t\mathbf{Z_0} + \mathbf{R}E_0(\sum_{j=0}^{t-1}(\mathbf{I}-\mathbf{R})^j\mathbf{X_{t-j}}) + \sum_{j=0}^{t-1}(\mathbf{I}-\mathbf{R})^j E_0(\mathbf{X_{t-j}}-\mathbf{X_{t-j-1}}) \\
&= (\mathbf{I}-\mathbf{R})^t\mathbf{Z_0} + \mathbf{R}\sum_{j=0}^{t-1}(\mathbf{I}-\mathbf{R})^j E_0(\mathbf{X_{t-j}}) \\
&= (\mathbf{I}-\mathbf{R})^t\mathbf{Z_0} + \mathbf{R}\sum_{j=0}^{t-1}(\mathbf{I}-\mathbf{R})^j \boldsymbol{\mu_{0,X}} \\
&= (\mathbf{I}-\mathbf{R})^t\mathbf{Z_0} + \mathbf{R}\frac{(\mathbf{I}-(\mathbf{I}-\mathbf{R})^{\mathbf{t}}}{(\mathbf{I}-(\mathbf{I}-\mathbf{R})}\boldsymbol{\mu_{0,X}}
\end{aligned}$$

$$= (\mathbf{I}-\mathbf{R})^{\mathbf{t}}\mathbf{Z_0} + (\mathbf{I}-(\mathbf{I}-\mathbf{R})^{\mathbf{t}}\boldsymbol{\mu_{0,X}}.$$

Covariance matrix for the control statistic

Suppose that $Cov_0(\mathbf{X_t}, \epsilon_\mathbf{t}) = \mathbf{0},\ E(\epsilon_\mathbf{t}) = \mathbf{0},\ E(\epsilon_\mathbf{t}\epsilon_\mathbf{t}^{'}) = \mathbf{U}$, then the in-control covariance matrix is

$$\begin{aligned}
Cov_0(\mathbf{Z_t}) &= Cov_0\bigg((\mathbf{I}-\mathbf{R})^t\mathbf{Z_0} + \mathbf{R}\sum_{j=0}^{t-1}(\mathbf{I}-\mathbf{R})^j\mathbf{X_{t-j}} + \sum_{j=0}^{t-1}(\mathbf{I}-\mathbf{R})^j(\mathbf{X_{t-j}}-\mathbf{X_{t-j-1}})\bigg)\\
&= Cov_0\bigg(\mathbf{R}\sum_{j=0}^{t-1}(I-R)^j\mathbf{X_{t-j}}\bigg) + Cov_0\bigg(\sum_{j=0}^{t-1}(I-R)^j(\mathbf{X_{t-j}}-\mathbf{X_{t-j-1}})\bigg) +\\
&\quad Cov_0\bigg(\mathbf{R}\sum_{j=0}^{t-1}(\mathbf{I}-\mathbf{R})^j\mathbf{X_{t-j}}, \sum_{j=0}^{t-1}(\mathbf{I}-\mathbf{R})^j(\mathbf{X_{t-j}}-\mathbf{X_{t-j-1}})\bigg)\\
&= \mathbf{R}\Big(\sum_{j=0}^{t-1}(\mathbf{I}-\mathbf{R})^j Cov_0(\mathbf{X_{t-j}})(\mathbf{I}-\mathbf{R})^j)\Big)\mathbf{R}\\
&\quad + \sum_{j=0}^{t-1}(\mathbf{I}-\mathbf{R})^j Cov_0(\mathbf{X_{t-j}}-\mathbf{X_{t-j-1}})(\mathbf{I}-\mathbf{R})^j\\
&\quad + \sum_{j=0}^{t-1}(\mathbf{I}-\mathbf{R})^j Cov_0(\mathbf{R}\mathbf{X_{t-j}}, \mathbf{X_{t-j}}-\mathbf{X_{t-j-1}})(\mathbf{I}-\mathbf{R})^j\\
&= \mathbf{R}\frac{\boldsymbol{I}}{\boldsymbol{I}-(\boldsymbol{I}-\boldsymbol{R})^2}\mathbf{R}V_0(\mathbf{X_t}).
\end{aligned}$$

It can be proved that

$$\sum_{j=0}^{t-1}(\mathbf{I}-\mathbf{R})^j Var_0(\mathbf{Y_{t-j}})(\mathbf{I}-\mathbf{R})^j = \frac{\mathbf{I}-(\mathbf{I}-\mathbf{R})^{\mathbf{2t}}}{\mathbf{I}-(\mathbf{I}-\mathbf{R})^{\mathbf{2}}}\boldsymbol{\Sigma}_\mathbf{Y}.$$

Also, we have that

$$\lim_{t\to\infty}\frac{\mathbf{I}-(\mathbf{I}-\mathbf{R})^{\mathbf{2t}}}{\mathbf{I}-(\mathbf{I}-\mathbf{R})^{\mathbf{2}}} = \frac{\mathbf{I}}{\mathbf{I}-(\mathbf{I}-\mathbf{R})^{\mathbf{2}}}.$$

Appendix B

Tables

VAR	No. of elements	Σ_e	Σ_{mm}	ρ^Q	δ_1	ρ_{ml}	ρ_{mm}	ρ_{ll}	ρ_{lm}	δ_0	c^Q	c_m	c_l
Ω_2^*	N_e	X											
Ω_m^*	$N_m(N_m+1)/2$		X										
ψ_{1m}^*	$N_l N_m$			X	X								
ϕ_{2m}^*	$N_e N_m$			X	X								
ϕ_{21}^*	$N_e N_l$			X	X								
Ω_1^*	$N_l(N_l+1)/2$			X	X								
ϕ_{m1}^*	$N_m N_l$			X	X	X							
ϕ_{mm}^*	N_m^2			X	X	X	X						
ϕ_{11}^*	N_l^2			X	X			X					
ϕ_{1m}^*	$N_l N_m$			X	X			X	X				
A_2^*	N_e		X	X	X					X	X		
A_m^*	N_m		X	X	X	X				X		X	
A_1^*	N_l		X	X	X			X		X			X

Table B.0.1: Mapping between structural and reduced-form parameters for the ATSM model.

Maturity	*3 month*	*t-Statistic*	*5 year*	*t-Statistic*	*10 year*	*t-Statistic*
Intercept	0.0035 (0.1800*1e-03)	19.6709	0.0047 (0.4670*1e-03)	10.1299	0.0051 (0.0644*1e-03)	79.0791
CPI	0.0034 (0.1709*1e-03)	19.9140	0.0028 (0.4434*1e-03)	6.4156	0.0026 (0.0612*1e-03)	42.3099
IP	-7.5713e-06 (0.1587*1e-03)	-0.0477	6.4410e-06 (0.4116*1e-03)	0.0156	-3.7569e-06 (0.0568*1e-03)	-0.06625
$adj.R^2$	0.1112		0.1391		0.2128	

Table B.0.2: Regressing U.S. Treasury yields on macroeconomic factors.

3M	*48M*	*60M*	*72M*	*84M*	*120M*
1.0000	0.1445	0.3650	0.2697	0.3008	-0.1696
0.1445	1.0000	0.1655	0.9798	0.8138	0.8326
0.3650	0.1655	1.0000	0.1714	0.6826	-0.3383
0.2697	0.9798	0.1714	1.0000	0.8067	0.7795
0.3008	0.8138	0.6826	0.8067	1.0000	0.4126
-0.1696	0.8326	-0.3383	0.7795	0.4126	1.0000

Table B.0.3: Correlation coefficients for U.S. Treasury bond expected returns.

λ \ u	1.5	2	2.5	3	3.5	4	4.5
0.05	10.9052 (6)	10.1504 (6)	9.3015 (6)	8.5742 (5)	7.5604 (5)	6.6746 (5)	5.8821 (4)
0.1	10.4735 (7)	10.0032 (6)	9.3625 (6)	8.6141 (6)	7.8398 (5)	6.7949 (5)	6.3112 (4)
0.15	4.6401 (6)	4.5863 (6)	4.5285 (5)	4.3028 (5)	4.1521 (5)	3.8635 (5)	3.7039 (4)
0.2	6.1538 (7)	6.0879 (7)	5.8557 (7)	5.6442 (6)	5.3134 (5)	4.9711 (5)	4.6929 (5)
0.25	6.2345 (7)	6.0457 (7)	5.9630 (6)	5.5580 (6)	5.2661 (5)	5.0370 (5)	4.6644 (5)
0.3	6.3382 (7)	6.1988 (6)	6.0654 (6)	5.7349 (6)	5.4512 (5)	5.1801 (5)	4.8956 (5)
0.35	4.2689 (7)	4.1450 (7)	4.0805 (6)	3.9716 (6)	3.7859 (5)	3.6668 (5)	3.4729 (5)
0.4	4.5479 (7)	4.3657 (6)	4.2784 (6)	4.1053 (6)	3.9930 (5)	3.7932 (5)	3.6039 (5)
0.45	4.7380 (7)	4.6270 (6)	4.4198 (6)	4.3756 (6)	4.1834 (5)	4.0068 (5)	3.8220 (5)
0.5	4.81811 (5)	4.8303 (5)	4.6982 (5)	4.5100 (4)	4.6883 (4)	4.1049 (5)	4.0258 (5)
0.75	6.4559 (5)	6.2989 (5)	6.3188 (5)	6.0857 (5)	5.8935 (5)	5.6704 (5)	5.5211 (5)
0.9	5.9822 (6)	5.9012 (6)	5.7933 (5)	5.6725 (5)	5.5070 (5)	5.400 (5)	5.2461 (4)

Table B.0.4: Out-of-control ARLs for n=40 and in-control ARL=6 for the case of control chart based on Mahalanobis distance for unconstrained portfolios. In parentheses the MRLs are presented.

λ \ u	1.5	2	2.5	3	3.5	4	4.5
0.05	5.7647 (4)	5.4942 (4)	5.2403 (4)	4.9013 (4)	4.554 (3)	3.9979 (3)	3.9514 (3)
0.1	5.9874 (4)	5.6457 (4)	5.4315 (4)	5.0503 (4)	4.661 (4)	4.1433 (3)	3.7668 (3)
0.15	5.8075 (5)	5.6026 (4)	5.3753 (4)	4.9159 (4)	4.6268 (3)	4.1407 (3)	3.7748 (3)
0.2	5.8304 (4)	5.6859 (4)	5.3572 (4)	5.0197 (4)	4.6309 (3)	4.2401 (3)	3.8680 (3)
0.25	5.6773 (4)	5.5410 (4)	5.2776 (4)	4.9200 (4)	4.5306 (4)	4.1454 (3)	3.8527 (3)
0.3	5.8985 (4)	5.6726 (3)	5.4226 (4)	5.1959 (4)	4.7568 (4)	4.3851 (3)	4.0227 (3)
0.35	5.9271 (4)	5.7277 (4)	5.5195 (4)	5.1419 (4)	4.8185 (4)	4.4227 (3)	4.0606 (3)
0.4	5.9286 (4)	5.6923 (4)	5.4714 (4)	5.1928 (4)	4.7971 (4)	4.4854 (3)	4.0788 (3)
0.45	5.9849 (5)	5.7179 (5)	5.5457 (5)	5.2854 (4)	4.8729 (4)	4.5943 (4)	4.2015 (3)
0.5	5.4718 (5)	5.4366 (4)	5.2036 (4)	4.9585 (4)	4.6863 (4)	4.4031 (4)	4.0940 (3)
0.75	5.4578 (5)	5.3463 (5)	5.2082 (5)	5.0806 (5)	4.8743 (5)	4.5602 (4)	4.3138 (4)
0.9	7.3793 (5)	7.3455 (4)	7.0636 (4)	7.0084 (4)	6.8983 (4)	6.6646 (4)	6.3441 (4)

Table B.0.5: Out-of-control ARLs for n=40 and in-control ARL=6 for the case of control chart based on MEWMA statistic for unconstrained portfolios.

λ \ u	1.5	2	2.5	3	3.5	4	4.5
0.05	3.1238 (1)	2.1804 (1)	1.7700 (1)	1.5558 (1)	1.4020 (1)	1.3174 (1)	1.2158 (1)
0.1	1.1212 (1)	1.0668 (1)	1.0320 (1)	1.0252 (1)	1.0178 (1)	1.0106 (1)	1.0050 (1)
0.15	2.1586 (1)	1.6672 (1)	1.4656 (1)	1.3498 (1)	1.2586 (1)	1.2174 (1)	1.1690 (1)
0.2	2.1104 (1)	1.6924 (1)	1.4666 (1)	1.3740 (1)	1.2884 (1)	1.2178 (1)	1.1670 (1)
0.25	2.0806 (1)	1.6784 (1)	1.4746 (1)	1.4060 (1)	1.2986 (1)	1.2236 (1)	1.1844 (1)
0.3	1.9454 (1)	1.5938 (1)	1.4330 (1)	1.3390 (1)	1.2848 (1)	1.2188 (1)	1.1884 (1)
0.35	1.9224 (1)	1.5950 (1)	1.4514 (1)	1.3630 (1)	1.3036 (1)	1.2350 (1)	1.1912 (1)
0.4	2.4336 (1)	1.8506 (1)	1.6898 (1)	1.3788 (1)	1.4372 (1)	1.3514 (1)	1.2816 (1)
0.45	2.3126 (1)	1.8616 (1)	1.6670 (1)	1.5278 (1)	1.4132 (1)	1.3502 (1)	1.2772 (1)
0.5	2.0582 (1)	1.7088 (1)	1.5524 (1)	1.4552 (1)	1.3788 (1)	1.3278 (1)	1.2620 (1)
0.75	1.9428 (1)	1.6896 (1)	1.5242 (1)	1.4390 (1)	1.3568 (1)	1.3090 (1)	1.2548 (1)
0.9	1.9192 (1)	1.6098 (1)	1.5020 (1)	1.4144 (1)	1.3594 (1)	1.3076 (1)	1.2504 (1)

Table B.0.6: Out-of-control ARLs for n=40 and in-control ARL=6 for the case of control chart based on Mahalanobis distance for constrained portfolio.

λ \ u	1.5	2	2.5	3	3.5	4	4.5
0.05	1.3646 (1)	1.3824 (1)	1.4120 (1)	1.0168 (1)	1.0136 (1)	1.0118 (1)	1.0114 (1)
0.1	1.4506 (1)	1.1986 (1)	1.0656 (1)	1.0240 (1)	1.0160 (1)	1.0102 (1)	1.0106 (1)
0.15	1.6190 (1)	1.3068 (1)	1.1134 (1)	1.0576 (1)	1.0312 (1)	1.0218 (1)	1.0112 (1)
0.2	1.7244 (1)	1.3822 (1)	1.1984 (1)	1.0990 (1)	1.0544 (1)	1.0302 (1)	1.0222 (1)
0.25	1.7562 (1)	1.4404 (1)	1.2264 (1)	1.1206 (1)	1.0674 (1)	1.0430 (1)	1.0340 (1)
0.3	1.8254 (1)	1.4662 (1)	1.2742 (1)	1.1540 (1)	1.0942 (1)	1.0550 (1)	1.0358 (1)
0.35	1.8864 (1)	1.5068 (1)	1.3096 (1)	1.2070 (1)	1.1274 (1)	1.0852 (1)	1.0472 (1)
0.4	1.8558 (1)	1.5510 (1)	1.3498 (1)	1.2170 (1)	1.1534 (1)	1.1030 (1)	1.0562 (1)
0.45	1.9938 (1)	1.6310 (1)	1.4224 (1)	1.2832 (1)	1.1842 (1)	1.1346 (1)	1.0948 (1)
0.5	1.9882 (1)	1.6574 (1)	1.4476 (1)	1.2994 (1)	1.2222 (1)	1.1572 (1)	1.1168 (1)
0.75	2.4472 (1)	2.0778 (1)	1.8260 (1)	1.6198 (1)	1.5304 (1)	1.4188 (1)	1.3174 (1)
0.9	5.8965 (1)	5.2398 (1)	5.6694 (1)	4.9970 (1)	4.1104 (1)	3.5460 (1)	3.1660 (1)

Table B.0.7: Out-of-control ARLs for n=40 and in-control ARL=6 for the case of control chart based on MEWMA statistic for constrained portfolio.

ϕ	0.87181	-0.017812	0.012011	0.0034272	-0.0053583
	(2.5431e-08)	(5.1461e-08)	(2.0137e-07)	(0.0536e-07)	(2.1606e-07)
	-0.30186	0.80995	0.099164	0.01879	-0.0587
	(3.0271e-08)	(6.2142e-08)	(2.4061e-07)	(0.0205e-07)	(2.3962e-07)
	0.097158	-0.58839	0.98951	0.016938	-0.08426
	(1.3344e-08)	(8.5078e-08)	(5.4005e-07)	(0.0859e-07)	(1.0933e-07)
	-0.08554	-0.028417	-0.03024	0.93816	0.01096
	(5.6615e-08)	(1.4567e-07)	(4.9868e-07)	(0.0440e-07)	(4.1624e-07)
	0.5685	0.21583	0.2952	0.15714	0.7043
	(8.6810e-08)	(2.4387e-07)	(5.3895e-07)	(0.0590e-07)	(4.4603e-07)
δ_0	-3.3432e-04				
	(4.4166e-07)				
δ_1	3.1952e-05	0.00013014	1.2125e-05	0.0001709	0.00016569
	(1.2858e-07)	2.3255e-07)	(1.8357e-07)	(2.6514e-07)	(4.4406e-05)
μ^Q	1.3919	-0.81477	0	0	0
	(1.212e-07)	(2.1755e-07)			
Σ	0.20883	0	0	0	0
	(5.913e-09)				
	0.029512	0.61729	0	0	0
	(0.1693e-08)	(0.1197e-08)			
	0	0	1	0	0
	0	0	0	1	0
	0	0	0	0	1
μ	0.025387	0.42077	0.67457	-0.25218	2.6127
	(3.0755e-08)	(3.3529e-07)	(1.0075e-8)	(4.1247e-08)	(5.1066e-08)
ϕ^Q	1.0633	0.82035	-0.32955	0.47331	0.26845
	(1.5812e-05)	(3.1240e-05)	(6.9610e-06)	(5.3160e-05)	(3.8894e-05)
	-0.26035	0.61316	-0.28452	-0.28316	-0.1324
	(3.1898e-05)	(6.3245e-05)	(1.0625e-05)	(1.0247e-04)	(7.8352e-05)
	-0.10367	0.071545	0.91015	0	0
	(1.1166e-04)	(1.0089e-04)	(2.6895e-05)		
	0.013353	-0.5	0.051817	0.78713	-0.20236
	(1.8092e-05)	(2.4970e-05)	(1.4491e-05)	(1.0026e-04)	(3.6707e-05)
	-0.17911	-0.24853	0.33837	-0.1458	0.78713
	(3.5119e-05)	(2.8875e-05)	(1.3749e-05)	(8.2879e-04)	(1.0026e-05)

Table B.0.8: The table reports the parameter estimates and standard errors in parentheses applying the minimum-chi-square method. The sample period is 1988:01 to 1997:07.

B.1 Shifts in the factor loadings of the state evolution process

B.1.1 Positive shifts in Yield curve

λ \ d	0.05	0.1	0.15	0.2	0.25	0.3	0.35	0.4
0.1	15.23	16.98	16.82	17.71	19.46	19.24	20.31	20.86
0.2	10.9	11.07	11.67	11.75	11.96	12.65	13.2	13.19
0.25	10.85	11.24	11.46	12	12.11	12.25	12.47	12.73
0.35	11.17	11.16	11.8	12.05	12.11	12.35	12.59	12.84
0.45	11.53	11.48	11.66	12.71	12.22	12.4	12.82	12.86
0.5	9.97	9.99	10.17	10.32	10.33	10.65	10.86	10.96
0.75	11.57	11.54	11.74	12.04	12.27	12.38	12.25	12.69
0.9	10.21	10.41	10.74	10.52	10.81	11.1	11.1	11.27

Table B.1.1: Out-of-control ARLs for in-control ARL=11 months for the case of modified control chart based on Mahalanobis distance.

λ \ d	0.05	0.1	0.15	0.2	0.25	0.3	0.35	0.4
0.1	6.65	3.52	2.07	1.45	1.17	1.06	1.02	1
0.2	10.81	5.87	2.99	1.88	1.33	1.13	1.05	1.01
0.25	15.69	8.25	4.2	2.34	1.55	1.2	1.08	1.02
0.35	5.12	3.7	2.39	1.64	1.26	1.09	1.03	1
0.45	20.42	14.1	8.35	4.74	2.79	1.78	1.34	1.11
0.5	10.11	7.61	5.23	3.19	2.04	1.5	1.2	1.06
0.75	11.05	9.46	7.47	5.38	3.8	2.52	1.81	1.38
0.9	9.45	8.85	7.17	5.69	4.2	3.06	2.28	1.67

Table B.1.2: Out-of-control ARLs for in-control ARL=11 months for the case of modified control chart based on MEWMA statistic.

λ \ d	0.05	0.1	0.15	0.2	0.25	0.3	0.35	0.4
0.1	14.26	12.45	15.81	20.47	22.22	17.22	18.51	19.09
0.2	9.82	10.06	10.52	10.64	11.2	11.51	11.67	11.89
0.25	9.45	9.44	9.83	9.94	10.39	10.4	10.76	10.73
0.35	9.56	10.04	10.5	10.35	10.82	11.21	11.25	11.74
0.45	9.38	9.7	9.68	9.99	10.28	10.18	10.36	10.97
0.5	10.35	10.41	10.43	10.8	10.89	11.42	11.7	11.28
0.75	9.99	9.97	10.35	10.43	10.17	10.32	10.54	10.91
0.9	11.49	12.03	12.14	11.81	12.77	13.22	12.16	12.05

Table B.1.3: Out-of-control ARLs for in-control ARL=11 months for the case of Residual control chart based on Mahalanobis distance.

λ \ d	0.05	0.1	0.15	0.2	0.25	0.3	0.35	0.4
0.1	1.01	1.04	1.08	1.26	1.86	3.18	6.06	10.66
0.2	1.18	1.37	1.88	2.52	3.75	5.33	7.56	10.35
0.25	1.42	1.74	2.35	3.2	4.59	5.9	7.97	10.26
0.35	2.5	3.11	3.98	5.04	6.49	7.72	9.57	11.41
0.45	3.32	4	4.8	5.86	7	8.28	9.53	10.63
0.5	3.74	4.59	5.42	6.37	7.41	8.54	9.7	11.05
0.75	6	6.84	7.72	8.45	9.26	10.1	10.91	11.5
0.9	6.23	6.87	7.34	8.05	8.79	9.38	9.58	10.25

Table B.1.4: Out-of-control ARLs for in-control ARL=11 months for the case of Residual control chart based on MEWMA statistic.

g \ d	0.05	0.1	0.15	0.2	0.25	0.3	0.35	0.4
0.1	11.18	11.62	11.28	11.53	11.72	11.26	12.1	12
0.3	10.96	11.08	10.96	11.38	11.69	11.84	11.75	12.42
0.5	13.22	13.56	13.68	13.75	14.02	14.05	13.83	14.13
0.7	9.16	9.32	9.35	9.22	9.54	9.33	9.36	9.7
1	10.41	10.77	10.84	11.01	11.04	11.2	11.27	11.34
1.5	9.16	9.24	9.36	9.58	9.56	9.79	9.92	9.87
2	8	8.22	8.17	8.25	8.48	8.23	8.79	8.78
2.5	16.57	16.9	17.08	17.68	17.85	17.77	18.22	17.78

Table B.1.5: Out-of-control ARLs for in-control ARL=11 months for the case of MCUSUM control chart.

λ \ d	0.05	0.1	0.15	0.2	0.25	0.3	0.35	0.4
0.1	6.66	3.36	2.02	1.41	1.17	1.05	1.02	1
0.2	8	4.33	2.5	1.59	1.22	1.09	1.02	1
0.25	7.94	4.37	2.55	1.63	1.26	1.09	1.03	1
0.35	8.86	5.54	3.19	1.99	1.4	1.15	1.04	1.01
0.45	9.93	6.81	4.16	2.45	1.68	1.26	1.09	1.02
0.5	10.46	7.39	4.66	2.87	1.86	1.34	1.12	1.04
0.75	11.14	9.03	6.9	4.71	3.17	2.18	1.56	1.24
0.9	10.67	9.52	7.77	5.7	4	2.85	2.04	1.55

Table B.1.6: Out-of-control ARLs for in-control ARL=11 months for the case of MMOEWMA control chart.

B.1.2 Negative Shifts in the Yield curve

λ \ d	-0.05	-0.1	-0.15	-0.2	-0.25	-0.3	-0.35	-0.4
0.1	14.56	13.32	13.39	12.99	12.23	11.44	10.78	10.01
0.2	10.19	10.18	9.78	9.56	8.89	9.09	8.50	8.25
0.25	10.32	10.21	9.78	9.87	9.44	8.99	8.83	8.84
0.35	10.63	10.61	10.23	10.09	9.86	9.52	9.26	9.07
0.45	10.73	10.64	10.49	10.3	9.91	9.9	9.7	9.49
0.5	9.43	9.29	8.92	8.73	8.77	8.6	8.38	8.24
0.75	10.83	10.67	10.91	10.35	10.43	10.16	9.9	10.24
0.9	9.98	10.02	9.77	9.8	9.6	9.25	9.39	9.12

Table B.1.7: Out-of-control ARLs for in-control ARL=11 months for the case of modified control chart based on Mahalanobis distance.

λ \ d	-0.05	-0.1	-0.15	-0.2	-0.25	-0.3	-0.35	-0.4
0.1	13.49	8.26	4.77	3.06	2.17	1.7	1.406	1.26
0.2	19.54	11.54	10.68	8.87	5.85	4.11	3.28	2.71
0.25	15.87	9.96	6.46	5.93	5	4.01	3.31	2.7
0.35	11.02	8	5.85	4.09	2.98	2.34	1.97	1.78
0.45	5.69	4.59	3.7	2.8	2.34	1.91	1.69	1.53
0.5	5.91	4.85	3.96	3.17	2.55	2.16	1.87	1.73
0.75	15.32	13.23	10.6	8.8	7.5	6.08	5.29	4.7
0.9	15.59	14.1	11.94	10.27	8.57	7.5	6.37	5.95

Table B.1.8: Out-of-control ARLs for in-control ARL=11 months for the case of modified control chart based on MEWMA statistic.

λ \ d	-0.05	-0.1	-0.15	-0.2	-0.25	-0.3	-0.35	-0.4
0.1	12.67	11.32	10.53	9.66	8.98	8.22	7.62	6.93
0.2	8.94	8.53	7.83	7.73	7.06	6.9	6.4	6.4
0.25	8.55	7.07	7.84	6.29	5.98	6.72	5.56	5.98
0.35	9.43	9.13	8.6	8.16	7.84	7.62	7.27	7.35
0.45	9.05	8.44	8.45	8.22	7.42	7.57	7.25	7.08
0.5	9.62	9.14	9.04	8.77	8.43	8.35	7.97	7.76
0.75	9.92	9.44	9.12	9.18	8.88	8.56	8.67	8.41
0.9	11.12	10.75	10.83	10.31	10.36	9.98	9.82	9.78

Table B.1.9: Out-of-control ARLs for in-control ARL=11 months for the case of Residual control chart based on Mahalanobis distance.

λ \ d	-0.05	-0.1	-0.15	-0.2	-0.25	-0.3	-0.35	-0.4
0.1	30.56	5.66	1.38	1.01	1	1	1	1
0.2	14.91	5.82	2.28	1.22	1.02	1	1	1
0.25	12.68	5.89	2.5	1.4	1.06	1	1	1
0.35	11.82	6.23	3.3	1.9	1.25	1.06	1	1
0.45	10.11	6.48	3.64	2.26	1.52	1.18	1.05	1
0.5	9.87	6.48	4.14	2.49	1.68	1.28	1.09	1.02
0.75	15.81	15.42	15.48	15.35	15.45	15.64	15.66	15.64
0.9	12.75	12.85	13.04	12.57	12.98	12.68	12.7	12.86

Table B.1.10: Out-of-control ARLs for in-control ARL=11 months for the case of Residual control chart based on MEWMA statistic.

g \ d	-0.05	-0.1	-0.15	-0.2	-0.25	-0.3	-0.35	-0.4
0.1	11.16	11.45	10.78	10.87	10.52	10.52	10.35	10.61
0.3	11.35	10.38	10.8	10.34	10.26	10.34	10.45	9.88
0.5	12.84	12.63	12.4	12.34	12.39	12.42	11.91	11.68
0.7	8.86	8.57	8.34	8.41	8.37	8.5	8.46	8.29
1	10.23	10.38	9.94	9.79	9.69	9.56	9.64	9.42
1.5	8.97	8.76	8.91	8.51	8.56	8.6	8.67	8.3
2	7.99	7.85	7.85	7.74	7.46	7.57	7.35	7.6
2.5	16.23	16.12	15.77	15.35	15.3	15.11	14.91	14.87

Table B.1.11: Out-of-control ARLs for in-control ARL=11 months for the case of MCUSUM control chart.

λ \ d	-0.05	-0.1	-0.15	-0.2	-0.25	-0.3	-0.35	-0.4
0.1	7.54	4.06	2.35	1.62	1.25	1.1	1.03	1
0.2	7.29	4.78	2.92	1.85	1.4	1.17	1.06	1.02
0.25	7.71	5.09	3.06	2	1.48	1.22	1.08	1.03
0.35	7	4.85	3.27	2.16	1.58	1.29	1.11	1.05
0.45	8.27	6.02	4.09	2.7	1.9	1.49	1.24	1.11
0.5	7.49	5.67	3.9	2.75	1.96	1.51	1.26	1.13
0.75	8.28	6.77	5.15	3.77	2.79	2.15	1.69	1.41
0.9	8.79	7.44	5.92	4.55	3.48	2.63	2.07	1.69

Table B.1.12: Out-of-control ARLs for in-control ARL=11 months for the case of MMOEWMA control chart.

B.2 Parallel shifts in Yield curve

B.2.1 Positive shifts

λ \ d	0.05	0.1	0.15	0.2	0.25	0.3	0.35	0.4
0.1	85.38	51.46	23.65	8.73	2.84	1.23	1.01	1
0.2	34.22	23.77	13.46	7.44	3.45	1.77	1.18	1.02
0.25	28.78	21.67	13.48	7.61	4.08	2.12	1.3	1.06
0.35	25.19	19.08	12.74	8.07	4.71	2.77	1.71	1.25
0.45	23.77	18.02	12.78	8.46	5.29	3.29	2.15	1.49
0.5	18.91	15.22	10.98	7.39	4.8	3.11	2.13	1.52
0.75	19.7	16.06	12.04	8.82	5.97	4.3	3	2.24
0.9	16.48	14.09	10.89	8.19	5.74	4.13	3.08	2.37

Table B.2.1: Out-of-control ARLs for in-control ARL=11 months for the case of EWMA control chart based on Mahalanobis distance.

λ \ d	0.05	0.1	0.15	0.2	0.25	0.3	0.35	0.4
0.1	9.73	5.66	3.19	1.98	1.41	1.19	1.07	1.02
0.2	12.4	7.04	3.99	2.52	1.75	1.34	1.15	1.06
0.25	10.14	6.38	3.81	2.51	1.71	1.34	1.17	1.06
0.35	7.74	5.41	3.71	2.45	1.8	1.41	1.21	1.09
0.45	4.38	3.5	2.69	2.02	1.61	1.32	1.17	1.08
0.5	4.56	3.7	2.81	2.25	1.7	1.41	1.21	1.11
0.75	11.92	9.75	7.34	5.47	4.06	3	2.28	1.83
0.9	12.88	10.8	8.64	6.73	5.08	3.91	3.05	2.38

Table B.2.2: Out-of-control ARLs for in-control ARL=11 months for the case of control chart based on MEWMA statistic.

λ \ d	0.05	0.1	0.15	0.2	0.25	0.3	0.35	0.4
0.1	3.97	2.38	1.44	1.07	1	1	1	1
0.2	4.19	2.95	2.03	1.35	1.09	1	1	1
0.25	4.48	3.34	2.16	1.55	1.2	1.05	1	1
0.35	5.29	4.03	2.87	2	1.49	1.19	1.06	1
0.45	5.46	4.2	3.15	2.3	1.7	1.35	1.15	1.03
0.5	5.9	4.72	3.48	2.61	1.93	1.48	1.21	1.08
0.75	6.08	4.94	3.83	2.98	2.34	1.91	1.58	1.33
0.9	7.21	5.6	4.56	3.42	2.71	2.21	1.84	1.57

Table B.2.3: Out-of-control ARLs for in-control ARL=11 months for the case of Residual control chart based on Mahalanobis distance.

λ \ d	0.05	0.1	0.15	0.2	0.25	0.3	0.35	0.4
0.1	30.66	5.75	1.35	1.01	1	1	1	1
0.2	15.11	5.8	2.21	1.2	1.02	1	1	1
0.25	12.35	5.62	2.48	1.35	1.06	1	1	1
0.35	11.68	6.23	3.22	1.8	1.23	1.06	1	1
0.45	10	6.42	3.63	2.21	1.5	1.16	1.05	1
0.5	10.01	6.56	3.86	2.41	1.64	1.28	1.09	1.02
0.75	9.38	6.98	4.92	3.36	2.37	1.77	1.44	1.21
0.9	8.04	6.48	4.82	3.53	2.63	2.03	1.64	1.37

Table B.2.4: Out-of-control ARLs for in-control ARL=11 months for the case of Residual control chart based on MEWMA statistic.

g \ d	0.05	0.1	0.15	0.2	0.25	0.3	0.35	0.4
0.1	2.81	1.02	1	1	1	1	1	1
0.3	3.34	1.05	1	1	1	1	1	1
0.5	5.69	1.56	1	1	1	1	1	1
0.7	8.94	8.78	8.91	9.07	9.05	9.06	8.96	8.69
1	6.83	4.52	2.08	1.07	1	1	1	1
1.5	6.72	5.53	4.03	2.55	1.45	1.03	1	1
2	6.14	5.46	4.38	3.32	2.43	1.71	1.18	1
2.5	11.95	10.35	8.2	6.04	4.6	3.27	2.33	1.62

Table B.2.5: Out-of-control ARLs for in-control ARL=11 months for the case of MCUSUM control chart.

λ \ d	0.05	0.1	0.15	0.2	0.25	0.3	0.35	0.4
0.1	9.63	5.45	3.1	1.91	1.4	1.17	1.06	1
0.2	7.5	4.68	2.82	1.9	1.42	1.19	1.07	1.03
0.25	7.54	4.97	3.11	2.04	1.51	1.25	1.1	1.04
0.35	6.68	4.84	3.24	2.24	1.66	1.3	1.15	1.07
0.45	7.85	5.96	4.06	2.76	2.04	1.56	1.29	1.15
0.5	7.4	5.48	3.92	2.81	2.1	1.64	1.32	1.17
0.75	8.26	6.68	5.18	3.95	2.96	2.33	1.85	1.5
0.9	8.8	7.35	6.14	4.81	3.6	2.88	2.29	1.88

Table B.2.6: Out-of-control ARLs for in-control ARL=11 months for the case of MMOEWMA control chart.

B.2.2 Negative shifts

λ \ d	-0.05	-0.1	-0.15	-0.2	-0.25	-0.3	-0.35	-0.4
0.1	82.87	50.95	22.99	8.46	2.68	1.24	1	1
0.2	33.73	24.21	14.04	7.13	3.41	1.78	1.15	1.02
0.25	30.4	21.79	13.64	7.68	3.92	2.06	1.32	1.06
0.35	25.43	19.35	13.14	8.07	4.69	2.81	1.77	1.25
0.45	22.87	18.07	12.87	8.38	5.18	3.2	2.17	1.51
0.5	19.11	15.03	10.92	7.27	4.81	3.16	2.12	1.51
0.75	20.13	16.51	12.44	8.66	6.25	4.17	3.02	2.25
0.9	16.59	14.34	10.8	8.02	5.86	4.24	3.09	2.38

Table B.2.7: Out-of-control ARLs for in-control ARL=11 months for the case of modified control chart based on Mahalanobis distance.

λ \ d	-0.05	-0.1	-0.15	-0.2	-0.25	-0.3	-0.35	-0.4
0.1	9.98	5.68	3.18	1.94	1.44	1.19	1.07	1.02
0.2	12.59	7.16	4.07	2.48	1.71	1.31	1.15	1.05
0.25	10.18	6.41	3.86	2.45	1.72	1.34	1.17	1.05
0.35	7.64	5.47	3.61	2.49	1.8	1.41	1.19	1.08
0.45	4.44	3.55	2.66	2.02	1.6	1.32	1.17	1.08
0.5	4.53	3.72	2.87	2.17	1.71	1.41	1.21	1.1
0.75	11.96	9.68	7.26	5.33	3.97	3.02	2.32	1.83
0.9	12.77	10.69	8.68	6.69	5.15	3.9	3.01	2.35

Table B.2.8: Out-of-control ARLs for in-control ARL=11 months for the case of modified control chart based on MEWMA statistic.

λ \ d	-0.05	-0.1	-0.15	-0.2	-0.25	-0.3	-0.35	-0.4
0.1	3.9	2.53	1.46	1.07	1	1	1	1
0.2	4.22	2.99	1.95	1.33	1.09	1.01	1	1
0.25	4.45	3.39	2.28	1.56	1.18	1.04	1	1
0.35	5.2	4.03	2.9	2.07	1.47	1.19	1.05	1
0.45	5.51	4.27	3.14	2.33	1.74	1.33	1.14	1.04
0.5	5.98	4.56	3.51	2.56	1.93	1.48	1.21	1.07
0.75	6.23	5.08	3.77	2.95	2.36	1.89	1.57	1.35
0.9	7.15	5.84	4.33	3.46	2.69	2.25	1.85	1.58

Table B.2.9: Out-of-control ARLs for in-control ARL=11 months for the case of Residual control chart based on Mahalanobis distance.

λ \ d	-0.05	-0.1	-0.15	-0.2	-0.25	-0.3	-0.35	-0.4
0.1	29.47	5.5	1.4	1.01	1	1	1	1
0.2	14.93	5.61	2.18	1.19	1.02	1	1	1
0.25	12.3	5.73	2.49	1.36	1.05	1	1	1
0.35	11.64	6.34	3.32	1.81	1.27	1.06	1	1
0.45	10.28	6.23	3.69	2.22	1.48	1.15	1.04	1
0.5	10.08	6.64	3.96	2.41	1.61	1.26	1.09	1.02
0.75	9.68	7.15	4.94	3.39	2.38	1.81	1.44	1.23
0.9	8.11	6.5	4.72	3.44	2.58	2.02	1.63	1.39

Table B.2.10: Out-of-control ARLs for in-control ARL=11 months for the case of Residual control chart based on MEWMA statistic.

g \ d	-0.05	-0.1	-0.15	-0.2	-0.25	-0.3	-0.35	-0.4
0.1	11.12	11.33	11.3	10.99	11.01	11.1	10.9	10.91
0.3	10.75	11.29	10.85	10.54	11.01	10.91	10.56	10.6
0.5	12.73	12.67	12.76	12.82	13	12.88	13.25	13.23
0.7	9.19	8.9	8.78	8.98	8.81	8.72	8.95	8.97
1	10.33	10.23	10.19	10.38	10.32	10.08	10.35	10.41
1.5	9.05	9.01	9.31	9.31	9.12	9.34	9	9
2	8.07	8.09	7.94	8.16	8.14	8.01	8.05	7.95
2.5	16.47	16.42	16.22	16.1	16.67	16.14	16.75	16.55

Table B.2.11: Out-of-control ARLs for in-control ARL=11 months for the case of MCUSUM control charts.

λ \ d	-0.05	-0.1	-0.15	-0.2	-0.25	-0.3	-0.35	-0.4
0.1	7.84	4.29	2.51	1.7	1.31	1.12	1.04	1.02
0.2	8.15	5.02	3.14	2.02	1.48	1.19	1.09	1.03
0.25	8.22	5.45	3.27	2.14	1.55	1.26	1.12	1.04
0.35	7.07	5.21	3.39	2.37	1.7	1.34	1.16	1.07
0.45	8.33	6.29	4.34	2.94	2.07	1.59	1.32	1.16
0.5	7.74	6.12	4.24	3	2.18	1.69	1.36	1.18
0.75	8.35	7.13	5.51	4.23	3.12	2.41	1.89	1.54
0.9	8.8	7.81	6.46	5.09	3.9	2.94	2.4	1.98

Table B.2.12: Out-of-control ARLs for in-control ARL=11 months for the case of MMOEWMA control chart.

B.3 Non-parallel shifts in yield curve

B.3.1 Positive shifts for a twist in the yield curve

λ \ d	0.05	0.1	0.15	0.2	0.25	0.3	0.35
0.1	47.74	2.95	1	1	1	1	1
0.2	66.53	43.68	22.26	10.35	4.3	1.74	1
0.25	51.99	36.84	20.86	10.53	4.73	2.01	1.18
0.35	40.83	30.34	18.92	11.04	5.82	2.95	1.61
0.45	35.62	27.05	17.61	10.88	6.2	3.63	2.01
0.5	28.37	21.9	14.92	9.49	5.8	3.67	2.03
0.75	12.22	5.51	2.35	1.2	1.02	1	1
0.9	11.17	5.47	2.62	1.38	1.06	1	1

Table B.3.1: Out-of-control ARLs for in-control ARL=11 months for the case of EWMA control chart based on Mahalanobis distance.

λ \ d	0.05	0.1	0.15	0.2	0.25	0.3	0.35
0.1	9.88	4.85	2.72	1.72	1.31	1.13	1.04
0.2	13.7	6.81	3.5	2.15	1.47	1.2	1.06
0.25	12.12	6.34	3.46	2.13	1.48	1.19	1.07
0.35	9.33	5.99	3.51	2.24	1.55	1.23	1.09
0.45	5.23	3.82	2.71	1.85	1.42	1.17	1.05
0.5	12.36	8.86	5.79	3.69	2.42	1.73	1.31
0.75	14.78	12.2	8.88	6.4	4.55	3.21	2.33
0.9	15.48	13.12	10.57	8.04	5.92	4.23	3.18

Table B.3.2: Out-of-control ARLs for in-control ARL=11 months for the case of MEWMA control chart.

λ \ d	0.05	0.1	0.15	0.2	0.25	0.3	0.35
0.1	1.57	1.1	1	1	1	1	1
0.2	2.16	1.43	1.05	1	1	1	1
0.25	2.44	1.69	1.12	1.01	1	1	1
0.35	3.07	2.2	1.43	1.06	1	1	1
0.45	3.35	2.59	1.7	1.15	1.01	1	1
0.5	3.74	2.84	1.13	1.29	1.03	1	1
0.75	4.21	3.44	2.64	1.78	1.26	1.04	1
0.9	4.75	4	3.09	2.23	1.58	1.18	1.02

Table B.3.3: Out-of-control ARLs for in-control ARL=11 months for the case of Residual EWMA control chart based on Mahalanobis distance.

λ \ d	0.05	0.1	0.15	0.2	0.25	0.3	0.35
0.1	39.3	4.5	1.06	1	1	1	1
0.2	19.65	5.84	1.65	1.03	1	1	1
0.25	16.88	6.04	2.05	1.11	1	1	1
0.35	15.84	7.54	3.15	1.54	1.07	1.01	1
0.45	14.03	7.59	3.91	1.98	1.26	1.09	1
0.5	13.58	8.14	4.3	2.24	1.39	1.1	1.01
0.75	13.48	9.22	5.87	3.54	2.3	1.6	1.25
0.9	11.36	8.95	5.92	3.93	2.7	1.96	1.46

Table B.3.4: Out-of-control ARLs for in-control ARL=11 months for the case of Residual control chart based on the MEWMA statistic.

g \ d	0.05	0.1	0.15	0.2	0.25	0.3	0.35
0.1	2.15	1	1	1	1	1	1
0.3	3.75	1	1	1	1	1	1
0.5	7.3	1.25	1	1	1	1	1
0.7	6.89	2.39	1	1	1	1	1
1	9.3	5.61	2.02	1	1	1	1
1.5	8.39	6.73	4.77	2.77	1.25	1	1
2	7.76	6.57	5.32	3.85	2.66	1.65	1.06
2.5	15.9	12.99	10.45	7.55	5.29	3.64	2.39

Table B.3.5: Out-of-control ARLs for in-control ARL=11 months for the case of MCUSUM control chart.

λ \ d	0.05	0.1	0.15	0.2	0.25	0.3	0.35
0.1	14.03	13.86	14.06	14.27	14.33	14.3	13.71
0.2	13.84	13.46	13.65	13.58	13.8	13.52	13.58
0.25	13.57	13.73	13.58	13.94	13.41	13.45	13.74
0.35	11.66	11.51	11.14	11.51	11.47	11.49	11.4
0.45	13.25	13.33	12.92	13.09	13.01	12.99	13.13
0.5	11.51	11.3	11.46	11.59	11.37	11.56	11.41
0.75	11.08	11.52	11.31	11.06	11.13	11.2	11.53
0.9	11.33	11.84	11.38	11.78	11.35	11.45	11.5

Table B.3.6: Out-of-control ARLs for in-control ARL=11 months for the case of MMOEWMA control chart.

B.3.2 Negative shifts for a twist in the yield curve

λ \ d	-0.05	-0.1	- 0.15	-0.2	-0.25	-0.3	-0.35
0.1	69.2	38.1	28.36	12.4	5.4	1.86	1.2
0.2	66.45	4.31	22.4	10.1	4.18	1.74	1.07
0.25	53.4	36.84	20.99	10.42	4.73	2.13	1.18
0.35	41.7	30.62	19.73	10.74	5.65	2.91	1.59
0.45	35.79	27.33	17.38	10.95	6.3	3.47	1.94
0.5	27.55	21.44	15.23	9.75	5.8	3.42	2
0.75	26.88	22.17	16.14	11.15	7.29	4.76	3.19
0.9	21.87	18.39	14.18	9.81	6.86	4.71	3.27

Table B.3.7: Out-of-control ARLs for in-control ARL=11 months for the case of EWMA control chart based on Mahalanobis distance.

λ \ d	-0.05	-0.1	- 0.15	-0.2	-0.25	-0.3	-0.35
0.1	9.16	4.35	2.38	1.54	1.23	1.07	1.02
0.2	19.02	9.38	4.41	2.37	1.55	1.22	1.08
0.25	15.07	8.15	4.19	2.42	1.56	1.23	1.08
0.35	11.03	7.17	4.15	2.53	1.65	1.25	1.1
0.45	5.59	4.26	3	2.01	1.5	1.21	1.07
0.5	5.99	4.52	3.27	2.22	1.63	1.26	1.1
0.75	15.64	13.18	10.06	6.92	4.88	3.32	2.33
0.9	16.2	13.69	11.1	8.55	6.39	4.65	3.31

Table B.3.8: Out-of-control ARLs for in-control ARL=11 months for the case of MEWMA control chart.

λ \ d	-0.05	-0.1	- 0.15	-0.2	-0.25	-0.3	-0.35
0.1	1.58	1.11	1	1	1	1	1
0.2	2.12	1.43	1.05	1	1	1	1
0.25	2.48	1.63	1.12	1	1	1	1
0.35	3.22	2.25	1.41	1.06	1	1	1
0.45	3.38	2.6	1.67	1.16	1	1	1
0.5	3.78	2.91	1.96	1.3	1.03	1	1
0.75	4.1	3.47	2.62	1.75	1.24	1.04	1
0.9	4.69	4.05	3.15	2.25	1.56	1.17	1.02

Table B.3.9: Out-of-control ARLs for in-control ARL=11 months for the case of Residual EWMA chart based on Mahalanobis distance.

λ \ d	-0.05	-0.1	- 0.15	-0.2	-0.25	-0.3	-0.35
0.1	38.31	4.41	1.05	1	1	1	1
0.2	19.64	5.95	1.7	1.03	1	1	1
0.25	16.29	6.33	2.12	1.11	1	1	1
0.35	16.34	7.47	3.09	1.53	1.07	1	1
0.45	14.47	7.72	3.81	1.94	1.25	1.04	1
0.5	14.02	8.14	4.32	2.22	1.4	1.69	1.01
0.75	13.44	9.52	5.8	3.6	2.28	1.63	1.27
0.9	11.22	8.74	5.99	4.04	2.7	1.93	1.46

Table B.3.10: Out-of-control ARLs for in-control ARL=11 months for the case of Residual MEWMA control chart.

g \ d	-0.05	-0.1	- 0.15	-0.2	-0.25	-0.3	-0.35
0.1	2.25	1	1	1	1	1	1
0.3	3.56	1	1	1	1	1	1
0.5	7.55	1.23	1	1	1	1	1
0.7	6.61	2.35	1	1	1	1	1
1	8.84	5.55	2.02	1	1	1	1
1.5	8.52	6.88	4.84	2.79	1.25	1	1
2	7.76	6.89	5.22	3.87	2.7	1.68	1.01
2.5	15.46	13.23	10.11	7.55	5.27	3.62	2.44

Table B.3.11: Out-of-control ARLs for in-control ARL=11 months for the case of MCUSUM control charts.

λ \ d	-0.05	-0.1	- 0.15	-0.2	-0.25	-0.3	-0.35
0.1	13.42	13.71	13.75	13.46	14	13.78	13.67
0.2	13.76	13.31	13.64	13.97	13.69	13.75	13.42
0.25	13.79	13.49	14	13.94	13.62	14.07	13.66
0.35	11.74	11.44	11.38	11.71	11.42	11.32	11.4
0.45	13.17	13.09	13.03	12.82	13.03	13.29	13.13
0.5	11.52	11.35	11.46	11.45	11.7	11.43	11.47
0.75	11.46	11.27	11.21	11.02	11.28	11.12	10.99
0.9	11.35	11.57	11.41	11.64	11.47	11.56	11.45

Table B.3.12: Out-of-control ARLs for in-control ARL=11 months for the case of MMOEWMA control chart.

B.3.3 Negative shifts in positive butterfly

λ \ d	-0.05	-0.1	- 0.15	-0.2	-0.25	-0.3
0.1	-	-	81.18	38.46	9.12	2.25
0.2	62.74	41.81	33.45	19.91	7.72	3.11
0.25	50.94	35.32	29.76	18.72	8.31	3.71
0.35	40.76	30.3	24.76	17.41	8.77	4.68
0.45	34.34	26.83	22.79	16.74	9.12	5.39
0.5	26.59	21.96	18.61	14.26	8.04	4.92
0.75	26.3	21.91	19.72	15.26	9.7	6.43
0.9	21.73	18.83	16.59	13.32	9.03	6.24

Table B.3.13: Out-of-control ARLs for in-control ARL=11 months for the case of EWMA control chart based on the Mahalanobis distance. With '-' we denote that the control charts failed to detect the out-of-control situation.

λ \ d	-0.05	-0.1	- 0.15	-0.2	-0.25	-0.3
0.1	12.24	8.03	4.59	3.02	2.04	1.43
0.2	23.11	15.75	9.28	5.56	3.45	2.06
0.25	17.57	13.12	8.25	5.43	3.35	2.07
0.35	12.04	9.67	7.06	4.87	3.55	2.19
0.45	5.92	5.33	4.2	3.42	2.65	1.87
0.5	6.12	5.55	4.52	3.65	2.92	2.04
0.75	15.76	14.41	11.98	9.86	7.61	5.7
0.9	16.49	15	12.97	10.99	8.91	7

Table B.3.14: Out-of-control ARLs for in-control ARL=11 months for the case of MEWMA control chart.

λ \ d	-0.05	-0.1	- 0.15	-0.2	-0.25	-0.3
0.1	1.75	1.38	1.17	1.05	1	1
0.2	2.29	2.06	1.54	1.33	1.07	1
0.25	2.56	2.28	1.75	1.53	1.16	1.03
0.35	3.21	2.94	2.44	2.02	1.45	1.16
0.45	3.6	3.16	2.73	2.36	1.79	1.31
0.5	3.89	3.65	2.93	2.59	2	1.48
0.75	4.35	4.03	3.5	3.21	2.55	2
0.9	4.9	4.53	4	3.67	3	2.38

Table B.3.15: Out-of-control ARLs for in-control ARL=11 months for the case of Residual control chart based on the Mahalanobis distance.

λ \ d	-0.05	-0.1	- 0.15	-0.2	-0.25	-0.3
0.1	79.4	27.74	6.83	2.2	1.11	1
0.2	28.09	15.9	6.96	3.43	1.75	1.04
0.25	22.26	13.81	7.3	3.84	2.07	1.13
0.35	19.79	13.91	8.54	5.04	3.05	1.52
0.45	16.87	13.11	8.31	5.49	3.71	2.01
0.5	16.24	12.56	8.61	5.72	3.94	2.18
0.75	15.04	12.4	9.62	7.31	5.54	3.39
0.9	12.16	10.89	8.89	7.08	5.73	3.75

Table B.3.16: Out-of-control ARLs for in-control ARL=11 months for the case of Residual MEWMA control chart.

g \ d	-0.05	-0.1	- 0.15	-0.2	-0.25	-0.3
0.1	6.75	1.86	1	1	1	1
0.3	7.58	2.62	1.04	1	1	1
0.5	10.21	5.46	1.67	1.03	1	1
0.7	7.97	5.66	2.66	1.28	1.01	1
1	9.68	7.89	5.62	3.25	1.63	1
1.5	8.82	7.98	6.56	5.23	3.85	2.28
2	7.91	7.29	6.52	5.61	4.51	3.43
2.5	15.76	14.35	12.82	10.64	8.95	6.57

Table B.3.17: Out-of-control ARLs for in-control ARL=11 months for the case of MCUSUM control charts.

λ \ d	-0.05	-0.1	- 0.15	-0.2	-0.25	-0.3
0.1	14.37	14.01	14.21	13.87	13.86	14.25
0.2	13.56	13.61	13.95	13.97	13.88	13.92
0.25	13.66	13.48	13.44	14.08	13.63	13.86
0.35	11.11	11.33	11.46	11.57	11.23	11.78
0.45	13.3	13.24	13.4	13.17	13.26	13.48
0.5	11.35	11.56	11.34	11.49	11.41	11.4
0.75	11.48	11.1	11.27	11.19	11.42	11.15
0.9	11.68	11.21	11.29	11.46	11.55	11.38

Table B.3.18: Out-of-control ARLs for in-control ARL=11 months for the case of MMOEWMA control chart.

B.3.4 Negative shifts in negative butterfly

λ \ d	-0.03	-0.06	- 0.09	-0.12	-0.15	-0.2
0.1	-	-	112.32	62	30.19	9.92
0.2	14.61	13.25	10.93	8.96	6.56	4.34
0.25	57.48	47.7	35.37	24.74	16.19	8.17
0.35	43.97	37.32	29.31	20.9	15.15	8.7
0.45	37.47	31.75	25.79	19.51	14.62	8.94
0.5	29.48	25.51	21.14	16.23	12.05	7.77
0.75	27.82	24.93	21	16.25	13.14	9.15
0.9	22.15	20.46	17.46	14.3	11.46	8.5

Table B.3.19: Out-of-control ARLs for in-control ARL=11 months for the case of EWMA control chart based on Mahalanobis distance. With "-" we dentote that the control chart failed to detect the out-of-control situation.

λ \ d	-0.03	-0.06	- 0.09	-0.12	-0.15	-0.2
0.1	12.36	8.06	4.76	3.07	2.07	1.43
0.2	22.63	15.58	9.01	5.6	3.46	2.1
0.25	17.78	13.19	8.16	5.33	3.47	2.07
0.35	11.96	9.96	7.04	5.01	3.49	2.23
0.45	6	5.27	4.29	3.43	2.58	1.91
0.5	6.22	5.46	4.54	3.67	2.81	2.08
0.75	15.74	14.23	12.03	9.47	7.73	5.63
0.9	16.63	15.24	13	10.93	8.76	6.92

Table B.3.20: Out-of-control ARLs for in-control ARL=11 months for the case of MEWMA control chart.

λ \ d	-0.03	-0.06	- 0.09	-0.12	-0.15	-0.2
0.1	1.65	1.39	1.16	1.06	1	1
0.2	2.22	1.99	1.56	1.3	1.08	1
0.25	2.72	2.18	1.77	1.53	1.16	1.02
0.35	3.36	2.92	2.41	2	1.5	1.15
0.45	3.48	3.2	2.69	2.35	1.76	1.3
0.5	3.93	3.64	2.99	2.62	2	1.44
0.75	4.24	3.97	3.59	3.17	2.56	1.94
0.9	4.77	4.59	4.03	3.67	3.02	2.43

Table B.3.21: Out-of-control ARLs for in-control ARL=11 months for the case of Residual EWMA control chart based on Mahalanobis distance.

λ \ d	-0.03	-0.06	- 0.09	-0.12	-0.15	-0.2
0.1	81.31	27.93	6.9	2.21	1.11	1
0.2	28.56	15.95	6.9	3.39	1.75	1.05
0.25	21.74	14.2	7.17	3.93	2.13	1.13
0.35	19.23	13.66	8	5.02	3.12	1.53
0.45	16.44	12.57	8.46	5.59	3.7	1.98
0.5	16.21	12.76	8.8	5.91	3.98	2.21
0.75	14.7	13.09	10.48	8.63	6.31	3.44
0.9	12.19	11.08	9.25	7.56	6.01	3.68

Table B.3.22: Out-of-control ARLs for in-control ARL=11 months for the case of Residual MEWMA control chart.

g \ d	-0.03	-0.06	- 0.09	-0.12	-0.15	-0.2
0.1	6.62	1.97	1	1	1	1
0.3	7.43	2.74	1.05	1	1	1
0.5	10.6	5.36	1.59	1.02	1	1
0.7	7.91	5.47	2.72	1.27	1.01	1
1	9.71	7.6	5.52	3.18	1.53	1.01
1.5	9	8.06	6.91	5.32	3.98	2.18
2	7.97	7.32	6.47	5.7	4.51	3.29
2.5	15.8	14.43	12.88	10.58	8.84	6.62

Table B.3.23: Out-of-control ARLs for in-control ARL=11 months for the case of MCUSUM control charts.

λ \ d	-0.03	-0.06	- 0.09	-0.12	-0.15	-0.2
0.1	14.29	14.12	13.88	14.31	14.25	14.21
0.2	13.67	13.71	14.16	13.71	13.81	14.11
0.25	14.01	14.06	13.85	13.58	13.66	13.82
0.35	11.37	11.56	11.25	11.47	11.63	11.65
0.45	12.89	12.9	13.03	13.13	13.02	13.05
0.5	11.52	11.34	11.38	11.57	11.37	11.48
0.75	11.11	11.5	11.19	11.61	11.31	11.37
0.9	11.7	11.35	11.21	11.42	11.84	11.49

Table B.3.24: Out-of-control ARLs for in-control ARL=11 months for the case of MMOEWMA control chart.

B.3.5 Positive shifts in positive butterfly

λ \ d	0.05	0.1	0.15	0.2	0.25	0.3
0.1	-	-	55.15	45.25	9.17	2.29
0.2	63.19	41.69	33.2	20.19	7.52	3.05
0.25	49.76	36.3	29.35	19.24	8.25	3.7
0.35	40.19	30.09	24.78	17.46	4.13	2.34
0.45	34.06	27.28	22.7	17	9.16	5.41
0.5	26.63	21.59	18.61	14.27	8.1	4.88
0.75	26.19	21.65	19.57	15.37	9.67	6.52
0.9	21.66	19.08	16.27	13.46	8.89	6.38

Table B.3.25: Out-of-control ARLs for in-control ARL=11 months for the case of EWMA control chart based on the Mahalanobis distance. With "-" we denote that the control chart failed to detect the out-of-control situation.

λ \ d	0.05	0.1	0.15	0.2	0.25	0.3
0.1	10.62	5.6	4.06	2.64	1.56	1.23
0.2	38.66	18.06	12.17	6.66	3.01	1.84
0.25	71.65	33.02	21.47	11.97	4.87	2.66
0.35	-	44.52	35.2	31.58	12.66	6.04
0.45	-	56.15	41.9	72.02	29.17	13.62
0.5	-	-	-	-	41.75	20.30
0.75	-	-	-	-	42.49	20.37
0.9	-	-	-	-	45.8	22.14

Table B.3.26: Out-of-control ARLs for in-control ARL=11 months for the case of MEWMA control chart. With "-" we denote that the control chart failed to detect the out-of-control situation.

λ \ d	0.05	0.1	0.15	0.2	0.25	0.3
0.1	1.18	1	1	1	1	1
0.2	1.63	1.11	1.04	1	1	1
0.25	1.84	1.25	1.11	1	1	1
0.35	2.51	1.64	1.4	1.04	1	1
0.45	2.91	1.92	1.61	1.16	1	1
0.5	3.12	2.23	1.86	1.28	1	1.01
0.75	3.64	2.79	2.48	1.79	1.07	1.06
0.9	4.23	3.37	3.02	2.18	1.75	1.09

Table B.3.27: Out-of-control ARLs for in-control ARL=11 months for the case of Residual EWMA control chart based on Mahalanobis distance.

λ \ d	0.05	0.1	0.15	0.2	0.25	0.3
0.1	27.63	3.74	1.64	1.02	1	1
0.2	16.4	5.3	3.1	1.4	1	1
0.25	14.53	5.94	3.54	1.71	1.03	1
0.35	14.11	7.17	5	2.66	1.26	1.03
0.45	13.09	7.57	5.62	3.38	1.6	1.14
0.5	12.09	7.88	5.92	3.77	1.86	1.24
0.75	12.96	9.26	7.82	5.43	3	2.03
0.9	11.07	8.7	7.59	5.64	3.44	2.4

Table B.3.28: Out-of-control ARLs for in-control ARL=11 months for the case of Residual MEWMA control chart.

g \ d	0.05	0.1	0.15	0.2	0.25	0.3
0.1	1.23	1	1	1	1	1
0.3	2.08	1	1	1	1	1
0.5	5.58	1.1	1	1	1	1
0.7	6.04	2.13	1.2	1	1	1
1	8.67	5.34	3.75	1.58	1	1
1.5	8.11	6.9	6.05	4.44	2.06	1.06
2	7.57	6.66	6.13	4.98	3.42	2.36
2.5	15	13.05	12.07	9.75	6.88	4.85

Table B.3.29: Out-of-control ARLs for in-control ARL=11 months for the case of MCUSUM control charts.

λ \ d	0.05	0.1	0.15	0.2	0.25	0.3
0.1	14.04	14.17	13.97	14.31	14.05	14.13
0.2	13.77	13.78	13.61	13.62	13.58	13.73
0.25	13.86	13.66	13.48	13.83	14.13	13.85
0.35	11.45	11.62	11.71	11.4	11.4	11.68
0.45	13.06	13.18	13.04	13	12.72	13.33
0.5	11.73	11.6	11.2	11.6	11.45	11.01
0.75	11.41	11.26	11.23	11.52	11.52	11.37
0.9	11.55	11.43	11.56	11.47	11.54	11.33

Table B.3.30: Out-of-control ARLs for in-control ARL=11 months for the case of MMOEWMA control chart.

B.3.6 Positive shifts in negative butterfly

λ \ d	0.03	0.06	0.09	0.12	0.15	0.2
0.1	-	-	-	62.3	30.33	10.36
0.2	-	-	40.33	27.06	16.91	8.01
0.25	-	-	35.53	24.09	16.13	8.04
0.35	-	-	28.74	21.49	14.91	8.64
0.45	-	-	25.99	19.34	14.21	9.02
0.5	-	-	20.82	16.07	12.18	7.77
0.75	-	-	20.71	16.82	13.28	9.07
0.9	22.73	20.88	17.93	14.92	11.55	8.54

Table B.3.31: Out-of-control ARLs for in-control ARL=11 months for the case of EWMA control chart based on the Mahalanobis distance. With "-" we denote that the control chart failed to detect the out-of-control situation.

λ \ d	0.03	0.06	0.09	0.12	0.15	0.2
0.1	13.47	9.46	5.51	3.32	2.18	1.49
0.2	20.42	13.05	7.92	4.9	3.13	1.9
0.25	16.05	11.32	7.1	4.65	3.16	1.98
0.35	11.48	8.92	6.17	4.41	3.1	2.09
0.45	5.81	4.94	4.07	3.18	2.52	1.81
0.5	5.92	5.25	4.25	3.43	2.7	1.99
0.75	15.19	13.51	11.15	8.8	6.89	5.22
0.9	16.05	14.39	12.66	10.36	8.21	6.50

Table B.3.32: Out-of-control ARLs for in-control ARL=11 months for the case of MEWMA control chart.

λ \ d	0.03	0.06	0.09	0.12	0.15	0.2
0.1	-	-	78.72	48.54	17.11	4.87
0.2	-	-	22.73	16.51	8.65	3.9
0.25	-	21.75	16.13	12.43	7.11	3.41
0.35	14.95	12.71	10.41	8.38	5.39	3.12
0.45	10.6	9.43	7.72	6.5	4.49	2.94
0.5	9.12	8.28	6.91	5.92	4.24	2.77
0.75	5.8	5.34	4.63	4.17	3.23	2.56
0.9	4.80	4.52	4.05	3.65	2.99	2.45

Table B.3.33: Out-of-control ARLs for in-control ARL=11 months for the case of Residual EWMA control chart based on the Mahalanobis distance. With "-" we denote that the control chart failed to detect the out-of-control situation.

λ \ d	0.03	0.06	0.09	0.12	0.15	0.2
0.1	63.15	32.93	12.89	5.69	2.72	1.16
0.2	59.28	32.73	14.71	7.49	3.67	1.46
0.25	54.33	34.55	17.72	9.86	5.65	2.37
0.35	50.51	35.29	20.21	12	7.32	3.39
0.45	49.89	35.7	27.07	13.2	8.25	4.01
0.5	50.16	35.51	21.43	13.41	8.05	3.89
0.75	48.53	39.73	27.03	19.16	12.56	7.09
0.9	48.18	40.52	30.65	23.32	15.89	9.35

Table B.3.34: Out-of-control ARLs for in-control ARL=11 months for the case of Residual MEWMA control chart.

g \ d	0.03	0.06	0.09	0.12	0.15	0.2
0.1	6.93	1.97	1.01	1	1	1
0.3	50.68	14.46	2.16	1.04	1	1
0.5	-	-	17.16	2.8	1.07	1
0.7	-	-	-	23.89	3.62	1
1	-	-	-	-	86.1	5.66
1.5	-	-	-	-	55.14	8.61
2	-	-	-	-	66.18	11.5
2.5	-	-	-	-	42.1	8.4

Table B.3.35: Out-of-control ARLs for in-control ARL=11 months for the case of MCUSUM control charts. With "-" we denote that the control chart failed to detect the out-of-control situation.

λ \ d	0.03	0.06	0.09	0.12	0.15	0.2
0.1	14.26	14.33	13.73	13.98	13.57	14.36
0.2	13.99	13.35	13.14	13.95	13.8	13.79
0.25	13.59	13.94	13.77	13.36	13.7	13.77
0.35	11.43	11.3	11.53	11.25	11.56	11.6
0.45	13.24	13.27	13.42	12.81	13.4	13.05
0.5	11.57	11.28	11.65	11.41	11.58	11.25
0.75	11.42	11.25	11.39	11.46	11.28	11.19
0.9	11.55	11.43	11.56	11.47	11.54	11.33

Table B.3.36: Out-of-control ARLs for in-control ARL=11 months for the case of MMOEWMA control chart.

B.4 VARMA ATSM Simulation study results

B.4.1 Modified EWMA chart based on the Mahalanobis distance

$\lambda = 0.1$

d_1 \ d_2	-0.4	-0.3	-0.2	-0.1	0.1	0.2	0.3	0.4
-0.4	2.1746	2.0526	2.1510	2.1982	2.1106	2.0124	2.0454	2.0960
-0.3	2.2663	2.1504	2.0807	2.0880	2.1467	2.0113	2.2723	2.0563
-0.2	2.1537	2.0230	1.9936	2.0330	2.1913	2.2877	2.1020	2.5280
-0.1	2.0720	2.5447	2.0830	2.1502	2.0177	2.1707	2.2613	2.0917
0.1	2.0450	2.4773	2.0917	2.3950	2.1408	2.1403	2.2823	2.2867
0.2	2.2350	2.0413	2.0647	2.1943	1.9867	2.0854	2.0477	2.1810
0.3	2.0240	2.3497	2.0907	2.0680	2.1320	2.0327	2.1586	2.0870
0.4	2.1352	2.0506	2.1164	2.1372	2.1026	2.1062	2.1772	2.1264

$\lambda = 0.2$

d_1 \ d_2	-0.4	-0.3	-0.2	-0.1	0.1	0.2	0.3	0.4
-0.4	2.2348	2.1382	2.2426	2.2240	2.2912	2.3828	2.1810	2.2916
-0.3	2.1990	2.1888	2.4617	2.4800	2.4023	2.1560	2.4150	2.4233
-0.2	2.4817	2.1617	2.2612	2.3380	2.2347	2.3177	2.1730	2.1507
-0.1	2.4443	2.9130	2.1327	2.1546	2.5187	2.3507	2.2343	2.3887
0.1	2.1280	2.1527	2.1310	2.2783	2.2782	2.1577	2.1510	2.1793
0.2	2.2953	2.0730	2.3103	2.2277	2.3827	2.7654	2.0903	2.2793
0.3	2.3160	2.1663	2.1307	2.1833	2.2220	2.2200	2.1796	2.1713
0.4	2.1878	2.0802	2.2252	2.1500	2.6322	2.4902	2.1598	2.2712

$\lambda = 0.3$

d_1 \ d_2	-0.4	-0.3	-0.2	-0.1	0.1	0.2	0.3	0.4
-0.4	2.7018	2.4554	2.4614	2.4598	2.2822	2.569	2.4400	2.5812
-0.3	2.3313	2.4406	2.3120	2.4190	2.5197	3.0630	2.3233	2.3193
-0.2	2.4573	2.4200	2.2998	2.4787	2.8077	2.6193	2.3630	2.5767
-0.1	2.3153	2.4883	2.3923	2.3090	2.2783	2.4030	2.5150	2.4147
0.1	2.7567	2.5030	2.6960	2.2580	2.3400	2.4380	2.3367	2.2950
0.2	2.3157	2.5430	2.6210	2.4793	2.3957	2.5242	2.3993	2.7067
0.3	2.7097	2.4233	2.9137	2.2577	2.3987	2.3443	2.4130	2.3923
0.4	2.2203	2.5563	2.4120	2.2357	2.7347	2.5140	2.2577	2.3368

$\lambda = 0.4$

d_1 \ d_2	-0.4	-0.3	-0.2	-0.1	0.1	0.2	0.3	0.4
-0.4	2.5308	2.5854	2.4962	2.3934	2.7636	2.5654	2.5846	2.5836
-0.3	2.5093	2.5594	2.3253	2.3420	2.7040	2.4990	2.7520	2.6410
-0.2	2.3813	2.4637	2.5378	2.8347	2.2510	2.5777	2.4513	2.5833
-0.1	2.7097	2.9893	2.4757	2.6258	3.0120	2.7393	2.7997	2.8717
0.1	2.3953	2.4310	2.9023	2.3903	2.6662	2.4623	2.6017	2.4710
0.2	2.2.2893	2.7713	3.1333	2.3697	2.4470	2.5742	2.5583	2.3507
0.3	2.7363	2.6433	2.7607	2.6450	2.9433	2.4380	2.9292	2.5933
0.4	2.6177	2.6753	2.5380	2.5540	2.7947	2.6703	3.0030	2.5088

$\lambda = 0.5$

d_1 \ d_2	-0.4	-0.3	-0.2	-0.1	0.1	0.2	0.3	0.4
-0.4	3.0578	3.0676	2.8860	3.2692	3.8950	3.4368	2.7330	3.6520
-0.3	2.8373	2.9654	3.0230	2.9420	3.1023	3.1550	2.5827	2.9360
-0.2	2.7147	4.7203	3.1712	3.0203	3.0173	3.0630	3.4377	4.1413
-0.1	3.5513	2.6247	3.0607	2.8652	2.7803	3.2157	2.7027	2.9830
0.1	3.2830	2.9803	2.8067	2.9113	2.7452	3.0967	4.2123	2.7283
0.2	3.0117	4.2037	3.2603	2.7690	2.8247	3.5020	3.0243	3.0127
0.3	3.4933	2.7867	2.7113	3.0820	3.3570	3.1783	4.5844	3.9463
0.4	2.5663	3.0143	3.3353	2.7323	3.3420	3.2433	2.7963	3.0748

$\lambda = 0.6$

d_1 \ d_2	-0.4	-0.3	-0.2	-0.1	0.1	0.2	0.3	0.4
-0.4	3.4494	3.4508	3.2046	3.6150	3.9324	3.9856	3.3424	3.4370
-0.3	3.3157	3.2684	3.4287	3.6600	3.2297	3.0533	3.1480	3.0737
-0.2	3.4340	3.5527	3.8704	4.4390	4.1063	3.5357	3.2867	2.7683
-0.1	2.9857	3.1110	3.2267	3.4940	3.6280	3.2447	3.2937	3.2407
0.1	3.7063	3.3830	3.1240	2.9673	3.1346	3.0817	3.0207	3.3240
0.2	3.0480	3.8617	3.5153	2.8410	3.1340	3.1822	3.7650	3.6370
0.3	3.5370	3.4617	2.9813	3.0040	5.8447	3.0090	3.0800	3.2447
0.4	3.0767	4.2893	4.1510	2.9980	3.3153	4.8187	2.7660	3.0336

$\lambda = 0.7$

d_1 \ d_2	-0.4	-0.3	-0.2	-0.1	0.1	0.2	0.3	0.4
-0.4	4.7072	4.1002	4.8674	6.7524	5.5128	5.5464	5.1988	3.7088
-0.3	3.8227	4.0136	3.8700	4.4720	4.1603	5.0490	3.7123	4.1017
-0.2	4.4203	4.0873	3.6768	3.5950	4.2263	4.6687	3.9560	4.1100
-0.1	3.5800	4.4280	5.3150	6.2754	5.5390	5.1283	6.4270	4.4410
0.1	4.9090	3.9223	4.2303	4.4940	3.8526	3.5197	3.3527	3.6867
0.2	3.7373	4.1940	3.8720	3.6447	3.7157	5.3226	4.0407	4.4923
0.3	3.9627	4.2223	5.5920	6.8543	3.5147	4.0953	4.9716	4.0030
0.4	4.0157	3.8897	3.6310	3.7860	3.2443	3.7637	3.3313	3.5836

$\lambda = 0.9$

d_1 \ d_2	-0.4	-0.3	-0.2	-0.1	0.1	0.2	0.3	0.4
-0.4	10.3270	14.7660	12.3940	9.8972	15.6692	14.1892	15.1136	11.6218
-0.3	9.0983	10.5170	8.7407	8.2530	7.5270	12.2537	11.1547	9.9680
-0.2	9.6420	7.3993	11.1047	11.6790	9.9697	8.2740	10.1030	12.8937
-0.1	13.7073	10.8523	10.6483	10.7620	10.4703	7.3540	10.8960	8.8590
0.1	7.8907	17.4400	17.0293	9.9747	12.8333	7.7073	10.8470	11.3843
0.2	9.3217	8.3690	12.9400	10.7497	9.6837	7.7073	10.8470	11.3843
0.3	7.9960	11.0257	7.1170	10.4750	10.8583	7.6193	11.1587	11.2940
0.4	9.8030	14.3847	12.7297	10.9877	14.7320	10.1297	10.3057	10.9793

B.4.2 Modified Chart Based on the Multivariate EWMA Statistic

$\lambda = 0.1$

d_1 \ d_2	-0.4	-0.3	-0.2	-0.1	0.1	0.2	0.3	0.4
-0.4	8.1905	8.3250	8.0892	8.2360	8.1227	8.2555	8.2927	8.3313
-0.3	8.1828	8.2775	8.1950	8.4055	8.0378	8.3462	8.2148	8.1475
-0.2	8.3872	8.3455	8.2180	8.4392	8.1532	8.4772	8.4330	8.1807
-0.1	8.2982	8.2523	8.2568	8.3845	8.4927	8.3855	8.3810	8.1500
0.1	8.2900	8.1438	8.5068	8.3993	8.5305	8.4205	8.2065	8.4010
0.2	8.4288	8.2402	8.2833	8.3277	8.2797	8.3630	8.4135	8.0642
0.3	8.2372	8.0593	8.1265	8.2892	8.1950	8.3255	8.2150	8.1990
0.4	8.2583	8.0183	8.0158	8.4243	8.4665	8.2510	8.1990	8.3110

$\lambda = 0.2$

d_1 \ d_2	-0.4	-0.3	-0.2	-0.1	0.1	0.2	0.3	0.4
-0.4	8.7602	8.7312	8.8703	9.0017	8.6828	9.0533	8.6877	8.8227
-0.3	9.0162	8.9012	9.1600	8.9105	8.8730	8.6468	8.9765	8.8997
-0.2	8.8788	8.7127	9.0777	8.7058	8.8727	8.9283	8.6760	8.8460
-0.1	8.8945	9.0290	8.6935	8.8778	8.9462	8.8562	8.9482	8.7892
0.1	8.6485	8.7505	8.9727	8.9355	8.9078	8.7755	8.8473	8.7425
0.2	8.6342	8.7560	8.5715	8.9678	8.9395	8.7513	9.1542	8.8130
0.3	8.7610	8.7807	8.8737	8.6845	8.9507	8.6150	8.8565	8.9273
0.4	8.6540	8.8060	9.1380	8.7290	8.9128	9.0233	8.9273	8.7293

$\lambda = 0.3$

d_1 \ d_2	-0.4	-0.3	-0.2	-0.1	0.1	0.2	0.3	0.4
-0.4	8.6922	8.8325	8.7082	9.0457	8.9465	8.7050	8.9440	8.9070
-0.3	8.8250	9.0570	8.6535	8.6155	8.6445	8.6888	8.7427	8.8200
-0.2	8.8432	8.7090	8.9165	8.8280	8.7937	8.6080	8.6945	8.8148
-0.1	8.6550	8.8383	8.7535	9.0140	8.8825	8.6568	8.9042	8.9817
0.1	9.0175	8.7602	8.9548	8.6877	8.5665	8.7152	8.5973	8.7668
0.2	8.8285	8.8245	8.7472	8.6565	9.0500	8.6795	8.8085	8.7345
0.3	8.8912	8.8283	8.7133	8.5582	8.6738	8.8323	8.7752	8.8242
0.4	8.7338	8.8443	8.8490	8.6598	8.6768	8.7317	8.9335	8.9040

$\lambda = 0.4$

d_1 \ d_2	-0.4	-0.3	-0.2	-0.1	0.1	0.2	0.3	0.4
-0.4	6.3613	6.4207	6.5113	6.2382	6.3472	6.4203	6.3890	6.5625
-0.3	6.2533	6.6913	6.5160	6.5285	6.2908	6.6357	6.3735	6.5195
-0.2	6.5625	6.4140	6.4742	6.4588	6.4190	6.3120	6.5427	6.4165
-0.1	6.3950	6.4135	6.3370	6.2690	6.4772	6.4848	6.4400	6.4895
0.1	6.4810	6.4982	6.3540	6.6753	6.3935	6.2793	6.4680	6.4283
0.2	6.4275	6.4285	6.3863	6.5345	6.4307	6.4648	6.4832	6.5205
0.3	6.3982	6.4028	6.4748	6.2955	6.4085	6.3092	6.4920	6.5338
0.4	6.2965	6.4480	6.3055	6.5252	6.2957	6.4385	6.4588	6.5140

$\lambda = 0.5$

d_1 \ d_2	-0.4	-0.3	-0.2	-0.1	0.1	0.2	0.3	0.4
-0.4	5.5633	5.5225	5.4100	5.4195	5.4240	5.3875	5.4795	5.5095
-0.3	5.4367	5.5352	5.4508	5.3838	5.4997	5.4088	5.2603	5.4153
-0.2	5.5347	5.5215	5.4352	5.4532	5.5432	5.4523	5.5362	5.2880
-0.1	5.5285	5.4465	5.5053	5.3228	5.4060	5.4502	5.5045	5.4713
0.1	5.3765	5.4655	5.4088	5.4902	5.5925	5.3412	5.5243	5.3907
0.2	5.5125	5.4290	5.5713	5.6070	5.4627	5.4110	5.4935	5.4908
0.3	5.4662	5.4932	5.4527	5.4158	5.3735	5.4955	5.4612	5.4547
0.4	5.4328	5.3563	5.5115	5.5198	5.5255	5.5827	5.4923	5.4502

$\lambda = 0.6$

d_1 \ d_2	-0.4	-0.3	-0.2	-0.1	0.1	0.2	0.3	0.4
-0.4	4.5762	4.6018	4.5105	4.6470	4.6200	4.5790	4.5793	4.5738
-0.3	4.5883	4.5660	4.5985	4.5968	4.5427	4.5003	4.4843	4.5918
-0.2	4.6050	4.6268	4.6673	4.5050	4.5462	4.6655	4.6605	4.6342
-0.1	4.6413	4.6270	4.6700	4.6292	4.5295	4.4930	4.5370	4.4547
0.1	4.6327	4.5702	4.6195	4.5905	4.5423	4.4173	4.5385	4.5435
0.2	4.4975	4.7780	4.6145	4.5505	4.5047	4.5682	4.5225	4.6487
0.3	4.6480	4.5894	4.5700	4.5888	4.5122	4.7118	4.4967	4.6917
0.4	4.6558	4.4417	4.5580	4.5347	4.6075	4.4943	4.5118	4.5278

$\lambda = 0.7$

d_1 \ d_2	-0.4	-0.3	-0.2	-0.1	0.1	0.2	0.3	0.4
-0.4	3.8733	3.8055	3.7015	3.8197	3.7778	3.7925	3.8270	3.6605
-0.3	3.7452	3.7578	3.8035	3.8405	3.8140	3.7420	3.7220	3.8287
-0.2	3.8657	3.7692	3.7710	3.8102	3.7593	3.8207	3.8293	3.6702
-0.1	3.7045	3.8080	3.8218	3.7572	3.8030	3.9220	3.7393	3.8298
0.1	3.8222	3.9143	3.7723	3.7687	3.8575	3.7410	3.8468	3.8803
0.2	3.7763	3.8763	3.8810	3.8635	3.7468	3.7985	3.7872	3.9038
0.3	3.7458	3.7778	3.7980	3.8535	3.7683	3.7342	3.7920	3.8345
0.4	3.8245	3.9017	3.8825	3.8977	3.7612	3.8268	3.8013	3.8400

$\lambda = 0.9$

d_1 \ d_2	-0.4	-0.3	-0.2	-0.1	0.1	0.2	0.3	0.4
-0.4	2.8098	2.7753	2.7923	2.8050	2.7492	2.8258	2.7942	2.7793
-0.3	2.7770	2.7440	2.8310	2.8330	2.8105	2.7832	2.8740	2.8150
-0.2	2.8218	2.7978	2.8450	2.7948	2.8070	2.7628	2.7473	2.8392
-0.1	2.8685	2.8255	2.7445	2.8403	2.7520	2.7520	2.8390	2.7418
0.1	2.7690	2.8382	2.8312	2.8592	2.7767	2.8502	2.8518	2.7830
0.2	2.8450	2.8093	2.8555	2.8108	2.8145	2.8045	2.7938	2.8155
0.3	2.8180	2.7927	2.8683	2.8050	2.8308	2.8255	2.8400	2.7538
0.4	2.8235	2.7877	2.8080	2.7920	2.8105	2.8763	2.8708	2.8268

B.4.3 EWMA Residual Chart Based on the Mahalanobis Distance

$\lambda = 0.1$

d_1 \ d_2	-0.4	-0.3	-0.2	-0.1	0.1	0.2	0.3	0.4
-0.4	3.0125	3.3208	3.2167	2.8625	3.2625	2.7042	2.9917	2.8458
-0.3	3.3208	2.7917	2.7000	2.8417	3.0208	2.8833	3.1042	3.1792
-0.2	2.6667	3.4458	2.8500	2.9083	3.2375	2.6625	2.9042	3.6625
-0.1	3.3750	3.0667	2.9000	2.9625	3.0042	3.1833	3.1542	3.1833
0.1	3.0042	3.2208	2.9542	2.9250	3.0792	2.8250	3.4750	2.6375
0.2	3.0458	2.9833	2.9625	3.2625	2.6750	3.0542	2.8542	3.1750
0.3	3.0708	2.6833	2.8375	3.5042	3.1417	2.9375	3.0875	3.5792
0.4	3.5625	2.8583	2.5542	2.8292	2.7708	2.7667	3.0250	2.7792

$\lambda = 0.2$

d_1 \ d_2	-0.4	-0.3	-0.2	-0.1	0.1	0.2	0.3	0.4
-0.4	4.8875	6.0833	6.5542	5.5500	7.4125	6.8083	6.0167	5.0792
-0.3	5.7625	5.9917	6.7708	5.9125	7.6833	5.5417	6.3458	7.7708
-0.2	6.5125	5.9667	6.6542	5.4875	5.9292	7.4375	4.8750	6.5583
-0.1	4.8042	6.6708	6.8917	5.3542	5.3083	5.9458	7.2250	6.0958
0.1	6.6583	6.5875	6.1417	6.8667	7.2917	6.1792	8.2208	6.4625
0.2	5.8542	4.7083	5.7833	6.4542	5.9292	6.2875	6.8708	4.6500
0.3	8.5125	6.7375	5.6583	6.9500	6.2292	5.8292	6.1542	6.4333
0.4	5.4750	5.2000	5.1667	4.3958	4.8458	5.4292	6.8083	6.2000

$\lambda = 0.3$

d_1 \ d_2	-0.4	-0.3	-0.2	-0.1	0.1	0.2	0.3	0.4
-0.4	10.5208	12.1500	9.8167	8.9417	12.8083	10.6167	13.1917	10.8000
-0.3	12.4917	10.7042	10.9708	9.5000	10.9500	11.1500	9.4958	13.7708
-0.2	11.9083	10.0083	12.7542	14.4500	10.6083	9.6000	11.3083	10.9167
-0.1	10.4042	8.8708	9.3958	8.6750	9.9792	9.4708	9.0083	10.3458
0.1	9.0458	9.9292	8.6125	12.4542	14.8292	8.3042	14.6917	10.2375
0.2	11.2583	11.3417	8.6125	10.0750	8.0917	10.7125	7.9208	10.3625
0.3	9.0125	10.0042	12.9042	9.9875	10.7042	10.1625	11.9750	9.4917
0.4	7.9667	10.8042	7.8708	8.4542	11.4667	9.3667	13.9583	13.9458

$\lambda = 0.4$

d_1 \ d_2	-0.4	-0.3	-0.2	-0.1	0.1	0.2	0.3	0.4
-0.4	20.7875	13.2000	20.9042	16.5000	17.5500	19.5750	21.1625	20.7583
-0.3	18.8542	23.7667	18.0250	15.3542	18.5208	17.5542	17.5500	24.5208
-0.2	20.5167	23.0500	19.5250	20.6375	20.6500	14.8917	18.9833	18.5292
-0.1	17.2917	15.8208	20.0500	17.2458	17.1583	20.1333	14.1958	19.1000
0.1	19.5833	17.8667	20.4500	20.2833	17.0833	17.1708	18.7208	19.0708
0.2	18.2458	15.8667	17.6292	14.4833	17.7500	19.6000	18.8583	21.2250
0.3	17.4500	21.2333	16.4875	19.3083	20.0958	11.0917	18.4208	17.8500
0.4	18.6083	14.6792	17.9000	20.7000	21.8167	17.7375	14.6750	16.7750

$\lambda = 0.5$

d_1 \ d_2	-0.4	-0.3	-0.2	-0.1	0.1	0.2	0.3	0.4
-0.4	27.8667	28.0833	30.5333	32.0667	29.2917	34.8083	28.2083	26.5958
-0.3	29.2917	27.7333	26.3208	27.5375	29.9917	32.3208	29.8292	23.8375
-0.2	28.0833	23.3625	23.8750	28.4083	23.7042	26.6875	25.8792	23.3167
-0.1	26.8500	25.3917	27.3083	24.1458	29.4042	29.1333	28.2167	25.2667
0.1	22.9458	29.0917	28.8667	30.0708	33.6333	25.9292	32.2042	31.9000
0.2	24.4042	29.8792	29.4833	27.8250	29.1000	32.4917	26.5208	24.7417
0.3	24.6875	35.0458	26.5167	24.7417	26.2250	29.1875	30.7167	22.7792
0.4	29.6167	29.7167	27.4292	29.2375	28.3792	28.4875	29.8333	28.1542

$\lambda = 0.6$

d_1 \ d_2	-0.4	-0.3	-0.2	-0.1	0.1	0.2	0.3	0.4
-0.4	44.0875	44.2417	36.2250	40.7042	45.9000	41.8125	41.0000	35.5750
-0.3	40.7875	42.0125	50.3292	45.3208	32.7792	35.6958	41.6875	38.6667
-0.2	43.0208	45.6208	32.5125	38.0833	40.4417	44.2292	41.4417	43.0250
-0.1	47.1083	31.8833	47.6333	41.3250	39.1917	41.1583	38.0583	41.7583
0.1	41.2708	34.6500	34.5667	39.4750	41.0208	40.2542	38.2917	36.3083
0.2	37.8417	37.8042	44.9125	39.3000	38.2542	41.2792	42.1750	40.4583
0.3	35.4083	40.7333	45.2333	42.8292	41.6208	39.4042	40.1750	37.0750
0.4	47.3958	42.7667	36.6917	40.6708	51.6625	35.6458	36.0792	43.8417

$\lambda = 0.7$

d_1 \ d_2	-0.4	-0.3	-0.2	-0.1	0.1	0.2	0.3	0.4
-0.4	48.0000	53.9542	49.3375	46.0333	46.9333	51.3125	44.1250	49.0792
-0.3	41.8875	49.7833	50.3292	45.3208	32.7792	35.6958	41.6875	38.6667
-0.2	42.0250	47.2250	45.9458	46.9375	43.7542	40.5500	52.4292	55.8000
-0.1	47.3083	53.3458	41.5208	48.4833	51.9875	46.0417	45.4458	49.6917
0.1	49.7375	47.1833	48.4292	50.4250	47.0500	53.2250	54.1000	43.7042
0.2	47.2458	46.3292	45.1375	53.9250	51.2542	51.1292	45.7375	57.0625
0.3	41.8542	47.5375	51.7583	47.1083	48.1833	44.9583	42.2000	43.1958
0.4	44.3292	41.8583	45.2125	49.9458	44.1917	54.6792	54.1125	48.3958

$\lambda = 0.9$

d_1 \ d_2	-0.4	-0.3	-0.2	-0.1	0.1	0.2	0.3	0.4
-0.4	54.9167	57.5708	61.8042	52.9250	55.0750	55.1125	66.3292	57.6667
-0.3	60.8708	53.6125	60.1500	57.6083	58.3625	53.0250	56.3708	60.7083
-0.2	50.0583	64.1208	59.5000	60.0792	58.2208	56.0167	53.5958	50.3500
-0.1	55.1375	57.9625	59.9417	59.9208	61.9000	50.0375	55.5500	60.8375
0.1	61.5667	55.4375	59.2833	63.6125	60.4792	49.7583	50.8875	52.0583
0.2	52.1958	58.7833	53.0125	54.3000	55.6625	61.0542	46.4000	59.6875
0.3	50.1875	61.5583	59.0542	48.1458	58.9000	61.7042	59.5833	60.4208
0.4	51.9250	56.9125	55.9708	61.7208	57.8375	55.8750	55.8292	58.8875

B.4.4 Residual Chart Based on the Multivariate EWMA Statistic

$\lambda = 0.1$

d_1 \ d_2	-0.4	-0.3	-0.2	-0.1	0.1	0.2	0.3	0.4
-0.4	20.3852	21.0040	21.4632	20.6268	21.0802	21.1227	20.9750	20.9443
-0.3	21.4390	20.9930	20.8863	21.1710	21.4853	21.2305	21.3890	21.5975
-0.2	20.9348	21.4110	21.5065	21.0485	20.8900	21.4597	21.5910	20.4110
-0.1	21.6172	21.0415	20.8128	21.2347	20.6968	21.4123	21.1687	20.9500
0.1	21.0727	20.4932	21.4830	20.3970	21.0162	21.3115	20.7285	20.7685
0.2	20.4803	20.9627	21.0338	20.5008	20.9617	21.1762	21.0182	20.8663
0.3	21.5897	21.9262	21.6460	20.9013	21.5948	21.2055	20.9735	21.1310
0.4	21.1567	20.7718	21.3785	21.5748	21.3407	21.4175	21.4247	21.1125

$\lambda = 0.2$

d_1 \ d_2	-0.4	-0.3	-0.2	-0.1	0.1	0.2	0.3	0.4
-0.4	11.2747	10.8505	10.7282	10.6110	10.8210	11.0053	10.8530	10.7095
-0.3	11.1245	10.9710	10.8277	10.6360	10.8902	10.9340	10.6728	11.0360
-0.2	10.7703	11.0173	10.9010	10.9738	10.5732	10.7508	11.0770	10.9977
-0.1	10.8995	10.9217	10.6990	10.9927	10.8262	10.8933	10.5757	10.9425
0.1	11.0285	11.2650	10.8050	10.9712	10.7272	10.6888	10.4855	11.0292
0.2	10.9625	10.9458	11.1080	11.1118	11.1060	11.1802	11.3340	10.9908
0.3	10.8595	10.9582	10.7828	10.8250	10.7035	10.5633	10.9797	10.7660
0.4	11.10808	10.9070	10.8425	11.0427	10.9770	10.9878	11.3085	10.9648

$\lambda = 0.3$

d_1 \ d_2	-0.4	-0.3	-0.2	-0.1	0.1	0.2	0.3	0.4
-0.4	7.3520	7.3442	7.3905	7.4040	7.3593	7.4798	7.1475	7.2145
-0.3	7.2685	7.1585	7.3247	7.3208	7.1357	7.2005	7.3350	7.2767
-0.2	7.4940	7.2443	7.3373	7.3907	7.4192	7.2805	7.2893	7.3070
-0.1	7.2960	7.2378	7.1505	7.2905	7.0423	7.2467	7.2188	7.3217
0.1	7.2370	7.2400	7.1707	7.3448	7.3647	7.1780	7.2203	7.3765
0.2	7.3115	7.2847	7.3762	7.1785	7.3420	7.2770	7.1935	7.2153
0.3	7.3327	7.2428	7.4238	7.3353	7.4240	7.3325	7.2935	7.3792
0.4	7.2758	7.2393	7.3637	7.4698	7.3420	7.2953	7.4605	7.3797

$\lambda = 0.4$

d_1 \ d_2	-0.4	-0.3	-0.2	-0.1	0.1	0.2	0.3	0.4
-0.4	5.2068	5.1790	5.1232	5.1875	5.2693	5.1818	5.1615	5.1465
-0.3	5.2645	5.0972	5.2900	5.2302	5.0903	5.3135	5.1770	5.2367
-0.2	5.1297	5.1997	5.1405	5.1558	5.2973	5.1377	5.2515	5.1505
-0.1	5.0660	5.2870	5.0995	5.1410	5.3362	5.2930	5.2995	5.1745
0.1	5.2438	5.3160	5.2432	5.1513	5.3155	5.2637	5.2533	5.1463
0.2	5.2910	5.3175	5.2685	5.1940	5.2590	5.2227	5.2278	5.2637
0.3	5.3362	5.2428	5.2142	5.1865	5.2505	5.2285	5.1547	5.2607
0.4	5.2055	5.2103	5.1815	5.2218	5.3310	5.2950	5.3105	5.1137

$\lambda = 0.5$

d_1 \ d_2	-0.4	-0.3	-0.2	-0.1	0.1	0.2	0.3	0.4
-0.4	4.3020	4.2503	4.3928	4.2603	4.2328	4.3068	4.2475	4.1855
-0.3	4.3315	4.3275	4.3398	4.3033	4.2405	4.2815	4.2053	4.2805
-0.2	4.2430	4.2680	4.2685	4.2912	4.2947	4.2410	4.2875	4.2000
-0.1	4.3335	4.3492	4.3338	4.3305	4.2592	4.2668	4.2850	4.2763
0.1	4.3822	4.2477	4.3450	4.3320	4.2715	4.3662	4.3325	4.2983
0.2	4.3195	4.2380	4.2775	4.4245	4.2873	4.2032	4.2603	4.2518
0.3	4.3535	4.3215	4.2540	4.2942	4.1818	4.4180	4.3330	4.4115
0.4	4.2580	4.1570	4.2555	4.2698	4.2800	4.2805	4.1685	4.2280

$\lambda = 0.6$

d_1 \ d_2	-0.4	-0.3	-0.2	-0.1	0.1	0.2	0.3	0.4
-0.4	3.6248	3.5795	3.5793	3.8018	3.5772	3.7088	3.6442	3.5878
-0.3	3.6282	3.6827	3.7163	3.6452	3.6858	3.5993	3.6740	3.7222
-0.2	3.5940	3.6970	3.5910	3.7287	3.6923	3.6630	3.6820	3.6805
-0.1	3.5725	3.5855	3.6560	3.6865	3.6528	3.7083	3.7110	3.7367
0.1	3.6923	3.6700	3.7405	3.5920	3.6322	3.6307	3.6370	3.7080
0.2	3.6985	3.6945	3.6307	3.5978	3.6568	3.6085	3.6347	3.6437
0.3	3.7037	3.5297	3.6852	3.6848	3.6827	3.6810	3.6757	3.5860
0.4	3.6685	3.7062	3.6603	3.6058	3.5722	3.7730	3.6395	3.6495

$\lambda = 0.7$

d_1 \ d_2	-0.4	-0.3	-0.2	-0.1	0.1	0.2	0.3	0.4
-0.4	3.3500	3.3173	3.2687	3.3218	3.3270	3.3262	3.3687	3.3125
-0.3	3.3298	3.2917	3.2767	3.2955	3.2912	3.3105	3.2662	3.3165
-0.2	3.3485	3.3965	3.2480	3.3218	3.3130	3.3397	3.3510	3.3445
-0.1	3.3653	3.3060	3.3595	3.3708	3.3675	3.3733	3.3740	3.3283
0.1	3.1735	3.3135	3.3385	3.2820	3.4112	3.3468	3.2957	3.3525
0.2	3.2615	3.3025	3.2887	3.3093	3.3342	3.2847	3.3558	3.3670
0.3	3.3165	3.2292	3.3363	3.3758	3.3573	3.2325	3.2650	3.3782
0.4	3.3203	3.3485	3.2830	3.3053	3.3628	3.2748	3.3268	3.3472

$\lambda = 0.9$

d_1 \ d_2	-0.4	-0.3	-0.2	-0.1	0.1	0.2	0.3	0.4
-0.4	3.0032	3.0105	3.0620	3.0100	3.0412	3.1012	2.9973	3.0848
-0.3	3.0753	3.0507	3.0240	3.0473	2.9983	2.9600	2.9870	2.9800
-0.2	2.9693	3.0930	3.0873	2.9733	2.9630	2.9663	3.0337	2.9882
-0.1	3.0315	2.9947	3.0177	2.9595	3.0183	2.9278	3.0850	2.9848
0.1	3.0118	3.0048	3.0190	3.0975	2.9080	3.0248	3.0032	3.0090
0.2	3.0722	2.9880	3.0332	3.0042	3.0120	3.0703	3.0290	3.0547
0.3	2.9882	3.0097	3.0270	3.0528	3.0130	2.9562	3.0408	2.9863
0.4	3.0227	3.0303	3.0025	2.9943	3.0215	3.0515	2.9482	3.0082

B.4.5 MMOEWMA control chart

$\lambda = 0.1$

d_1 \ d_2	-0.4	-0.3	-0.2	-0.1	0.1	0.2	0.3	0.4
-0.4	2.2825	2.2908	2.2545	2.3325	2.2730	2.3160	2.2883	2.2675
-0.3	2.0173	2.2447	2.2803	2.3035	2.2742	2.2828	2.2725	2.3148
-0.2	1.9910	2.2578	2.2327	2.2560	2.3395	2.3100	2.2923	2.2535
-0.1	2.0232	2.2700	2.0383	2.3170	2.3080	2.3200	2.2982	2.2677
0.1	1.9757	2.2668	1.9932	2.0562	2.2670	2.2738	2.2978	2.2510
0.2	2.0558	2.2942	2.0055	1.9880	1.9770	2.3450	2.2810	2.3055
0.3	2.0190	2.2740	2.0045	2.0313	1.9883	2.0180	2.2515	2.3020
0.4	2.0135	2.2870	1.9952	2.0057	2.0402	2.0227	2.0307	2.2917

$\lambda = 0.2$

d_1 \ d_2	-0.4	-0.3	-0.2	-0.1	0.1	0.2	0.3	0.4
-0.4	2.7422	2.6963	2.7440	2.7778	2.6980	2.7230	2.7203	2.6463
-0.3	2.3955	2.7403	2.7075	2.8270	2.7353	2.7462	2.7363	2.7872
-0.2	2.4370	2.7532	2.7335	2.7375	2.7418	2.6972	2.8037	2.7412
-0.1	2.3803	2.6760	2.4472	2.7585	2.7035	2.7525	2.7840	2.7705
0.1	2.4750	2.7765	2.4550	2.4655	2.7410	2.6648	2.7700	2.7372
0.2	2.3725	2.7147	2.4655	2.4432	2.4177	2.7500	2.7255	2.7357
0.3	2.3803	2.7207	2.4388	2.4697	2.5030	2.4617	2.7687	2.7760
0.4	2.4552	2.7542	2.4325	2.4190	2.4962	2.4600	2.4700	2.6982

$\lambda = 0.3$

d_1 \ d_2	-0.4	-0.3	-0.2	-0.1	0.1	0.2	0.3	0.4
-0.4	3.0282	3.0297	3.0402	3.0507	2.9823	3.0343	3.0775	3.0535
-0.3	2.7397	3.0177	3.0223	3.0692	3.0275	3.0245	3.0450	3.0685
-0.2	2.7820	2.9987	3.0377	3.0010	3.0340	3.0208	3.0810	3.0385
-0.1	2.7553	2.9575	2.7902	3.0697	3.0528	3.0553	3.1162	3.0177
0.1	2.7405	3.0947	2.7687	2.7505	3.0322	3.0150	3.0710	3.0980
0.2	2.7830	2.9780	2.8105	2.7767	2.8195	3.0475	3.0495	2.9503
0.3	2.7625	3.0535	2.8272	2.7935	2.7412	2.7750	3.0562	3.0213
0.4	2.7755	3.0705	2.7997	2.7628	2.7723	2.7940	2.8340	2.9965

$\lambda = 0.4$

d_1 \ d_2	-0.4	-0.3	-0.2	-0.1	0.1	0.2	0.3	0.4
-0.4	3.4663	3.5185	3.5008	3.5605	3.4598	3.4987	3.4817	3.5095
-0.3	2.9647	3.4655	3.4232	3.5265	3.4595	3.4330	3.4327	3.4987
-0.2	2.9958	3.3960	3.5088	3.3990	3.4588	3.5295	3.4038	3.4417
-0.1	3.0160	3.5105	2.9855	3.5175	3.4653	3.4348	3.4430	3.4487
0.1	2.9588	3.4355	2.9385	2.9453	3.4265	3.4880	3.3782	3.4505
0.2	2.9552	3.4398	3.0122	2.9962	2.9200	3.3770	3.4475	3.4638
0.3	2.9860	3.4478	2.9602	2.9562	2.9707	2.9457	3.5015	3.4842
0.4	2.9605	3.5313	2.9215	2.9500	3.0053	2.9590	2.9522	3.3853

$\lambda = 0.5$

d_1 \ d_2	-0.4	-0.3	-0.2	-0.1	0.1	0.2	0.3	0.4
-0.4	4.0365	4.0520	4.1355	4.0980	4.0380	4.0365	4.0500	4.0780
-0.3	3.1145	4.1057	3.9728	4.1303	4.0130	3.9405	4.0462	4.0125
-0.2	3.2043	4.1467	3.9710	4.1285	4.0617	4.0090	4.1050	4.0818
-0.1	3.2475	4.0892	3.2302	4.1028	4.0012	4.1502	3.9817	4.0637
0.1	3.1917	3.9567	3.2052	3.1987	4.0285	4.0530	4.0415	4.0492
0.2	3.2340	3.9455	3.2473	3.1785	3.1915	4.0682	4.0500	4.0310
0.3	3.1925	4.0667	3.2037	3.2557	3.2188	3.2435	4.0622	4.0865
0.4	3.2170	4.0000	3.2150	3.1975	3.2295	3.2175	3.1875	4.1283

$\lambda = 0.6$

d_1 \ d_2	-0.4	-0.3	-0.2	-0.1	0.1	0.2	0.3	0.4
-0.4	4.4037	4.3200	4.2562	4.3005	4.2867	4.2885	4.2905	4.2888
-0.3	3.4268	4.3513	4.3240	4.2915	4.3578	4.2923	4.2545	4.4342
-0.2	3.4672	4.3355	4.2035	4.2227	4.3915	4.4040	4.3210	4.3122
-0.1	3.4148	4.3265	3.3265	4.2547	4.3072	4.2947	4.2053	4.4437
0.1	3.4758	4.3355	3.4407	3.4055	4.2945	4.3565	4.2553	4.3680
0.2	3.4855	4.3485	3.4137	3.3638	3.4322	4.2918	4.2400	4.4235
0.3	3.5050	4.3498	3.4478	3.4475	3.4065	3.4060	4.3445	4.2227
0.4	3.4733	4.4750	3.4420	3.4075	3.4017	3.3222	3.4985	4.3232

$\lambda = 0.7$

d_1 \ d_2	-0.4	-0.3	-0.2	-0.1	0.1	0.2	0.3	0.4
-0.4	4.7707	4.8800	4.9132	4.7830	4.7607	4.7453	4.6880	4.8120
-0.3	3.7405	4.8472	4.9320	4.8262	4.5738	4.8498	4.8323	4.7715
-0.2	3.7160	4.7820	4.8200	4.7755	4.7252	4.8480	4.9485	4.8758
-0.1	3.7005	4.8068	3.6510	4.9473	4.8178	4.7953	4.7955	4.8643
0.1	3.7395	4.7523	3.6322	3.6267	4.7800	4.7490	4.7995	4.7598
0.2	3.7633	4.7168	3.6713	3.6520	3.6270	4.7855	4.8480	4.9185
0.3	3.7687	4.7348	3.7662	3.7400	3.6695	3.6910	4.7630	4.8275
0.4	3.6615	4.7598	3.7335	3.7738	3.5640	3.6985	3.6775	4.7218

$\lambda = 0.9$

d_1 \ d_2	-0.4	-0.3	-0.2	-0.1	0.1	0.2	0.3	0.4
-0.4	5.8982	5.8723	5.7998	5.8617	5.9760	5.9588	6.0040	6.0788
-0.3	4.3208	5.8395	5.9592	5.8705	5.8630	6.1002	6.0175	5.9820
-0.2	4.4170	5.8375	5.8308	5.9953	5.8660	5.7467	5.9360	5.9822
-0.1	4.2642	5.9725	4.3770	5.9710	5.9873	5.8338	5.9088	5.7942
0.1	4.3842	5.9020	4.3625	4.3933	5.8887	6.0713	6.0885	5.8552
0.2	4.4645	5.8785	4.3617	4.3703	4.3563	5.9112	5.8783	5.8955
0.3	4.4488	6.0008	4.4112	4.2852	4.4000	4.3918	6.0228	5.7767
0.4	4.3673	6.0000	4.2847	4.3228	4.3643	4.4402	4.3610	6.0285

Appendix C

Figures

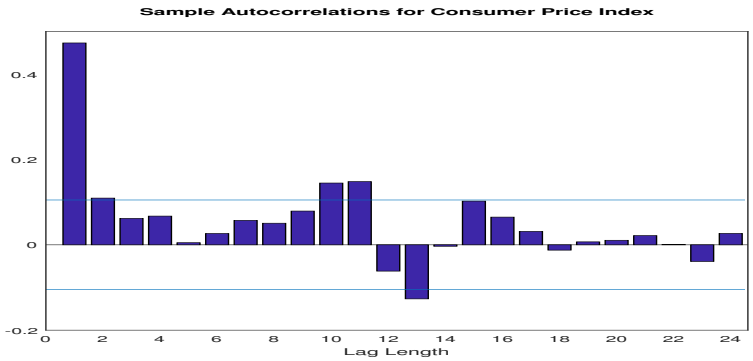

Figure C.0.1: The figure illustrates the autocorrelations for the Consumer Price Index for lag 1 to lag 24 over the sample period 1981:01 to 2009:12.

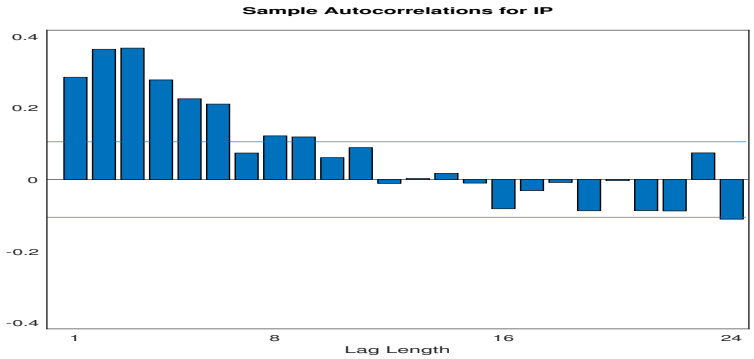

Figure C.0.2: The figure illustrates the autocorrelations for the Industrial Production Index for lag 1 to lag 24 over the sample period 1981:01 to 2009:12.

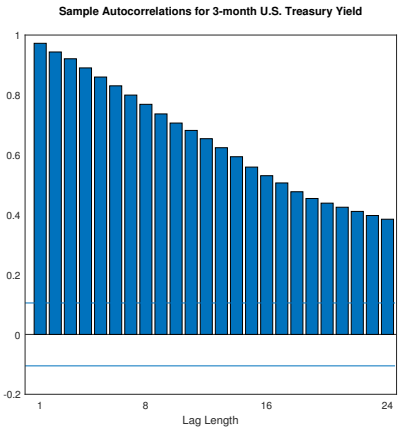

(a) Autocorrelation of 3m bond

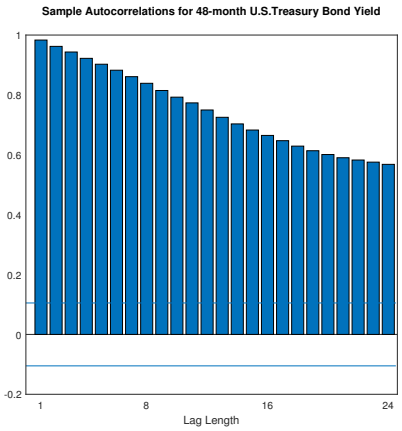

(b) Autocorrelation of 48m bond

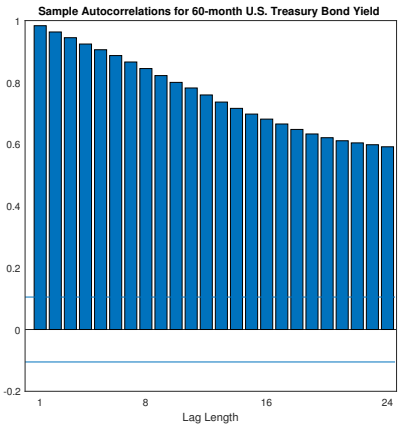

(c) Autocorrelation of 60m bond

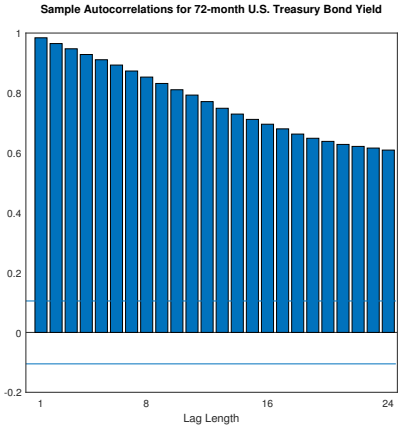

(d) Autocorrelation of 72m bond

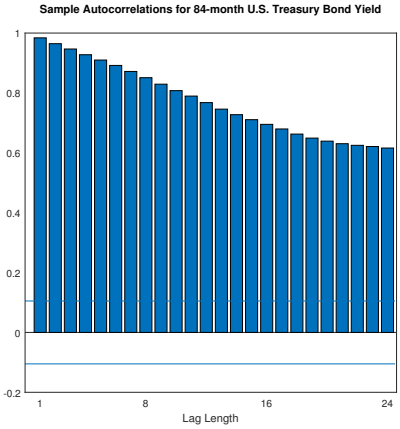

(e) Autocorrelation of 84m bond

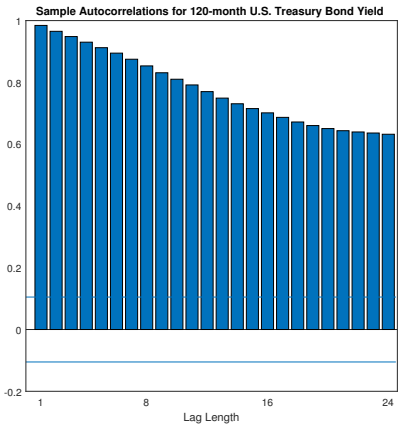

(f) Autocorrelation of 120m bond

Figure C.0.3: Autocorrelation of U.S. Treasury bond yields.

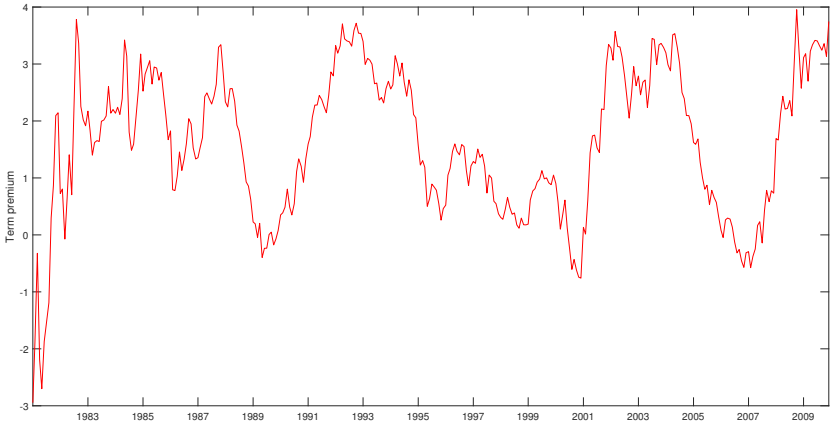

Figure C.0.4: The figure illustrates the yield term premia, the difference between the 10-year yield and the 3-month yield.

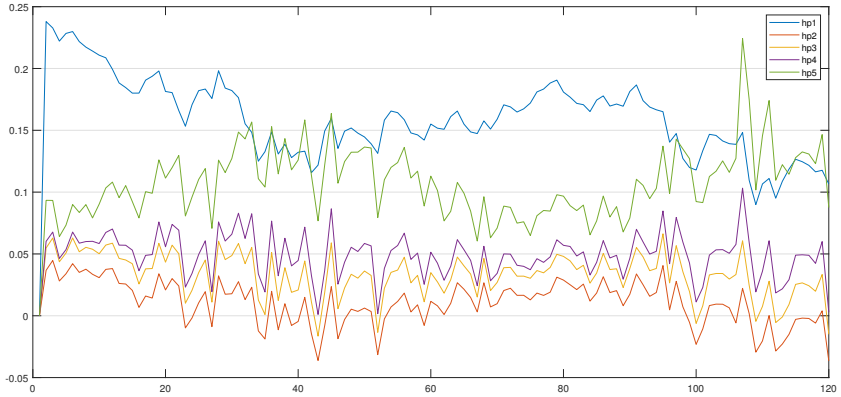

Figure C.0.5: One-step-ahead holding period returns for the out-of-sample period 2000:01 to 2009:12. Hpi, $i = \ldots, 5$ are the holding period returns from holding each of the bonds for one period of time and maturity decreases from $i + 1$ to i.

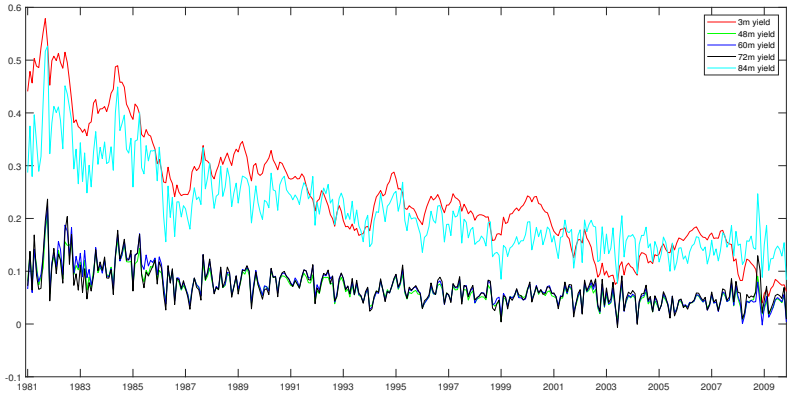

Figure C.0.6: Excess holding period returns for the out-of-sample period 2000:01 to 2009:12. Hpi, $i = \ldots, 5$ are the excess holding period returns from holding each of the bonds for one period of time and maturity decreases from $i+1$ to i net of the risk-free rate the federal funds rate.

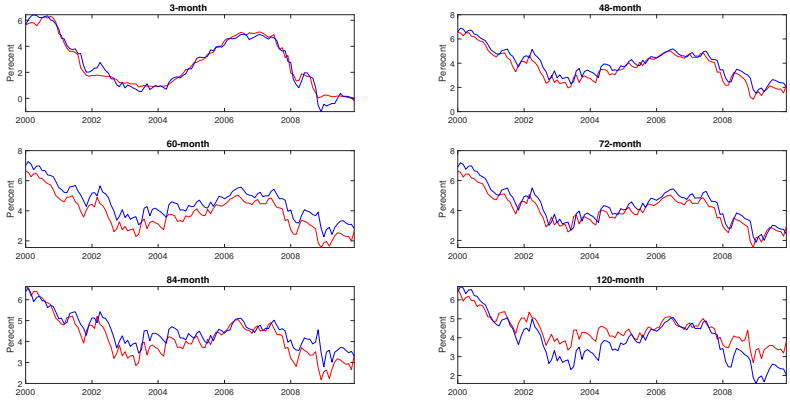

Figure C.0.7: Fitted and actual yield for the out-of-sample period 2000:01 to 2009:12. The blue line is the predicted values and the red line is the actual yields.

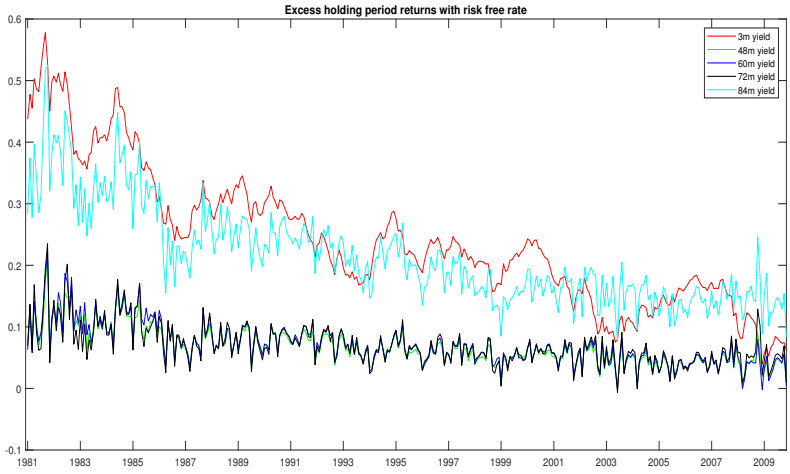

Figure C.0.8: Excess holding period returns with risk free rate the Federal Funds rate. The sample period is 1982:01 to 2009:12.

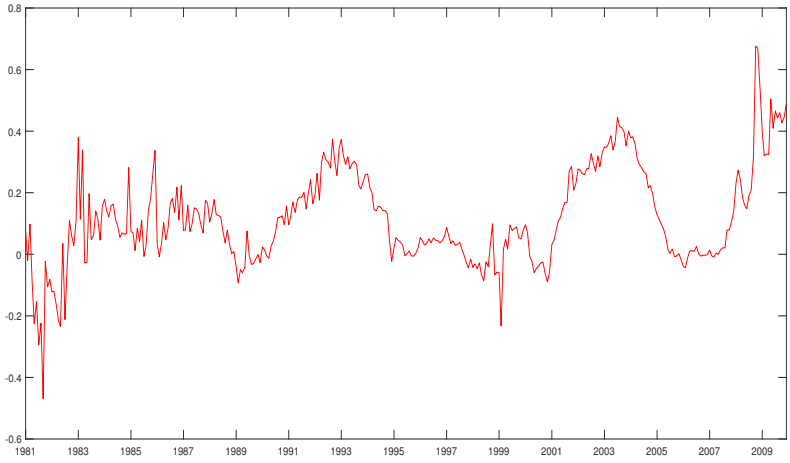

Figure C.0.9: Five-by-ten year forward rate for the sample period 1982:01 to 2009:12.

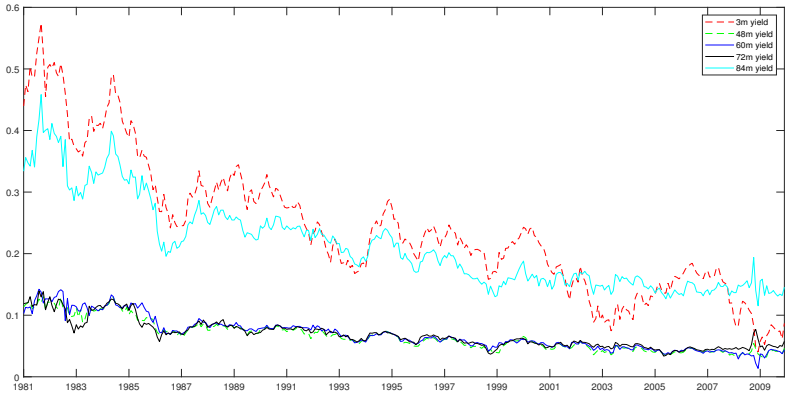

Figure C.0.10: Forward spread rates for the sample period 1982:01 to 2009:12.

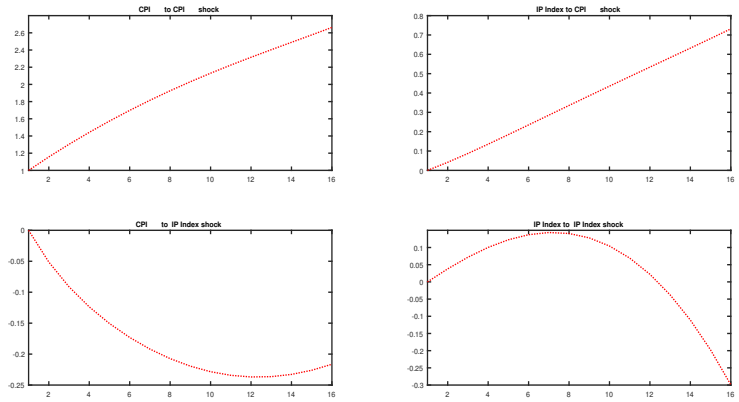

Figure C.0.11: Impulse responses for the macroeconomic factors.

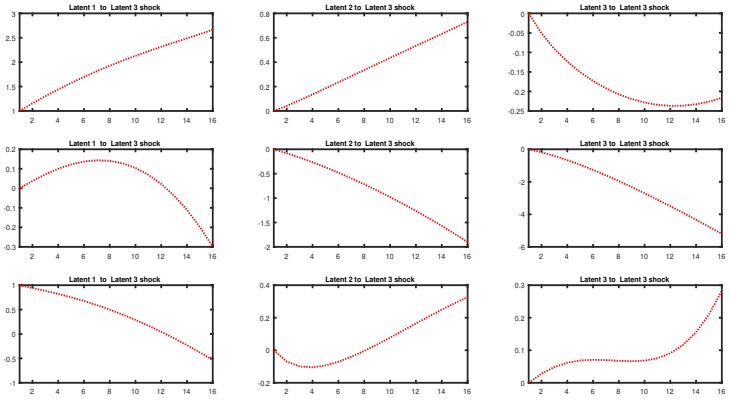

Figure C.0.12: Impulse responses for the latent factors.

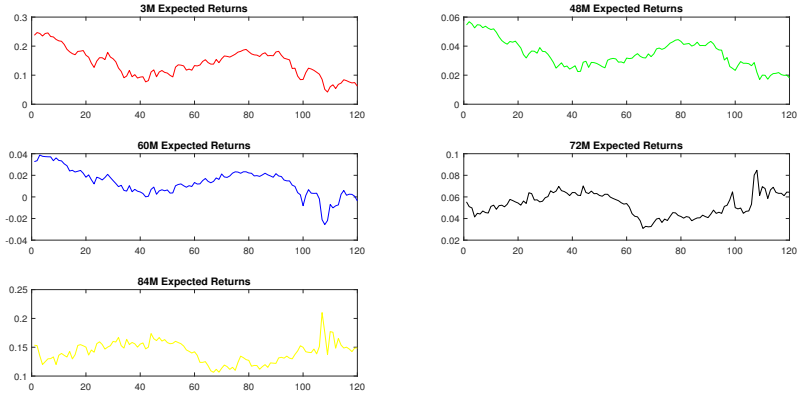

Figure C.0.13: Out-of-sample expected returns for the U.S. government bonds.

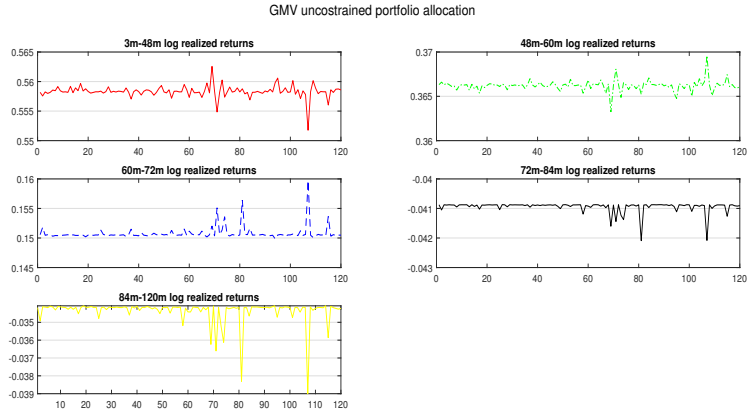

Figure C.0.14: GMVP allocation for the period 2000:01 to 2009:12 when short selling is allowed.

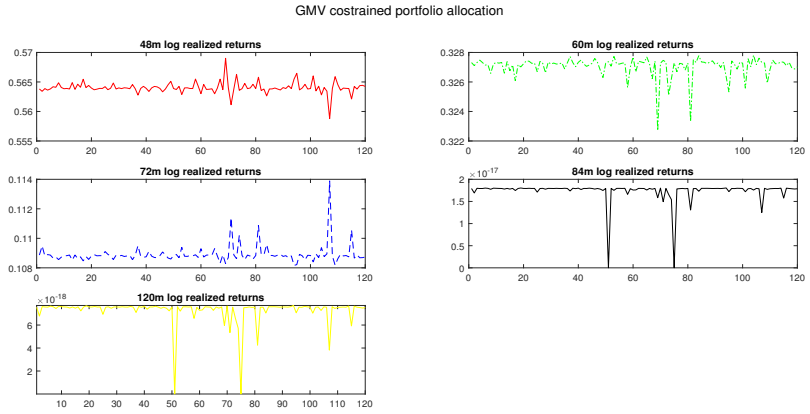

Figure C.0.15: GMV constrained portfolio allocation for the period 2000:01 to 2009:12

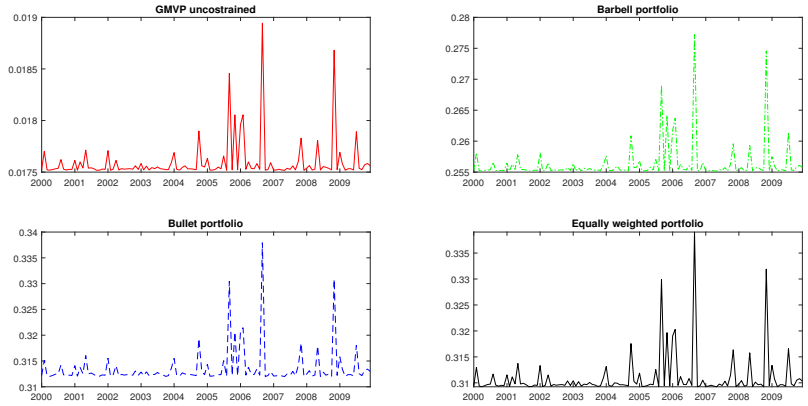

Figure C.0.16: Monthly GMVP standard deviation with short selling for the out-of-sample period 2000:01 to 2009:12.

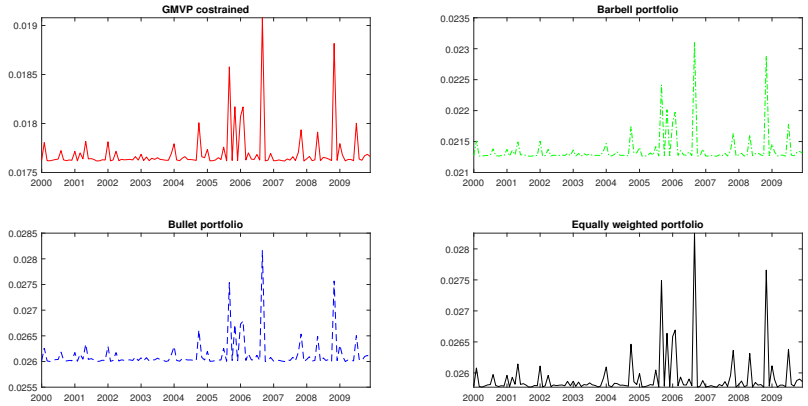

Figure C.0.17: Monthly GMVP standard deviation with no short selling for the out-of-sample period 2000:01 to 2009:12.

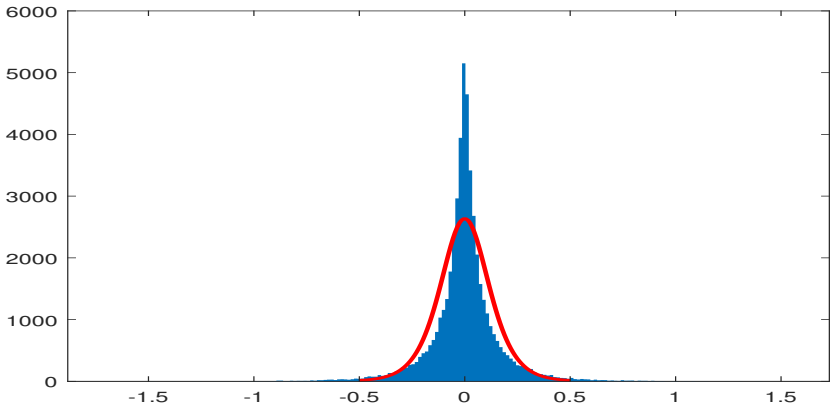

Figure C.0.18: Distribution fitting plot for simulated optimal GMVP weights in the case of asset correlation and the logistic distribution.

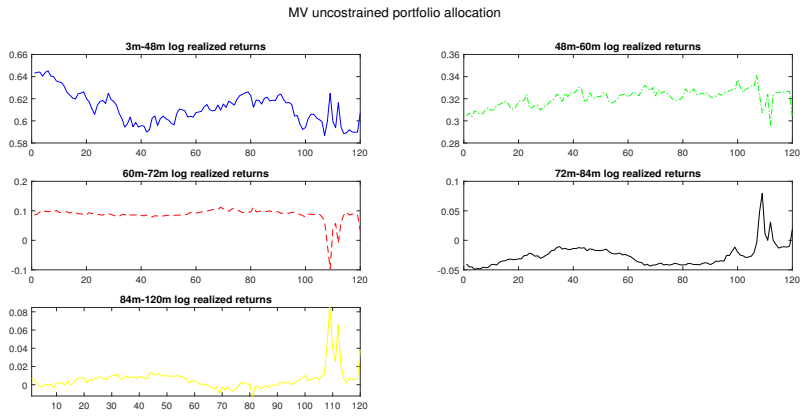

Figure C.0.19: MV unconstrained portfolio weights for risk aversion $\delta = 0.001$.

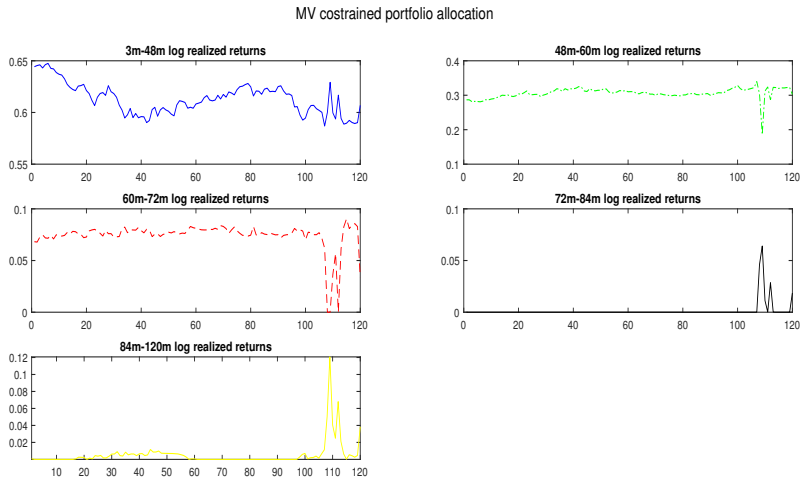

Figure C.0.20: MV constrained portfolio weights for risk aversion $\delta = 0.001$.

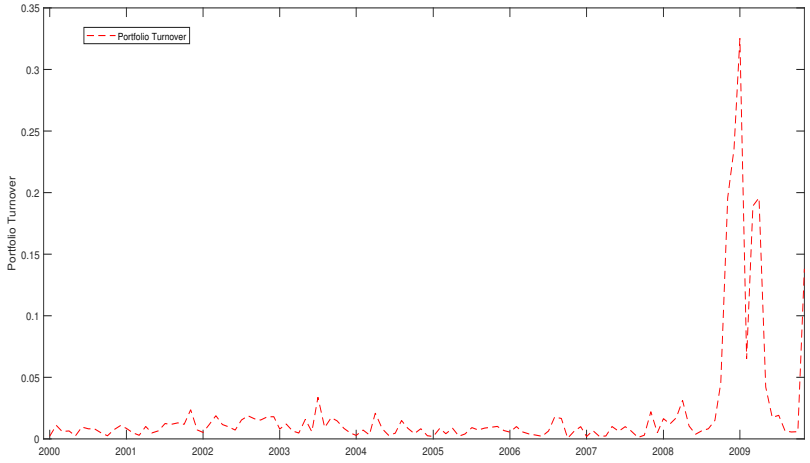

Figure C.0.21: Portfolio turnover for constrained MV portfolio for the out-of-sample period 2000:01 to 2009:12.

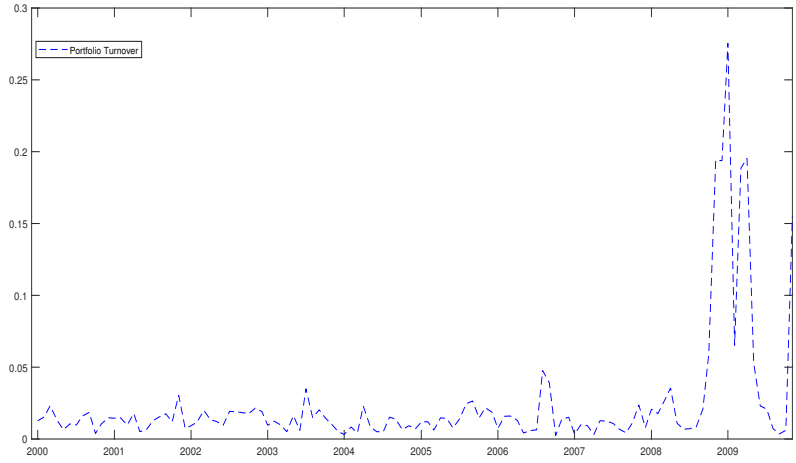

Figure C.0.22: Portfolio turnover for unconstrained MV portfolio for the out-of-sample period 2000:01 to 2009:12.

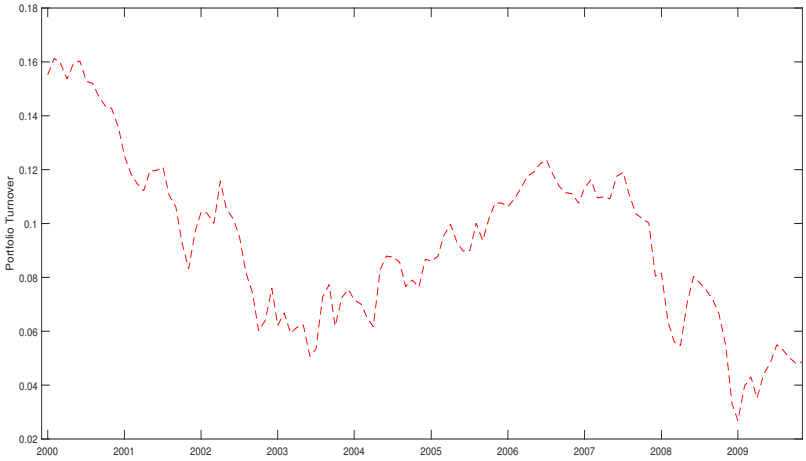

Figure C.0.23: Realized returns net of transaction costs of unconstrained MV portfolio for the out-of-sample period 2000:01 to 2009:12.

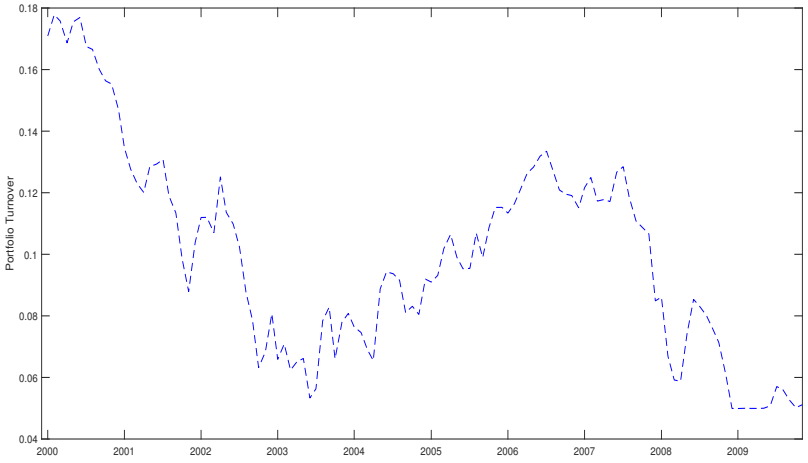

Figure C.0.24: Realized returns net of transaction costs of constrained MV portfolio for the out-of-sample period 2000:01 to 2009:12.

C.0.1 Control statistics without reestimation of the target process

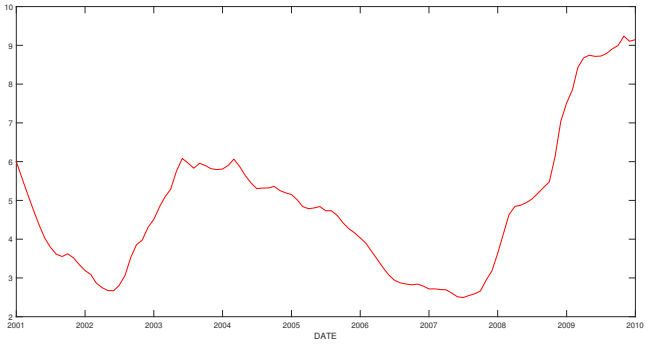

Figure C.0.25: Control statistic for the case of EWMA control chart based on Mahalanobis distance when $\lambda = 0.1$. The sample period is 2001:01 to 2009:12.

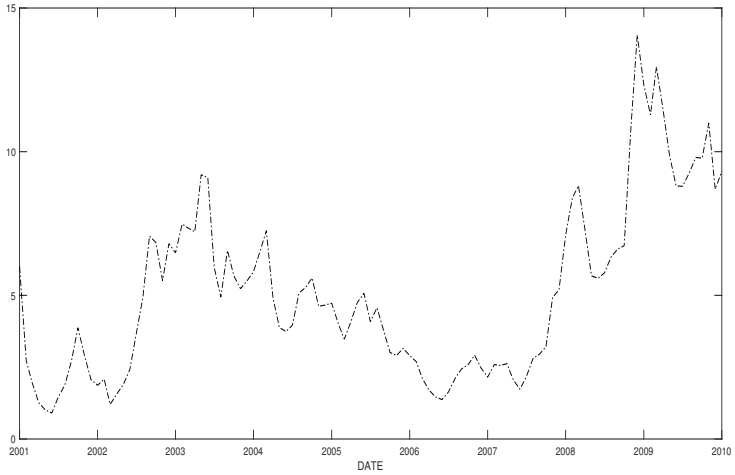

Figure C.0.26: Control statistic for the case of EWMA control chart based on Mahalanobis distance when $\lambda = 0.75$. The sample period is 2001:01 to 2009:12.

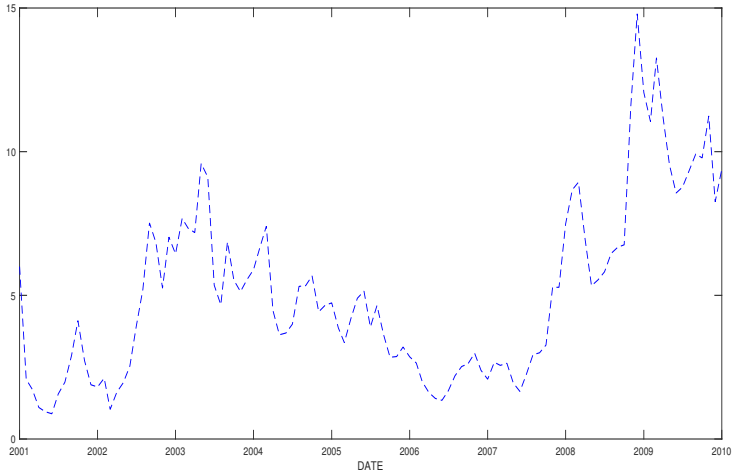

Figure C.0.27: Control statistic for the case of EWMA control chart based on Mahalanobis distance when $\lambda = 0.9$. The sample period is 2001:01 to 2009:12.

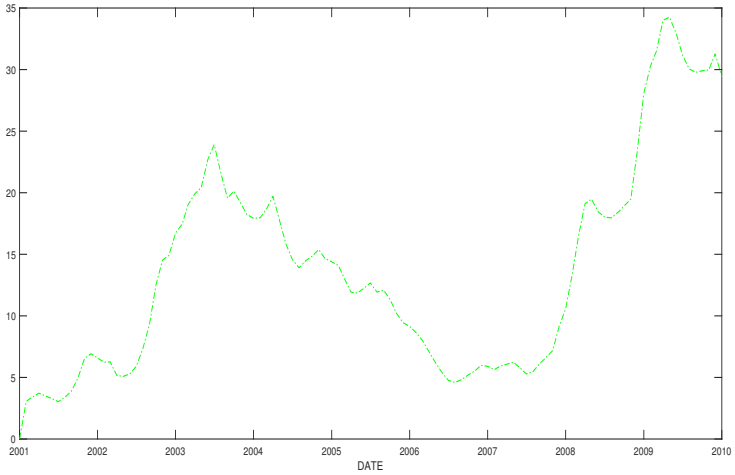

Figure C.0.28: Control statistic for the case of MEWMA control chart when $\lambda = 0.25$. The sample period is 2001:01 to 2009:12.

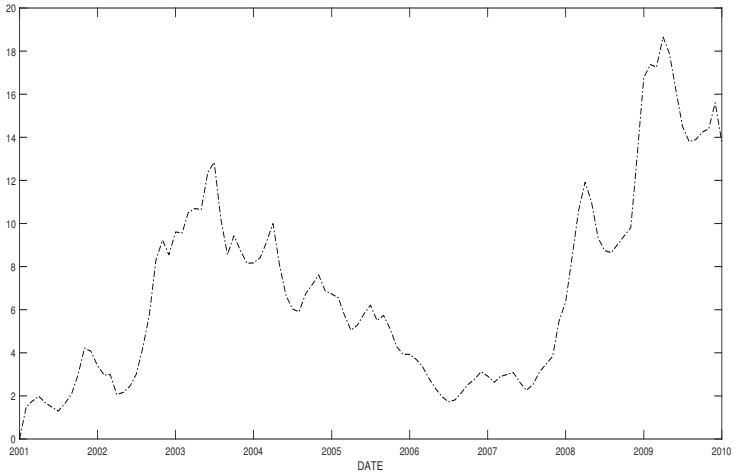

Figure C.0.29: Control statistic for the case of MEWMA control chart when $\lambda = 0.45$. The sample period is 2001:01 to 2009:12.

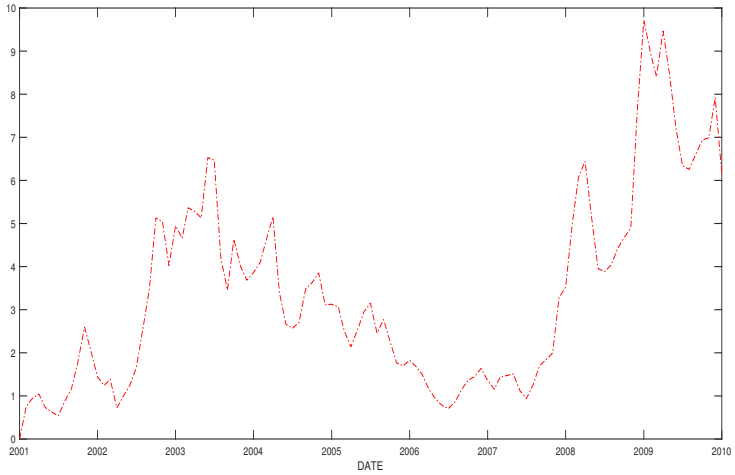

Figure C.0.30: Control statistic for the case of MEWMA control chart when $\lambda = 0.75$. The sample period is 2001:01 to 2009:12.

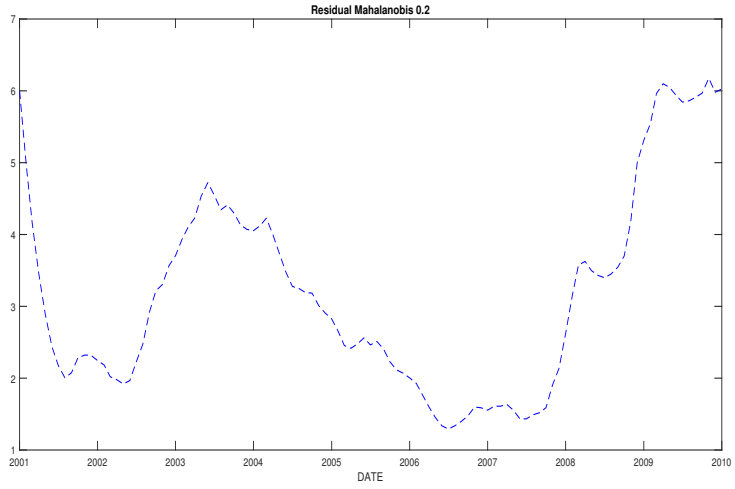

Figure C.0.31: Control statistic for the case of Residual EWMA control chart based on Mahalanobis distance when $\lambda = 0.2$. The sample period is 2001:01 to 2009:12.

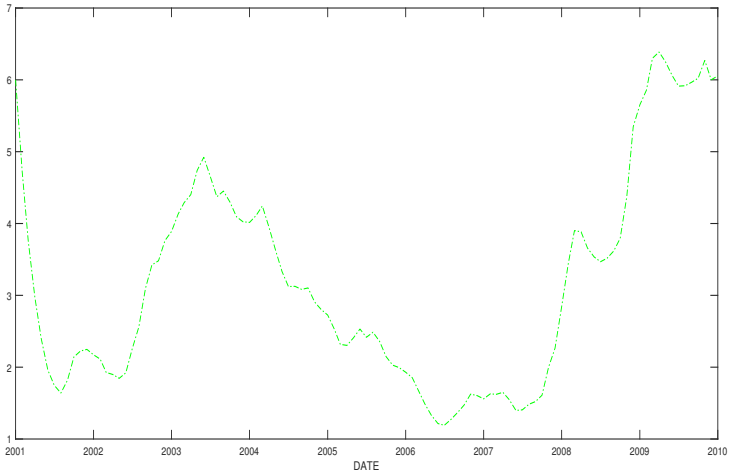

Figure C.0.32: Control statistic for the case of Residual EWMA control chart based on Mahalanobis distance when $\lambda = 0.25$. The sample period is 2001:01 to 2009:12.

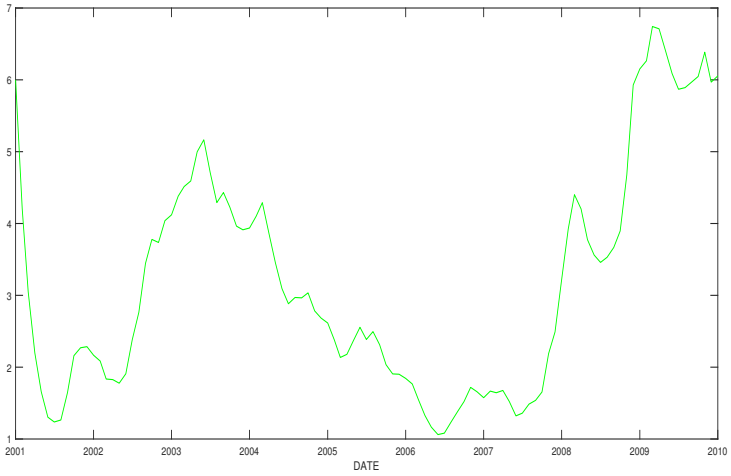

Figure C.0.33: Control statistic for the case of Residual EWMA control chart based on Mahalanobis distance when $\lambda = 0.35$. The sample period is 2001:01 to 2009:12.

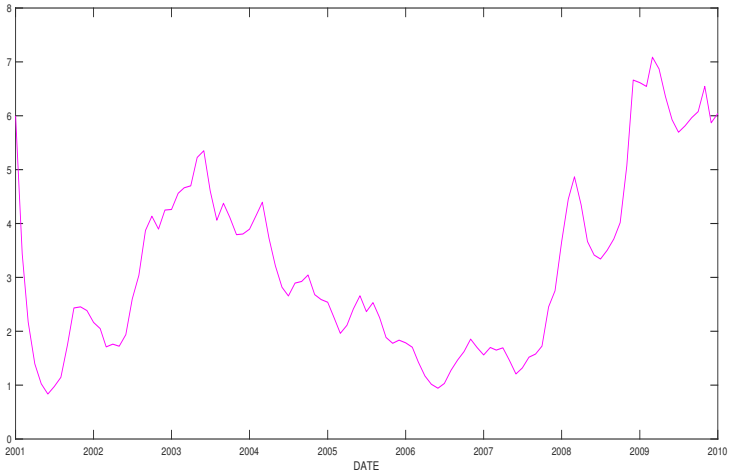

Figure C.0.34: Control statistic for the case of Residual EWMA control chart based on Mahalanobis distance when $\lambda = 0.5$. The sample period is 2001:01 to 2009:12.

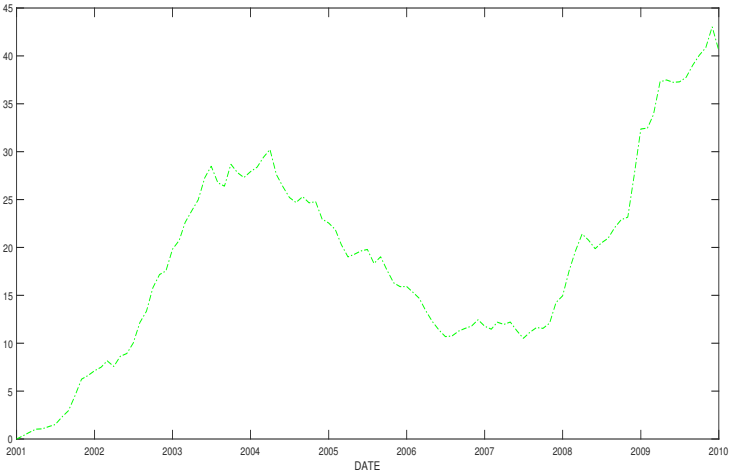

Figure C.0.35: Control statistic for the case of Residual MEWMA control chart when $\lambda = 0.25$. The sample period is 2001:01 to 2009:12.

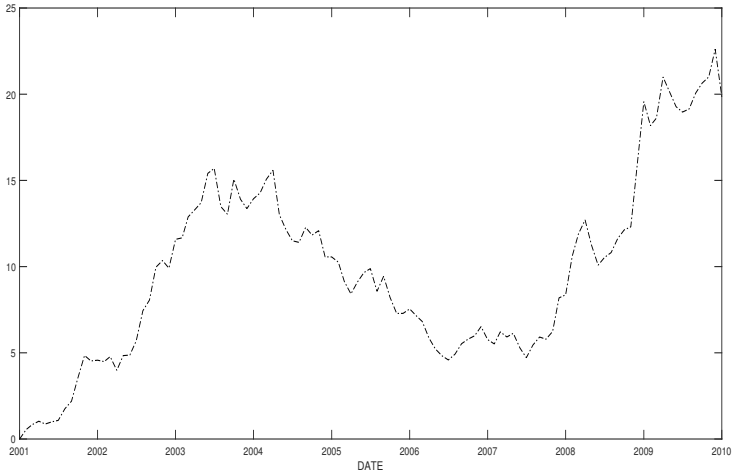

Figure C.0.36: Control statistic for the case of Residual MEWMA control chart when $\lambda = 0.45$. The sample period is 2001:01 to 2009:12..

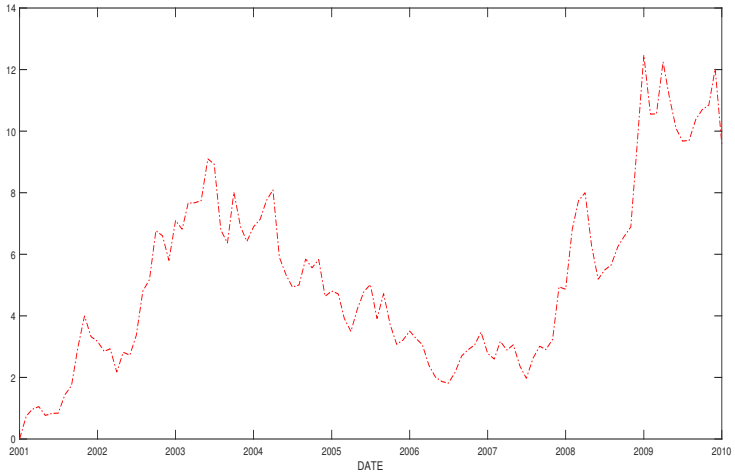

Figure C.0.37: Control statistic for the case of Residual MEWMA control chart when $\lambda = 0.75$. The sample period is 2001:01 to 2009:12.

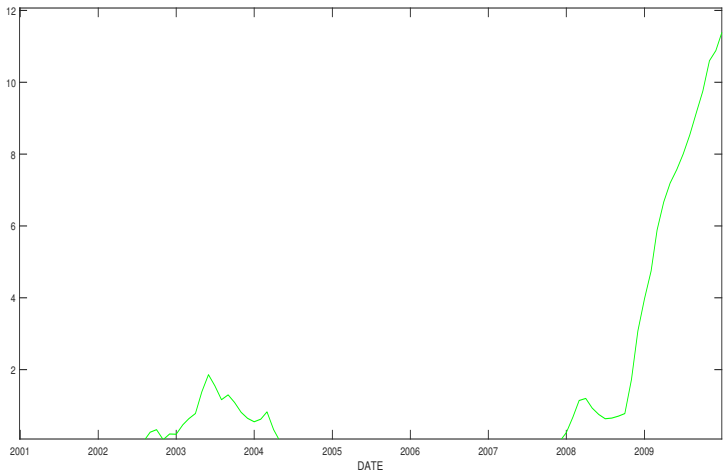

Figure C.0.38: Control statistic for the case of MCUSUM control chart when $g = 2.5$. The sample period is from 2001:01 to 2009:12.

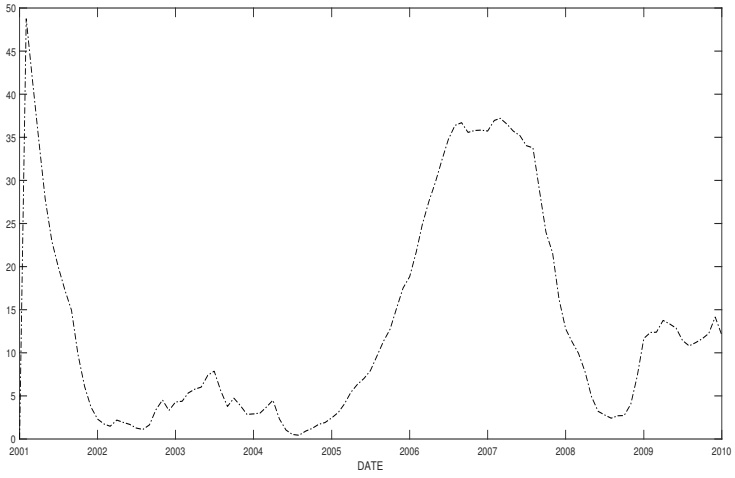

Figure C.0.39: Control statistic for the case of MMOEWMA control chart when $\lambda = 0.45$. The sample period is 2001:01 to 2009:12.

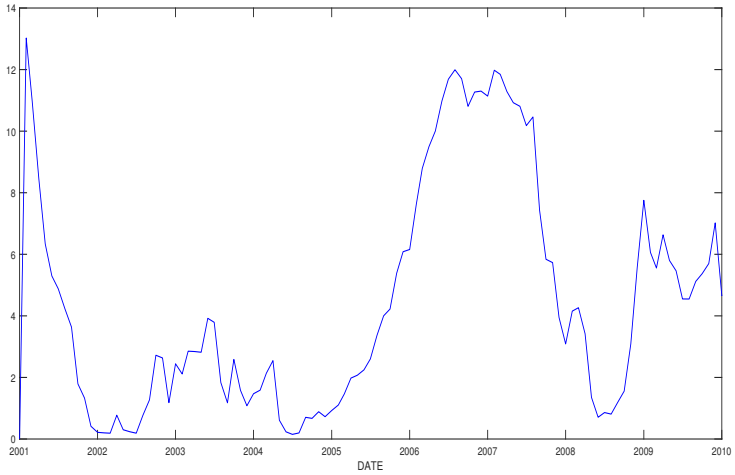

Figure C.0.40: Control statistic for the case of MMOEWMA control chart when $\lambda = 0.9$. The sample period is 2001:01 to 2009:12.

C.0.2 Control charts without reestimation of the target process

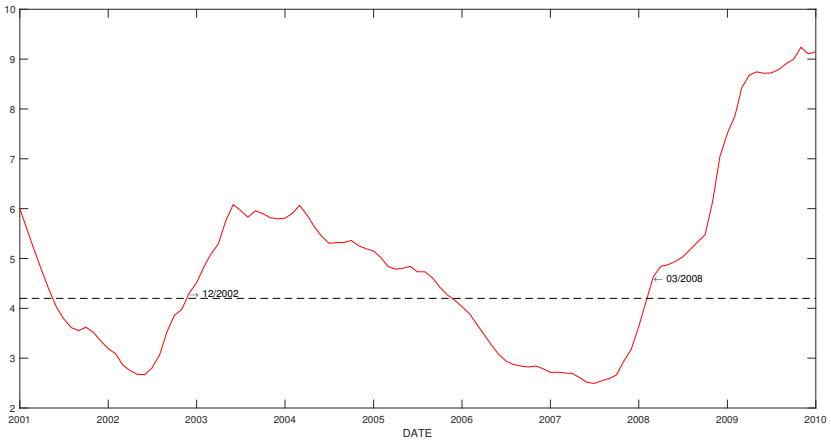

Figure C.0.41: Control chart for the case of EWMA control chart based on Mahalanobis distance when $\lambda = 0.1$. The sample period is 2001:01 to 2009:12.

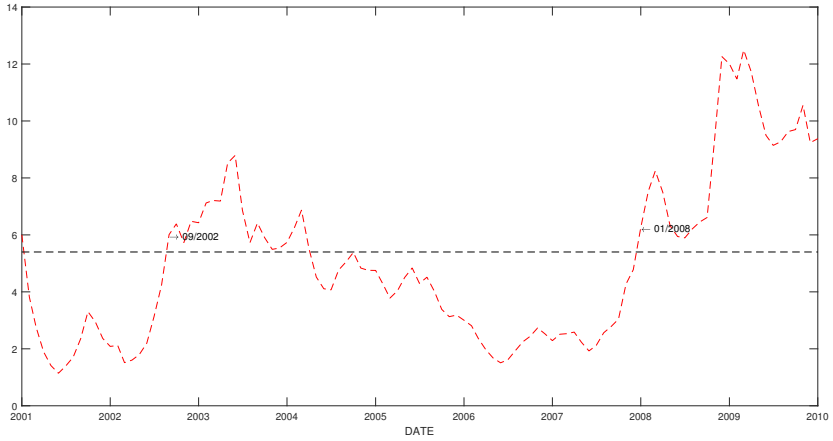

Figure C.0.42: Control chart for the case of EWMA control chart based on Mahalanobis distance when $\lambda = 0.75$. The sample period is 2001:01 to 2009:12.

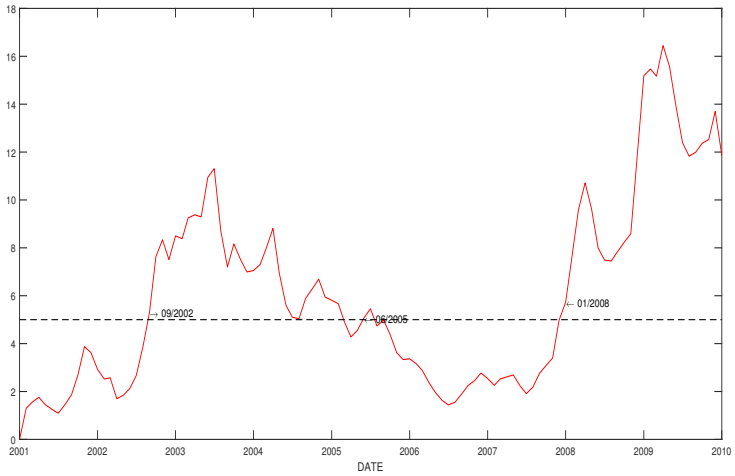

Figure C.0.43: Control chart for the case of MEWMA control chart when $\lambda = 0.5$. The sample period is 2001:01 to 2009:12.

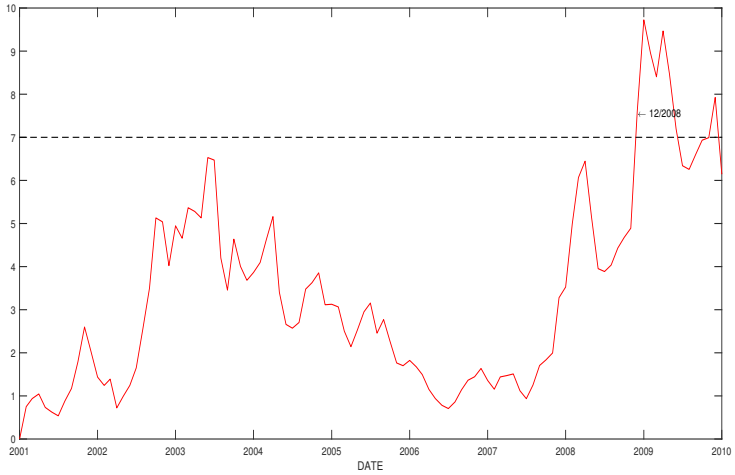

Figure C.0.44: Control chart for the case of MEWMA control chart when $\lambda = 0.75$. The sample period is 2001:01 to 2009:12.

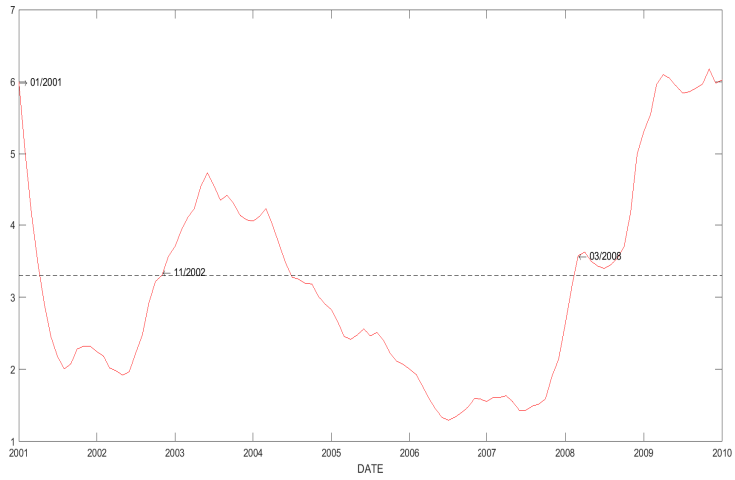

Figure C.0.45: Control chart for the case of Residual EWMA control chart based on Mahalanobis distance when $\lambda = 0.2$. The sample period is 2001:01 to 2009:12.

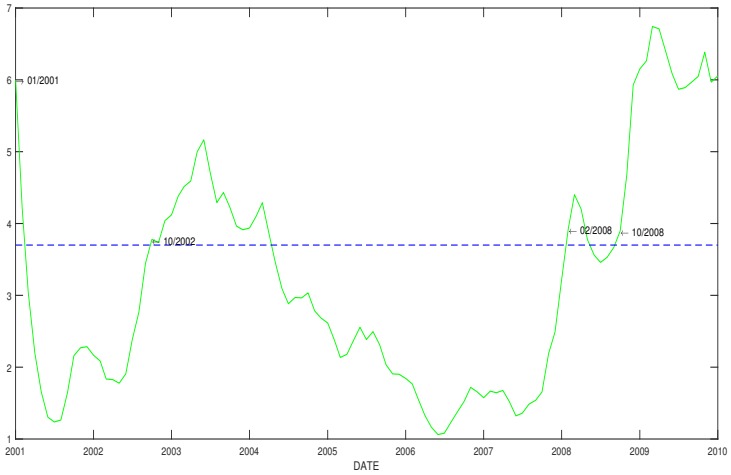

Figure C.0.46: Control chart for the case of Residual EWMA control chart based on Mahalanobis distance when $\lambda = 0.35$. The sample period is 2001:01 to 2009:12.

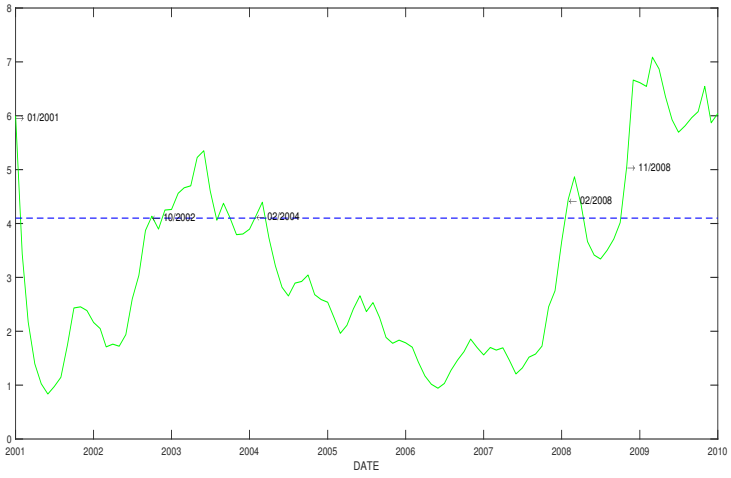

Figure C.0.47: Control chart for the case of Residual EWMA control chart based on Mahalanobis distance when $\lambda = 0.5$. The sample period is 2001:01 to 2009:12.

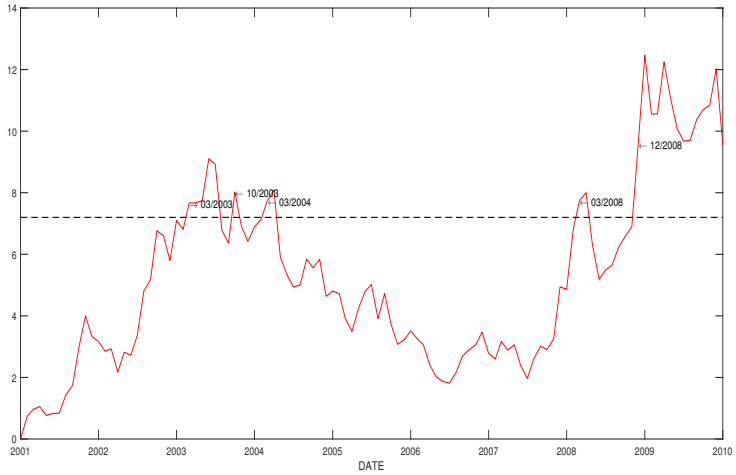

Figure C.0.48: Control chart for the case of Residual MEWMA control chart when $\lambda = 0.75$. The sample period is 2001:01 to 2009:12.

C.0.3 Control statistics with reestimation of the target process

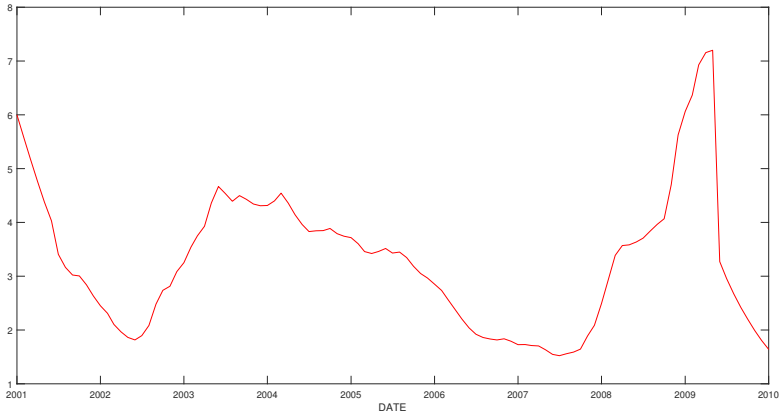

Figure C.0.49: Control statistic for the case of EWMA control chart based on Mahalanobis distance when $\lambda = 0.1$ and reestimation of the target process. The sample period is 2001:01 to 2009:12.

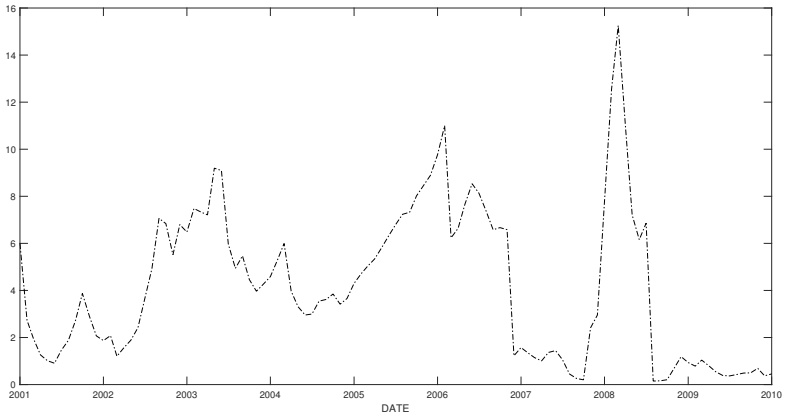

Figure C.0.50: Control statistic for the case of EWMA control chart based on Mahalanobis distance when $\lambda = 0.75$ and reestimation of the target process. The sample period is 2001:01 to 2009:12.

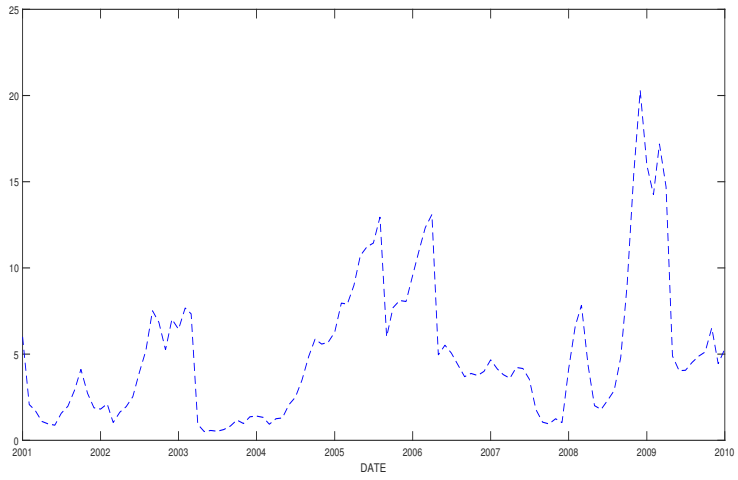

Figure C.0.51: Control statistic for the case of EWMA control chart based on Mahalanobis distance when $\lambda = 0.9$ and reestimation of the target process. The sample period is 2001:01 to 2009:12.

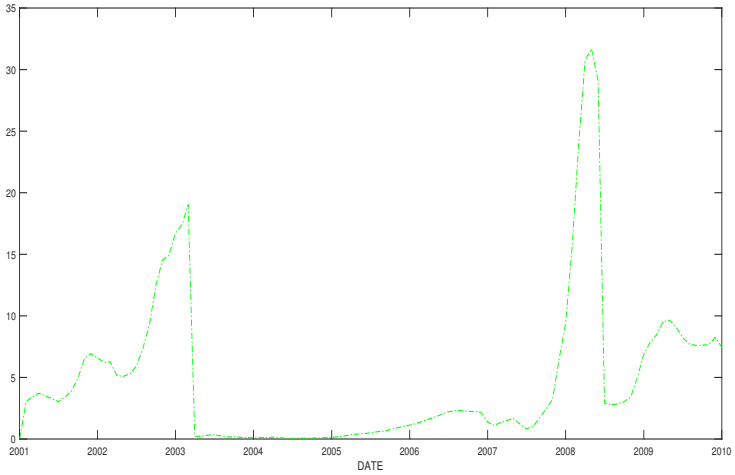

Figure C.0.52: Control statistic for the case of MEWMA control chart when $\lambda = 0.25$ and reestimation of the target process. The sample period is 2001:01 to 2009:12.

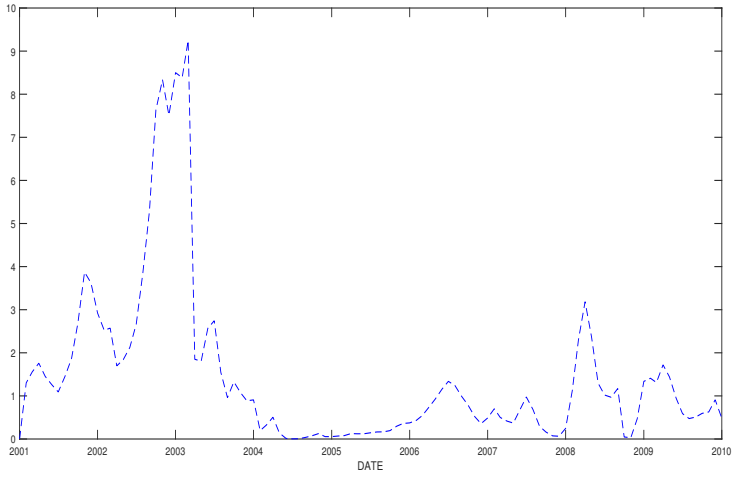

Figure C.0.53: Control statistic for the case of MEWMA control chart when $\lambda = 0.5$ and reestimation of the target process. The sample period is 2001:01 to 2009:12.

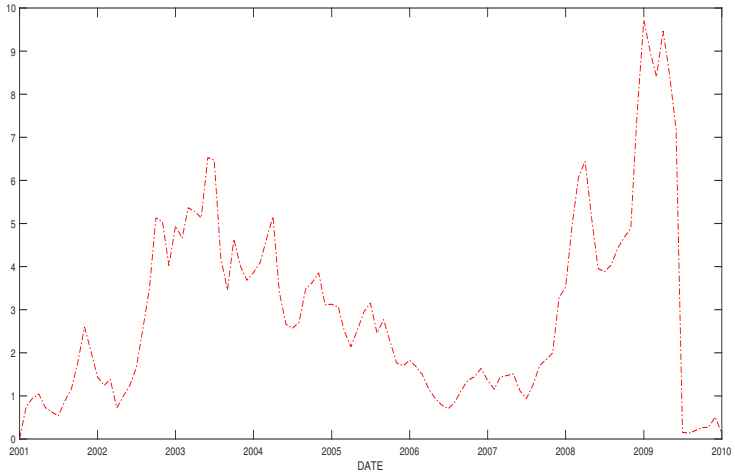

Figure C.0.54: Control statistic for the case of MEWMA control chart when $\lambda = 0.75$ and reestimation of the target process. The sample period is 2001:01 to 2009:12.

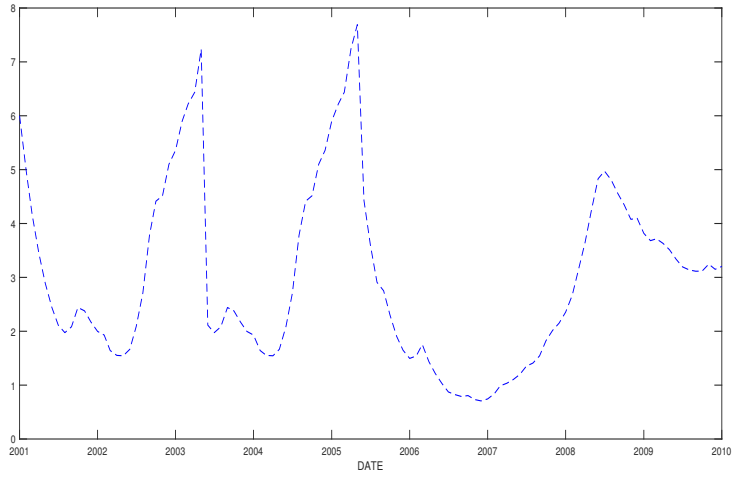

Figure C.0.55: Control statistic for the case of Residual EWMA control chart based on Mahalanobis distance when $\lambda = 0.2$ and reestimation of the target process. The sample period is 2001:01 to 2009:12.

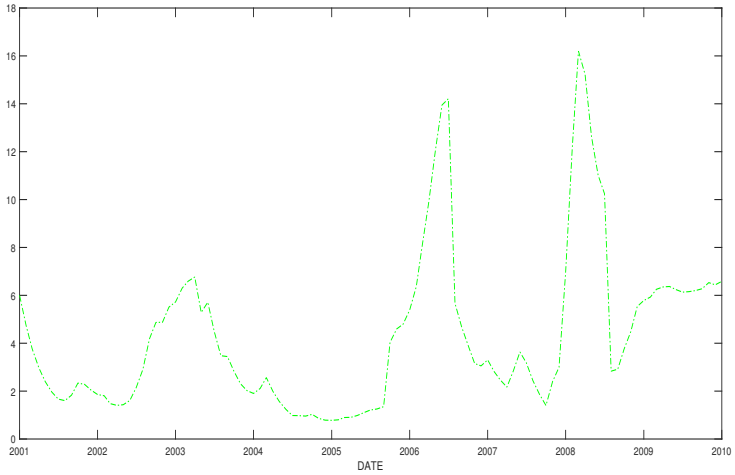

Figure C.0.56: Control statistic for the case of Residual EWMA control chart based on Mahalanobis distance when $\lambda = 0.25$ and reestimation of the target process. The sample period is 2001:01 to 2009:12.

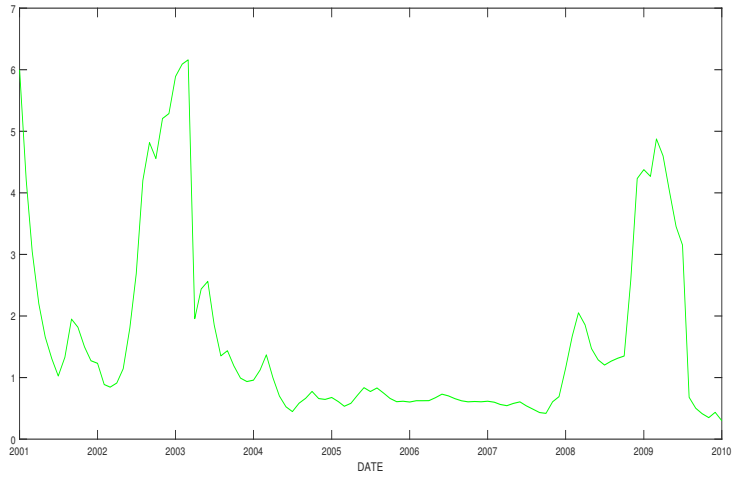

Figure C.0.57: Control statistic for the case of Residual EWMA control chart based on Mahalanobis distance when $\lambda = 0.35$ and reestimation of the target process. The sample period is 2001:01 to 2009:12.

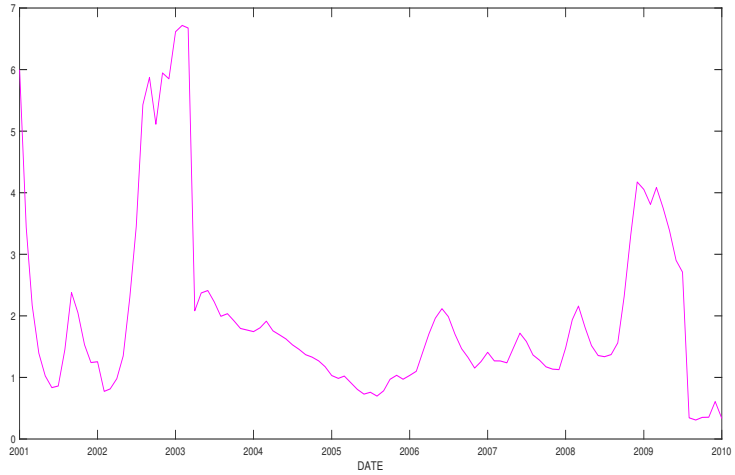

Figure C.0.58: Control statistic for the case of Residual EWMA control chart based on Mahalanobis distance when $\lambda = 0.5$ and reestimation of the target process. The sample period is 2001:01 to 2009:12.

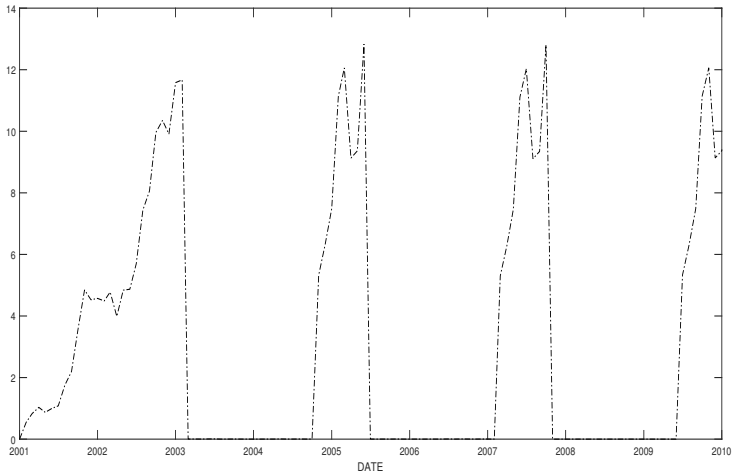

Figure C.0.59: Control statistic for the case of Residual MEWMA control chart when $\lambda = 0.45$ and reestimation of the target process. The sample period is 2001:01 to 2009:12.

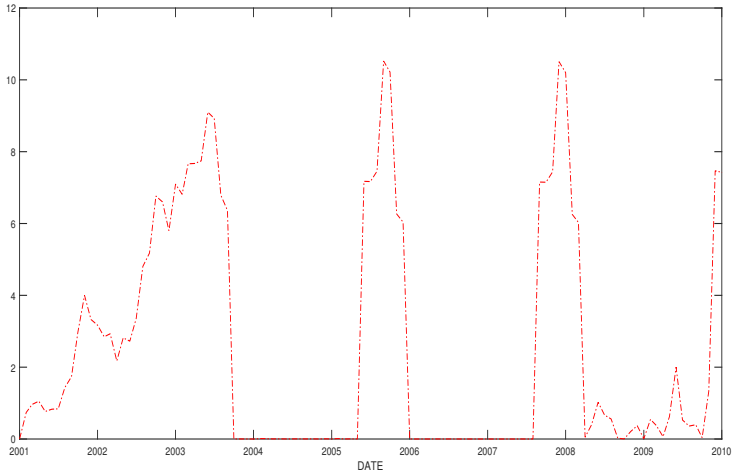

Figure C.0.60: Control statistic for the case of Residual MEWMA control chart when $\lambda = 0.75$ and reestimation of the target process. The sample period is 2001:01 to 2009:12.

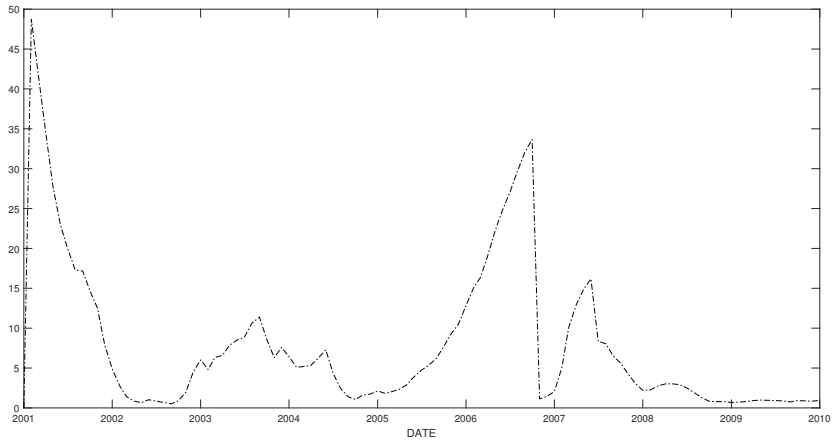

Figure C.0.61: Control statistic for the case of MMOMEWMA control chart when $\lambda = 0.45$ and reestimation of the target process. The sample period is 2001:01 to 2009:12.

C.0.4 Control charts with reestimation of the target process

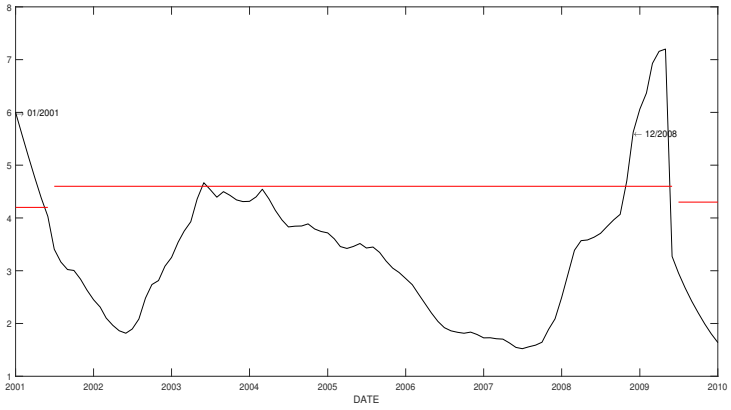

Figure C.0.62: Control chart for the case of EWMA control chart based on Mahalanobis distance when $\lambda = 0.1$ and reestimation of the target process. The sample period is 2001:01 to 2009:12.

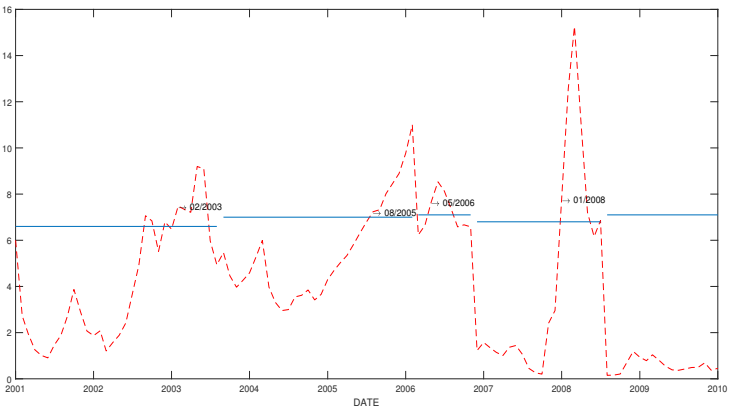

Figure C.0.63: Control chart for the case of EWMA control chart based on Mahalanobis distance when $\lambda = 0.75$ and reestimation of the target process. The sample period is 2001:01 to 2009:12.

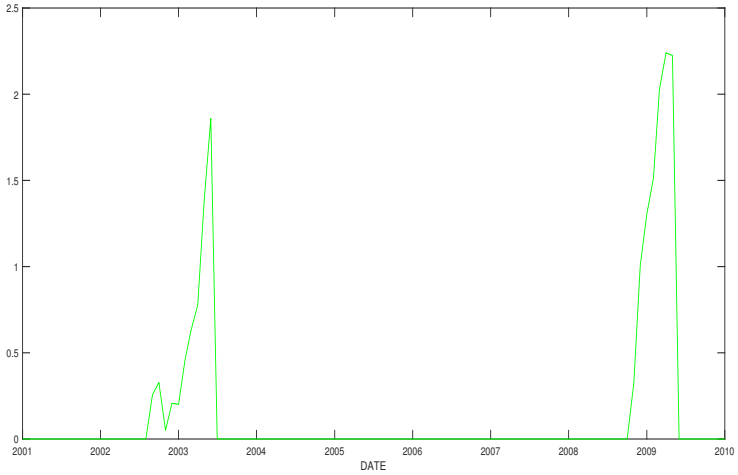

Figure C.0.64: Control chart for the case of MCUSUM control chart when $g = 2.5$ and reestimation of the target process. The sample period is 2001:01 to 2009:12.

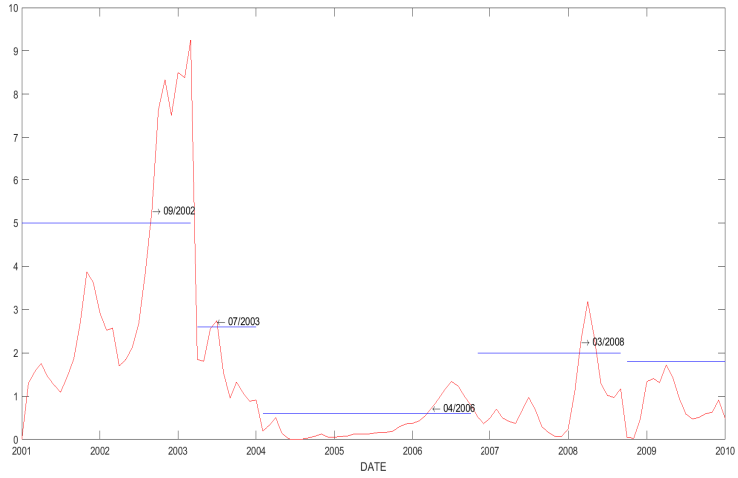

Figure C.0.65: Control chart for the case of MEWMA control chart when $\lambda = 0.5$ and reestimation of the target process. The sample period is 2001:01 to 2009:12.

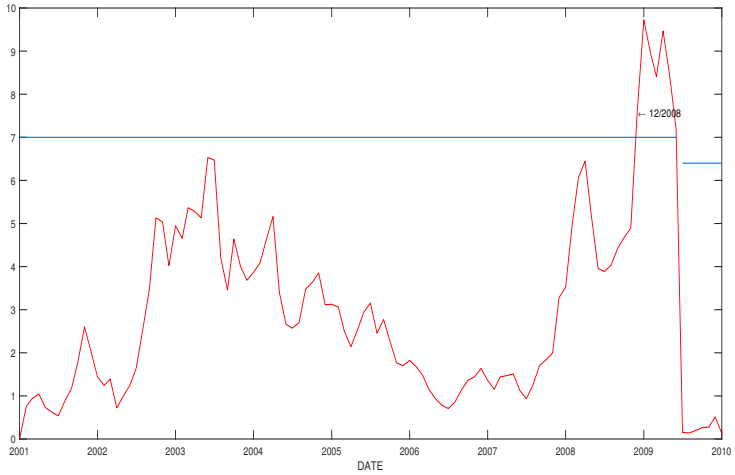

Figure C.0.66: Control chart for the case of MEWMA control chart when $\lambda = 0.75$ and reestimation of the target process. The sample period is 2001:01 to 2009:12.

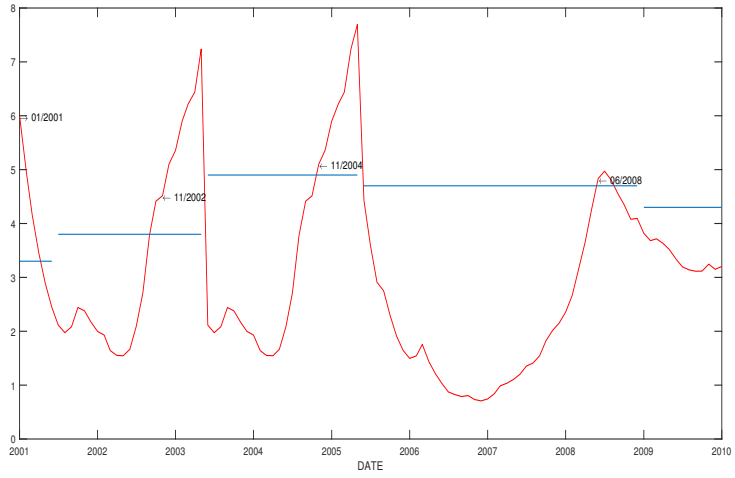

Figure C.0.67: Control chart for the case of Residual EWMA control chart based on Mahalanobis distance when $\lambda = 0.2$ and reestimation of the target process. The sample period is 2001:01 to 2009:12.

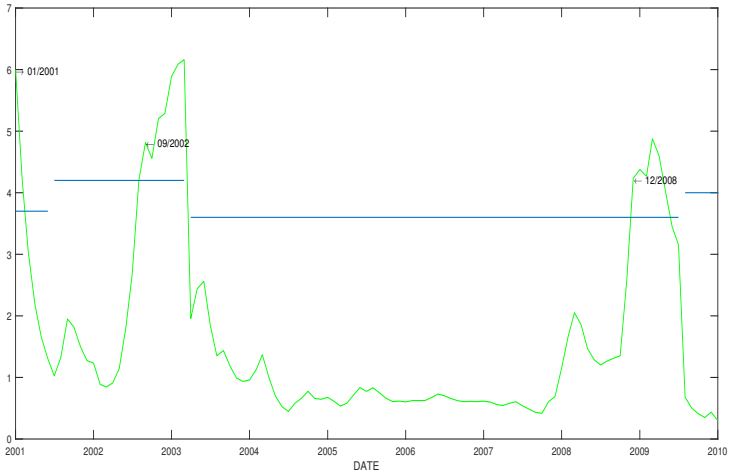

Figure C.0.68: Control chart for the case of Residual EWMA control chart based on Mahalanobis distance when $\lambda = 0.35$ and reestimation of the target process. The sample period is 2001:01 to 2009:12.

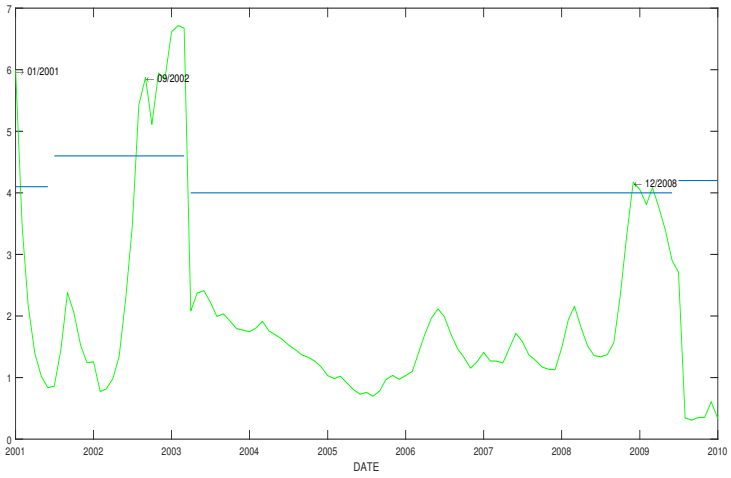

Figure C.0.69: Control chart for the case of Residual EWMA control chart based on Mahalanobis distance when $\lambda = 0.5$ and reestimation of the target process. The sample period is 2001:01 to 2009:12.

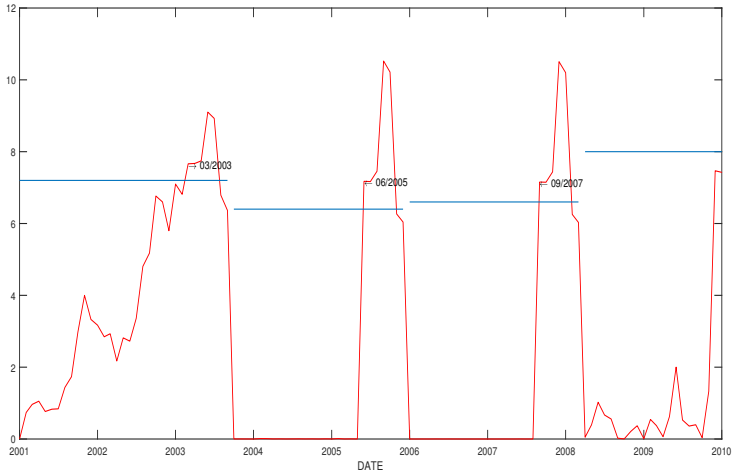

Figure C.0.70: Control chart for the case of Residual MEWMA control chart when $\lambda = 0.75$ and reestimation of the target process. The sample period is 2001:01 to 2009:12.

C.0.5 VARMA ATSM

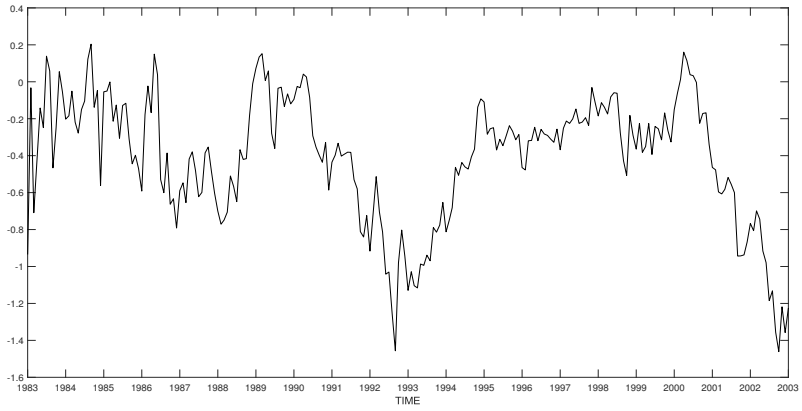

Figure C.0.71: Curvature of the yield curve. The sample period is 1983:01 to 2003:12.

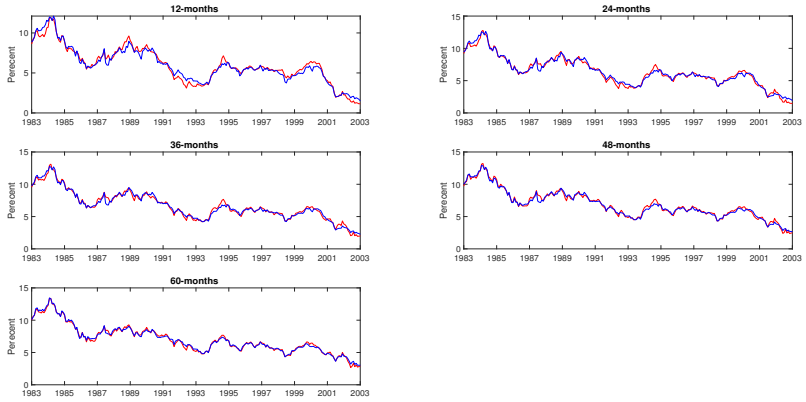

Figure C.0.72: Fitted and actual yields in-sample affine VARMA. The in-sample period is 1983:01 to 2003:12.

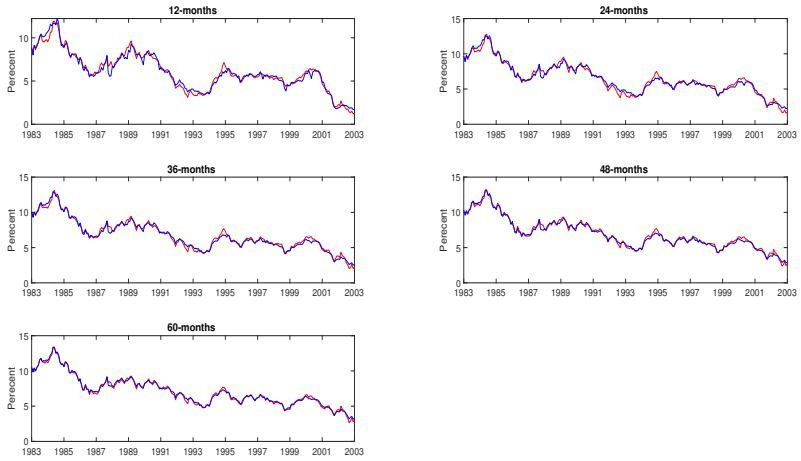

Figure C.0.73: Fitted and actual yields in-sample affine VAR. The in-sample period is 1983:01 to 2003:12.

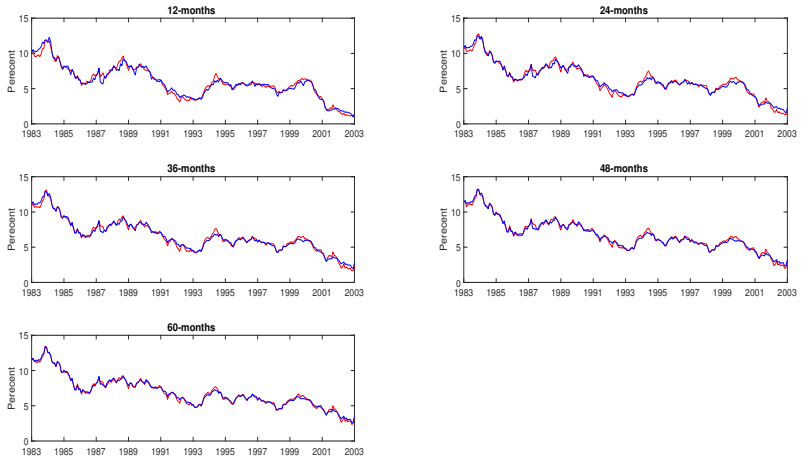

Figure C.0.74: Fitted and actual yields in-sample affine PMD-VARMA. The in-sample period is 1983:01 to 2003:12.

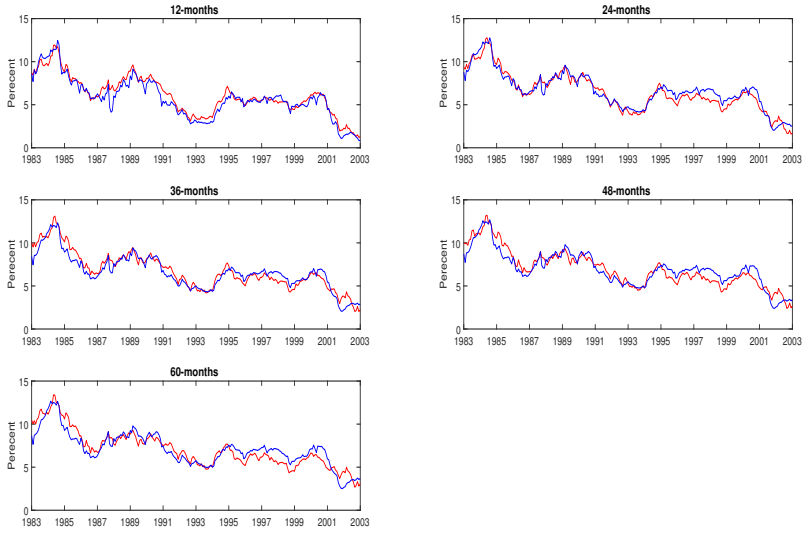

Figure C.0.75: Fitted and actual yields in-sample affine PMD-VAR. The in-sample period is 1983:01 to 2003:12.

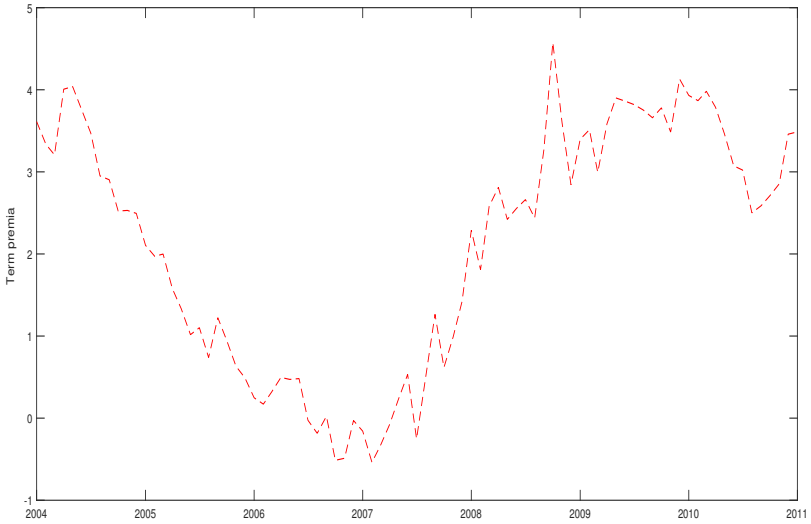

Figure C.0.76: Term Premia for the out-of-sample period, 2004:01 to 2011:12.

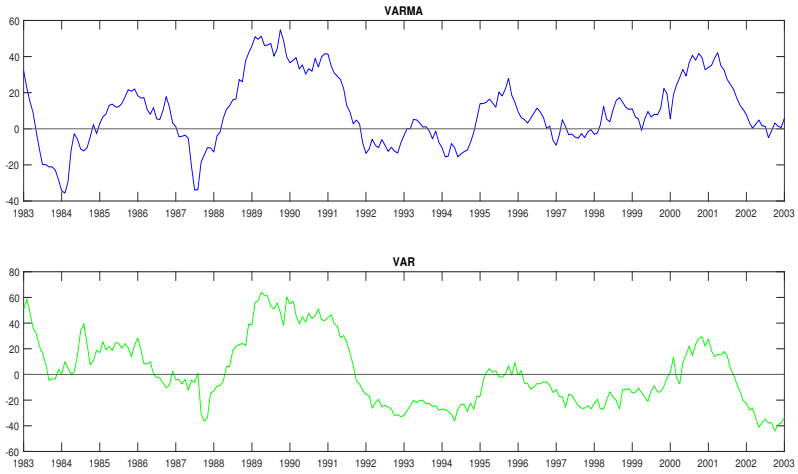

Figure C.0.77: Market price of risk for inflation for the in-sample period, 1983:01 to 2003:12.

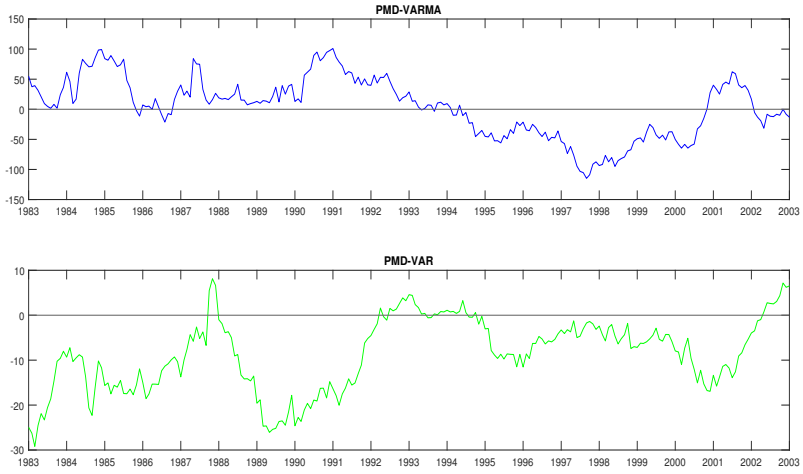

Figure C.0.78: Market price of risk for inflation from the PMD for the in-sample period, 1983:01 to 2003:12.

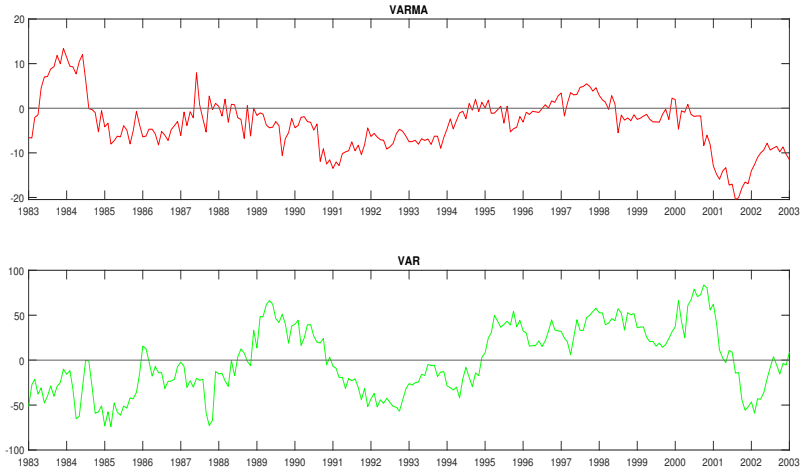

Figure C.0.79: Market price of risk for IP for the in-sample period, 1983:01 to 2003:12.

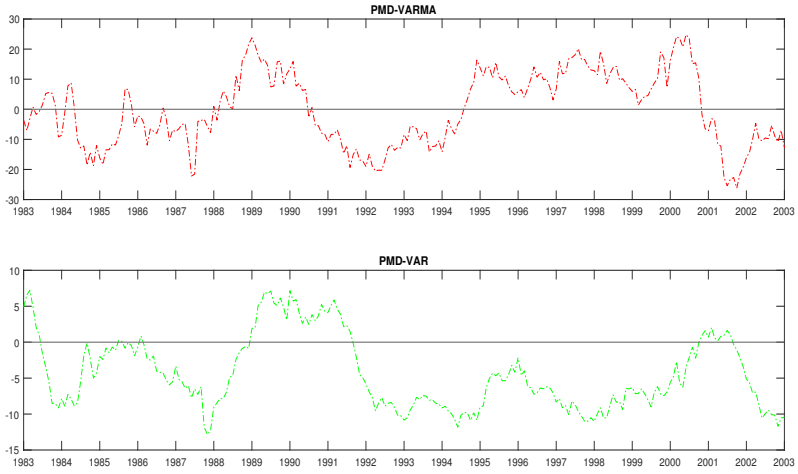

Figure C.0.80: Market price of risk for IP from the PMD for the in-sample period, 1983:01 to 2003:12.

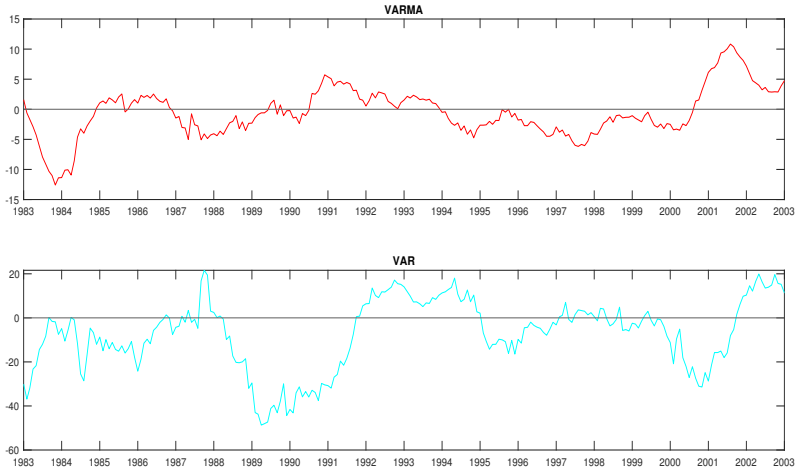

Figure C.0.81: Market price of risk for short rate for the in-sample period, 1983:01 to 2003:12.

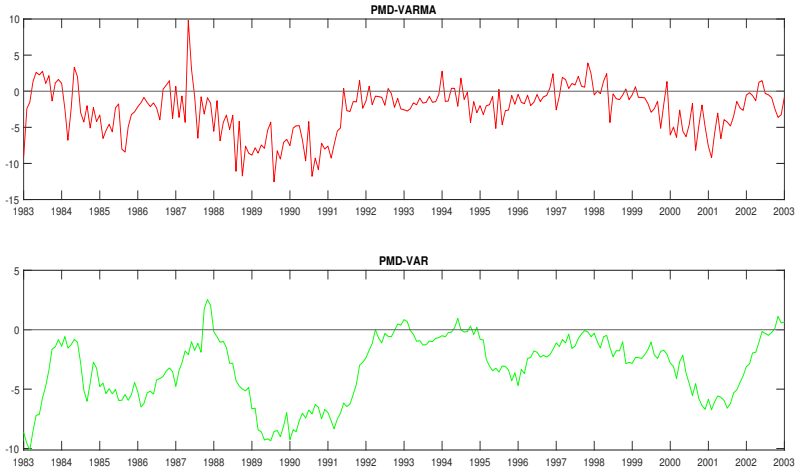

Figure C.0.82: Market price of risk for short rate from the PMD for the in-sample period, 1983:01 to 2003:12.

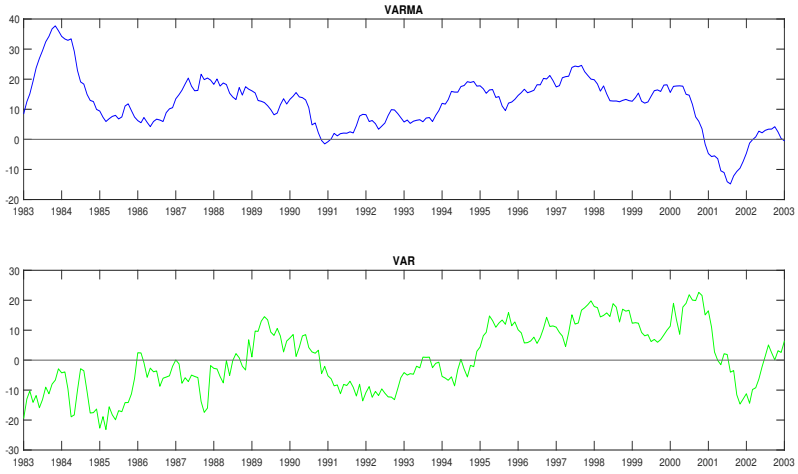

Figure C.0.83: Market price of risk for term premia for the in-sample period, 1983:01 to 2003:12.

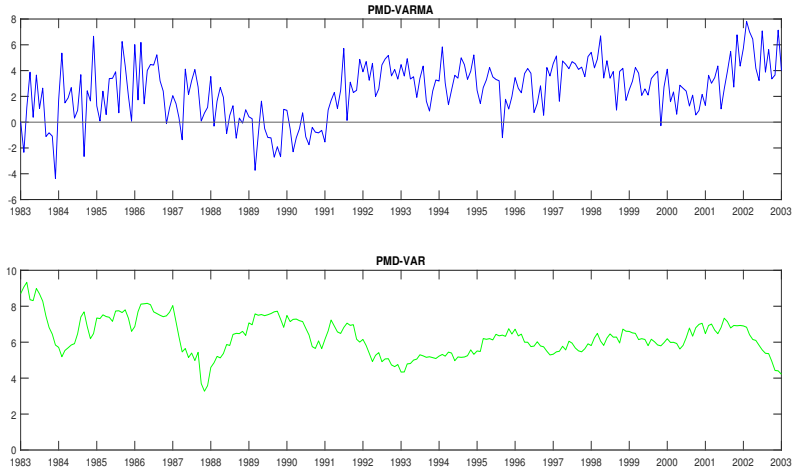

Figure C.0.84: Market price of risk for term premia from the PMD for the in-sample period, 1983:01 to 2003:12.